

Universidade Federal de Goiás  
Instituto de Ciências Biológicas  
Programa de Pós-Graduação em Genética e Biologia Molecular

**A HISTÓRIA EVOLUTIVA DE UMA PERERECA SUL-AMERICANA**

*Scinax squalirostris* (LUTZ, 1925) (ANURA, HYLIDAE):

**UM RESGATE DO PASSADO E CONSEQUÊNCIAS FUTURAS**

TATIANNE PIZA FERRARI ABREU JARDIM





Universidade Federal de Goiás  
Instituto de Ciências Biológicas  
Programa de Pós-Graduação em Genética e Biologia Molecular



TATIANNE PIZA FERRARI ABREU JARDIM

**A HISTÓRIA EVOLUTIVA DE UMA PERERECA SUL-AMERICANA**

***Scinax squalirostris* (LUTZ, 1925) (ANURA, HYLIDAE):**

**UM RESGATE DO PASSADO E CONSEQUÊNCIAS FUTURAS**

Goiânia  
2018

**TERMO DE CIÊNCIA E DE AUTORIZAÇÃO PARA DISPONIBILIZAR VERSÕES ELETRÔNICAS  
DE TESES E  
DISSERTAÇÕES NA BIBLIOTECA DIGITAL DA UFG**

Na qualidade de titular dos direitos de autor, autorizo a Universidade Federal de Goiás (UFG) a disponibilizar, gratuitamente, por meio da Biblioteca Digital de Teses e Dissertações (BDTD/UFG), regulamentada pela Resolução CEPEC nº 832/2007, sem ressarcimento dos direitos autorais, de acordo com a Lei nº 9610/98, o documento conforme permissões assinaladas abaixo, para fins de leitura, impressão e/ou *download*, a título de divulgação da produção científica brasileira, a partir desta data.

**1. Identificação do material bibliográfico:**       **Dissertação**       **Tese**

**2. Identificação da Tese ou Dissertação:**

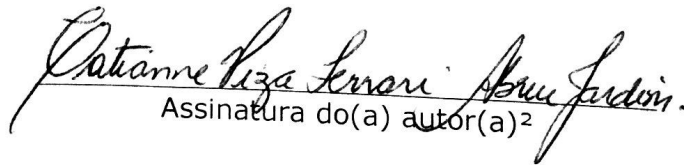
Nome completo do autor: Tatianne Piza Ferrari Abreu Jardim

Título do trabalho: A história evolutiva de uma perereca sul-americana *Scinax squalirostris* (Lutz, 1925) (Anura, Hylidae): Um resgate do passado e consequências futuras

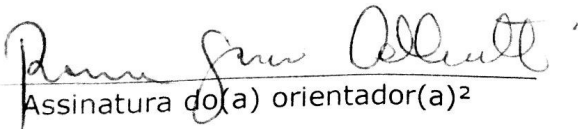
**3. Informações de acesso ao documento:**

Concorda com a liberação total do documento  SIM       NÃO<sup>1</sup>

Havendo concordância com a disponibilização eletrônica, torna-se imprescindível o envio do(s) arquivo(s) em formato digital PDF da tese ou dissertação.

  
Assinatura do(a) autor(a)<sup>2</sup>

Ciente e de acordo:

  
Assinatura do(a) orientador(a)<sup>2</sup>

Data: 12 / 11 / 2018

<sup>1</sup> Neste caso o documento será embargado por até um ano a partir da defesa. A extensão deste prazo suscita justificativa junto à coordenação do curso. Os dados do documento não serão disponibilizados durante o período de embargo.  
Casos de embargo:  
- Solicitação de registro de patente  
- Submissão de artigo em revista científica  
- Publicação como capítulo de livro  
- Publicação da dissertação/tese em livro

<sup>2</sup>A assinatura deve ser escaneada.

TATIANNE PIZA FERRARI ABREU JARDIM

**A HISTÓRIA EVOLUTIVA DE UMA PERERECA SUL-AMERICANA**

*Scinax squalirostris* (LUTZ, 1925) (ANURA, HYLIDAE):

**UM RESGATE DO PASSADO E CONSEQUÊNCIAS FUTURAS**

**Orientadora:** Prof.<sup>a</sup> Dr.<sup>a</sup> Rosane Garcia Collevatti  
**Co-orientador:** Prof. Dr. Natan Medeiros Maciel

Tese apresentada ao Programa de Pós-Graduação em Genética e Biologia Molecular, da Universidade Federal de Goiás, como parte das exigências para a obtenção do título de Doutora em Genética e Biologia Molecular.

Goiânia,  
Outubro / 2018

Ficha de identificação da obra elaborada pelo autor, através do Programa de Geração Automática do Sistema de Bibliotecas da UFG.

Piza Ferrari Abreu Jardim, Tatianne

A história evolutiva de uma perereca Sul-Americana *Scinax squalirostris* (Lutz, 1925) (Anura, Hylidae): Um resgate do passado e consequências futuras [manuscrito] / Tatianne Piza Ferrari Abreu Jardim. - 2018.

ccxxxvi, 236 f.: il.

Orientador: Profa. Dra. Rosane Garcia Collevatti; co-orientador Dr. Natan Medeiros Maciel.

Tese (Doutorado) - Universidade Federal de Goiás, Instituto de Ciências Biológicas (ICB), Programa de Pós-Graduação em Genética e Biologia Molecular, Goiânia, 2018.

Bibliografia. Apêndice.

Inclui tabelas, lista de figuras, lista de tabelas.

1. conservação. 2. delimitação. 3. diversidade genética. 4. filogeografia. 5. mudança climática. I. Garcia Collevatti, Rosane, orient. II. Título.

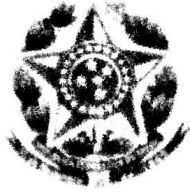
CDU 575



SERVIÇO PÚBLICO FEDERAL  
UNIVERSIDADE FEDERAL DE GOIÁS  
INSTITUTO DE CIÊNCIAS BIOLÓGICAS  
PROGRAMA DE PÓS-GRADUAÇÃO EM GENÉTICA E BIOLOGIA MOLECULAR

**ATA DA SESSÃO PÚBLICA DE DEFESA DE TESE DE Nº 015**

1  
2 Aos trinta e um dias do mês de outubro do ano de dois mil e dezoito  
3 (31/10/2018), às 08hs30min, no auditório do ICB V/UFG, reuniram-se os  
4 componentes da banca examinadora: Prof. Dr. Natan Medeiros Maciel, co-  
5 orientador; Profa. Dra. Daniela de Melo e Silva; Profa. Dra. Natácia  
6 Evangelista de Lima; Profa. Dra. Luciana Signorelli Faria Lima e Prof. Dr. Iberê  
7 Farina Machado, para, em sessão pública presidida pelo primeiro examinador  
8 citado, procederem à avaliação da defesa de tese intitulada: **"A HISTÓRIA**  
9 **EVOLUTIVA DE UMA PERERECA SUL-AMERICANA *Scinax squalirostris***  
10 **(LUTZ, 1925) (ANURA, HYLIDAE): UM RESGATE DO PASSADO E**  
11 **CONSEQUÊNCIAS FUTURAS"**, em nível de doutorado, área de concentração  
12 em **Genética e Biologia Molecular**, de autoria de **TATIANNE PIZA**  
13 **FERRARI ABREU JARDIM**, discente do Programa de Pós-Graduação em  
14 Genética e Biologia Molecular da Universidade Federal de Goiás. Em virtude da  
15 orientadora Profa. Dra. Rosane Garcia Colevatti ter sido convocada para  
16 missão no CNPq, assumiu a presidência da banca o co-orientador Prof. Dr.  
17 Natan Medeiros Maciel, que fez a apresentação formal dos membros da banca.  
18 A palavra, a seguir, foi concedida à autora da tese que, em cerca de  
19 45 minutos, procedeu à apresentação de seu trabalho. Terminada a  
20 apresentação, cada membro da banca arguiu a examinada, tendo-se adotado  
21 o sistema de diálogo sequencial. Terminada a fase de arguição, procedeu-se a  
22 avaliação da tese. Tendo-se em vista o que consta na Resolução nº 1294 de  
23 06 de Junho de 2014 do Conselho de Ensino, Pesquisa, Extensão e Cultura  
24 (CEPEC), que regulamenta o Programa de Pós-Graduação em Genética e  
25 Biologia Molecular, a tese foi APROVADA, considerando-se integralmente  
26 cumprido este requisito para fins de obtenção do título de Doutor (a) em  
27 Genética e Biologia Molecular pela Universidade Federal de Goiás. A conclusão



SERVIÇO PÚBLICO FEDERAL  
UNIVERSIDADE FEDERAL DE GOIÁS  
INSTITUTO DE CIÊNCIAS BIOLÓGICAS  
PROGRAMA DE PÓS-GRADUAÇÃO EM GENÉTICA E BIOLOGIA MOLECULAR

28 do curso dar-se-á quando da entrega da versão definitiva da tese na  
29 secretaria do programa, com as devidas correções sugeridas pela banca  
30 examinadora, no prazo de trinta dias a contar da data da defesa. Cumpridas  
31 as formalidades de pauta, às 12 horas e 17 minutos, encerrou-se a  
32 sessão de defesa e, para constar, o presidente da Banca lavrou a presente ata  
33 que, após lida e aprovada, será assinada pelos membros da banca  
34 examinadora em três vias de igual teor.

*Natan Medeiros Maciel*

35  
36 Prof. Dr. Natan Medeiros Maciel

37 **Presidente da Banca**

38 **UFG/GO**

39  
40  
41 *Daniela de Melo e Silva*

42 Profa. Dra. Daniela de Melo e Silva

43 **UFG/GO**

44  
45 *Natácia Evangelista de Lima*

46 Profa. Dra. Natácia Evangelista de Lima

47 **UFG/GO**

48  
49 *Luciana Signorelli Faria Lima*

50 Profa. Dra. Luciana Signorelli Faria Lima

51 **UFG/GO**

52  
53 *Iberê Farina Machado*

54 Prof. Dr. Iberê Farina Machado

55 **UFG/GO**

## AGRADECIMENTOS

Quero agradecer primeiramente a FAPEG uma vez que, graças à concessão da bolsa de doutorado, pude dedicar-me exclusivamente ao desenvolvimento dessa tese. Agradeço também aos órgãos de fomento CNPq e CAPES/PROCAD, pelos recursos para o desenvolvimento dessa tese, como coletas, materiais e equipamento para obtenção dos dados genéticos.

Agradeço aos meus orientadores, **Rosane Garcia Collevatti** e **Natan Medeiros Maciel**, que sempre estiveram presente e souberam me aconselhar e guiar ao longo desses anos. Graças a vocês pude crescer, amadurecer e me tornar uma pessoa melhor. Agradeço pela eterna paciência e pela maravilhosa oportunidade.

Quero agradecer as coleções que doaram alíquotas de tecidos e/ou emprestaram exemplares para que esse trabalho pudesse ser realizado. Agradeço às seguintes coleções zoológicas e suas instituições: **Coleção Célio F. B. Haddad** (CFBH), Departamento de Zoologia, Universidade Estadual Paulista, Campus de Rio Claro, São Paulo, **Coleção Herpetológica da Universidade de Brasília** (CHUNB), Brasília, Distrito Federal, **Colección Biológica Arnoldo da Winkelried Bertoni** (IIBP-H), Instituto de Investigación Biológica del Paraguay, Asunción, **Museu de Ciências e Tecnologia** (MCT), Pontifícia Universidade Católica do Rio Grande do Sul, Porto Alegre, Rio Grande do Sul, **Coleção do setor de herpetologia da Universidade Federal do Rio Grande do Sul** (UFRGS), Porto Alegre, Rio Grande do Sul, **Coleção Zoológica da Universidade Federal de Goiás** (ZUFG), Goiânia, Goiás, **Coleção Herpetológica do setor de Zoologia da Universidade Federal de Santa Maria** (ZUFMS), Santa Maria, Rio Grande do Sul, **Coleção da Universidade Federal de Minas Gerais** (UFMG), Belo Horizonte, Minas Gerais e por fim, ao **Museu Nacional do Rio de Janeiro** (MNRJ), Universidade Federal de Rio de Janeiro, Rio de Janeiro, e aqui deixo o meu lamento ao ocorrido no dia 02 de Setembro desse ano.

Agradeço aos **membros da banca**, que dedicaram uma parte do seu tempo e do seu conhecimento para contribuir com o meu trabalho e com o meu crescimento!

Agradeço aos laboratórios, professor@s, técnic@s e alun@s do Laboratório de Genética e Biodiversidade (**LGBio**) e do Laboratório de Herpetologia e Comportamento Animal (**LabHerp**). Dentro desses dois ambientes pude aprender muito, discutir, passar para frente o pouco que eu sabia, e viver muitas histórias.

Agradeço a **Núbia Esther, Liliane Meija-Ballesteros e Daniela Silva** por terem participado da minha qualificação e contribuído muito para meu crescimento a partir daquela fase. Aos outr@s professor@s do PGBM e EcoEvol, agradeço pelos ensinamentos nas disciplinas e palestras. Agradeço à **UFG** pela infraestrutura.

Ao longo desses 4 anos (e pouquinho) várias pessoas entraram e passaram pela minha vida, muitas que tenho um débito de gratidão por me apoiarem, me aconselharem, me ajudarem e que me inspiraram em como ser uma profissional e uma pessoa melhor. Agradecendo a ess@s grandes amig@s: **Daniela Elaine, Ramilla, Vanessa, Fernanda Fraga, Rhewter, Ueric, Elisa, Liliana Meija-Ballesteros, Núbia Esther, Jacqueline Lima, Ariane, Kassia, Rejane, Warita, Luciana V., Tatiana, Marcelo, Cintia, Thaís, Carol, Vinicius, Deusivan, Maurivan, Fernanda, James, Leonardo, Dani, Paola Nobre, Luciano Sgarbi, Marcos Vieira, Amanda Anjos, Tailise, Raísa, Geiziane, Bruno Ribeiro, Jesus, Lorena, Danilo, Davi, Dinei, Bruno Barreto, Ivy, Jacques, Bruno Vilela, Fabricio Vilalobos, Karlo, Renato, Rômulo**. Eu aprendi muito com cada um de vocês! Tenho certeza que mais pessoas merecem esse agradecimento, mas peço perdão a minha falta de memória neste momento, mas agradeço você que de alguma forma contribuiu em minha vida!

Aquele agradecimento especial e bem ‘falso’ para meus Falsianos *et al.*: **Priscila Cabral, Maria Augusta, Alejandro Valencia, Gabryella Mesquita e Nathane Queiroz**, vocês me ajudaram a crescer, tornaram os dias mais felizes, me mostraram que nas dificuldades não estamos sozinhos, obrigada por cada papo, cada café, cada companhia, cada ajuda, cada correção, cada riso, cada Aff, cada mão que me estenderam!

Quero agradecer aos **meus pais Vania Piza Ferrari e Julio César Abreu**, meu padrasto **Antônio José e Silva** e minha madrasta **Magali Lourenço**! Que cada um no seu jeito de ser, na sua distância ou presença, ao longo da minha vida, contribuíram para que eu pudesse crescer e chegar onde estou e ser o que sou! O agradecimento da contribuição, participação, incentivo, paciência e amor de vocês nunca será o suficiente! Obrigada por tudo, vocês são incríveis e são tudo na minha vida!!!

Agradeço aos meus irmãos **Julio César Abreu Jr., Marco Antônio e Felipe Silva** vocês são os melhores irmãos que alguém poderia ter vida, e eu tive a sorte de ser essa escolhida! Obrigada as irmãs **Jady Fernandes, Bárbara Zanini** e irmão **Bernardo Jardim** que ganhei de presente da vida. Agradeço aos meus **Tios e Tias**, meu lindo **Vô Luiz** e minha **vozinha Neuza** que não está mais aqui (e **Vó Lydia e Terezinha** que

ganhei de presente também), aos **meus primos e primas!** Vocês são parte fundamental da minha vida e do meu crescimento, obrigada por me apoiarem e estarem sempre ao meu lado!

Agradeço aos meus Sogrinhos **Suzana Caldas e Ricardo Zanini!** Obrigada por todo apoio, carinho e por me considerarem como filha! E finalmente, gostaria de agradecer ao meu marido **Lucas Lacerda Caldas Zanini Jardim,** um agradecimento que nem sei por onde começar e muito menos terminar! Agradeço pela pessoa maravilhosa que você é, devo muito a você! Obrigada por tornar cada momento maravilhoso melhor ainda e por tornar cada momento difícil, mais leve. Obrigada pela paciência, pela companhia, pelos risos, por sempre estar ao meu lado e pelo divertimento que é a nossa vida! Agradeço por me fazer crescer intelectualmente e como pessoa também! Obrigada por sempre me dar a mão e me mostrar que podemos passar por tudo, e tudo realmente fica mais fácil e mais leve ao seu lado. Obrigada por estar e construir a vida comigo!

## SUMÁRIO

RESUMO GERAL .....	10
GENERAL ABSTRACT .....	12
INTRODUÇÃO GERAL .....	14
OBJETIVO GERAL E ESPECÍFICOS .....	18
<b>CAPÍTULO 1: Inferring responses to Neogene-Quaternary climate dynamics from historical demography in a South American grassland treefrog.....</b>	<b>20</b>
ABSTRACT .....	21
1. INTRODUCTION .....	22
2. MATERIAL AND METHODS .....	25
2.1 Population sampling and genetic data .....	25
2.2 Genetic diversity and population structure .....	26
2.3 Population demographic history .....	27
2.4 Coalescent tree and Time of Most Recent Ancestor .....	28
2.5 Lineage Dispersal .....	28
2.6 Paleodistribution modelling .....	29
2.7 Demographical scenarios and simulations .....	30
2.8 Spatial patterns in genetic diversity .....	32
3. RESULTS .....	32
3.1 Genetic diversity and population structure .....	32
3.2 Demographic population history and Time of Most Common Ancestor .....	33
3.3 Lineage Dispersal .....	34
3.4 Paleodistribution modelling .....	34
3.5 Demographical scenarios and simulations .....	35
3.6 Spatial patterns in genetic diversity .....	35
4. DISCUSSION .....	36
ACKNOWLEDGEMENTS .....	40
REFERENCES .....	41
BIOSKETCH .....	47
TABLE .....	48
FIGURE LABELS .....	50

FIGURES .....	52
SUPPORTING INFORMATION: APPENDIX S1 SUPPLEMENTARY TABLES .....	58
SUPPORTING INFORMATION: APPENDIX S2 SUPPLEMENTARY MATERIAL AND METHODS .....	74
SUPPORTING INFORMATION: APPENDIX S3 SUPPLEMENTARY FIGURES .....	80
<b>CAPÍTULO 2: Revelando a diversidade do complexo de espécies de <i>Scinax squalirostris</i> (Lutz, 1925) (Anura, Hylidae), uma espécie com ampla distribuição disjunta .....</b>	<b>94</b>
RESUMO .....	94
1. INTRODUÇÃO .....	96
2. MATERIAL E MÉTODOS .....	99
2.1 Amostragem e dados moleculares .....	99
2.2 Dados morfométricos .....	100
2.3 Análises moleculares .....	101
2.4 Análises morfométricas .....	102
3. RESULTADOS .....	103
3.1 Análises moleculares .....	103
3.2 Análises morfométricas .....	104
4. DISCUSSÃO .....	104
4.1 Delimitação molecular .....	105
4.2 Análise morfométrica .....	106
4.3 Nomenclatura .....	107
AGRADECIMENTOS .....	108
REFERÊNCIAS .....	109
TABELAS .....	114
LISTA DE FIGURAS .....	119
FIGURAS .....	120
MATERIAL SUPLEMENTAR: APÊNDICE S1 SUPLEMENTAR TABELAS .....	124
MATERIAL SUPLEMENTAR: APÊNDICE S2 SUPLEMENTAR FIGURAS .....	128
MATERIAL SUPLEMENTAR: APÊNDICE S3 SUPLEMENTAR AMOSTRAS .....	129

<b>CAPÍTULO 3: Predicting impacts of global climatic change on distribution and genetic diversity of the treefrog <i>Scinax squalirostris</i> (Lutz, 1925) (Anura, Hylidae)</b> .....	132
ABSTRACT .....	132
1. INTRODUCTION .....	134
2. MATERIAL AND METHODS .....	137
2.1 Population sampling and genetic diversity .....	137
2.2 Ecological niche modelling: Future predictions .....	138
2.3 Simulations of genetic diversity under climatic changes .....	140
2.4 Forecasting and dynamic genetic clusters in future scenarios .....	141
2.5 Accessing the genetic richness and conservation of genetic diversity .....	142
3. RESULTS .....	143
3.1 Ecological niche modelling: Future predictions .....	143
3.2 Simulations of genetic diversity under climatic changes .....	144
3.3 Forecasting and dynamics in genetic clusters in future scenarios .....	144
3.4 Conservation of genetic diversity .....	145
4. DISCUSSION .....	146
ACKNOWLEDGEMENTS .....	150
REFERENCES .....	151
BIOSKETCH .....	159
TABLE .....	161
FIGURE LABELS .....	163
FIGURES .....	165
SUPPORTING INFORMATION: APPENDIX S1 SUPPLEMENTARY TABLES .....	171
SUPPORTING INFORMATION: APPENDIX S2 SUPPLEMENTARY FIGURES .....	227
CONCLUSÃO GERAL .....	231
REFERÊNCIAS .....	233

## RESUMO GERAL

Diferentes eventos, como geológicos do Neógeno e climáticos do Quaternário, tiveram um papel importante com alterações da paisagem e do clima na América do Sul, influenciando diretamente a história evolutiva dos organismos da região nos últimos milhões de anos. Essas mudanças levaram à alternância entre períodos quentes e úmidos com frios e secos, e essa alternância iniciou a dinâmica de retração e expansão de paisagens abertas e florestais. Espécies associadas a esses ambientes evoluíram seguindo essa dinâmica, levando a alteração na conformação genética, diferenciação de linhagens e até a especiação. Assim como no passado, mudanças climáticas futuras podem alterar a paisagem causando mudanças na distribuição geográfica das espécies. Além disso, o aquecimento global previsto pode levar a diminuição da diversidade genética e ocasionar a extinção devido à baixa capacidade das espécies de se adaptarem as mudanças drásticas tão rapidamente. Nesta tese utilizou-se duas regiões do DNA mitocondrial (Cytb e 12S) e uma nuclear (RAG-1) juntamente com simulações coalescentes, e de Modelagem de Nicho Ecológico para acessar a história evolutiva de uma espécie de perereca *Scinax squalirostris* (Lutz, 1925) associada aos Campos (*grasslands*) Sul-Americanos. No primeiro capítulo buscou-se entender como eventos geológicos do Neógeno e climáticos do Quaternário podem ter moldado a atual distribuição disjunta e o padrão de diversidade genética de *S. squalirostris*. Encontrou-se que as populações de *S. squalirostris* possuem alta diversidade genética, com nenhum sinal de fluxo gênico atual, uma alta diferenciação genética e história demográfica estável ao longo do tempo com origem de dispersão no Sul do Brasil. Eventos de coalescência dataram do Plioceno-Pleistoceno, com compartilhamento de haplótipos entre as populações geograficamente distantes, indicando um arranjo incompleto de linhagens. A modelagem de paleodistribuição sugere que as linhagens de *S. squalirostris* tinham uma ocorrência de ampla distribuição no último máximo glacial (LGM) com contração e mudança de área no período pós-LGM. Tais resultados indicam que a atual distribuição geográfica e diversidade genética de *S. squalirostris* é devido a contração de uma área amplamente distribuída no passado, gerada pela dinâmica de retração de *grasslands* nos períodos mais quentes devido à perda de áreas adequadas para sua ocorrência. No segundo capítulo testou-se a hipótese de que as populações atuais de *S. squalirostris* poderiam representar linhagens distintas, com potencial (is) espécie(s) candidata(s) não descrita(s), devido a atual distribuição disjunta. Com a utilização de dados moleculares e dados morfométricos resgatou-se a formação de dois grupos, sendo um destes com uma espécie a ser descrita, um grupo restrito a região Centro-Oeste do Brasil, e outro grupo abrangendo populações do Sul e Sudeste do Brasil, Paraguai, Uruguai e Argentina. No terceiro capítulo utilizou-se a modelagem de nicho ecológico, juntamente com as análises moleculares e as simulações de agrupamentos genéticos para verificar o quanto as mudanças climáticas futuras poderão alterar a diversidade genética e a distribuição de *S. squalirostris*. Através de dois cenários climáticos com diferentes alterações na temperatura para 2100 (cenário 4.5 RCP aumenta 1.8°C e estabiliza, e o cenário 8.5 aumenta 3.7°C e continua aumentando), a análise de modelagem de nicho

indicou uma diminuição de áreas adequadas na região Centro-Oeste e Sudeste, com um deslocamento em direção ao Sul do Brasil adentrando até a região central da Argentina em direção a áreas mais antropizadas. A maioria das populações do Centro-Oeste e norte da região Sudeste poderão ser extintas devido à ausência de áreas climáticas adequadas para a sua ocorrência e sua baixa diversidade genética. Além disso, foi observado que as Unidades de Conservação (UCs) detêm, atualmente, grande parte da diversidade genética de *S. squalirostris*. Com as mudanças climáticas previstas, as UCs em áreas que serão ideais para a ocorrência de *S. squalirostris* conseguirão manter altos níveis de diversidade genética, porém com perdas de diversidade na região Centro-Oeste e Sudeste. Este trabalho indica que as mudanças climáticas futuras afetarão negativamente essa espécie, pois as áreas adequadas para sua ocorrência serão reduzidas e deslocadas. A perda e as alterações nos agrupamentos genéticos, podem levar a uma possível perda do potencial evolutivo das populações de *S. squalirostris* em responder às mudanças climáticas futuras, o que poderia resultar na extinção de algumas populações.

**Palavras-chave:** conservação; delimitação; diversidade genética; simulação coalescente; filogeografia; mudança climática.

## GENERAL ABSTRACT

Geological events of the Neogene and the climatic fluctuations of the Quaternary played an important role in shaping the landscape and climate of South America therefore directly influencing the evolutionary history of the organisms of this area over the last million years. These changes led to the alternation between warm and humid, cold and dry periods. Such alternation dictated the dynamics of retraction and expansion of open and forest landscapes. Species associated to these environments evolved following this dynamic, which lead to alteration in genetic conformation, lineage differentiation and even speciation. As in the past, future changes in climate can modify the landscape causing changes in the geographical distribution of species. In addition, predicted global warming may lead to a decline in genetic diversity as well as lead to extinction due to species' low ability to adapt to drastic and quick changes. In this thesis two regions of mitochondrial DNA (Cytb and 12S) and one nuclear (RAG-1) were used together with coalescing simulations, and ecological niche modelling to access the evolutionary history of a *Scinax squalirostris* (Lutz, 1925), a species associated to the South American grasslands. In the first chapter, we sought to understand how Neogene and Quaternary geological or climatic events, respectively, may have shaped the current disjunct distribution and the genetic diversity pattern of *S. squalirostris*. The populations of *S. squalirostris* were found to have high genetic diversity, with no sign of current gene flow, a high genetic differentiation, and a stable demographic history over time with scattered origin in southern Brazil. Coalescence events date from Pliocene-Pleistocene, with haplotype sharing among geographically distant populations, which indicates incomplete lineage sorting. The paleodistribution models suggests that *S. squalirostris* lineages were widely distributed during the last glacial maximum (LGM) but afterwards contracting and changing their area of occurrence. These results indicate that the current geographic distribution and genetic diversity of *S. squalirostris* is due to the contraction of an area widely distributed in the past, generated by the dynamics of retraction of grasslands in warmer periods due to the loss of areas suitable for their occurrence. In the second chapter, we tested the hypothesis that the current populations of *S. squalirostris* could represent distinct lineages with candidate species not previously described, due to the current disjunct distribution. Using molecular and morphometric data the formation of two groups was rescued. One of them consists in a candidate species to be described, which is a lineage restricted to the Central-West region of Brazil. The other one comprises of populations from the South and Southeast Brazil, Paraguay, Uruguay and Argentina. In the third chapter, ecological niche modelling, molecular techniques and simulations of genetic groups were used to verify how future climate changes could alter the genetic diversity and distribution of *S. squalirostris*. Through two climatic scenarios with different temperature changes to 2100 (scenario 4.5 RCP increases 1.8 °C and stabilizes, and scenario 8.5 increases 3.7 °C and continues to increase), ecological niche modelling analysis indicated a decrease of suitable areas in the Central-West and Southeast regions, with a displacement towards the South of Brazil entering the central region of Argentina towards more anthropized areas. Most of

the Central West and Northern Southeast populations may be extinct due to the absence of climatic suitable areas for their occurrence and low genetic diversity. In addition, it was observed that Protections Areas (PAs) currently harbors a large part of the genetic diversity of *S. squalirostris*. Thus, PAs in areas that will be ideal for the occurrence of *S. squalirostris* will be able to maintain their high levels of genetic diversity, but with losses of genetic diversity in the Midwest and Southeast regions. This work indicates that future climate changes will negatively affect this species, since the appropriate areas for its occurrence will be reduced and displaced. The loss and changes in genetic clusters may lead to a possible loss of the evolutionary potential of *S. squalirostris* populations in responding to future climate changes, which could result in the extinction of some populations.

**Keywords:** coalescent simulations; conservation; climate change; delimitation; genetic diversity; phylogeography.

## INTRODUÇÃO GERAL

Os eventos geológicos do Neógeno e climáticos do Quaternário tiveram um papel importante nesse processo, com alterações da paisagem e do clima (Burnham & Graham, 1999) na América do Sul, influenciando diretamente a história evolutiva dos organismos da região nos últimos milhões de anos (Behling 2002, Ortiz-Jaureguizar & Cladera, 2006, Tuomisto, 2007). Eventos como retração e transgressão marinha, soerguimento e formações costeiras e flutuações climáticas levaram a expansão e a retração de florestas e áreas abertas (Behling, 2002, Ortiz-Jaureguizar & Cladera, 2006; Overbeck, 2007) moldando a distribuição da biota encontrada atualmente. Assim, entender e reconstruir a história dessas biotas pode nos ajudar a entender os padrões de organização espacial dos organismos e os processos que resultaram nesses padrões (Riddle et al., 2008) e termos um melhor conhecimento sobre como os eventos geológicos e climáticos do Neógeno e Quaternário podem ter afetado os organismos.

A Filogeografia (Avice et al., 1987) é um campo que trata tanto das relações filogenéticas entre os táxons de interesse bem como dos componentes históricos responsáveis pela distribuição espacial das linhagens (Avice et al., 1987; Freeland, 2005). Essa área tem por objetivo entender como os eventos históricos influenciaram na atual distribuição geográfica da diversidade genética, de populações e de espécies (Freeland, 2005). A obtenção dessa história demográfica através da análise filogeográfica é de grande importância para melhorar a compreensão de processos microevolutivos na escala espaço/temporal genética (Knowles e Maddison, 2002). A modelagem de paleodistribuição projetada em cenários climáticos passados podem (i) fornecer um contexto espacial da história demográfica da espécie para as análises filogeográficas, (ii) os prováveis precursores dos padrões de divergência e (iii) a distribuição observada atualmente nas espécies (e.g. Lima et al., 2014; Collevatti et al., 2015; Vitorino et al., 2017).

Além de entender a influência dos eventos históricos, é importante também prever o efeito das mudanças climáticas futuras na distribuição e diversidade genética dos organismos, e podemos acessar esses efeitos através da utilização da modelagem de nicho ecológico (ENM) (e.g. Lima et al., 2017; Vasconcelos *et al.*, 2018). A diversidade genética intraespecífica representa o potencial evolutivo das espécies, nas quais a

seleção natural atua para promover a evolução dos organismos e sua adaptação às mudanças ambientais (Urban et al., 2012, 2013). Altos níveis de diversidade genética podem favorecer uma rápida resposta evolutiva, mas populações com baixa diversidade genética têm seu potencial evolutivo reduzido e tornando-as propensas à extinção local (Spielman et al., 2004; Frankham, 2005). Como é esperado que até 2100 a temperatura aumente em aproximadamente 2°C a 4°C (New et al., 2011; Fischer et al., 2018) devido a emissão de gases de efeito estufa (IPCC, 2014), se faz necessário entender como essas mudanças podem afetar as espécies e se terão capacidade de responder de forma tão rápida quanto a intensidade que tais alterações ocorrem. Além disso, é importante compreender o quanto a diversidade genética dessas espécies está representada em Unidades de Conservação e avaliar se, devido às mudanças climáticas essa diversidade será mantida.

Estudos filogeográficos da biota sul-americana têm mostrado uma história complexa de diversificação, na qual a combinação dos eventos orogênicos do Neógeno e as oscilações climáticas do Quaternário contribuíram para moldar a presente diversidade e distribuição das linhagens do continente, inclusive para anuros (Rull, 2011; Turchetto-Zolet et al., 2013). Além disso, estudos elucidam que os anuros são os grupos que mais podem sofrer com mudanças climáticas futuras (Loyola et al., 2014; Vilela et al., 2018; Vasconcelos et al., 2018). Tendo em vista ao apresentado até aqui, nesta tese, nós buscamos resgatar a história evolutiva passada e prever os efeitos das mudanças climáticas, em um complexo de espécie de uma perereca sul-americana *Scinax squalirostris*.

*Scinax squalirostris* foi descrita por Adolpho Lutz em 1925, tendo como localidade tipo a Fazenda Bonito na Serra da Bocaina, fronteira entre os estados brasileiros de São Paulo e Rio de Janeiro. O nome específico se refere ao formato do focinho parecido com tubarão, *shark-like snout* (Lutz, 1925). *Scinax squalirostris* pertence ao clado *Scinax ruber* (Faivovich et al., 2005; Wiens et al., 2010). O clado *S. ruber* é bem diversificado e possui uma taxonomia complexa, sendo que algumas espécies podem representar um complexo de espécies (Fouquet et al., 2007). Duellman e colaboradores (2016) realizaram um estudo filogenético e biogeográfico com hilídeos a fim de tentar compreender melhor a relação e a história evolutiva dessa linhagem. Utilizando 44% espécies de hilídeos formalmente descritas obteve um clado bem suportado onde *S. squalirostris* se encontra. Foi sugerida então a criação de uma

subfamília chamada Scinaxinae para abrigar este clado. Em análises para essa subfamília Duellman et al. (2016) obtiveram a formação de clados com suportes baixos, indicando que o clado *Scinax ruber* é uma das linhagens que necessitam de estudos adicionais com o intuito de compreender com maior refinamento suas relações de parentesco.

Esta espécie de perereca possui uma ampla distribuição geográfica, mas de forma disjunta. Ocorre na região meridional do continente sul-americano, incluindo o Centro-Oeste, Sudeste e Sul do Brasil, Sul do Paraguai, Uruguai, Norte da Argentina e região Leste da Bolívia (Brandão et al., 1997; Uetanabaro et al., 2007). Possui como habitat áreas abertas, ocorrendo em áreas denominada de Campos (Eterovick & Sazima, 2004; Cruz et al., 2009). *Scinax squalirostris* é considerada uma espécie fora de perigo de extinção (IUCN, 2018). No meio científico esta espécie é considerada um complexo de espécies crípticas (Eterovick & Sazima, 2004), possuindo variação acústica (Faria et al., 2013) e variações em relação ao tamanho e coloração (observação pessoal).

Esta tese será apresentada e composta em capítulos, sendo composta por 3 capítulos. O primeiro capítulo abrange a filogeografia e os processos associados à distribuição de *S. squalirostris*. Neste capítulo nós utilizamos uma abordagem filogeográfica, com simulações coalescentes e modelagem de paleodistribuição, para compreender a atual distribuição geográfica e a diversidade genética das populações de *Scinax squalirostris*, bem como quais os eventos geológicos e/ou climáticos podem ter moldado e afetado a distribuição geográfica e diversidade genética dessa espécie.

O segundo capítulo é um trabalho de delimitação de espécie, em que testamos a existência de mais de uma linhagem evolutiva sob o mesmo nome de *S. squalirostris*. Como a sua distribuição é dada de forma disjunta e dada a sua baixa capacidade de dispersão, é esperado que haja uma alta estruturação genética populacional, devido à restrição do fluxo gênico. Isso poderia ter levado as populações a se diversificarem, e apresentarem linhagens evolutivas distintas. Assim, nós utilizamos uma abordagem de taxonomia integrativa, utilizando dados moleculares juntamente com dados morfométricos para testar a existência de linhagens candidatas a espécie.

No terceiro capítulo, verificamos como as mudanças climáticas previstas para 2100 poderão afetar a distribuição das populações de *S. squalirostris* e se essa espécie estaria ameaçada sob esses eventos. Para isso, nós utilizamos simulações genéticas e

modelagem de nicho ecológico para tentar compreender como as mudanças climáticas futuras poderão afetar a diversidade genética e a distribuição das populações de *S. squalirostris*. Além disso, avaliamos se a diversidade genética atual é bem representada em Unidades de Conservação e se, devido às mudanças climáticas futuras, essa diversidade genética ainda será preservada.

## **OBJETIVO GERAL**

O objetivo desta tese foi investigar a origem da distribuição geográfica e da variação genética, história evolutiva e as relações filogenéticas de *Scinax squalirostris*.

## **OBJETIVOS ESPECÍFICOS**

1. Investigar a história demográfica e origem da distribuição disjunta de *Scinax squalirostris* e avaliar a dinâmica de dispersão ao longo do tempo.

2. Verificar a existência de mais de uma linhagem evolutivamente distinta nas populações analisadas de *Scinax squalirostris*.

3. Compreender se e como as mudanças climáticas futuras podem apresentar risco para a distribuição e diversidade genética de *Scinax squalirostris*.

4. Verificar como a riqueza genética atual está representada em Unidades de Conservação e prever o quanto essa diversidade genética ainda será representada no futuro.



# Capítulo 1

---

Capítulo elaborado conforme as normas da revista e para submissão:  
*Journal of Biogeography*

RESEARCH PAPER

*Journal of Biogeography*

**Inferring responses to Neogene-Quaternary climate dynamics from historical demography in a South American grassland treefrog**

Tatianne P. F. Abreu-Jardim<sup>1,2\*</sup> | Rafael F. Magalhães<sup>3</sup> | Natan M. Maciel<sup>2</sup> | Matheus Souza Lima-Ribeiro<sup>4</sup> | Guarino R. Colli<sup>5</sup> | Célio F. B. Haddad<sup>6</sup> | Rosane G. Collevatti<sup>1</sup>

\*Correspondence: Laboratório de Genética & Biodiversidade, Instituto de Ciências Biológicas, Universidade Federal de Goiás (UFG), Campus Samambaia, 74001-970, Goiânia, Goiás, Brazil. E-mail: tatibio1@gmail.com.

<sup>1</sup>Laboratório de Genética & Biodiversidade, Instituto de Ciências Biológicas, Universidade Federal de Goiás (UFG), Campus Samambaia, 74001-970, Goiânia, Goiás, Brazil.

<sup>2</sup>Laboratório de Herpetologia e Comportamento Animal, Departamento de Ecologia, Instituto de Ciências Biológicas, Universidade Federal de Goiás, Campus Samambaia, 74001-970, Goiânia, Goiás, Brazil.

<sup>3</sup>Departamento de Zoologia – Instituto de Ciências Biológicas, Universidade Federal de Minas Gerais, Belo Horizonte, Minas Gerais, Brasil.

<sup>4</sup>Laboratório de Macroecologia. Universidade Federal de Goiás (UFG). Campus Jataí. 75801-615. Jataí. Goiás. Brazil.

<sup>5</sup>Departamento de Zoologia, Instituto de Ciências Biológicas, Universidade de Brasília, 70910-900 Brasília, Distrito Federal, Brazil.

<sup>6</sup>Departamento de Zoologia, Instituto de Biociências, Universidade Estadual Paulista Júlio de Mesquita Filho, 13506-900 Rio Claro, São Paulo, Brazil.

**Short running title:** Phylogeography of the anura *Scinax squalirostris* (Anura, Hylidae)

**Number of words:** 7.149

**Data accessibility:** It will be deposited to GenBank and TreeBASE

### **Abstract**

**Aim:** Our goal was to reconstruct the demographic history of lineages of *Scinax squalirostris* and to understand the dispersal dynamics through the Neogene-Quaternary periods. Additionally, we aimed to investigate how the climatic cycles of these periods influenced its current geographical distribution and genetic diversity patterns.

**Location:** grasslands of Meridional South America

**Methods:** We sampled 219 individuals of *Scinax squalirostris* from 26 localities in Southern South America and applied a statistical phylogeography framework, integrating coalescent simulations, ecological niche modelling and reconstruction of spatio-temporal dynamics. The genetic data was based on polymorphisms with different mutation rates from two mitochondrial and one nuclear regions.

**Results:** *Scinax squalirostris* populations were genetically structured and are characterized by high genetic diversity. Coalescent tree and Bayesian clusters showed incomplete lineage sorting with geographically distant populations sharing haplotypes

and even ancestral. The ancestral location reconstruction placed the root in South of Brazil, and the dispersal events were mediated by the suitable climatic conditions occurring during Pliocene-Pleistocene transition. Paleodistribution modelling showed a large area of occurrence during the LGM, with contraction in the Holocene until present.

**Main conclusions:** Incomplete lineage sorting and common ancestry among *Scinax squalirostris* populations from Pampas, Chaco, Atlantic Forest and Cerrado biome are evidences of the past connection among these biomes, indicating that the current disjunct distribution is most likely due to the range contraction of a previous ancient and wider distribution in response to climatic dynamics in Quaternary.

**Keywords:** anuran, coalescent analysis, climatic changes, discrete phylogeography, divergence times, genetic diversity, Scinaxinae, *Scinax squalirostris*.

## 1 | INTRODUCTION

A mosaic of vegetations comprising forests, open vegetations (e.g. Cerrado, Caatinga and Pampas) and grasslands (Behling, 2002) cover the Southeastern of South America. South America grasslands are patchy and discontinuous vegetation (Overback *et al.*, 2007) composed by a mixture of wood, shrubland and herbaceous plants, occurring in areas of strong environmental seasonality, ranging their annual precipitation from 600 mm to 1.500 mm and average annual temperatures from -5°C to 20°C (Woodward *et al.*, 2004). Grasslands lie on tropical, subtropical and temperate regions where they may be exemplified, respectively, by *campo limpo*, *campo sujo*, and *campos rupestres* in Cerrado biome, *campos de altitude* in Atlantic Forest and *campos sulinos* (temperate grassland) in Pampas biome of Argentina, Uruguay and Southern of Brazil (Leite &

Klein, 1990; Overback *et al.*, 2007). Additionally, grasslands could be also found associated with forests resulting a mosaic of vegetation, such as Araucaria Forest mosaic in Southern Brazilian Atlantic Forest (Leite & Klein, 1990; Overback *et al.*, 2007).

Grasslands have been shaped along time by an ancient and complex history since Miocene geologic events (Behling 2002, Ortiz-Jaureguizar & Cladera, 2006). In Miocene-Late and Pliocene periods, the widely distributed "Paranean Sea" regressed allowing grasslands to occupy plains extending from North/Northern Patagonia to central and Northern Argentina and Uruguay (Ortiz-Jaureguizar & Cladera, 2006). Thereafter, during Late Pliocene, the climate became drier and cooler promoting further expansion of the open vegetations (Ortiz-Jaureguizar & Cladera, 2006). Also, during Pleistocene glacial period, temperature decreased from 5° to 7°C, allowing grassland distribution to expand toward North of South America (Behling, 2002; Ortiz-Jaureguizar & Cladera, 2006). In this period of grassland expansions, Atlantic Forest retracted its distribution and became restricted to coastal areas (Behling, 2002). However, as temperature increased and climate became humid during the interglacial period, grasslands retracted their distributions allowing forests to expand again over South America (Ortiz-Jaureguizar & Cladera, 2006; Overbeck, 2007). Consequently, grasslands have been fragmented and lost suitable areas since the end of the dry and cold climatic conditions of Pliocene and Pleistocene, resulting their current disjunct distribution (Behling 2002, Ortiz-Jaureguizar & Cladera, 2006).

As grasslands distribution have been shaped by cycles of expansion and contraction, and the species inhabiting at these habitats may have been evolutionarily pressured it to adapt or to track grasslands dynamics. There are still few phylogeographic studies concerning species inhabiting open vegetations and grasslands of South America (Turchetto-Zolet *et al.*, 2013), most of them restricted to South and

Southeastern Brazil (e.g. Langone *et al.*, 2015; Silva *et al.*, 2017). Species do not respond equally to climatic cycles, such as expanding their distribution ranges or losing genetic diversity (see Turchetto-Zolet *et al.*, 2013). For instance, *Calibrachoa heterophylla*, which occurs in Southern Brazil, had a retraction of its distribution during the colder periods, but expanded along interglacial periods, due to formation of new suitable areas in response to warmer temperatures (Mäder *et al.*, 2013). Also, Langone *et al.* (2015) showed that the amphibian species *Pseudopaludicola falcipes*, from Southern temperate grassland, also expanded its distribution along interglacial periods favouring gene flow among its populations. For other species, colder and drier periods favoured expansion and stability of their geographic ranges, but warmer periods caused range retraction (Cristiano *et al.*, 2016), resulting in different demographic and genetic effects, such as divergence and genetic structuration (e.g. Collevatti, *et al.*, 2009; Lorenz-Lenke *et al.*, 2010, Maia *et al.*, 2017 and Peçanha *et al.*, 2017). In addition, some geomorphological events in the Quaternary, exemplified by marine transgressions or coastal plain development, drove species diversification (Mäder *et al.*, 2013, Silva *et al.*, 2017).

Thus, species strictly associated to grasslands requires more studies to understand the evolutionary history of South America diversity, especially amphibians, one of the least studied groups (see Turchetto-Zolet *et al.*, 2013). *Scinax squalirostris* Lutz, 1925, is a small treefrog (23 to 28 mm) (Cei, 1980) widely distributed throughout of the Meridional South America region, from central, Southeastern and Southern Brazil, Northern Bolivia, Southern Paraguay, Uruguay to Northeastern Argentina (Brandão *et al.*, 1997; De la Riva *et al.*, 2000; Leite *et al.*, 2008; Frost, 2018). Although its geographic distribution is continuous over Pampas and humid Chaco, it is spatially disjoint in the Atlantic Forest and the Cerrado region, occurring in areas of high altitudes

(sky-islands), being found in grasslands, shrublands and swamps (Brandão *et al.*, 1997; Leite *et al.*, 2008; Cruz *et al.*, 2009).

In order to investigate the demographic history and the origin of the disjunct geographical distribution of *S. squalirostris*, a useful approach is coupling coalescent simulations and paleoclimatic simulations using ecological niche modelling (ENM) in a multi-model inference framework (e.g., Carstens & Richards, 2007; Knowles & Carstens, 2007; Collevatti *et al.*, 2013; 2015a). In addition, spatio-temporal lineage dispersal inferences (Lemey *et al.*, 2009; 2010) may also give clues on the climatic footprint on demographic history and spatial pattern of genetic diversity of current populations (see also Collevatti *et al.*, 2015b). Here, we reconstruct the demographic history and the dispersal dynamics of treefrog *S. squalirostris*, using an extensive sampling and DNA regions with different mutation rates to investigate how the Neogene and Quaternary events shaped the current spatial pattern of genetic diversity and geographical distribution. We hypothesized that the disjunct distribution of *S. squalirostris* is due to range contraction of a previously more distributed species, caused by changes in climatic conditions that affected suitable habitat distribution. In this scenario, we expect a larger distribution area of *S. squalirostris* in the colder periods and range contractions in the hotter periods, causing habitat fragmentation. As consequence, current populations would have high genetic differentiation, low or absence of gene flow and an old time of their most recent common ancestor (TRMCA).

## **2 | MATERIAL AND METHODS**

### **2.1 | Population sampling and genetic data**

We sampled in field and gathered from museum collection 228 individuals of *Scinax squalirostris* from 26 localities, throughout its geographical distributions in Brazil,

Uruguay and Paraguay (Figure 1; Appendix S1: Table S1.1 in Supporting Information). We amplified and sequenced two mitochondrial (mtDNA) fragments: 12S and cytochrome B (Cytb), and nuclear DNA (nDNA) recombination activation gene (RAG1). For details of primers, amplifications and sequencing conditions see Appendix S1: Tables S1.2-S1.4. Information about alignment, saturation test (see Supporting Information: Appendix S3: Figure S3.1) and recombination tests and treatment of heterozygous individuals (see Appendix S2 in Supporting Information).

## **2.2 | Genetic diversity and population structure**

To investigate genetic diversity and population structure, mtDNA and nDNA were analysed separately. We estimated the overall and population nucleotide ( $\pi$ ) and haplotype ( $h$ ) diversities using ARLEQUIN 3.11 (Excoffier *et al.*, 2005a). We performed a Bayesian clustering analysis to verify the genetic admixture among populations using BAPS 5.0 (Corander *et al.*, 2008). We also tested the hypothesis of population genetic differentiation using an analysis of molecular variance (AMOVA) implemented in ARLEQUIN 3.11. We tested for isolation-by-distance (IBD) and isolation-by-environment (IBE) using a Multiple Regression on Distance Matrices (MRM) (Lichstein, 2007). For the genetic distance matrix, we used pairwise genetic differentiation (Slatkin's linearized pairwise  $F_{ST}$ ). The geographic distance matrix was obtained from the logarithm of the geodesic distances between pair of populations. For environment analysis, we selected the five variables that explained the most of the variance among populations of *S. squalirostris* from 19 bioclimatic variables. We tested regression significance 10,000 permutations using the function 'mrm' implemented in the package 'ecodist' (Goslee & Urban, 2007) in R 3.3.1 (for details on the generation of environmental matrices and data processing see Appendix S2).

## 2.3 | Population demographic history

We performed all coalescent analysis with concatenated partitions of mitochondrial and nuclear DNA, but assigning different priors for each DNA fragments. The best-fit evolutionary model for each gene and their maximum likelihood parameters were selected using the corrected Akaike Information Criterion (AICc) implemented in JMODELTEST 2 (Darriba *et al.*, 2012) (Appendix S1: Table S1.5). For molecular dating we used mutation rates previously estimated for mitochondrial and nuclear fragments for molecular dating to anura amphibians (Appendix S1: Table S1.6) because of the lack of Scinaxinae fossils.

We estimated the population effective size ( $N_e$ ) using the demographic parameter  $\theta$ , calculated by Bayesian estimation implemented in LAMARC 2.1.10 (Kuhner, 2006). Analyses were run with 20 initial chains of 15,000 steps and three final chains of 80,000 steps. The initial and final chains were sampled every 100 steps. We performed two independent runs to assess convergence. Results for each region were combined with LOGCOMBINER and checked convergence and stationarity (Effective Sample Size,  $ESS \geq 200$ ) using TRACER 16 (Rambaut *et al.*, 2013). The effective population size was obtained using a generation time of one year, based on data for the related (Kluge, 1981) treefrog *Boana rosenbergi* (Boulenger, 1898). To understand changes in effective population size throughout time we performed an Extended Bayesian Skyline Plot (EBSP) analysis (Drummond *et al.*, 2005) using BEAST (Drummond *et al.*, 2013). We used the substitution models and mutation rates reported above (see Appendix S1: Table S1.5 and S1.6) and the relaxed molecular clock model (uncorrelated lognormal). Two independent analyses were run for 100 million generations, sampled every 2,300 generations. Convergence and stationarity ( $ESS \geq$

200) were checked using TRACER 1.6. We combined runs and trees after removing a 20% burn-in with LOGCOMBINER (Drummond *et al.*, 2013).

## **2.4 | Coalescent tree and Time of Most Recent Common Ancestor**

We run a Bayesian coalescent analysis implemented in BEAST (Drummond *et al.*, 2013) to infer a coalescent tree and estimate the time of the most recent common ancestor (TMRCA). For this analysis, we used 139 haplotypes obtained from concatenated mtDNA and nDNA regions (see results below). We defined *Scinax fuscomarginatus* as outgroup based on Duellman *et al.* (2016). We used an uncorrelated lognormal molecular clock and the same priors of EBSP analysis (see above). For tree prior we used Coalescent Constant model based on EBPS results (see below). MCMC conditions and number of runs were the same as EBSP analysis. Convergence and stationarity were assessed (ESS were  $\geq 200$ ) using TRACER 1.6. We combined runs and trees after removing a 20% burn-in with LOGCOMBINER (Drummond *et al.*, 2013) and the Maximum Clade Credibility (MCC) tree was obtained with TREEANNOTATOR (Drummond *et al.*, 2013). We also ran an empty alignment (sampling only from priors) to verify the sensitivity of results to the assumed priors. The analysis showed that parameters posterior distribution was different from those obtained from the empty alignment, indicating that our data is informative. BEAST analyses were performed in Cyberinfrastructure for Phylogenetic Research CIPRES 3.3 (Miller *et al.*, 2010).

## **2.5 | Lineage Dispersal**

To reconstruct the spatio-temporal history of lineage dispersal we used the relaxed random walk model (RRW, Lemey *et al.*, 2009, 2010) implemented in the software BEAST (Drummond *et al.*, 2013). We performed the analyses for both concatenated

mitochondrial and nuclear partitions with unlinked priors. The diffusion process parameters were searched by a Bayesian Stochastic Search Variable Selection (BSSVS). We set the same priors for sequence evolution as TMRCA analysis, Coalescent GMRF Bayesian Skyride Model (Minin *et al.*, 2008) for tree prior and CTMC rate reference (Ferreira & Suchard, 2008) for location state rate prior. We performed two independent runs of 80 million generations, sampled at every 8,000 steps. We checked the convergence and stationarity ( $ESS \geq 200$ ) using TRACER 1.6. We combined the runs and trees with LOGCOMBINER (Drummond *et al.*, 2013) considering a burn-in of 10% and obtained the MCC tree using TREEANNOTATOR (Drummond *et al.*, 2013). After that, we reconstructed the spatio-temporal diffusion using SPREAD 1.0.6 (Bielejec *et al.*, 2011). Transitions rates between localities were considered only for strong support, Bayes factors  $> 8.0$ .

## **2.6 | Paleodistribution modelling**

To model the present and past potential geographic distributions of *S. squalirostris* we obtained 257 occurrence records (Appendix S1: Table S1.7) from the online databases VerNet (Vertebrate Network, available at <http://portal.vertnet.org>), GBIF (Global Biodiversity Information Facility, available at <http://www.gbif.org/>) and SpeciesLink (<http://slink.cria.org.br/>). All records were examined for errors and we excluded duplicate or imprecise occurrences. We mapped the occurrences records in a grid of cells of  $0.5 \times 0.5^\circ$  (longitude x latitude) encompassing the Neotropics. The environmental climatic layers were derived from five Atmosphere-Ocean General Circulation Models (AOGCMs) (see Appendix S1: Table S1.8; and Appendix S2 for analysis details). We used five bioclimatic variables (annual mean temperature, mean diurnal range, isothermality (mean diurnal range/temperature annual range),

precipitation of wettest three months and precipitation of driest three months) selected by factorial analysis using Varimax rotation from the 19 bioclimatic variables (see Appendix S2 for details). The distribution of *S. squalirostris* was inferred for pre-industrial (representing current climate conditions), middle Holocene (6Ka) and Last Glacial Maximum (LGM, 21ka) using 12 algorithms (Appendix S1: Table S1.9). We obtain the consensus map for each time period estimating the average of frequencies for each cell across the 60 models taking into account the TSS values as weights. The historical refugium map was the combination of the predictive maps from all time periods and considered all grid cells with suitability values  $\geq 0.5$  in the three time periods as refugium (more details in Appendix S2).

## 2.7 | Demographical scenarios and simulations

To set the demographic hypothesis, we classified the 60 predictive ENM maps, following Collevatti *et al.* (2013b; 2015) and classified the predictive maps according to three general demographic scenarios (i) ‘Range Retraction’ (77 % of the maps), range size was larger at LGM than in present-day; (ii) ‘Range Expansion’ (8 % of the maps), range size was smaller at LGM than in present-day, and (iii) ‘Range Stability’ (15 % of the maps), constant range size through time. Furthermore, we also set *a priori* biogeographic hypothesis of ‘Multiple Refugia’ based on Ab’Saber (2000). This model predicts an expansion-retraction in vegetation, during glacial-interglacial periods, with heterogeneous vegetation responses, creating many refuges of different effective sizes.

We simulated the demographic scenarios using coalescent models implemented in DIYABC 2.0 (Cornuet *et al.*, 2014). The relative fits of these models were calculated using the Approximate Bayesian Computation (ABC) method (Excoffier *et al.*; 2005b). Each scenario simulation (Figure 2) included seven populations according to the clades

(A, B, C, D, E, F and G) recovered in coalescent tree estimates (see results below) and the coalescent events ( $t_d$ ,  $t_5$ ,  $t_4$ ,  $t_3$ ,  $t_2$ ). Population admixture was also simulated and changes of effective population size ( $N_e$ ) through time,  $N_0$  (present effective population size) and  $N_1$  (past effective population size), following the demographic scenarios derived from the ENMs. To model calibration, we used the demographic parameters estimated in LAMARC and the mutation rates and evolutionary models used in coalescent analyses (see above).

For each scenario, we considered the change of effective population size according to ENMs. For instance, for scenarios with range expansion we attributed effective population size increase. All seven groups had the same population size  $N_0$  and the  $N_1$  shift according to our theoretical expectation for each scenario (see Figure 2 for a visual representation of these scenarios). For the "Range Expansion" hypothesis (scenario 1 and 5), we considered  $N_0 = 10,000$  and  $N_1 = 1,000$ . The "Range Retraction" hypothesis (scenario 2 and 6) was simulated with  $N_0 = 10,000$  and  $N_1 = 100,000$  for all populations. In "Stability Range" hypothesis (scenario 3 and 7) we simulated the effective population size as unchanged over the time ( $N_0 = 10,000$  and  $N_1 = 10,000$ ). For the "Multiple Refuges" hypothesis (scenario 4 and 8) we set  $N_0 = 10,000$  for each population, then we draw random  $N_1$  values from a set compound by 0; 10; 100; 1,000; 10,000; 100,000  $N_e$ , which represents extinction, bottleneck, stable and expansion processes (Figure 2). Scenarios 5, 6, 7 and 8 (Figure 2) comprised simulations with lineage admixture event between clades E, F and G. We performed 600,000 simulations (for mtDNA and nDNA separately), and all scenarios were compared using direct approach, which is the relative proportion of each scenario in the simulated dataset closest to the observed data set, and with logistic approach, which is the logistic

regression of each scenario probability being the deviation between simulated summary statistics and observed (Cornuet, *et al.* 2008).

## 2.8 | Patterns in genetic diversity

We used quantile regressions (Cade & Noon, 2003) to analyse the relationships of climatic suitability and stability through time with haplotype ( $h$ ) and nucleotide ( $\pi$ ) diversities. We defined climate stability as the differences in ensembled suitabilities between: LGM to present-day, Holocene to present-day and LGM to Holocene. Besides that, we analysed whether historical changes in the geographical range of *S. squalirostris* generated a spatial pattern in haplotype ( $h$ ) and nucleotide ( $\pi$ ) diversities. Therefore, we obtained the distance between each analysed population in relation to centroid and edge of the historical refuge, and then we performed quantile regressions of haplotype ( $h$ ) and nucleotide ( $\pi$ ) diversities against this spatial distance. We also analysed the genetic diversity against the altitude. Quantile regression was run using the function 'rq' implemented in package 'quantreg' (Koenker, 2017) in R.

## 3 | RESULTS

### 3.1 | Genetic diversity and population structure

Populations of *Scinax squalirostris* had high haplotype ( $h_{\text{mtDNA}} = 0.97071$  and  $h_{\text{nDNA}} = 0.93695$ ) and nucleotide diversities ( $\pi_{\text{mtDNA}} = 0.021735$ ,  $\text{SD} = 0.010878$  and  $\pi_{\text{nDNA}} = 0.016684$ ,  $\text{SD} = 0.008720$ ) for both mtDNA and nDNA (Table 1; Appendix S3: Figure 3.2). We found 63 haplotypes in 589 bp of mtDNA (12S and CytB) and 73 haplotypes in 413 bp of nDNA (RAG-1) (Figure 1; Appendix S1: Table S1.10). Overall, the majority of mitochondrial and nuclear haplotypes were unique haplotypes, but 16 populations shared mitochondrial haplotypes and 15 shared nuclear haplotypes (Figure

1; Appendix S1: Table S1.10). The Bayesian clustering (BAPS) indicated an optimal partition of eight clusters for mtDNA and six clusters for nDNA (Figure 3). Populations of Central-Western Brazil (CGO and BDF) were grouped in the same clusters (Figure 3a: green clusters, 4 and 5 for mtDNA, and Figure 3b: light pink cluster, 5 for nDNA). Populations of Southeast Brazil were grouped in the same clusters (Figure 3a: blue clusters mtDNA and Figure 3b for nDNA: 1, 2, 3), populations of South Brazil were grouped for mtDNA in clusters 7 and 8 (Figure 3a: light and dark pink clusters), and South/Southeast for nDNA in clusters 6 (Figure 3b: dark pink cluster). Populations of *S. squalirostris* showed high genetic differentiation for both mtDNA and nDNA ( $F_{STmtDNA} = 0.937$ ;  $p < 0.001$  and  $F_{STnDNA} = 0.651$ ;  $p < 0.001$ ) (Appendix S1: Table S1.11). In general, there were not strong patterns of IBD and IBE on genetic differentiation in MRM analysis ( $R^2$ : mitochondrial 0.0536 ( $p=0.18$ ) and nuclear 0.0746 ( $p=0.06$ ); Appendix S1: Table S1.12).

### **3.2 | Demographic population history and Time of Most Recent Common Ancestor**

Coalescent analysis showed low values of mutation parameter  $\theta$  for all populations and overall population ( $\theta = 0.0447$ , Table 1). Overall effective population size  $N_e$  was 6,114.06 (95% CI = 5,026.30-7,259.35), but most populations had low  $N_e$  (Table 1). The EBSP showed constant population size through time (Appendix S3: Figure S3.3). The TMRCA for *S. squalirostris* lineages dated from the Miocene ~7.6 Ma (95% CI = 1.1-23.2), with the coalescence of two major lineages comprising the clades ((A, B), (C), D) and (E, (F, G)) (Figure 4). Lineages of *S. squalirostris* started to diverge ~5.0 Ma (95% CI = 0.8-15Ma). Major divergence events occurred in the Pliocene/Pleistocene transition (~2.9 Ma; 95% CI = 0.4-9Ma) (Figure 4a, b) and resulted in incomplete lineage sorting, with geographically distant populations sharing haplotypes and

common ancestors. Haplotypes of populations from Cerrado and Atlantic Forest and Pampas, composed the strongly supported Northern clade, dated from ~5.0 Ma (Figure 4a, b). The Southern clade, dated from ~4.7 Ma, was formed by haplotypes of Atlantic Forest and Pampas populations (SJRS, BRS, SFRS, ISC and URU) also, Humid Chaco and Cerrado (APY, EPY, BMS) (Figure 4a, b). The large overlap of the 95% HPD in these estimates suggests that the Northern and Southern clades may have diversified during the same period.

### **3.3 | Lineage Dispersal**

The phylogeographic reconstruction of lineage dispersal showed the most probable ancestral location for *S. squalirostris* lineages in the South Brazil (BSC) (Figure 5a; Appendix S3: Figure S3.4). Lineages dispersed during the Pliocene-Pleistocene transition (~4.5-0.6 Ma), and no dispersal event was observed during the LGM. Lineages started spreading at ~4.5 Ma (Figure 5a; Appendix S3: Figure S3.4) in three main routes: from population BSC towards populations in South (ISC, PPR, PGPR, ASC), West (BMS) and Southwest Brazil (CGO, ISP, SMG, SVMG, SRMG) (Figure 5a, b; Appendix S3: Figure S3.4). The most of dispersal events occurred in cooler periods (Figure 5c, d; Appendix S3: Figure S3.4). After ~2.9 Ma, lineages dispersed to multiple directions (Figure 5c-d; Appendix S3: Figure S3.4). The last dispersal events, which occurred during Middle Pleistocene (~0.6 Ma), revealed connections among populations in different clades (Figure 4 and 5; Appendix S3: Figure S3.4).

### **3.4 | Paleodistribution modelling**

The ENM modelling were well evaluated by *True Skill* statistics (TSS) and the Area under the Curve (AUC) (Appendix S1: Table S1.13). The hierarchical ANOVA showed

higher variance for time component (see Appendix S1: Table S1.14 and Appendix S3: Figure S3.5), meaning that the ENMs were able to detect the effects of climatic changes through time on the distribution dynamics of *S. squalirostris*. The ENM ensembles predicted that *S. squalirostris* had a wider potential distribution at the LGM (Figure 6b) than at the Holocene or present day (Figure 6c, d). The highest levels of suitability were restricted to South, East and Southeast Brazil and Southern Paraguay and North Argentina in LGM. During the mid-Holocene (Figure 6c) climatic suitability decreased in the Central-Western Brazil and increased in the Southeast, East and South Brazil and Uruguay, which was maintained until the present day (Figure 6d). The geographical range size decreased over time, being higher at LGM than present-day. The range shifts were higher between present-day and LGM than Holocene and present-day, indicating quasi-stability between the Holocene and present-day (Appendix S3: Figure S3.6). The climatic historical refugium extended from the East and the Southeast Atlantic Forest towards South Brazil, Uruguay and Argentina (Figure 6e).

### **3.5 | Demographical scenarios and simulations**

The direct approach showed a small variation among the different demographic scenarios for both partitions (Appendix S1: Table S1.15; Appendix S3: Figure S3.7). However, the logistic approach showed that the scenario “Range retraction” (scenario 6) with admixture among clades E, F and G, were the most likely hypothesis to predict the observed genetic parameters of *S. squalirostris* for mtDNA and nDNA.

### **3.6 | Spatial patterns in genetic diversity**

Overall, quantile regression did not showed effects of climate change on the genetic diversity of mitochondrial and nuclear data (see Appendix S3: Figures S3.8 - S3.12).

Only for populations at greater distances from the historic refugium had lower nuclear and mitochondrial nucleotide diversity (Figure S3.12f and S3.13f).

#### 4 | DISCUSSION

Our findings from paleodistribution modelling, phylogeographic analysis and coalescent simulations supported the hypothesis that the disjunct distribution of *S. squalirostris* is most likely due to of an ancient wider distribution. The high genetic differentiation and diversity currently found in *S. squalirostris* together with results of stable demography and incomplete lineage sorting reinforces that a more continuous population have once occurred through South/Southeast of South America in the past.

Our results of lineage dispersal reconstruction showed an origin of dispersion in the Southern Brazil with multiple dispersions in many directions over time toward Central-West and Southeastern Brazil. The initial dispersal events occurred in Pliocene, when the climate was warm and the forests were still widespread. Which may have restricted the dispersions to geographically nearest areas. Thus, with precipitation decrease and the beginning of climatic cycles in the Late Pliocene, the forest environments began to retract (Ortiz-Jaureguizar & Cladera, 2006), and dispersion of these lineages become more frequent from Southern Brazil towards many directions. The last dispersions routes dated ~ 600.000 ka, in a colder Pleistocene period. We also observed that in the colder periods the dispersal events reached areas more distant (Central-West and Southeastern) from the center of dispersal (Southern Brazil). Such dispersal routes have most likely occurred because suitable climatic conditions were available across a wide region during cooler phases, allowing spatial displacements, acting as main factor for the uninterrupted dispersion of the lineages. For other Pampean grassland amphibian species, *Pseudopaludicola falcipes*, showed an opposite pattern of

dispersal, which had its initial dispersion in ca. 1.46 Ma and was continuous along interglacial periods (Langone *et al.*, 2015), being favored by warm climate. However, this contrast dispersal pattern between *P. falcipes* and *S. squalirostris*, despite their similar distributions in the South region, suggests that the effects of climate change also depend on the biological characteristics of each species, as well as geographic characteristics and climate changes at each site (Hewitt, 2000). For *S. squalirostris*, the preference for colder climate was also corroborated by paleodistribution models. Our results showed a larger distribution area of *S. squalirostris* during the LGM, in agreement with the greater distribution of grasslands during the LGM, when the climate was cold and dry (Behling, 2002; 2007). The paleodistribution models also showed a decrease of suitable areas in West areas of predicted distribution and increase of suitable areas in East, from LGM to Holocene, which has been maintained until today. Indeed, simulations of demographic hypotheses showed "Range Retraction" (range size was larger at LGM than in present-day) as the most likely scenario among alternative hypotheses, and paleodistribution modelling has, in fact, more changes in suitability over time and geographic decline, especially in West areas, than gains of new areas. Several studies have shown that species associated with grasslands were favored by the colder and drier climate and had larger suitable areas during LGM (Lorenz-Lenke *et al.*, 2010; Maäder *et al.*, 2013 and Maia *et al.*, 2017).

Nucleotide and haplotype diversities found for *S. squalirostris* were high and similar to found for other South American species, 12S: *Pseudopaludicola falcipes*,  $\pi = 0.2119$  (Langone *et al.*, 2015); RAG-1: *Scinax eurydice*,  $h = 0.81$  and  $\pi = 0.0057$  (Menezes *et al.*, 2016); CytB: *Pithecopus megacephalus*,  $h = 0.94$  and  $\pi = 0.0054$  (Ramos *et al.*, 2017). High levels of genetic diversity within populations have been associated with high effective population sizes over long periods of time (Pabijan *et al.*,

2012). Like this, the high genetic diversity and low mutation parameter may be the consequence of long-term stability in the geographical range of *S. squalirostris*. In fact, coalescent analysis (EBSP) showed historical constant population size. Other studies with species associated with the open vegetations and grasslands of South America also found low effect of glacial dynamics on the demography and genetic diversity (e.g. Langone *et al.*, 2015; Cristiano *et al.*, 2016; Vitorino *et al.*, 2016). In addition, the spatial dynamics of climatically suitable areas through time did not affect or caused differences in genetic diversity. However, areas farthest from the predicted historical refugium showed lower genetic diversity, likely due to cycles of range expansion and retraction in glaciation and interglacial periods, what has been shown to cause loss of genetic diversity in peripheral areas (Excoffier, *et al.*, 2009). Moreover, the wide historical refugium may have maintained the most of genetic diversity through time.

*S. squalirostris* had high values of genetic differentiation, comparable to other anurans species such as *Leptodactylus fuscus* (Camargo *et al.*, 2006) and *Physalaemus cuvieri* (Conte *et al.*, 2014). Amphibians generally have low dispersion capacity, and consequently, amphibians' populations are expected to be genetically structured and show limited gene flow, which facilitates isolation (Vences and Wake, 2007). High genetic differentiation indicates low or lack of gene flow among current populations of *S. squalirostris*. In fact, there was no correlation between genetic differentiation and geographical distance or environmental isolation, which may result from a rupture of the gene flow, likely due to the range contraction in warmer periods, when climatically suitable habitats became less available. This range contraction may have led to disjunct formation of a widely distributed area. Other species of plants, rodents and lizards from grasslands and open areas of South America, also had their ranges conformed disjunctly due to climatic oscillations and leading to vicariance events, for instance *Lychnophora*

*ericoides* (Collevatti *et al.*, 2009), *Micrablepharus atticolus* (Santos *et al.*, 2014), *Tabebuia serratifolia* (Vitorino *et al.*, 2016), *Oxymycterus nasutus* (Peçanha *et al.*, 2017) and *Cereus hildmannianus* (Silva *et al.*, 2017). Furthermore, the absence of gene flow found for *S. squalirostris* may indicate that the incongruence between the coalescent tree of haplotypes and geography may be a consequence of incomplete lineage sorting, with populations geographically distant sharing a common ancestral. Populations from Pampas and Chaco, Atlantic Forest and Cerrado biomes were connected in the past as showed by their shared haplotypes and Bayesian clustering of populations. In fact, the areas currently designated by these biomes were occupied by grassland up to the Quaternary (Behling & Hooghiemstra, 2001; Behling, 2003; Carnaval & Moritz, 2008), facilitating the wide and continuous distribution of *S. squalirostris* ancestral during cold and dry Quaternary climate.

Our results also indicate an ancient origin of *S. squalirostris*, from ~ 7.6 Ma, with subsequent divergence into two large clades, Northern and Southern. Northern clade was formed by populations from Pampas, Atlantic Forest and Cerrado grasslands. Southern clades were composed mainly by populations from Pampas and Chaco. Nonetheless, most of *S. squalirostris* divergences occurred in the Pliocene-Pleistocene transition. This period is also associated to divergences between South and Southeast Brazil clades in a co-generic species *Scinax eurydice* (Menezes *et al.*, 2016) and *Cereus hildmannianus* (Silva *et al.*, 2017), what is explained by primary events of Quaternary climate fluctuations, and there is no relationship to LGM effects. In fact, most coalescence events of *S. squalirostris* occurred before the LGM (ca. 2.8- 1.2 Ma). We hypothesized that the climatic conditions for *S. squalirostris* were spatially restricted during these periods, causing a compartmentalization of regional grasslands. Besides, times of coalescent events are directly related to effective population size (Kingman,

1982), so populations with higher  $N_e$  values tend to present older coalescent times, which is in accordance with the results found for *S. squalirostris*. Thus, despite the expansion during glacial periods, indicated by the paleodistribution modelling, the coalescent tree indicates a regional ancient process of differentiation without latter secondary contact. This suggests an ancient process of incomplete lineage sorting, probably mediated by warmer cycles, shaping the population structure of *Scinax squalirostris*.

In conclusion, our results support that the current disjunct distribution of *S. squalirostris* is most likely due to the range contraction of an ancient wider distribution due to climatic dynamics in Quaternary indicated by high haplotype and nucleotide diversity, older coalescent times and an incomplete lineage sorting. Moreover, our results showed that the Southern Brazil was the region of routes of the lines of *S. squalirostris* and this distribution was more widely in cold and dry climate until LGM. These results reinforce that Pliocene-Pleistocene played a fundamental role through dynamics of expansion and retraction of South America grasslands, affecting the species associated with these habitats. In addition, our study provides further evidence that more studies should be done on grasslands-associated species, since these habitats show a different and complex evolutionary history.

## **ACKNOWLEDGEMENTS**

This work was supported by a grant from CNPq (project no. 475333/2011-0, 475333/2011-0) and CAPES/PROCAD (project no. 88881.068425/2014-01). TPF AJ received a fellowship from FAPEG (Fundação de Amparo à Pesquisa do Estado de Goiás, project n°. 201410267000553). The authors would like to thank TF Rangel for providing access to the computational platform Bioensembles, and E. Barreto and A.

Anjos for help us in generated the genetic data. We thank P. Cabral and A. Valencia-Zuleta for help in English editing and L. Jardim and N. Esther for help with some analyses. We are grateful to many people and their institutions that kindly collected, donated specimens, sent sample tissues and loan specimens. CNPq have continuously support NMM, GRC, CFBH and RGC with grants and fellowships, which we gratefully acknowledge.

## REFERENCES

- Ab'Saber, N. (2000) Spaces occupied by the expansion of dry climates in South America during the Quaternary ice ages. *Revista do Instituto Geológico*, 21, 71-78.
- Behling, H. & Hooghiemstra, H. (2001) Chap. 18 - Neotropical Savanna environments in space and time: Late Quaternary Interhemispheric Comparisons. A2 Markgraf, Vera BT interhemispheric climate linkages. Academic Press, San Diego, 307–323.
- Behling, H. (2002). South and Southeast Brazilian grasslands during Late Quaternary times: a synthesis. *Palaeogeography, Palaeoclimatology and Palaeoecology*, 177, 19-27.
- Behling, H. & Pillar, V. D. (2007) Late Quaternary vegetation, biodiversity and fire dynamics on the southern Brazilian highland and their implication for conservation and management of modern *Araucaria* forest and grassland ecosystems. *Philosophical Transactions of the Royal Society B: Biological Sciences*, 362, 243-251.
- Bielejec, F., Rambaut, A., Suchard, M. A. & P. Lemey. (2011) Spatial phylogenetic reconstruction of evolutionary dynamics. *Bioinformatics*, 27, 2910-2912.
- Brandão, R. A. Duar, B. A. & SEBBEN, A. (1997). Geographic Distribution. *Scinax squalirostris*. *Herpetological Reviews*, 28.
- Cade, B. S. & Noon, B. R. (2003) A gentle introduction to quantile regression for ecologists. *Frontiers in Ecology and the Environmental*, 1, 412-420.

- Carnaval, A. C. & Moritz, C. (2008) Historical climate modelling predicts patterns of current biodiversity in the Brazilian Atlantic forest. *Journal of Biogeography*, 35,1187-1201.
- Carstens, B. C. & Richards, C. L. (2007) Integrating coalescent and ecological niche modeling in comparative phylogeography. *Evolution*, 61, 1439-1454.
- Cei, J. M. (1980) Amphibians of Argentina. *Monitore Zoologico Italiano. Nuova Serie, Monographia*, 2, 1-609.
- Collevatti, R. G., Rabelo, S. G. & Vieira, R. F. (2009) Phylogeography and disjunct distribution in *Lychnophora ericoides* (Asteraceae), an endangered cerrado shrub species. *Annals of Botany*, 104, 655-664.
- Collevatti, R. G., L. C. Terribile, J. A. F. Diniz-Filho, & M. S. Lima-Ribeiro. (2015a) Multi-model inference in comparative phylogeography: an integrative approach based on multiple lines of evidence. *Frontiers in Genetics*, 6.
- Collevatti, R. G., L. C. Terribile, S. G. Rabelo, and M. S. Lima-Ribeiro. 2015b. Relaxed random walk model coupled with ecological niche modeling unravel the dispersal dynamics of a Neotropical savanna tree species in the deeper Quaternary. *Frontiers in Plant Science*, 6.
- Collevatti, R. G., Terribile, L. C., Oliveira, G., Lima-Ribeiro, M. S., Nabout, J. C., Rangel, T. F. & Diniz-Filho, J. A. F. (2013) Drawbacks to paleodistribution modeling: the case of South American seasonally dry forests. *Journal of Biogeography*, 40, 345-358.
- Collevatti, R. G., Terribile, L. C., Lima-Ribeiro, M. S., Nabout, J. C., Oliveira, G., Rangel, T. F., Rabelo, S. G. & Diniz-Filho, J.A.F. (2012) A coupled phylogeographical and species distribution modelling approach recovers the demographical history of a neotropical seasonally dry forest tree species. *Molecular Ecology*, 21, 5845-5863.
- Conte, M., Tarqueta, C. P., Zucchi, M. I, Souza, A. P. & Recco-Pimentel, S. M. (2014). Unraveling the variability and genetic structure of Barker frog *Physalaemus cuvieri* (Leiuperiane) populations from different regions of Brazil. *Genetics and Molecular Research*, 13, 8055-8065.
- Corander, J., Marttinen, P., Sirén, J. & Tang, J. (2008) Enhanced Bayesian modeling in BAPS software for learning genetic structures of populations. *BMC Bioinformatics*, 9, 539.

- Cornuet, J. M., Pudlo, P., Veyssier, J., Dehne-Garcia, A., Gautier, M., Leblois, R., Marin, J. M. & Estoup, A. (2014) DIYABC v2.0: a software to make approximate Bayesian computation inferences about population history using single nucleotide polymorphism, DNA sequence and microsatellite data. *Bioinformatics*, 30, 1187.
- Cornuet, J. M., Santos, F., Beaumont, M. A., Robert, C. P., Marin, J. M., Balding, D. J., Guillemaud, T. & Estoup, A. (2008) Inferring population history with DIYABC: a user-friendly approach to Approximate Bayesian Computations. *Bioinformatics*, 24, 2713-2719.
- Cristiano, M. P., Cledes, Cardoso, D., Fernandes-Salomão, T. M., Heinze, J. (2016) Integrating Paleodistribution Models and Phylogeography in the Grass-Cutting Ant *Acromyrmex striatus* (Hymenoptera: Formicidae) in Southern Lowlands of South America. *PLoS ONE*, 11, e0146734.
- Cruz, C. A.G., Feio, R. N., & Caramaschi, U. (2009) Anfíbio do Ibitipoca. Ed. Bicho do Mato. Belo Horizonte.
- Darriba, D., Taboada, G. L., Doallo, R. & Posada, D. (2012) JModelTest 2: more models, new heuristics and parallel computing. *Nature Methods*, 9, 772.
- De la Riva, I., Köhler, J., Lötters, S. & Reichle, S. (2000). Ten years of research on Bolivian amphibians: updated checklist, distribution, taxonomic problems, literature and iconography. *Revista Espanola de Herpetologia*, 14, 19-164.
- Drummond, A. J., Rambaut, A., Shapiro, B. & Pybus, O. G. (2005) Bayesian coalescent inference of past population dynamics from molecular sequences. *Molecular Biology and Evolution*, 22, 1185–1192.
- Drummond, A.J., Rambaut, A., Suchard, M.A. (2013) BEASTv1.8.0. Available at: <http://beast.bio.ed.ac.uk/>.
- Duellman, W. E., Marion, A. B. & Hedges, S. B. (2016) Phylogenetics classification and biogeography of the treefrogs (Amphibia: Anura: Arboranae). *Zootaxa* 4104, 001-109.
- Excoffier, L., Foll, M. & Petit, R. J. (2009) *Genetic consequences of range expansions*. *Annual Review in Ecology, Evolution and Systematics*, 40, 48-501.
- Excoffier, L., Estoup, A. & Cornuet, J. M. (2005b) Bayesian analysis of an admixture model with mutations and arbitrarily linked markers. *Genetics*, 169, 1727-1738.
- Excoffier, L., Laval, G. & Schneider, S. (2005a) Arlequin ver. 3.0: an integrated software package for population genetics data analysis. *Evolutionary Bioinformatics Online*, 1, 47-50.

- Ferreira, M. A. R. & Suchard, M. A. (2008) Bayesian analysis of elapsed times in continuous-time Markov chains. *Canadian Journal of Statistics*, 26, 355-368.
- Frost, D. R. (2018). Amphibian Species of the World: An Online Reference. Version 5.7. Electronic Database accessible at <http://research.amnh.org/herpetology/amphibia/index.html>. American Museum of Natural History, New York, USA.
- Goslee, S. C. & Urban, D. L. (2007) The ecodist package for dissimilarity-based analysis of ecological data. *Journal of Statistical Software*, 22, 1-19
- Hewitt G. (2000) The genetic legacy of the Quaternary ice ages. *Nature*, 405, 907–913.
- Kingman JFC. 1982. *The coalescent. Stochastic Process and their Applications*, 13, 235-248.
- Kluge, A. G. (1981) The life history, social organization, and parental behavior of *Hyla rosenbergi* Boulenger, a nest-building gladiator frog. *Miscellaneous Publications Museum of Zoology*, 160, 1-180.
- Knowles, L.L., Carstens, B.C. (2007) Delimiting species without monophyletic gene trees. *Systematic Biology* 56, 887-895.
- Koenker, R. (2017) quantreg: Quantile Regression. R package version 5.33.
- Kuhner, M. K. (2006). Lamarc 2.0: Maximum likelihood and Bayesian estimation of population parameters. *Bioinformatics*, 22, 768-770.
- Langone, J. A., Camargo, A. & de Sá, R. O. (2015). High genetic diversity but low population structure in the frog *Pseudopaludicola falcipes* (Hensel, 1867) (Amphibia, Anura) from the Pampas of South America. *Molecular Phylogenetic and Evolution*, 95, 137-151.
- Leite, F. S. F.; Juncá, F. A.; Eterovick, P. (2008.) Status do conhecimento, endemismo e conservação de anfíbios anuros da Cadeia do Espinhaço, Brasil. *Megadiversidade*, 4, 158-176
- Leite, P.F., & Klein R.M., 1990. Geografia do Brasil: Região Sul. In: IBGE (Ed.), Vegetação, vol. 2. Instituto Brasileira de Geografia e Estatística, 113-150.
- Lemey, P., Rambaut, A., Drummond, A. J. & Suchard, M. A. (2009) Bayesian Phylogeography Finds Its Roots. *PLoS Computational Biology*, 5, e1000520.
- Lemey, P., Rambaut, A., Welch, J. J. & Suchard, M. A. (2010) Phylogeography takes a relaxed random walk in continuous space and time. *Molecular Biology and Evolution*, 27,1877-1885.
- Lichstein, J. (2007) Multiple regression on distance matrices: A multivariate spatial analysis tool. *Plant Ecology*, 188, 117-131.

- Lorenz-Lemke, A. P., Togni, P. D., Mäder, G. R., Kriedt, A., Stehmann, J. R., Salzano, F. M., Bonatto, S. L. & Freitas, L. B. (2010) Diversification of plant species in a subtropical region of eastern South American highlands: a phylogeographic perspective on native *Petunia* (Solanaceae). *Molecular Ecology*, 19, 5240-5251.
- Mäder, G., Fregonezi, J. N., Lorenz-Lemke, A. P., Bonatto, S. L. & Freitas, L. B. (2013) Geological and climatic changes in quaternary shaped the evolutionary history of *Calibrachoa heterophylla*, an endemic South-Atlantic species of petunia. *BMC Evolutionary Biology*, 13, 178.
- Maia, F. R., Zwiener, V. P., Morokawa, R., Silva-Pereira, V. & Goldenberg, R. (2017) Phylogeography and ecological niche modelling uncover the evolutionary history of *Tibouchina hatschbachii* (Melastomataceae), a taxon restricted to the subtropical grasslands of South America. *Botanical Journal of the Linnean Society*, 183, 616-632.
- Menezes, L., Canedo, C., Batalha-Filho, H., Garda, A. A., Gehara, M. & Napoli, M. F. (2016) Multilocus phylogeography of the treefrog *Scinax eurydice* (Anura, Hylidae) reveals a Plio-Pleistocene diversification in the Atlantic Forest. *PLoS ONE*, 11, e0154626.
- Miller, M.A., Schwartz, T., Pickett, B. E., et al. (2015) A RESTful API for Access to Phylogenetic Tools via the CIPRES Science Gateway. *Evolutionary Bioinformatics*, 11, 43-48.
- Minin, V. N., Bloomquist, E. W. & Suchard, M. A. (2008) Smooth Skyride through a Rough Skyline: Bayesian Coalescent-Based Inference of Populations Dynamics. *Molecular Biology and Evolution*, 25, 1459-1471.
- Ortiz-Jaureguizar, E. & Cladera, G. A. (2006) Paleoenvironmental evolution of Southern South America during the Cenozoic. *Journal of Arid Environments*, 66, 498-532.
- Overbeck, G. E.; Müller, S. C.; Fidelis, A.; Pfadenhauer, J.; Pillar, V. D.; Blanco, C. C.; Boldrini, I. I.; Both, R. & Forneck, E. D. (2007) Brazil's neglected biome: The South Brazilian Campos. *Perspectives in Plant Ecology, Evolution and Systematics*, 9, 101-116.
- Pabijan, M., Wollenberg, K.C. & Vences, M. (2012) Small body size increases the regional differentiation of populations of tropical mantellid frogs (Anura: Mantellidae). *Journal of Evolutionary Biology*, 25, 2310–2324.

- Peçanha, W. T., Althoff, S. L., Galiano, D., Quintela, F.M., Maestri, R., Gonçalves, G. L., et al. (2017) Pleistocene climatic oscillations in Neotropical open areas: Refuge isolation in the rodent *Oxymycterus nasutus* endemic to grasslands. *PLoS ONE*, 12, e0187329.
- Rambaut, A., Suchard, M.A., Xie, W., Drummond, A.J. (2013) TRACER v1.6. Available at: <http://tree.bio.ed.ac.uk/software/tracer>.
- Ramos, E. K., Magalhães, R. F., Sari, E. H. R., Rosa, A. H. B., Garcia, P. C. A. & Santos, F. R. S. (2017) Population genetics and distribution data reveal conservation concerns to the sky island endemic *Pithecopus megacephalus* (Anura, Phyllomedusidae). *Conservation Genetics*, 19, 99-110.
- Santos, M. G., Nogueira, C., Giugliano, L. G. & Colli, G. R. (2014) Landscape evolution and phylogeography of *Micrablepharus atticolus* (Squamata, Gymnophthalmidae), an endemic lizard of the Brazilian Cerrado. *Journal of Biogeography*, 41, 1506-1519.
- Silva, G. A. R., Antonelli, A., Lendel, A., Moraes, E. M., Manfrin, M. H. (2017) The impact of early Quaternary climate change on the diversification and population dynamics of a South American cactus species. *Journal of Biogeography*, 1-13.
- Turchetto-Zolet, A. C., Pinheiro, F., Salgueiro, F. & Palma-Silva, C. (2013) Phylogeographical patterns shed light on evolutionary process in South America. *Molecular Ecology*, 22, 1193-1213.
- Vences, M., Wake, D. (2007) Speciation, species boundaries and phylogeography of amphibians. In: Heatwole, H. (Ed.), *Amphibian Biology*, vol. 7. Surrey Beatty and Sons, Chipping Norton, pp. 2613–2671.
- Vitorino, L. C., Lima-Ribeiro, M. S., Terribile, L. C. & Collevatti, R. G. (2017) Demographical history and palaeodistribution modelling show range shift towards Amazon Basin for a Neotropical tree species in the LGM. *BMC Evolutionary Biology*, 16-213.
- Woodward, F. I., Lomas, M. R. & Kelly, C. K. (2004) Global climate and the distribution of plant biomes. *Philosophical Transactions of the Royal Society B*, 359, 1465-1476.

## **BIOSKETCH**

The authors work with bridging macroecology and population genetics, with particular emphasis on phylogeography and geographical patterns of genetic diversity in Neotropical species.

**Author contributions:** R.G.C., N. M. M., R. F. M., M. S. L. R., G. R. C., C. F. B. H. and T. P. F. A. J. conceived the overall study; R. F. M and T. P. F. A. J. generated the genetic data; T. P. F. A. J. performed the phylogeographical analyses; M. S. L. R. and T. P. F. A. J. performed niche modelling analyses. T. P. F. A. J., R.G.C. and N. M. M wrote the manuscript.

## **SUPPORTING INFORMATION**

Additional Supporting information may be found in the online version of this article:

**Appendix S1** Supplementary tables (Tables S1.1 - S1.15) with sampling locations, details of genetic sampling, mutation rates, haplotype information, details of ecological niche modelling, AMOVA and demography simulations probabilities.

**Appendix S2** Supplementary additional information of details of Material and Methods.

**Appendix S3** Supplementary figures (Figures S3.1 - S3.13) with details of saturation analysis, details of sampled, Bayesian Analysis of Population Structure, EBSP, location diffusion tree, details of ecological niche modelling, details of demography simulations and quantile regressions.

**Conflict of Interest Statement** The authors declare no conflict of interest.

**TABLE 1** Genetic diversity and demographic parameters of *Scinax squaleirostris* populations. N – sample size,  $k$  - number of haplotypes,  $h$  – haplotype diversity,  $\pi$  - nucleotide diversity and standard deviation (s.d.),  $\theta$  – coalescent parameter and 95% CI,  $Ne$  – effective population size and 95% CI. See Table S1 for population names.

Population Code	mtDNA				nDNA				mtDNA+nDNA			
	N	$h$	$\pi$ (s.d.)	$nh$	N	$h$	$\pi$ (s.d.)	$nh$	$\theta$	$\theta$ -95% CIi-CIs	$Ne$	$Ne$ -95% CIi-CIs
ISP	5	0.4000	0.000000 ± 0.000000	2	5	0.4000	0.009685 ± 0.006791	2	0.000677	0.00002 - 0.00331	92.50282	2.76005 - 452.53963
BSP	12	0.9091	0.000540 ± 0.000663	8	11	0.7091	0.009509 ± 0.005820	4	0.000194	0.00009 - 0.00092	26.50745	12.61153 - 125.84209
SRMG	11	0.7455	0.003118 ± 0.002184	4	12	0.3182	0.000000 ± 0.000000	1	0.000394	0.00005 - 0.00099	53.83473	6.94112 - 135.81654
OMG	16	0.6833	0.002221 ± 0.001637	5	16	0.1250	0.002421 ± 0.001926	2	0.000694	0.00009 - 0.00164	94.82564	13.51197 - 224.35690
CMG	3	0.0000	0.000000 ± 0.000000	1	3	1.0000	0.006457 ± 0.005795	3	-	-	-	-
PMG	1	0.0000	0.000000 ± 0.000000	1	-	-	-	-	-	-	-	-
SMG	16	0.8167	0.001042 ± 0.000975	7	16	0.6667	0.001957 ± 0.001663	5	0.001309	0.00054 - 0.00307	178.85700	74.87672 - 419.74690
SVMG	22	0.5628	0.000154 ± 0.000319	5	21	0.7333	0.003517 ± 0.002483	8	0.000838	0.00040 - 0.00154	114.50127	55.74763 - 210.69327
SCMG	13	0.4615	0.000000 ± 0.000000	2	12	0.5758	0.000734 ± 0.000919	3	0.000315	0.00001 - 0.00077	43.04045	2.66440 - 106.30309
CGO	24	0.5833	0.001556 ± 0.001243	5	23	0.2451	0.000613 ± 0.000794	3	0.000387	0.00011 - 0.0010	52.87827	15.43990 - 146.20090
BDF	19	0.6433	0.000318 ± 0.000474	4	18	0.1111	0.000000 ± 0.000000	1	0.000157	0.00002 - 0.00055	21.45191	2.82837 - 75.96981
BMS	7	0.8571	0.003881 ± 0.002762	3	7	0.9048	0.011991 ± 0.007602	5	0.006335	0.00239 - 0.02047	865.59136	327.51736 - 2797.49290
ISC	26	0.8492	0.000846 ± 0.000831	12	24	0.9565	0.008861 ± 0.005180	18	0.004665	0.00430 - 0.00920	637.40864	588.08290 - 1257.7377
SJRS	10	0.4667	0.000000 ± 0.000000	2	10	1.0000	0.007802 ± 0.004968	10	0.007237	0.00505 - 0.00814	988.83736	690.97009 - 1112.62990
SFRS	2	1.0000	0.052632 ± 0.053474	2	2	1.0000	0.019370 ± 0.02054	2	-	-	-	-
BRS	1	0.0000	0.000000 ± 0.000000	1	1	0.0000	0.000000 ± 0.000000	1	-	-	-	-
PPR	2	1.0000	0.000000 ± 0.000000	2	2	1.0000	0.014528 ± 0.015692	2	-	-	-	-
PGPR	8	0.6071	0.000000 ± 0.000000	3	8	0.8929	0.010896 ± 0.006829	6	0.001567	0.000673 - 0.00326	214.10918	91.95627 - 445.84445
CBSC	1	0.0000	0.000000 ± 0.000000	1	1	0.0000	0.000000 ± 0.000000	1	-	-	-	-
CNSC	2	0.0000	0.000000 ± 0.000000	1	2	1.0000	0.009685 ± 0.010828	2	-	-	-	-
BSC	5	0.4000	0.000000 ± 0.000000	2	5	1.0000	0.013075 ± 0.008861	5	0.000525	0.001482 - 0.21940	71.74775	202.49509 - 29978.56472
CSC	3	0.0000	0.000000 ± 0.000000	2	2	1.0000	0.014528 ± 0.015692	2	-	-	-	-

ASC	1	0.0000	0.000000 ± 0.000000	2	2	1.0000	0.016949 ± 0.018119	2	-	-	-	-
EPY	1	0.0000	0.000000 ± 0.000000	1	1	0.0000	0.000000 ± 0.000000	1	-	-	-	-
APY	7	0.2857	0.000000 ± 0.000000	2	4	1.0000	0.008071 ± 0.006213	3	0.002072	0.000397 - 0.00880	283.11055	54.24463 - 1202.400000
URU	1	0.0000	0.000000 ± 0.000000	1	1	0.0000	0.000000 ± 0.000000	1	-	-	-	-
										0.036786 -		
Overall	219	0.9686	0.017793 ± 0.009009	69	209	0.9333	0.013087 ± 0.007007	73	0.044747	0.053129	6114.06736	5026.30527 - 7259.35336

## Figures Labels

**FIGURE 1.** Geographical distribution of the 26 *Scinax squalirostris* populations sampled and haplotypes for (a) concatenated mitochondrial and (b) nuclear sequence data. Different colours were assigned for each haplotype following the legends. The size of the circle represents the sample size in each population and the circle sections represent the haplotype frequency in each sampled population.

**FIGURE 2.** Demographical and biogeographical scenarios considered in ABC analyses for *Scinax squalirostris* populations. Each scenario simulation included seven populations according to the clades (1: clade A, 2: clade B, 3: clade C, 4: clade D, 5: clade E, 6: clade F and 7 clades: G) and the coalescent events (td, t5, t4, t3, t2) recovered in coalescent tree estimates (Figure 4). The admixture of populations was simulated between populations of Pampas/Chaco and Atlantic Forest. Changes of effective population size ( $N_e$ ) were simulated through time ( $N_0$  present-day and  $N_1$ -Pleistocene period), following the demographic scenarios derived from the ENMs.

**FIGURE 3.** Bayesian clustering of populations of *Scinax squalirostris* obtained from the (a) concatenated mitochondrial and (b) nuclear sequence data. Different colours were assigned to different clusters following the figure legends. The bar plot represents the clusters populations ( $k= 8$  for mitochondrial data and  $k= 6$  for nuclear). For details on population codes and localities see Table S1.1 in Appendix S1.

**FIGURE 4.** Time for the most recent common ancestor of *Scinax squalirostris* haplotypes. (a) Coalescent tree. The blue bars correspond to the credibility interval at 95% of the average time for the common ancestor. The numbers below the branches correspond to the support of the node (posteriori probabilities) and the numbers above the branches represent the node age. The scale is in millions of years (Ma) before present. For details on population codes and localities see Table S1.1 in Appendix S1. (b) Geographical distribution of seven clades showed in coalescent tree across Humid Chaco, Pampas, Atlantic Forest and Cerrado. Colors represent each clade according legend.

**FIGURE 5.** Spatio-temporal dynamics of lineage diffusion among the 26 populations of *Scinax squalirostris*. Arrows between locations represent branches in the tree along which the relevant location transition occurs. Grey area represents the historical refugium for *S. squalirostris*, predicted using palaeodistribution models. The  $\delta^{18}$  curve corresponds to the composite benthic stable oxygen isotope ratios (Lisiecki & Raymo, 2005). For details on population codes and localities see Table S1.1 in Appendix S1.

**FIGURE 6.** Maps of consensus expressing the ensemble climatic suitability for *Scinax squalirostris*, based on paleodistribution modelling. (a) Occurrence records of *Scinax squalirostris*, used to generate the paleodistribution models. Potential distribution across the Neotropics during the (b) Last Glacial Maximum (LGM – 21ka), (c) mid-Holocene (6 ka), (d) present-day and (e) Historical refugium predicted in ecological niche modeling analysis.

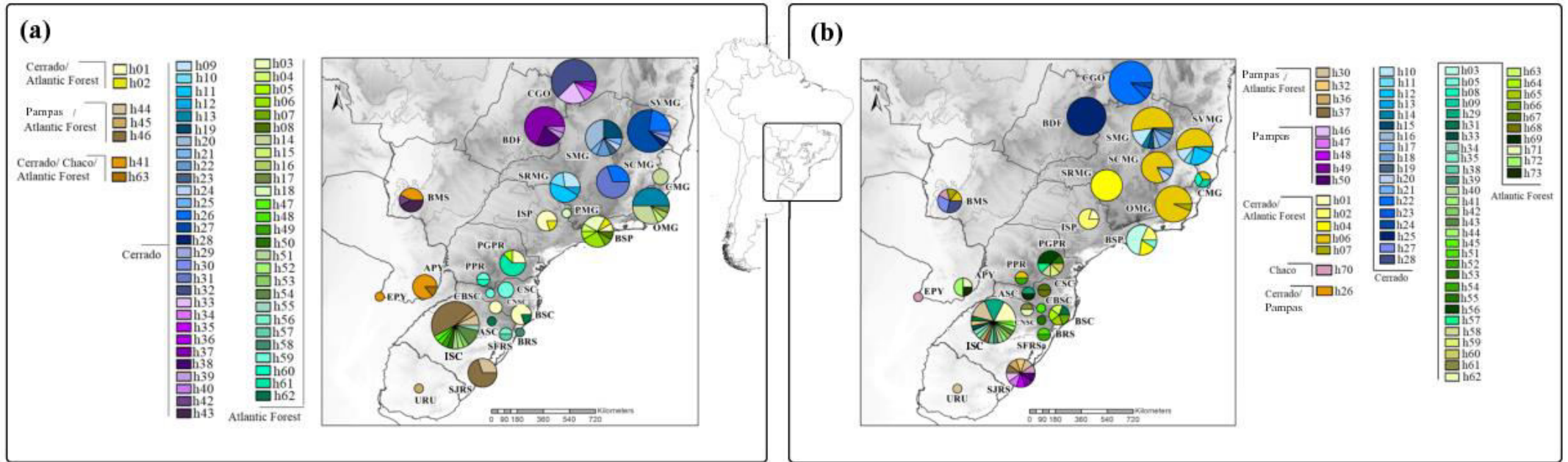


Figure 1

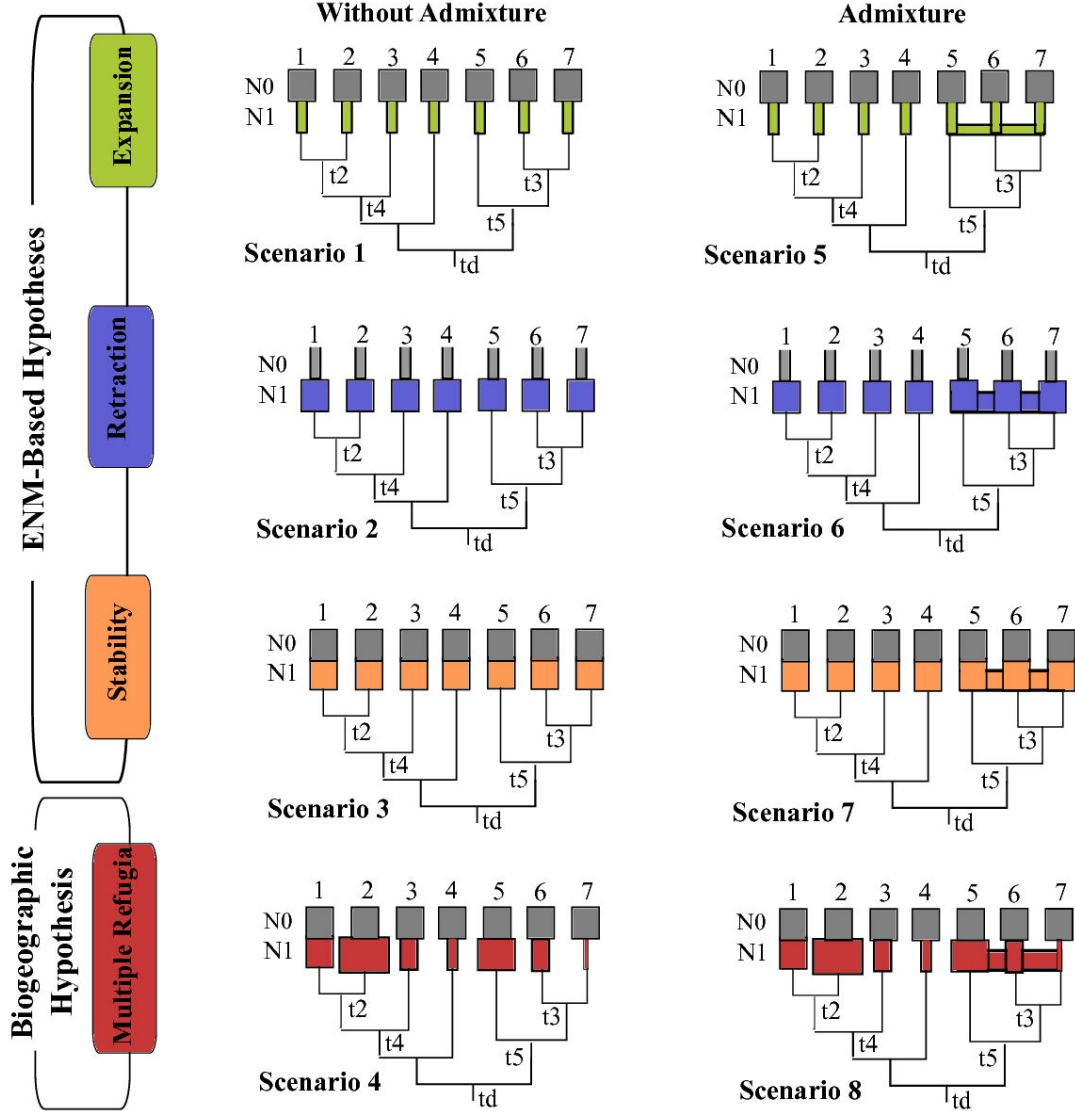


Figure 2

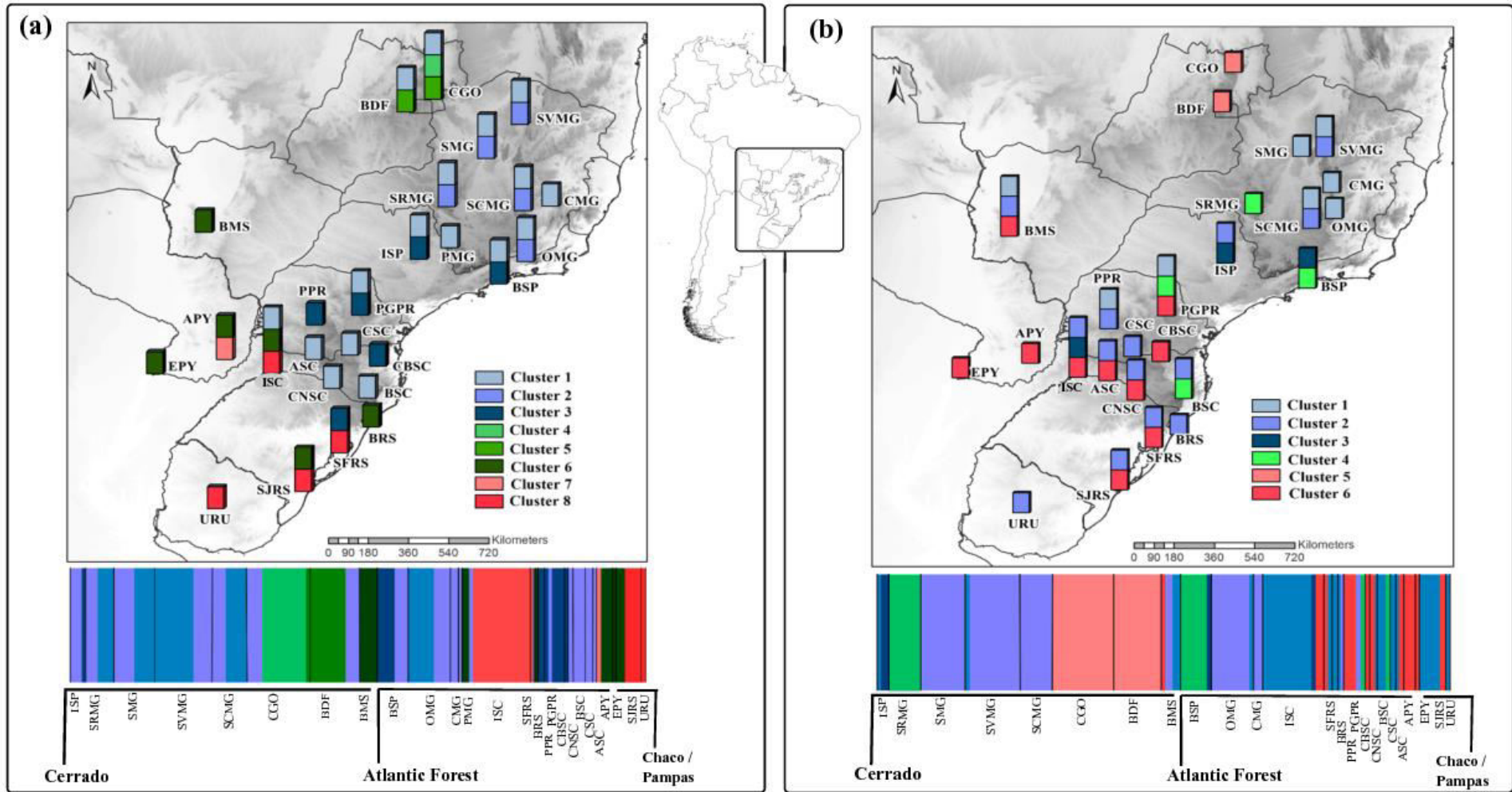
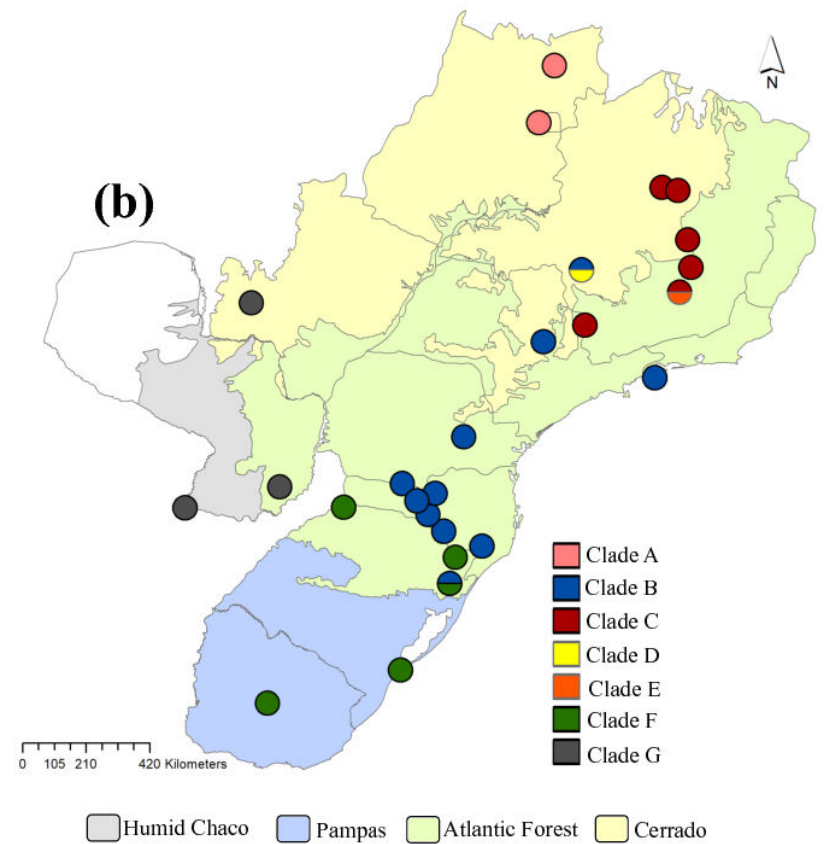
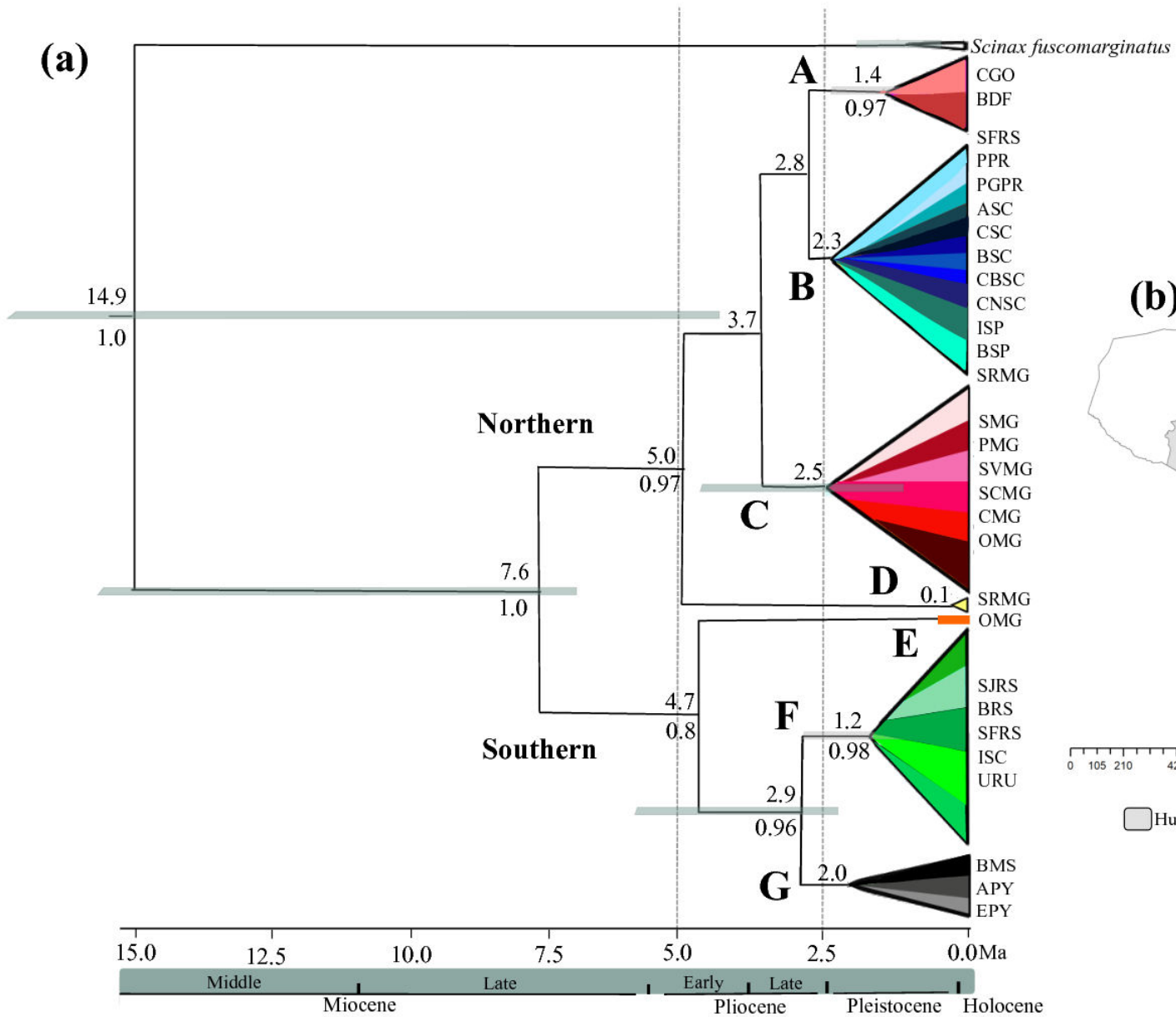
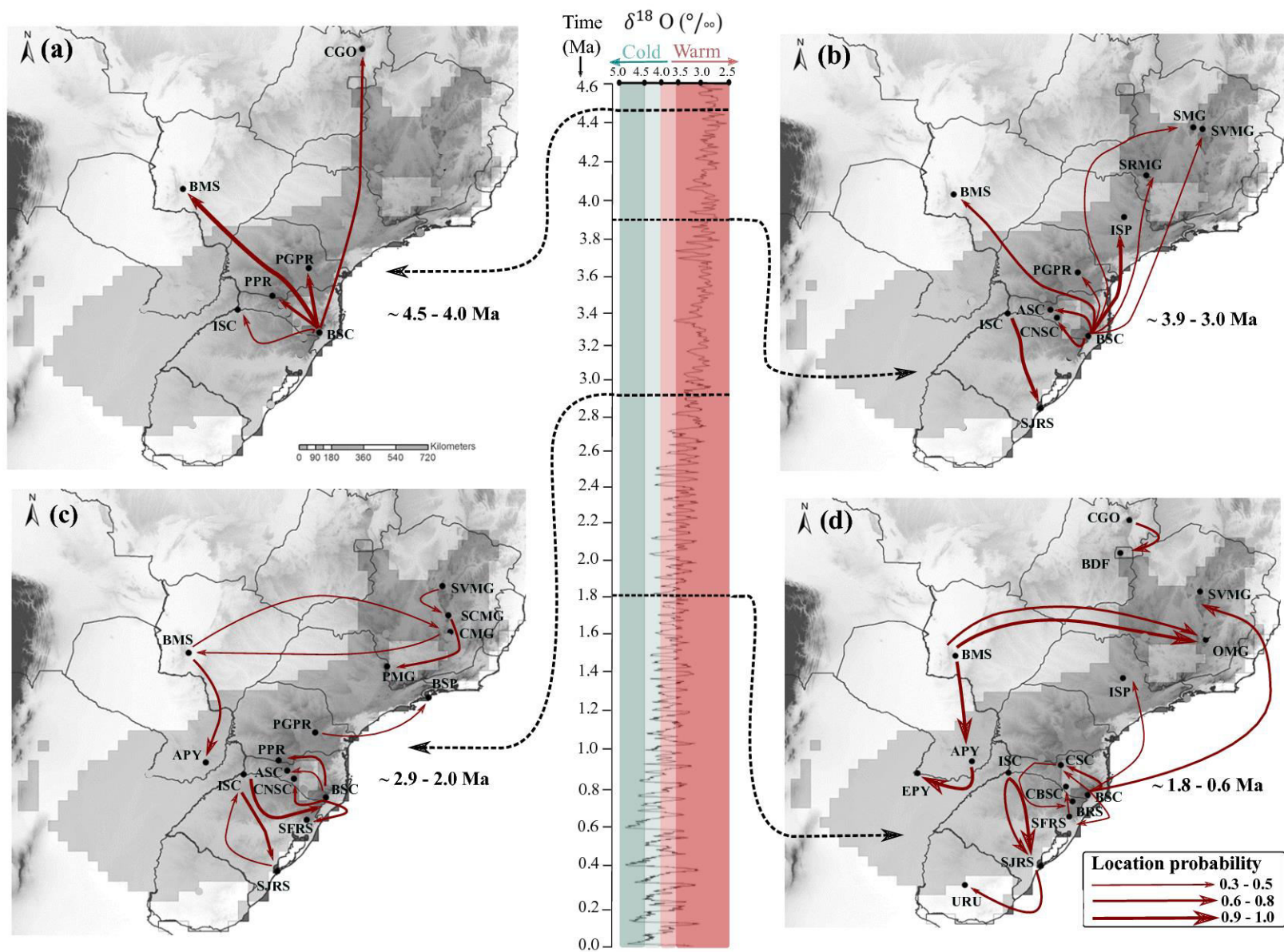
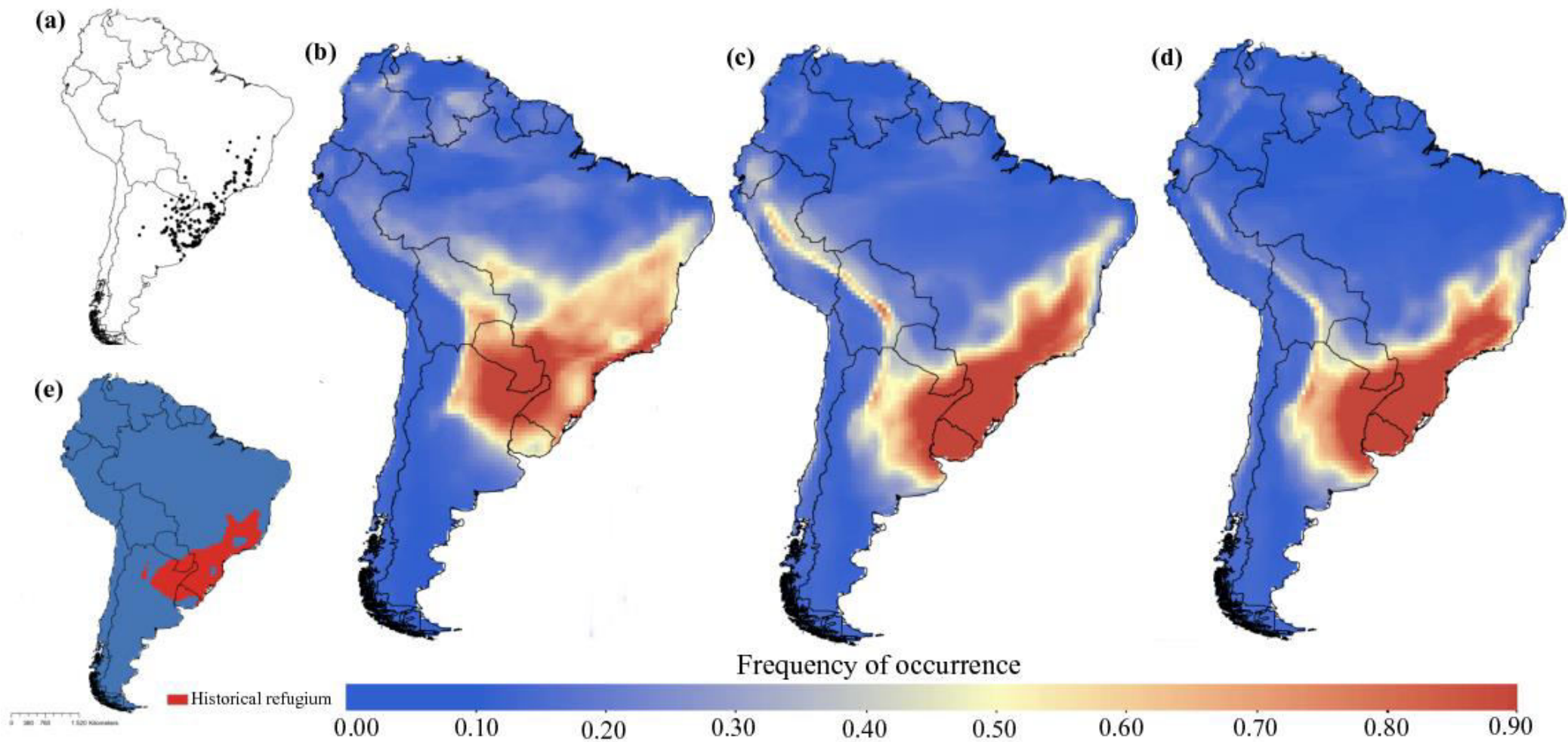


Figure 3







**SUPPORTING INFORMATION**

**Inferring responses to Neogene-Quaternary climate dynamics from historical demography in a South American grassland treefrog**

Tatianne P. F. Abreu-Jardim | Rafael F. Magalhães | Natan M. Maciel | Matheus Souza

Lima-Ribeiro | Guarino R. Colli | Célio F. B. Haddad and Rosane G. Collevatti.

**Appendix S1** Supplementary tables (Tables S1.1- S1.15) analyses details: with sampling locations, details of genetic sampling, mutation rates, haplotype information, details of ecological niche modelling, AMOVA and demography simulations probabilities.

**Table S1.1** Sampling locations of the 26 populations of *Scinax squalirostris*. Name of localities in the Population column we presented the abbreviation of Brazilian states and a Paraguayan department. Collection column we presented the abbreviation of donor institutions. (Amphibian Collection Célio F. B. Haddad (CFBH), Collection of the Universidade Federal de Minas Gerais (UFMG), Zoological Collection of the Universidade Federal de Goiás (ZUFG), Collection Elaine Maria Lucas Gonsales (EMLG), Museum of Ciências e Tecnologia da PUCRS (MCT), Collection of the Universidade Federal do Rio Grande do Sul (UFRGS), Herpetology Collection of the Instituto de Investigación Biológica del Paraguay (IIBPH).

<b>Population</b>	<b>Population Code</b>	<b>Collection</b>	<b>Latitude</b>	<b>Longitude</b>
Itirapina-SP	ISP	CFBH	-22.2744	-47.7958
PARNA Bocaina-SP	BSP	CFBH	-23.3458	-44.4825
São Roque de Minas-MG	SRMG	CFBH	-20.1461	-46.6628
Ouro Preto-MG	OMG	CFBH	-20.2875	-43.5081
Catas Altas-MG	CMG	UFMG	-20.0747	-43.4075
Poços de Caldas-MG	PMG	UFMG	-21.7878	-46.5614
Serra do Cabral-MG	SMG	LOD	-17.6992	-44.2714
PARNA Sempre Vivas-MG	SVMG	ZUFG	-17.7883	-43.7977
PARNA Serra do Cipó-MG	SCMG	ZUFG	-19.2469	-43.5100
PARNA Chapada dos Veadeiros-GO	CGO	ZUFG	-14.0833	-47.4667
Brasília-DF	BDF	ZUFG	-15.7797	-47.9297
Bonito-MS	BMS	ZUFG	-21.1211	-56.4819
Itaparinga-SC	ISC	CFBH	-27.1833	-53.7333
São José do Norte-RS	SJRS	UFRGS	-32.0147	-52.0417
São Francisco de Paula-RS	SFRS	MCP	-29.4481	-50.5836
Bom Jesus-RS	BRS	CFBH	-28.6678	-50.4167
Palmas-PR	PPR	ZUFG	-26.4842	-51.9906
Ponta Grossa-PR	PGPR	ZUFG	-25.095	-50.1619
Campo Belo do Sul-SC	CBSC	MCP	-27.8992	-50.7608
Campos Novos-SC	CNSC	CFBH	-27.4017	-51.2250
Bom Jardim da Serra-SC	BSC	CFBH	-28.3369	-49.6247
Caçador-SC	CSC	EMLG	-26.7753	-51.0150
Água Doce-SC	ASC	EMLG	-26.9978	-51.5561
Estancia San José-Ñeembucú-Py	EPY	IIBPH	-27.2016	-58.4486
Alto Vera, Yataí-Itapuá-Py	APY	IIBPH	-26.5833	-55.6333
Uruguai	URU	-	-33.0000	-56.0000

**Table S1.2** PCR Primers used to sequence CytB, 12S and RAG-1 genes used in this study. Nucleotide sequence based primers: 12Sa-12Sb; Reeder, 1995, MVZ15L - Moritz *et al.*, 1992 and H15149 – Kocher *et al.*, 1989, Heinicke *et al.*, 2007.

Gene region	Primer	Direction	Nucleotide Sequence (5'-3')
CytB	MVZ15	forward	GAACTAATGGCCCACACWWTACGNAA
	H1415 (cyt-b2) (H15149)	reverse	AAACTGCAGCCCCTCAGAATGATATTTGTCCTCA
12S	12S	forward	AAACTGGGATTAGATACCCCACTAT
	12S	reverse	GAGGGTGACGGGCGGTGTGT
RAG	RAG1	forward	ATGCATCRAAAATTCARCAAT
	RAG1	reverse	CCYCCTTTRTTGATAKGGWCATA

**Table S1.3** PCR mix components and quantities for each of the amplified fragments used in this study.

Reagent	Cytb, 12S and RAG-1
Deionized water	8.5 $\mu$ L
DNA	2.0 $\mu$ L
Forward primer (2mM)	3.0 $\mu$ L
Reverse primer (2mM)	3.0 $\mu$ L
Buffer 1X*	2.0 $\mu$ L
DNTPs (2,5 mM)	1.2 $\mu$ L
Taq polymerase (5u/ $\mu$ L)	0.3 $\mu$ L
Total volume	20 $\mu$ L

\*Buffer 1X (10 mM Tris-HCl, pH 8.3, 50 mM KCl, 1.5 mM MgCl<sub>2</sub>)

**Table S1.4** PCR thermal program for each of the amplified fragments used in this study.

Gene region	Initial heating	Desnaturation	Annealing	Extension	Final extension
	<b>35 cycles</b>				
CytB	2 min at 94°C	60 sec at 94°C	60 sec at 56°C	90 sec at 72°C	6 min at 72°C
12S	2 min at 94°C	60 sec at 94°C	60 sec at 54°C	90 sec at 72°C	6 min at 72°C
RAG	2 min at 94°C	60 sec at 94°C	60 sec at 58°C	90 sec at 72°C	6 min at 72°C

**Table S1.5** Parameters of selected models for fragments used in this study.

Datasets	Cytb	12S	RAG-1
Model	K80+I	K80+G	JC
p-inv	0.8790	-	-
Kappa	17.7938	5.4465	
gamma shape	-	0.1200	-
Nst	2	2	1
Ncat	-	4	-

**Table S1.6** Mutation rates for each DNA region used in coalescent analyses.

	Mutation rate region (subs./millions of years)	Reference
	Mean -SD	
12S	0.0026 - 0.0001	Evans <i>et al.</i> , 2004
CytB	0.0069 - 0.0010	Macey <i>et al.</i> , 1998
RAG	0.0015 - 0.0001	Heinicke <i>et al.</i> , 2007

**Table S1.7** Geographical coordinates of 257 occurrence records of *Scinax squalirostris* used in ecological niche modelling.

longitude	latitude	longitude	latitude	longitude	latitude
-54.80	-34.70	-55.67	-26.83	-50.42	-28.67
-56.46	-34.75	-56.17	-27.23	-51.23	-27.40
-54.92	-34.80	-49.63	-28.33	-53.57	-30.16
-54.10	-31.92	-56.77	-27.14	-43.31	-17.06
-54.28	-34.03	-57.02	-26.01	-44.27	-18.11
-56.69	-34.71	-58.40	-33.87	-46.01	-17.01
-53.77	-34.35	-58.58	-34.33	-50.58	-29.45
-57.54	-30.90	-58.23	-28.05	-51.18	-29.17
-55.67	-26.76	-64.87	-31.10	-52.53	-26.56
-56.74	-27.36	-54.42	-25.72	-43.68	-18.81
-56.50	-27.42	-65.63	-32.65	-43.69	-20.52
-56.17	-27.23	-56.68	-36.75	-42.54	-15.61
-55.94	-25.07	-58.54	-34.63	-44.18	-17.87

-56.76	-27.14	-58.05	-29.79	-41.77	-13.15
-57.23	-24.69	-59.26	-29.14	-43.80	-20.25
-55.73	-27.18	-61.11	-32.16	-55.06	-34.83
-56.83	-25.68	-58.60	-33.78	-58.52	-33.01
-57.27	-27.40	-58.88	-32.37	-60.08	-31.10
-57.54	-25.46	-58.54	-34.58	-46.37	-20.25
-55.67	-26.83	-58.52	-33.02	-46.62	-21.13
-46.52	-23.67	-60.44	-26.79	-48.35	-23.40
-47.35	-21.92	-60.64	-32.06	-56.33	-34.86
-44.75	-22.57	-60.57	-31.71	-44.57	-22.64
-49.55	-28.40	-59.02	-33.69	-58.99	-27.47
-46.32	-23.78	-60.30	-31.73	-46.56	-21.79
-35.73	-84.83	-58.44	-32.35	-51.32	-264.28
-48.43	-22.87	-59.22	-31.48	-49.20	-25.93
-59.50	-32.67	-60.52	-31.73	-51.32	-26.43
-58.73	-34.38	-57.85	-35.02	-51.63	-26.52
-58.84	-33.69	-57.33	-37.62	-46.62	-21.78
-58.87	-32.37	-54.91	-34.80	-44.58	-22.65
-58.96	-31.99	-54.28	-34.04	-51.74	-27.01
-59.24	-31.54	-54.13	-34.58	-46.37	-20.25
-58.88	-33.91	-57.53	-30.95	-51.02	-30.08
-57.17	-28.54	-56.45	-34.74	-50.23	-30.25
-58.70	-34.58	-54.17	-31.87	-50.21	-30.18
-58.10	-27.92	-55.06	-34.83	-52.10	-32.04
-58.64	-34.36	-56.30	-34.87	-51.23	-30.03
-60.38	-29.42	-55.60	-30.87	-50.07	-28.75
-58.06	-29.79	-53.80	-34.39	-51.93	-29.83
-58.87	-33.89	-57.88	-30.53	-51.76	-29.91
-57.93	-35.78	-57.87	-30.58	-53.67	-31.56
-58.35	-34.61	-57.73	-30.78	-56.00	-28.66
-60.15	-31.19	-55.90	-34.82	-50.07	-29.59
-59.26	-29.15	-56.03	-34.82	-48.78	-28.48
-57.17	-28.54	-56.03	-34.88	-52.34	-31.77

-57.72	-35.73	-55.72	-34.73	-49.73	-29.34
-58.44	-34.54	-54.20	-31.87	-51.34	-27.63
-59.19	-25.61	-53.67	-32.72	-51.13	-29.68
-43.75	-19.51	-55.28	-32.63	-50.70	-26.93
-43.71	-19.17	-56.65	-34.50	-50.76	-27.90
-43.71	-19.17	-54.98	-34.33	-50.22	-29.45
-43.74	-19.51	-54.57	-34.78	-52.10	-32.04
-46.57	-22.07	-55.27	-34.80	-50.38	-29.42
-43.88	-21.68	-54.95	-34.97	-51.18	-28.33
-43.41	-20.07	-56.35	-34.80	-51.98	-31.36
-44.18	-17.87	-56.83	-31.83	-50.01	-28.84
-44.20	-20.14	-57.62	-31.82	-50.22	-30.20
-43.43	-19.04	-55.55	-31.03	-55.36	-30.77
-43.60	-18.25	-55.60	-31.32	-52.99	-32.05
-43.31	-18.47	-53.45	-33.68	-57.18	-29.95
-43.61	-20.45	-53.58	-33.68	-55.34	-29.60
-43.47	-20.08	-53.53	-33.98	-54.54	-29.92
-46.53	-23.67	-53.77	-34.28	-56.47	-30.18
-46.53	-23.67	-53.78	-34.33	-56.01	-28.62
-47.82	-22.25	-53.78	-34.35	-52.52	-31.74
-48.44	-22.88	-54.33	-34.48	-50.92	-31.11
-47.35	-21.92	-54.15	-34.60	-48.43	-22.87
-44.75	-22.57	-57.87	-30.93	-57.54	-30.90
-46.32	-23.78	-57.53	-30.95	-53.77	-34.35
-48.13	-22.28	-56.67	-34.73	-49.55	28.40
-48.77	-24.22	-56.97	-34.38	-47.80	-22.27
-53.81	-29.68	-56.37	-34.82	-46.48	-20.35
-51.02	-30.08	-55.47	-32.43	-46.66	-20.15
-51.46	-29.69	-54.40	-32.97	-46.56	-21.79
-51.18	-29.92	-54.62	-33.00	-44.27	-17.70
-52.34	-31.77	-54.48	-33.22	-43.80	-17.79
-52.15	-32.02	-54.38	-33.23	-43.51	-19.25
-50.16	-25.10	-54.83	-34.00	-51.56	-27.00

-51.99	-26.48	-53.87	-33.03	-51.02	-26.78
-50.62	-24.32	-48.00	-22.25	-52.04	-32.01
-49.18	-25.92	-44.61	-22.72	-53.73	-27.18
-52.62	-27.19	-43.51	-20.29	-47.47	-14.08
-47.82	-22.25	-49.62	-28.34	-47.93	-15.78
-44.57	-22.64	-56.48	-21.12	-58.45	-27.20
-50.16	-25.10	-51.99	-26.48		

---

**Table S1.8** Details on Atmosphere-Ocean Global Circulation Models (AOGCMs) used for ecological niche modelling of *Scinax squalirostris*

<b>Model ID</b>	<b>Modelling Centre</b>	<b>Resolution*</b>	<b>Source</b>	<b>Year</b>
CCSM4	University of Miami – RSMAS, USA	0.9° × 1.25°	CMIP5/PMIP3	2012
CNRM-CM5	Centre National de Recherches Meteorologiques / Centre Europeen de Recherche et Formation Avancees en Calcul Scientifique, France	1.4° x 1.4°	CMIP5/PMIP3	2012
MIROC-ESM	Atmosphere and Ocean Research Institute (University of Tokyo), National Institute for Environmental Studies, and Japan Agency for Marine-Earth Science and Technology, Japan	2.8° × 2.8°	CMIP5/PMIP3	2012
MPI-ESM-P	Max Planck Institute for Meteorology, Germany	1.9° × 1.9°	CMIP5/PMIP3	2011
MRI-CGCM3	Meteorological Research Institute, Japan	1.1° x 1.1°	CMIP5/PMIP3	2012

\* longitude × latitude

CMIP5 –Coupled Model Intercomparison Project, Phase 5 (<http://cmip-pcmdi.llnl.gov/>)

PMIP3 –Paleoclimate Modelling Intercomparison Project, Phase 3 (<http://pmip3.lsce.ipsl.fr/>)

**Table S1.9** Ecological niche modeling methods used to estimate *Scinax squalirostris* potential distribution.

<b>Method</b>	<b>Species data type</b>
Bioclimatic Envelope (BioClim)	Presence only
Ecological Niche Factor Analysis (ENFA)	Presence only
Euclidian Distance (EuclidDist)	Presence only
Flexible discriminant analysis (FDA)	Presence and absence
Generalized additive models (GAM)	Presence and absence
Generalized Linear Models (GLM)	Presence and absence
Gower Distance (GowerDist)	Presence only
Mahalanobis Distance (MahalDist)	Presence only
Multivariate adaptive regression splines (MARS)	Presence and absence
Maximum Entropy (MaxEnt)	Presence/background
Neural Networks (NNet)	Presence and absence
Random Forest (RNDFOR)	Presence and absence

**Table S1.10** Characteristics of the 26 populations sampled for the analysis Phylogeography of *Scinax squaleirostris*. Individuals (N), haplotypes by population (K) and relation of the haplotypes by population. Haplotypes in bold show the haplotype shared among some populations.

Population		mtDNA		nrDNA		
Code	N	k	Haplotypes	N	k	Haplotypes
ISP	5	2	<b>h01, h02</b>	5	2	<b>h01, h02</b>
BSP	12	8	<b>h01, h02</b> , h03, h04, <b>h05</b> , h06, h07, h08	11	4	<b>h02</b> , h03, <b>h04</b> , h05
SRMG	11	4	h09, h10, h11, h12	12	1	<b>h04</b>
OMG	16	5	h13, <b>h14</b> , h15, h16, h17	16	2	<b>h06, h07</b>
CMG	3	1	<b>h14</b>	3	3	<b>h06</b> , h08, h09
PMG	1	1	h18	-	-	-
SMG	16	7	h19, h20, h21, h22, h23, h24, h25	16	5	<b>h06, h10</b> , h11, h12, h13
SVMG	22	5	<b>h26</b> , h27, h28, h29, h30	21	8	<b>h06, h10</b> , h14, h15, h16, h17, h18, h19
SCMG	13	2	<b>h26</b> , h31	12	3	<b>h06</b> , h20, h21
CGO	24	5	h32, h33, h34, h35, h36	23	3	h22, h23, h24
BDF	19	4	h37, h38, h39, h40	18	1	h25
BMS	7	3	<b>h41</b> , h42, h43	7	5	<b>h06, h07, h26</b> , h27, h28
ISC	26	12	h44, <b>h45</b> , h46, h47, h48, h49, h50, h51, h52, h53, h54, h55	24	18	<b>h01, h29, h30, h31, h32</b> , h33, h34, h35, <b>h36, h37</b> , h38, h39, h40, h41, h42, h43, h44, h45
SJRS	10	2	h44, h46	10	10	<b>h26, h30, h32, h36, h37</b> , h46, h47, h48, h49, h50

SFRS	2 2	h56, h57	2 2	<b>h51</b> , h52
BRS	1 1	h58	1 1	h53
PPR	2 2	<b>h59</b> , h60	2 2	<b>h06</b> , h54
PGPR	8 3	<b>h01</b> , <b>h05</b> , h61	8 6	h55, h56, h57, h58, h59, h60
CBSC	1 1	<b>h62</b>	1 1	<b>h51</b>
CNSC	2 1	<b>h01</b>	2 2	h61, h62
BSC	5 2	<b>h01</b> , <b>h62</b>	5 5	<b>h31</b> , h63, h64, h65, h66
CSC	3 2	<b>h59</b>	2 2	h67, h68
ASC	1 2	<b>h59</b>	2 2	<b>h29</b> , h69
EPY	1 1	<b>h41</b>	1 1	h70
APY	7 2	<b>h41</b> , h63	4 3	h71, h72, h73
URU	1 1	<b>h45</b>	1 1	<b>h30</b>

---

**Table S1.11** Analysis of Molecular Variance (AMOVA) for populations of *Scinax squalirostris*.

DNA Region	Source of Variation	d.f	SSD	Variance components	% of variation	Fixation Index
Mitochondrial	Among populations	25	1075.276	5.24081 Va	93.78	FST= 0.93
	Within populations	193	67.075	0.34754 Vb	6.22	
Nuclear	Among populations	24	380.776	1.83940 Va	65.11	FST= 0.65
	Within populations	184	181.329	0.98548 Vb	34.89	

Significant test with 10,100 permutations; p <0.000.

**Table S1.12** Coefficients of MRM analyses for calculated isolation by environmental. Environmental variables Bio4 - ‘Temperature Seasonality’, Bio6 - ‘Minimum Temperature of Coldest Month’, Bio11 - ‘Mean Temperature of Coldest Quarter’, Bio14 - ‘Precipitation of Driest Month’, Bio19 - ‘Precipitation of Coldest Quarter’. Values in bold are significant \*p < 0.05.

MRM	Mitochondrial			Nuclear		
	Coefficients	p-value	R <sup>2</sup>	Coefficients	p-value	R <sup>2</sup>
Intercept	-12.1328	0.874		-8.2777	0.505	
Geographic Distance	18.9238	0.312	0.0086	4.9931	0.202	0.043
Bio4	-1.8132	0.876	0.0002	2.2835	0.363	0.006
Bio6	-3.7484	0.743	0.0005	0.1250	0.0962	0.00001
Bio11	<b>-20.2499</b>	<b>0.048</b>	<b>0.0190</b>	-0.6186	0.787	0.0003
Bio14	-9.9699	0.491	0.0030	3.1278	0.290	0.006
Bio19	5.1204	0.373	0.0040	0.9448	0.407	0.003
R <sup>2</sup> (p-value)	0.0583 (0.171)			0.0762 (0.061)		
F-test (p-value)	3.2856 (0.171)			4.0298 (0.061)		

\*p-value calculated with 10,000 random permutations.

**Table S1.13** Values of true skill statistics (TSS) and values of area under the curve (AUC), with mean and standard deviation, for all ecological niche models (ENM) and Atmosphere-Ocean Global Circulation Model (AOGCM) combinations (ENM x AOGCM) in *Scinax squaleirostris* paleodistribution modelling.

ENM/AOGCM	CCSM		CNRM		MIROC		MPI		MRI		Mean		SD	
	TSS	AUC	TSS	AUC	TSS	AUC	TSS	AUC	TSS	AUC	TSS	AUC	TSS	AUC
BioClim	0.698	0.937	0.690	0.936	0.678	0.920	0.722	0.949	0.647	0.927	0.690	0.936	0.028	0.011
ENFA	0.515	0.849	0.480	0.798	0.503	0.840	0.521	0.841	0.541	0.841	0.515	0.841	0.022	0.020
EuclidDist	0.645	0.895	0.465	0.825	0.625	0.888	0.673	0.903	0.551	0.883	0.625	0.888	0.084	0.031
FDA	0.759	0.961	0.730	0.945	0.724	0.940	0.793	0.963	0.751	0.950	0.751	0.950	0.027	0.010
GAM	0.768	0.960	0.780	0.967	0.767	0.942	0.821	0.966	0.758	0.956	0.768	0.960	0.025	0.010
GowerDist	0.662	0.921	0.647	0.889	0.683	0.900	0.746	0.927	0.616	0.915	0.662	0.915	0.049	0.016
MahalonobisDit	0.725	0.935	0.561	0.845	0.545	0.867	0.724	0.927	0.707	0.923	0.707	0.923	0.091	0.041
GLM	0.714	0.942	0.761	0.952	0.704	0.915	0.820	0.967	0.754	0.954	0.754	0.952	0.046	0.020
MARS	0.747	0.951	0.761	0.952	0.780	0.955	0.837	0.969	0.761	0.954	0.761	0.954	0.035	0.007
MaxEnt	0.762	0.958	0.727	0.957	0.768	0.960	0.836	0.978	0.777	0.972	0.768	0.960	0.039	0.009
NNet	0.564	0.882	0.686	0.962	0.688	0.951	0.694	0.920	0.670	0.966	0.686	0.951	0.054	0.035
RndFor	0.792	1.000	0.767	1.000	0.789	1.000	0.827	1.000	0.798	1.000	0.792	1.000	0.022	0.000
<b>Mean</b>	0.720	0.939	0.709	0.948	0.696	0.930	0.769	0.956	0.729	0.952	-	-	-	-
<b>SD</b>	0.085	0.041	0.111	0.064	0.091	0.044	0.093	0.043	0.089	0.043	-	-	-	-

**Table S1.14** Relative contributions of each modeling component (time, methods, AOGCMs and their interaction) to the variability of the predictions of the ENMs for *Scinax squaleirostris*. The suitability column shows the median proportion and amplitude of the sum of squares from the hierarchical ANOVA calculated for each cell of the grid covering the Neotropical region.

Sources of uncertainty	Median (SS)%	Min-Máx
ENMs*Time	0.26	0.00 - 0.78
AOGCMs*Time	0.14	0.00 - 0.76
Time	0.04	0.02 - 0.92
Residual	0.46	0.06 - 0.78

**Table S1.15** Probability values and 95% confidence intervals for the 10 subsets of closest simulated data. We use the logistic approach in Approximate Bayesian Computation (ABC) to evaluate all demographic scenarios (8 scenarios). In bold the best-supported scenarios in this comparison.

	N	Scenario 1	Scenario 2	Scenario 3	Scenario 4	Scenario 5	Scenario 6	Scenario 7	Scenario 8
Mitochondrial	1000	0.00 [0.0000,1.0000]	0.00 [0.0000,1.0000]	0.00 [0.0000,1.0000]	0.00 [0.0000,1.0000]	0.00 [0.0000,1.0000]	<b>1.00 [1.0000,1.0000]</b>	0.00 [0.0000,1.0000]	0.00 [0.0000,1.0000]
	2000	0.00 [0.0000,1.0000]	0.00 [0.0000,1.0000]	0.00 [0.0000,1.0000]	0.00 [0.0000,1.0000]	0.00 [0.0000,1.0000]	<b>1.00 [1.0000,1.0000]</b>	0.00 [0.0000,1.0000]	0.00 [0.0000,1.0000]
	3000	0.00 [0.0000,1.0000]	0.00 [0.0000,1.0000]	0.00 [0.0000,1.0000]	0.00 [0.0000,1.0000]	0.00 [0.0000,1.0000]	<b>1.00 [1.0000,1.0000]</b>	0.00 [0.0000,1.0000]	0.00 [0.0000,1.0000]
	4000	0.00 [0.0000,1.0000]	0.00 [0.0000,1.0000]	0.00 [0.0000,1.0000]	0.00 [0.0000,1.0000]	0.00 [0.0000,1.0000]	<b>1.00 [1.0000,1.0000]</b>	0.00 [0.0000,1.0000]	0.00 [0.0000,1.0000]
	5000	0.00 [0.0000,1.0000]	0.00 [0.0000,1.0000]	0.00 [0.0000,1.0000]	0.00 [0.0000,1.0000]	0.00 [0.0000,1.0000]	<b>1.00 [1.0000,1.0000]</b>	0.00 [0.0000,1.0000]	0.00 [0.0000,1.0000]
	6000	0.00 [0.0000,1.0000]	0.00 [0.0000,1.0000]	0.00 [0.0000,1.0000]	0.00 [0.0000,1.0000]	0.00 [0.0000,1.0000]	<b>1.00 [1.0000,1.0000]</b>	0.00 [0.0000,1.0000]	0.00 [0.0000,1.0000]
	7000	0.00 [0.0000,1.0000]	0.00 [0.0000,1.0000]	0.00 [0.0000,1.0000]	0.00 [0.0000,1.0000]	0.00 [0.0000,1.0000]	<b>1.00 [1.0000,1.0000]</b>	0.00 [0.0000,1.0000]	0.00 [0.0000,1.0000]
	8000	0.00 [0.0000,1.0000]	0.00 [0.0000,1.0000]	0.00 [0.0000,1.0000]	0.00 [0.0000,1.0000]	0.00 [0.0000,1.0000]	<b>1.00 [1.0000,1.0000]</b>	0.00 [0.0000,1.0000]	0.00 [0.0000,1.0000]
	9000	0.00 [0.0000,1.0000]	0.00 [0.0000,1.0000]	0.00 [0.0000,1.0000]	0.00 [0.0000,1.0000]	0.00 [0.0000,1.0000]	<b>1.00 [1.0000,1.0000]</b>	0.00 [0.0000,1.0000]	0.00 [0.0000,1.0000]
	10000	0.00 [0.0000,1.0000]	0.00 [0.0000,1.0000]	0.00 [0.0000,1.0000]	0.00 [0.0000,1.0000]	0.00 [0.0000,1.0000]	<b>1.00 [1.0000,1.0000]</b>	0.00 [0.0000,1.0000]	0.00 [0.0000,1.0000]
Nuclear	1000	0.00 [0.0000,1.0000]	0.00 [0.0000,1.0000]	0.00 [0.0000,1.0000]	0.00 [0.0000,1.0000]	0.00 [0.0000,1.0000]	<b>1.00 [1.0000,1.0000]</b>	0.00 [0.0000,1.0000]	0.00 [0.0000,1.0000]
	2000	0.00 [0.0000,1.0000]	0.00 [0.0000,1.0000]	0.00 [0.0000,1.0000]	0.00 [0.0000,1.0000]	0.00 [0.0000,1.0000]	<b>1.00 [1.0000,1.0000]</b>	0.00 [0.0000,1.0000]	0.00 [0.0000,1.0000]
	3000	0.00 [0.0000,1.0000]	0.00 [0.0000,1.0000]	0.00 [0.0000,1.0000]	0.00 [0.0000,1.0000]	0.00 [0.0000,1.0000]	<b>1.00 [1.0000,1.0000]</b>	0.00 [0.0000,1.0000]	0.00 [0.0000,1.0000]
	4000	0.00 [0.0000,1.0000]	0.00 [0.0000,1.0000]	0.00 [0.0000,1.0000]	0.00 [0.0000,1.0000]	0.00 [0.0000,1.0000]	<b>1.00 [1.0000,1.0000]</b>	0.00 [0.0000,1.0000]	0.00 [0.0000,1.0000]
	5000	0.00 [0.0000,1.0000]	0.00 [0.0000,1.0000]	0.00 [0.0000,1.0000]	0.00 [0.0000,1.0000]	0.00 [0.0000,1.0000]	<b>1.00 [1.0000,1.0000]</b>	0.00 [0.0000,1.0000]	0.00 [0.0000,1.0000]
	6000	0.00 [0.0000,1.0000]	0.00 [0.0000,1.0000]	0.00 [0.0000,1.0000]	0.00 [0.0000,1.0000]	0.00 [0.0000,1.0000]	<b>1.00 [1.0000,1.0000]</b>	0.00 [0.0000,1.0000]	0.00 [0.0000,1.0000]
	7000	0.00 [0.0000,1.0000]	0.00 [0.0000,1.0000]	0.00 [0.0000,1.0000]	0.00 [0.0000,1.0000]	0.00 [0.0000,1.0000]	<b>1.00 [1.0000,1.0000]</b>	0.00 [0.0000,1.0000]	0.00 [0.0000,1.0000]
	8000	0.00 [0.0000,1.0000]	0.00 [0.0000,1.0000]	0.00 [0.0000,1.0000]	0.00 [0.0000,1.0000]	0.00 [0.0000,1.0000]	<b>1.00 [1.0000,1.0000]</b>	0.00 [0.0000,1.0000]	0.00 [0.0000,1.0000]
	9000	0.00 [0.0000,1.0000]	0.00 [0.0000,1.0000]	0.00 [0.0000,1.0000]	0.00 [0.0000,1.0000]	0.00 [0.0000,1.0000]	<b>1.00 [1.0000,1.0000]</b>	0.00 [0.0000,1.0000]	0.00 [0.0000,1.0000]
	10000	0.00 [0.0000,1.0000]	0.00 [0.0000,1.0000]	0.00 [0.0000,1.0000]	0.00 [0.0000,1.0000]	0.00 [0.0000,1.0000]	<b>1.00 [1.0000,1.0000]</b>	0.00 [0.0000,1.0000]	0.00 [0.0000,1.0000]

## REFERENCES

- Evans, B. J., Kelley, D. B., Tinsley, R. C., Melnick, D. J. & Cannatella, D. C. (2004) A mitochondrial DNA phylogeny of African clawed frogs: phylogeography and implications for polyploid evolution. *Molecular Phylogenetics and Evolution*, 33, 197-213.
- Heinicke, M. P., Duellman, W. E. & Hedges, S. B. (2007) Major Caribbean and Central American frog faunas originated by ancient oceanic dispersal. *Proceedings of the National Academy of Sciences*, 104, 10092–10097.
- Macey, J. R., Schulte, J. A., Larson, A., Fang, Z. L., Wang, Y. Z., Tuniyev, B.S. & Papenfuss, T. J. (1998) Phylogenetic relationships of toads in the *Bufo bufo* species group from the eastern escarpment of the Tibetan Plateau: a case of vicariance and dispersal. *Molecular Phylogenetics and Evolution*, 9, 80-87.

**SUPPORTING INFORMATION**

**Inferring responses to Neogene-Quaternary climate dynamics from historical demography in a South American grassland treefrog**

Tatianne P. F. Abreu-Jardim | Rafael F. Magalhães | Natan M. Maciel | Matheus Souza  
Lima-Ribeiro | Guarino R. Colli | Célio F. B. Haddad and Rosane G. Collevatti.

**Appendix S2** Supplementary additional information of Details of Material and Methods.

**Genetic data**

We extracted the DNA of muscle and liver tissue samples preserved in ethanol, using the Dneasy Blood & Tissue Kit (Quiagen<sup>®</sup>, InR., Chatsworth, CA). DNA were amplified by polymerase chains reaction (PCR), and sequenced in an ABI 3500 automated DNA sequencer (Applied Biosystems<sup>®</sup>, CA) using the BigDye<sup>®</sup> Terminator Cycle Sequencing kit, according to the manufacturer's instructions. We sequenced all fragments in the forward and reverse directions.

The consensus sequences were assembled for each individual using the software SEQSCAPE 2.7 (Applied Biosystems) and to obtain the multiple sequence alignments, we used CLUSTALX (Thompson et al., 1997) implemented in BIOEDIT 7.2.5 (Hall, 1999). *Coding sequences were tested for saturation by plotting transitions and transversions with TN93 distance (Tamura & Nei, 1993) using DAMBE software (Xia, 2013). As third codon positions of CytB showed high levels of saturation (see Appendix S3: Figure S3.1; in supporting information), they were excluded from the final alignment. The sequences of RAG-1 showed heterozygous individuals (138 individuals, 47 characters), therefore,*

we used the most frequent haplotype, estimated by PHASED implemented in DNAsp 5.0 (Librado & Rozas, 2009). No signal of recombination was founded.

### **Structure of populations: IBD and IBE test**

Environmental distance matrices were calculated as pairwise Euclidian distances for each environmental variable. We selected the variables that explained the most of the variance among populations: (Bio4- ‘Temperature Seasonality’ (16%), Bio6- ‘Minimum Temperature of Coldest Month’ (27%), Bio11- ‘Mean Temperature of Coldest Quarter’ (17%), Bio14- ‘Precipitation of Driest Month’ (66%), Bio19- ‘Precipitation of Coldest Quarter’ (67%), obtained in the EcoClimate database ([www.ecoclimate.org](http://www.ecoclimate.org); Lima-Ribeiro *et al.*, 2015). Before obtaining the environmental distance matrix, we standardized each variable to zero mean and unity variance (Z standardization) (Diniz-Filho *et al.*, 2013). All distance matrices were log-scaled.

### **Demographic population history: Lamarc**

The analyses were run with 20 initial chains of 15,000 steps and three final chains of 80,000 steps, sampling by each 100 steps. The demographic parameters were estimated with populations that had at least five individuals, due to the limitation in the number of populations for reliable estimation in LAMARC. The convergence, stability and the effective sample size ( $ESS \geq 200$ ) were checked using TRACER 1.6 (Rambaut *et al.*, 2013).

### **Species distribution modeling**

To overcome the multicollinearity problem among all bioclimatic variables in the ENMs predictions, we performed a factorial analysis using Varimax rotation from 19

bioclimatic variables obtained in the EcoClimate database ([www.ecoclimate.org](http://www.ecoclimate.org); Lima-Ribeiro *et al.*, 2015) which are available at 0.5° x 0.5° of resolution.

The distribution of *S. squalirostris* was inferred using presence-only and presence-absence algorithms (Table S10), represented by 12 algorithms: bioclimatic envelopes (Bioclim), ecological niche factor analysis (ENFA), Euclidean distance, flexible discriminant analysis (FDA), generalized additive models (GAM), generalized linear models (GLM), Gower distance, Mahalanobis distance, multivariate adaptive regression splines (MARS), maximum entropy (Maxent), neural networks (NNET), and random forest (RNDFOR). There are not reliable real absence data available, so we used pseudo-absences were randomly generated for all Neotropical grid cells excluding cells with presence, maintaining prevalence equal to 0.5 to maximize model performance. To assess the model stability, we used a random data partitioning 75% training (calibration) and 25% testing (evaluation), replicated 50 repetitions for each model, due to the absence of independent testing data. This procedure and ENMs were run in the integrated computational platform BIOENSEMBLES (Diniz-Filho *et al.*, 2009). Model accuracy was assessed through two accuracy metrics, the calculation of the area under the receiver operator characteristics (ROC) curve – AUC, which is a threshold-independent statistic that is considered a highly effective measure for the performance of ordinal score models whose AUC ranges from 0 to 1 (Allouche *et al.*, 2006). The other metric is the true skill statistic (TSS), that take into account both omission and commission errors, with range from -1 to 1 and values close to 1 indicate a perfect fit (Allouche *et al.*, 2006). We used an ensemble approach (Araújo & New, 2006) to calculate a consensus map that included only models with AUC > 0.75 and TSS > 0.5, and the models with poor performance were eliminated from the ensemble process (values of AUC and TSS in Table S11). We used the remaining models to compute the

frequency of occurrence in the cells covering the Neotropical, after truncation using specific thresholds based on the ROC curve (maximum specificity + sensibility). The frequency of occurrence in each cell provide a surrogate for the environmental suitability and was used for *Scinax squalirostris* across the Neotropical grid cells.

The combination of all ENMs and AOGCMs resulted in 60 independent predictive maps (12 ENMs x 5 AOGCMs) for each time period (pre-industrial, 6 Ka, 21 Ka). We applied a hierarchical ANOVA using the predicted suitability from all models (12 ENMs x 5 AOGCMs x 3 times periods) as response variables to identify and map the uncertainties due to modeling components. For this, the ENMs and AOGCMs components were nested into the time component, but crossed by a two-way factorial design within each time period (see Terrible *et al.*, 2012). The 60 predictive maps were combined to obtain the consensus map for each time period, and then they were combined to generate a map of the historical refuge (stable environments through time). We considered all grid cells with suitability values  $\geq 0.5$  in the three time periods as refuge. To quantify the range sizes between the three time periods, we first tested 0.5 and 0.75 binary thresholds and selected 0.5 because it better recovered the current distribution area of *S. squalirostris*. Then, we used this threshold to transform occurrence frequency maps into presence and absence maps, and thus we calculated range size by summing the numbers of cells predicted as presence for each of the 60 predictive maps. After that, we subtracted the range sizes between current and Holocene, current and LGM, Holocene and LGM to calculate range shift.

## REFERENCES

- Allouche, O., Tsoar, A. & Kadmon, R. (2006) Assessing the accuracy of species distribution models: prevalence, kappa and the true skill statistic (TSS). *Journal of Applied Ecology*, 43,1223-1232.
- Araújo, M. B., & New, M. (2006) Ensemble forecasting of species distributions. *Trends in Ecology and Evolution*, 22, 42–47.
- Diniz-Filho, J. A. F., Bini, L. M., Rangel, T. F.; Loyola, R. D., Hof, C., Nogués-Bravo, D. & Araújo, M. B. (2009) Partitioning and mapping uncertainties in ensembles of forecasts of species turnover under climate change. *Ecography*, 32, 897-906.
- Diniz-Filho, J. A. F., Soares, T. N., Lima, J. S., Dobrovolski, R., Landeiro, V. L., Telles, M. P. C., Rangel, T. F & Bini, L. M. (2013) Mantel test in population genetics. *Genetics and Molecular Biology*, 36, 476-485.
- Hall, T. A. (1999) BioEdit: a user-friendly biological sequence alignment editor and analysis program for Windows 95/98/NT. *Nucleic Acids Symposium Series*, 41, 95-98.
- Librado, P. & Rozas, J. (2009) Dnasp: software for comprehensive analysis of DNA polymorphism data.
- Lima-Ribeiro, M. S., Varela, S., González-Hernández, J., Oliveira, G., Diniz-Filho, J. A. F. & Terribile, L. C. (2015) ecoClimate: a database of climate data from multiple models for past, present and future for Macroecologists and Biogeographers. *Biodiversity Informatics*, 10, 1-21.
- Rambaut, A., Suchard, M. A., Xie, W. & Drummond, A. J. (2013) Tracer v1.6. Available: <http://tree.bio.ed.ac.uk/software/tracer>.
- Tamura, K. & M. Nei. (1993) Estimation of the number of nucleotide substitutions in the control region of mitochondrial DNA in humans and chimpanzees. *Molecular Biology and Evolution*, 10, 512-526.
- Terribile, L. C., Lima-Ribeiro, M. S., Araújo, M. B., Bizão, N., Collevatti, R. G. *et al.* (2012) Areas of Climate Stability of Species ranges in the Brazilian Cerrado: Disentangling Uncertainties through Time. *Natureza & Conservação*, 10, 152-159.
- Thompson, J. D., Gibson, T. J., Plewniak, F., Jeanmougin, F. & Higgins, D. G. (1997) The Clustal X windows interface: flexible strategies for multiple sequence alignment aided by quality analysis tools. *Nucleic Acids Research*, 24, 4876–4882.

Xia, X. (2013) DAMBE5: A comprehensive software package for data analysis in molecular biology and evolution. *Molecular Biology and Evolution*, 30, 1720-1728.

**SUPPORTING INFORMATION**

**Inferring responses to Neogene-Quaternary climate dynamics from historical demography in a South American grassland treefrog**

Tatianne P. F. Abreu-Jardim | Rafael F. Magalhães | Natan M. Maciel | Matheus Souza

Lima-Ribeiro | Guarino R. Colli | Célio F. B. Haddad and Rosane G. Collevatti.

**Appendix S3** Supplementary figures (Figs S3.1-S3.13) with saturation analysis, genetic diversities maps, Bayesian Analysis of Population Structure, EBSP, location diffusion tree, details of ecological niche modelling, demography simulations and quantile regressions.

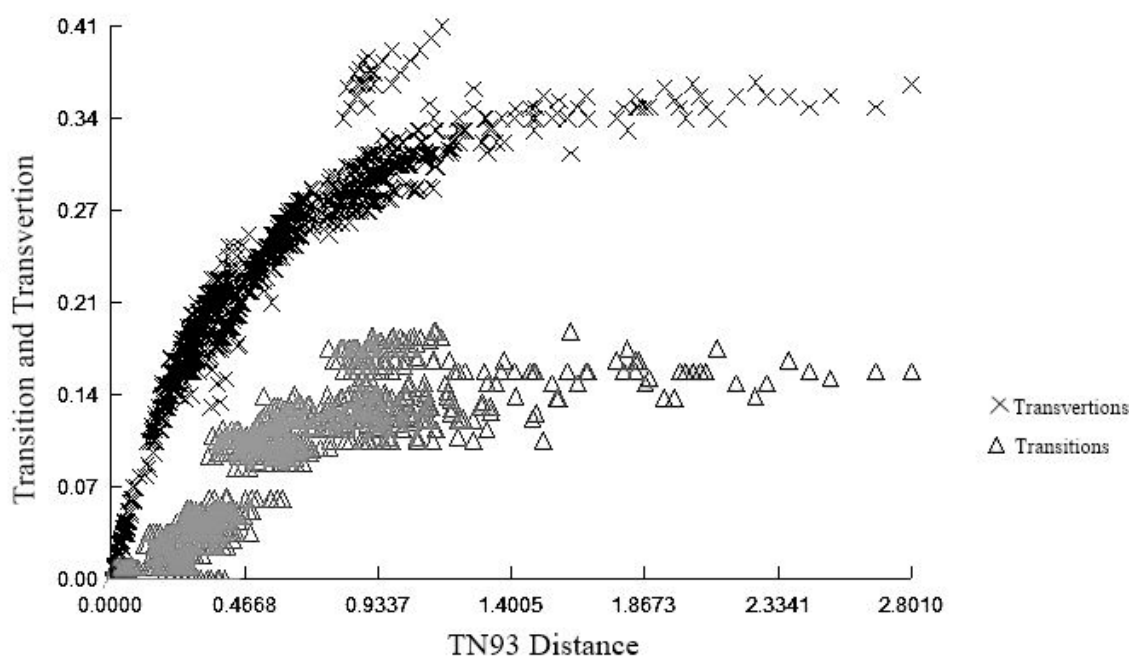


**Figure S3.1** Transition and transversion saturation plot for third codon positions of Cytochrome b sequences.

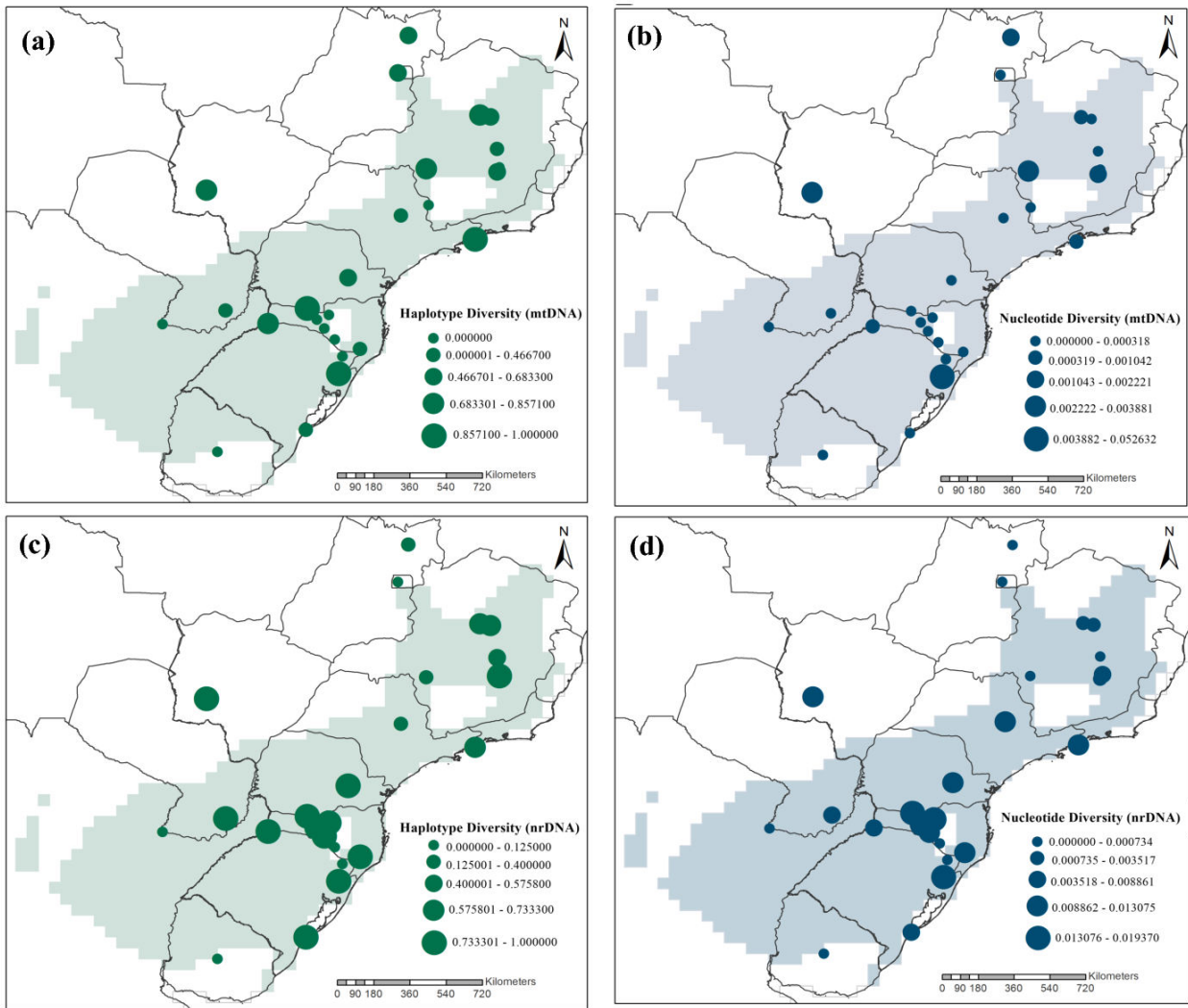


**Figure S3.2** Maps of geographic distribution of mitochondrial (mtDNA) and nuclear (nDNA) genetic diversity (nucleotide and haplotype) in the historical refuge predicted by paleodistribution modelling for *Scinax squalirostris*: (a) haplotype diversity for mtDNA, (b) nucleotide diversity for mtDNA, (c) haplotype diversity for nDNA, and (d) nucleotide diversity for nDNA.

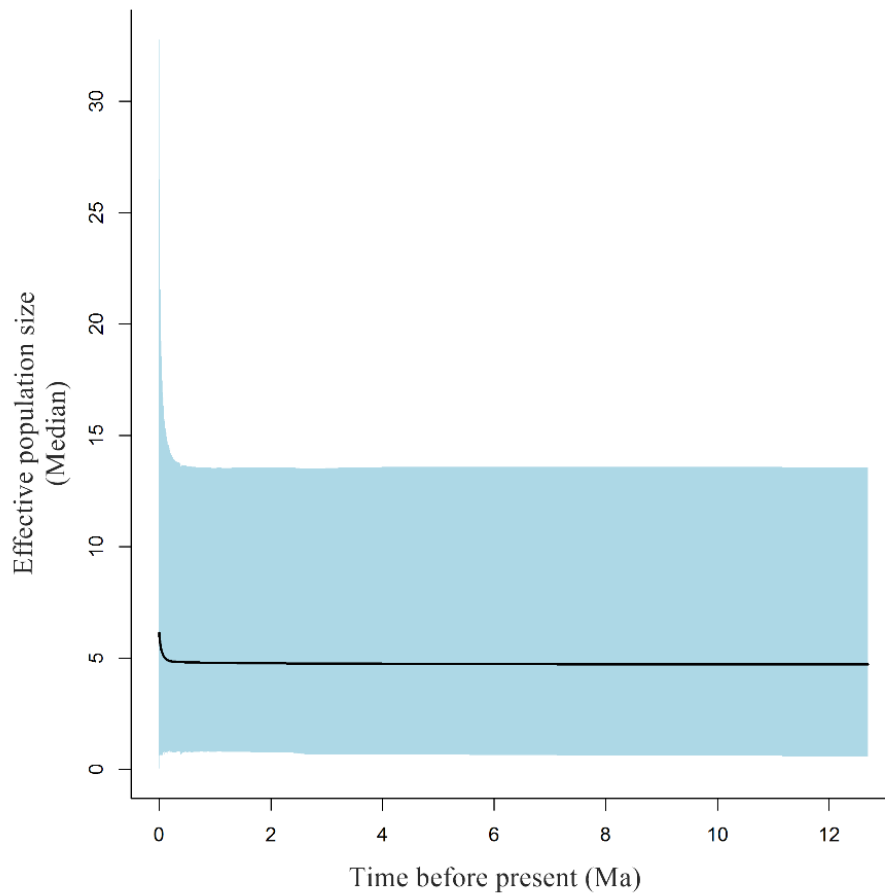


**Figure S3.3** Extended Bayesian Skyline Plot of *Scinax squalirostris* populations of concatenated fragments (mtDNA and nDNA). The black line represents the median of the effective population size estimates and the blue bands indicate the upper and lower credibility interval (95%). The scale is in millions of years (Ma) before present.

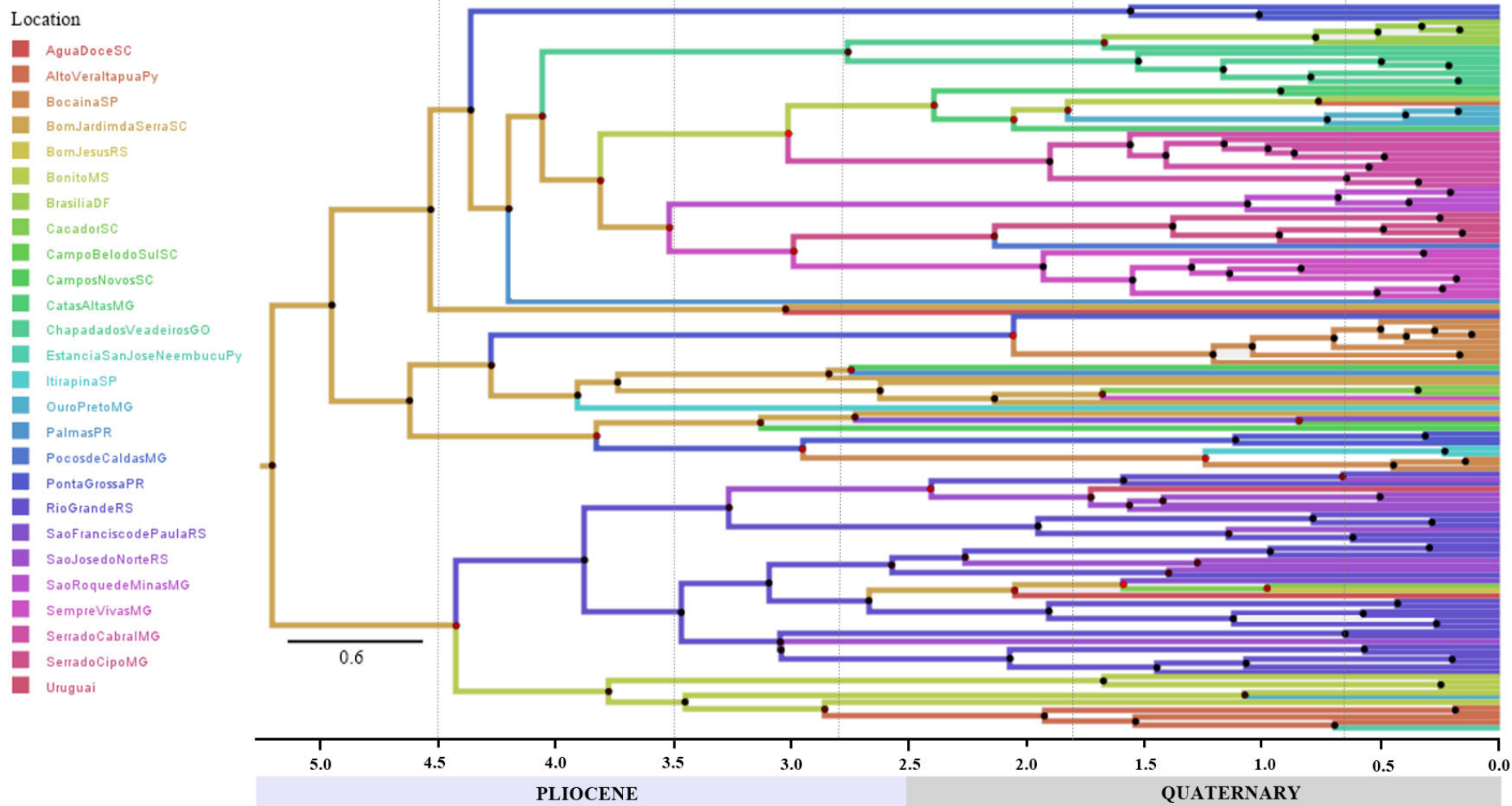


**Figure S3.4** Annotated tree showing the spatio-temporal dynamics of *Scinax squalirostris* lineages diffusion among the 26 sampled populations. The black dots represent the location probability upper to 0.8 and the red dots represent the location probability below to 0.79.

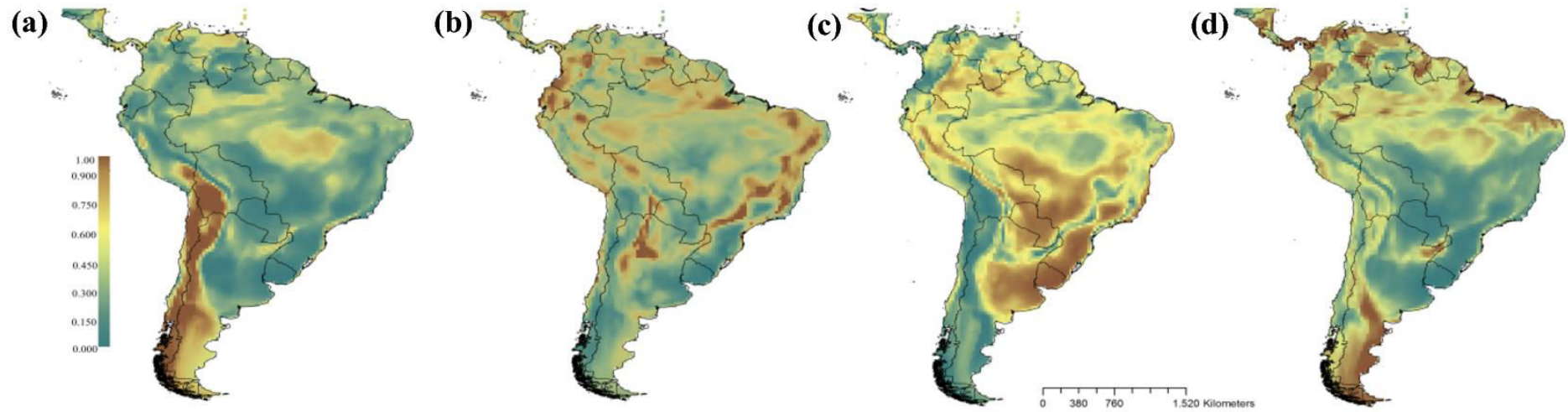


**Figure S3.5** Maps of uncertainty (relative sum of squares) for the modelling components for *Scinax squalirostris*: (a) ecological niche models (ENMs), (b) atmosphere–ocean global circulation models (AOGCMs), (c) time, and (d) residual (ENM \* AOGCM interaction).

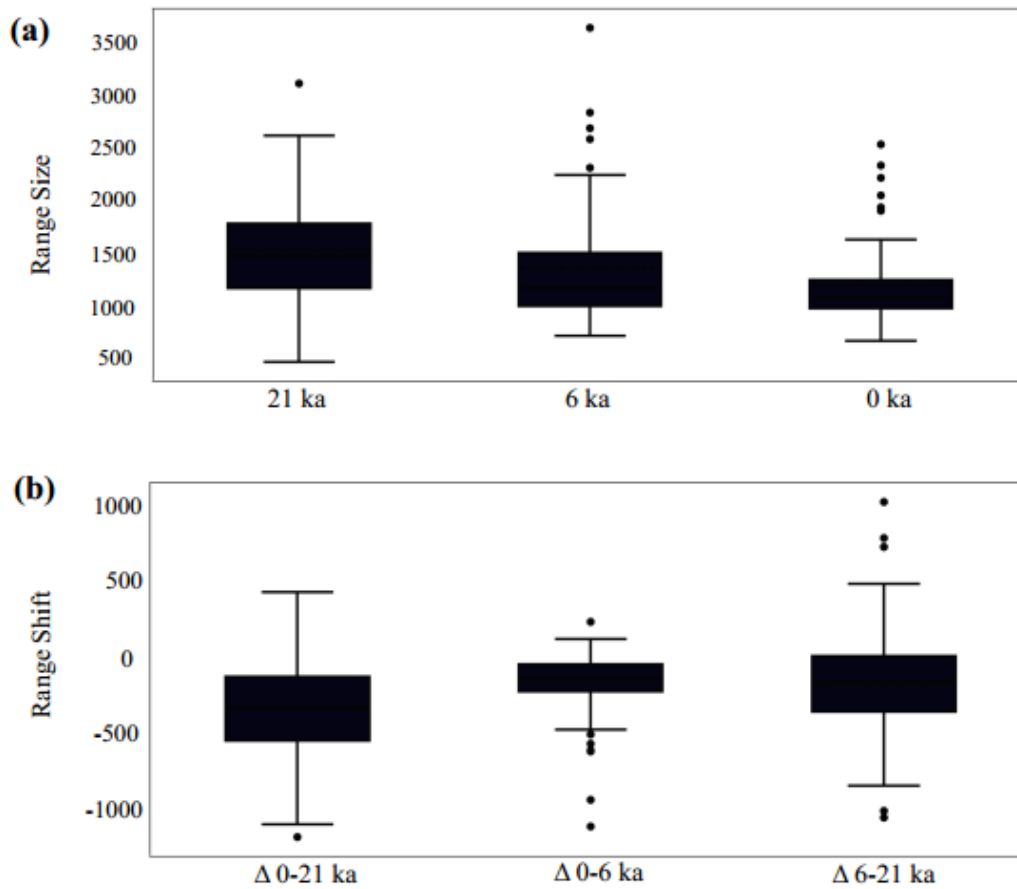


**Figure S3.6** Median and 0.05 – 0.95 quantiles among the 60 maps of (a) range size and (b) range shift (difference of range size among time periods in number of cells) predicted for *Scinax squalirostris* at present-day (0 Ka), mid-Holocene (6 Ka) and LGM (21 Ka).

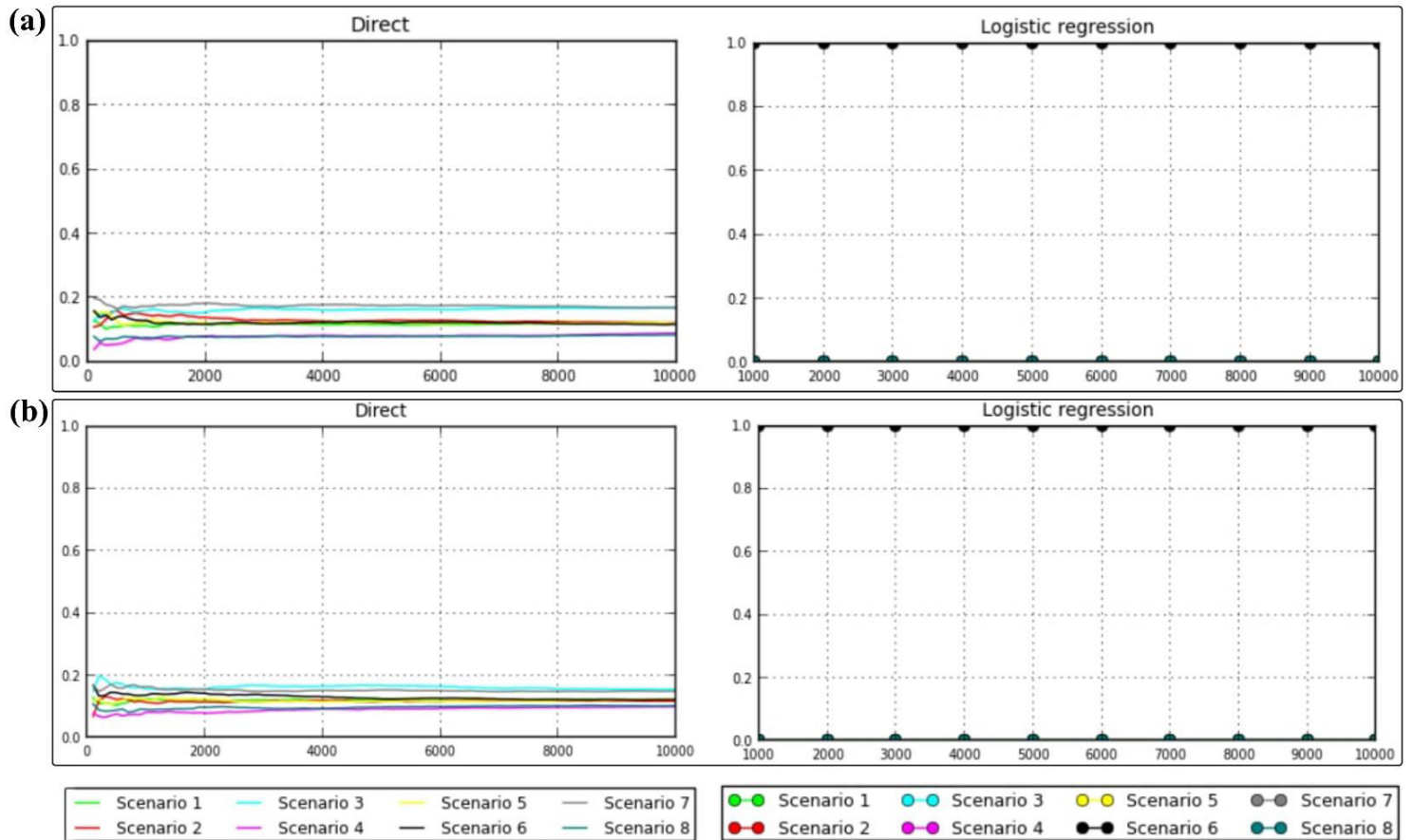


**Figure S3.7** Posterior probabilities of demographic scenarios for populations of *Scinax squalirostris* using approximate Bayesian computation (ABC), (a) scenarios tested with mtDNA and (b) scenarios tested with nrDNA. Scenarios without admixture: range expansion (scenario 1), range retraction (scenario 2), range stability (scenario 3) and multiples refuges (scenario 4). Scenarios with admixture: range expansion (scenario 3), range retraction (scenario 6), range stability (scenario 7) and multiples refuges (scenario 8).

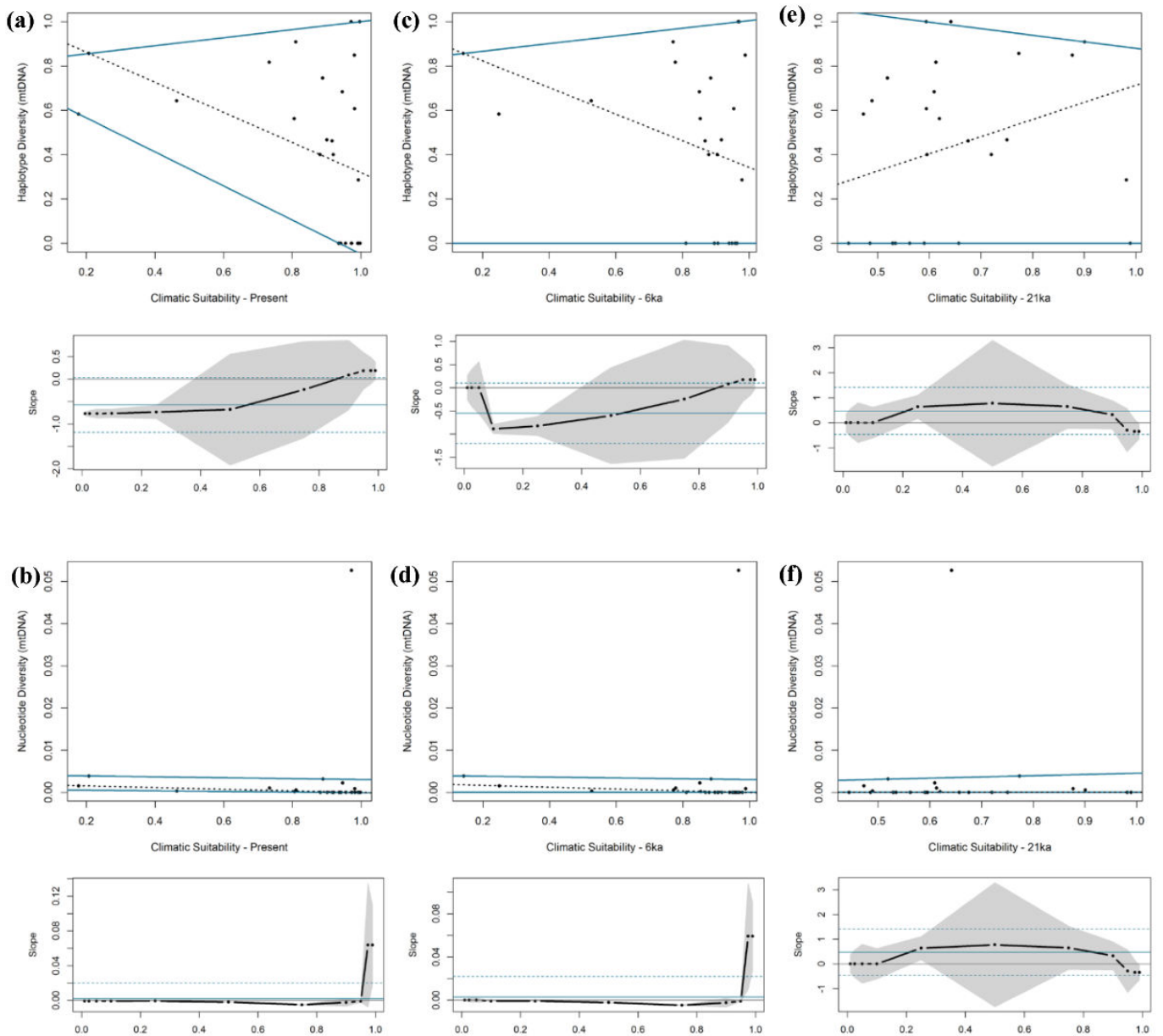


**Figure S3.8** Quantile regression for the relationships of haplotype and nucleotide diversities for mtDNA among the 26 populations of *Scinax squalirostris* with suitability in climatic conditions: (a) and (b) climatic suitability in present; (c) and (d) climatic suitability in 6 Ka; (e) and (f) climatic suitability in 21 Ka. The upper figures show the triangle-shaped envelopes from 0.05 (lower line) and 0.95 (upper line) quantiles. The lower figures show the slope estimate for 0.01, 0.025, 0.05, 0.1, 0.25, 0.5, 0.75, 0.9, 0.95, 0.975 and 0.99 quantiles (area in grey indicates 95% confidence interval around estimates).

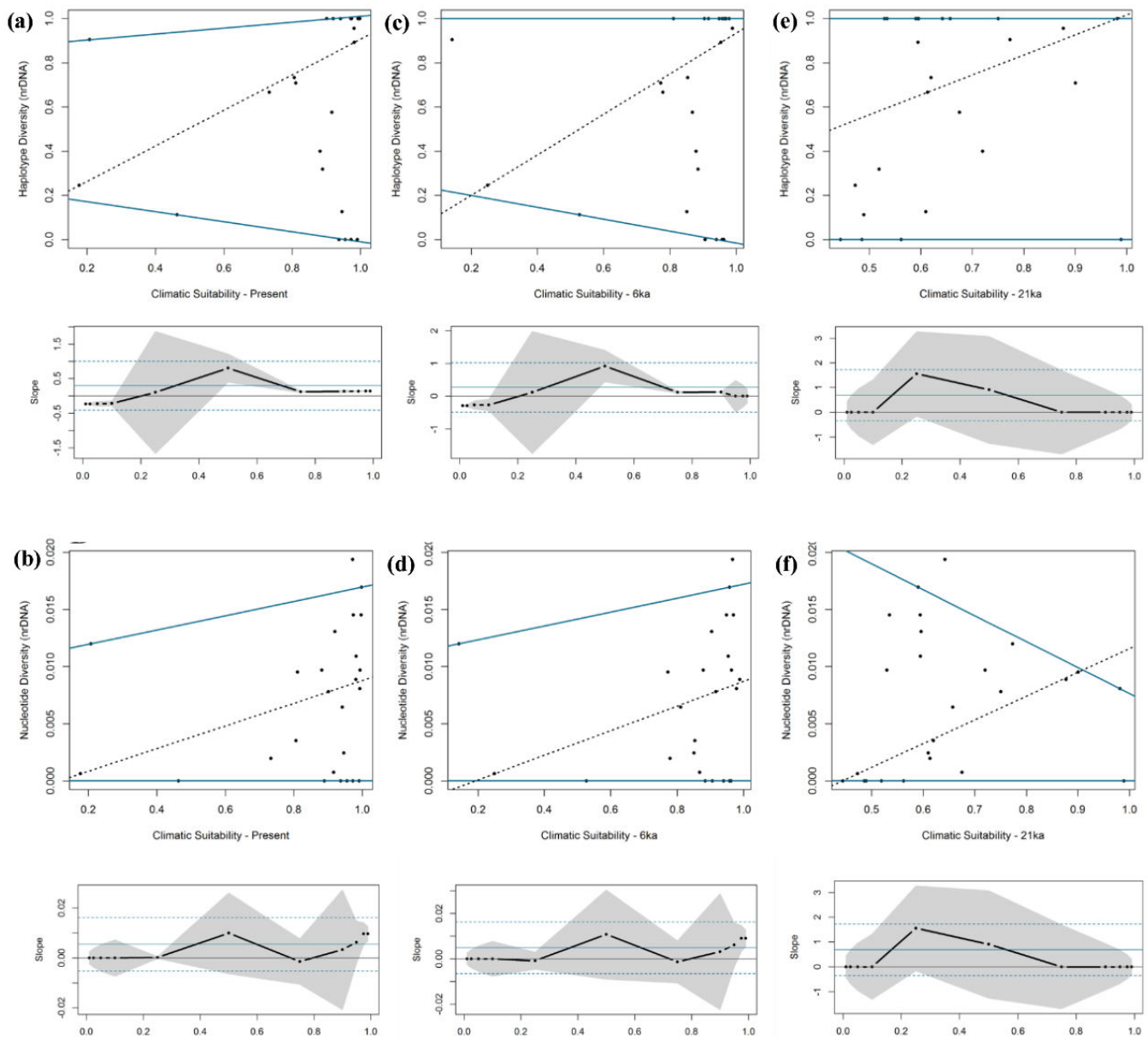


**Figure S3.9** Quantile regression for the relationships of haplotype and nucleotide diversities for nDNA among the 26 populations of *Scinax squalirostris* with suitability in climatic conditions: (a) and (b) climatic suitability in present; (c) and (d) climatic suitability in 6 Ka; (e) and (f) climatic suitability in 21 Ka. The upper figures show the triangle-shaped envelopes from 0.05 (lower line) and 0.95 (upper line) quantiles. The lower figures show the slope estimate for 0.01, 0.025, 0.05, 0.1, 0.25, 0.5, 0.75, 0.9, 0.95, 0.975 and 0.99 quantiles (area in grey indicates 95% confidence interval around estimates).

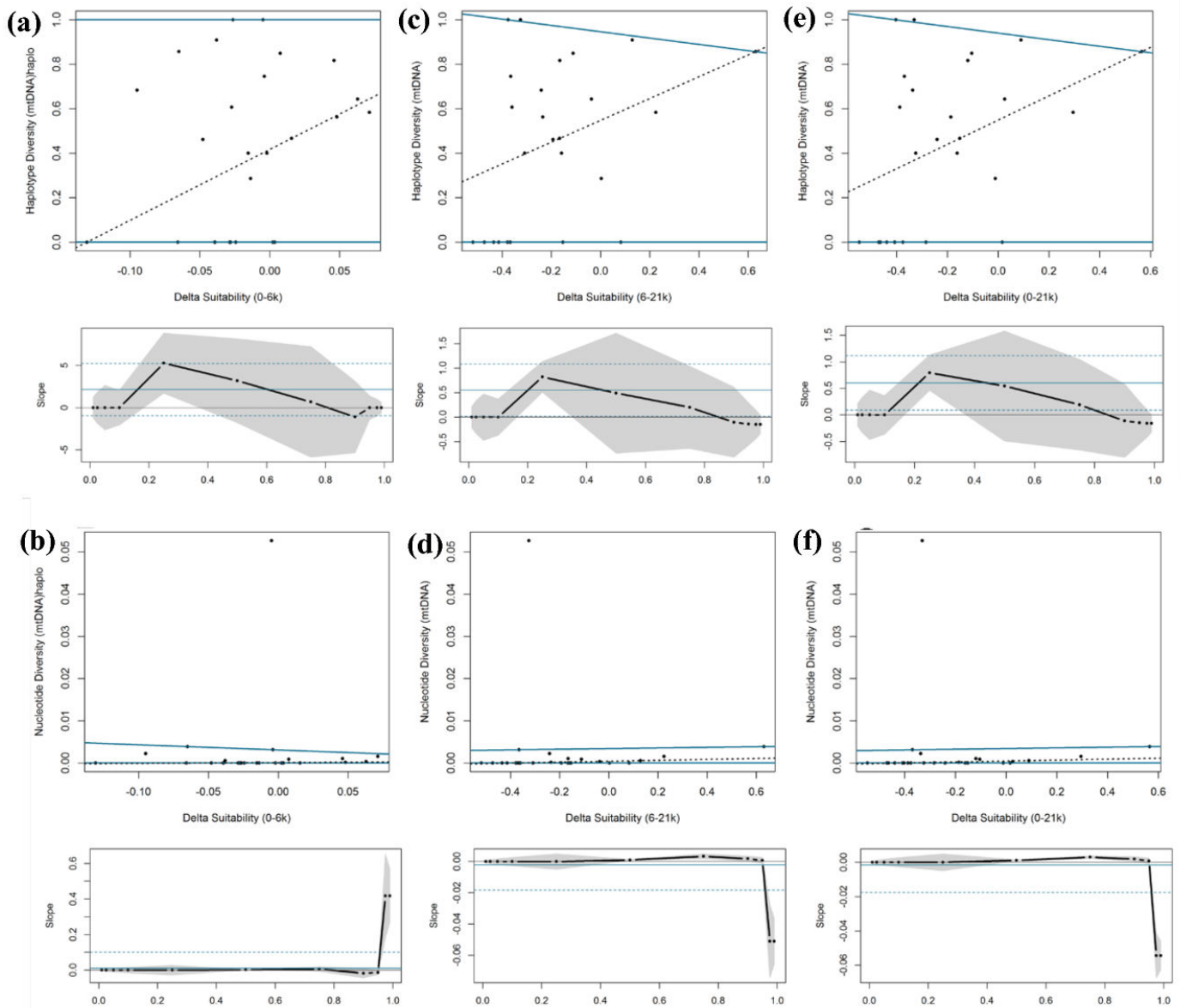


**Figure S3.10** Quantile regression for the relationships of haplotype and nucleotide diversities for mtDNA among the 26 populations of *Scinax squalirostris* with stability and suitability in climatic conditions: (a) and (b) climatic stability through 6 Ka to present; (c) and (d) climatic stability through 21 Ka to 6 Ka; (e) and (f) climatic stability through 21 Ka to present. The upper figures show the triangle-shaped envelopes from 0.05 (lower line) and 0.95 (upper line) quantiles. The lower figures show the slope estimate for 0.01, 0.025, 0.05, 0.1, 0.25, 0.5, 0.75, 0.9, 0.95, 0.975 and 0.99 quantiles (area in grey indicates 95% confidence interval around estimates).

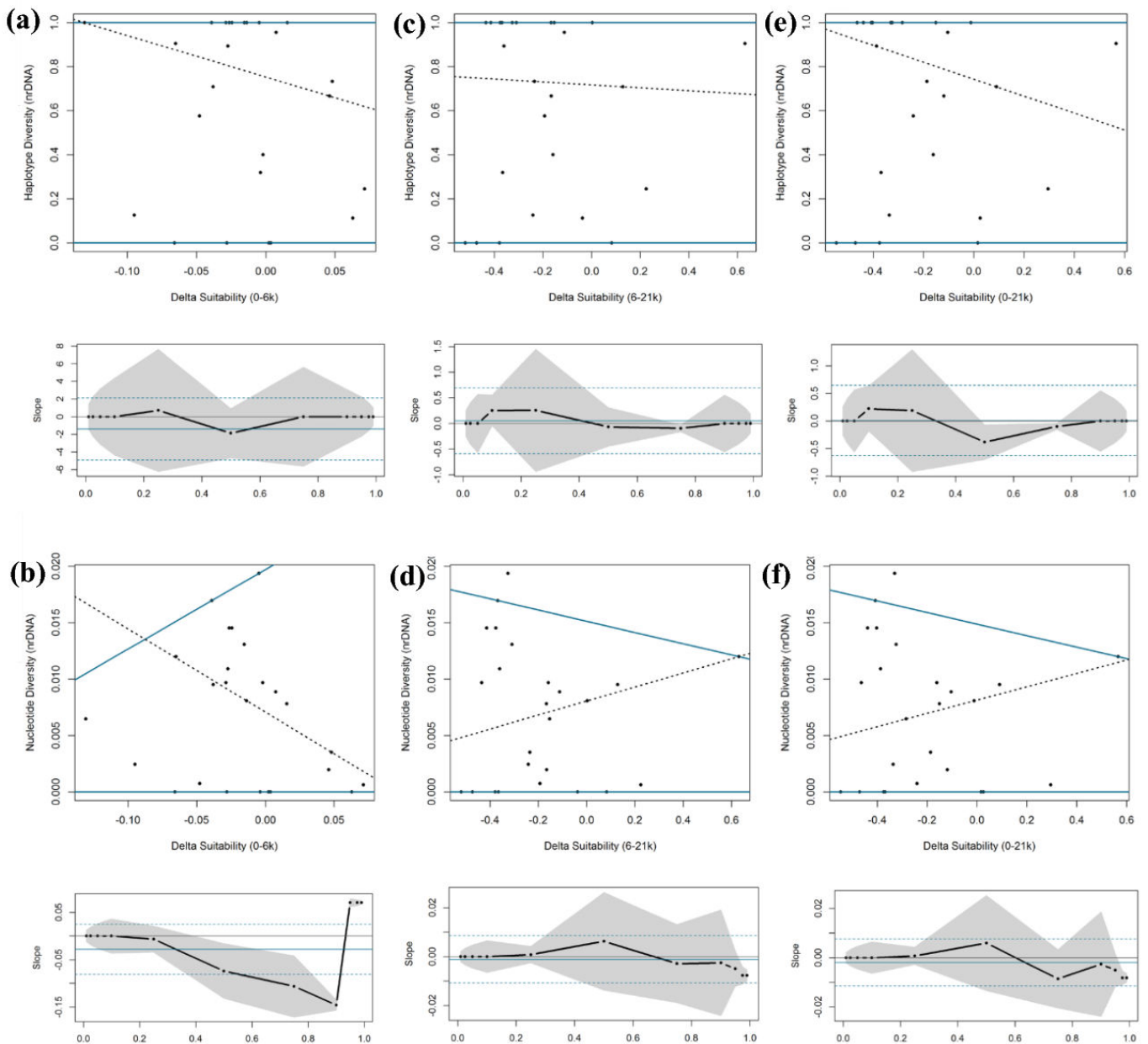


**Figure S3.11** Quantile regression for the relationships of haplotype and nucleotide diversities for nDNA among the 26 populations of *Scinax squalirostris* with stability and suitability in climatic conditions: (a) and (b) climatic stability through 6 Ka to present; (c) and (d) climatic stability through 21 Ka to 6 Ka; (e) and (f) climatic stability through 21 Ka to present. The upper figures show the triangle-shaped envelopes from 0.05 (lower line) and 0.95 (upper line) quantiles. The lower figures show the slope estimate for 0.01, 0.025, 0.05, 0.1, 0.25, 0.5, 0.75, 0.9, 0.95, 0.975 and 0.99 quantiles (area in grey indicates 95% confidence interval around estimates).

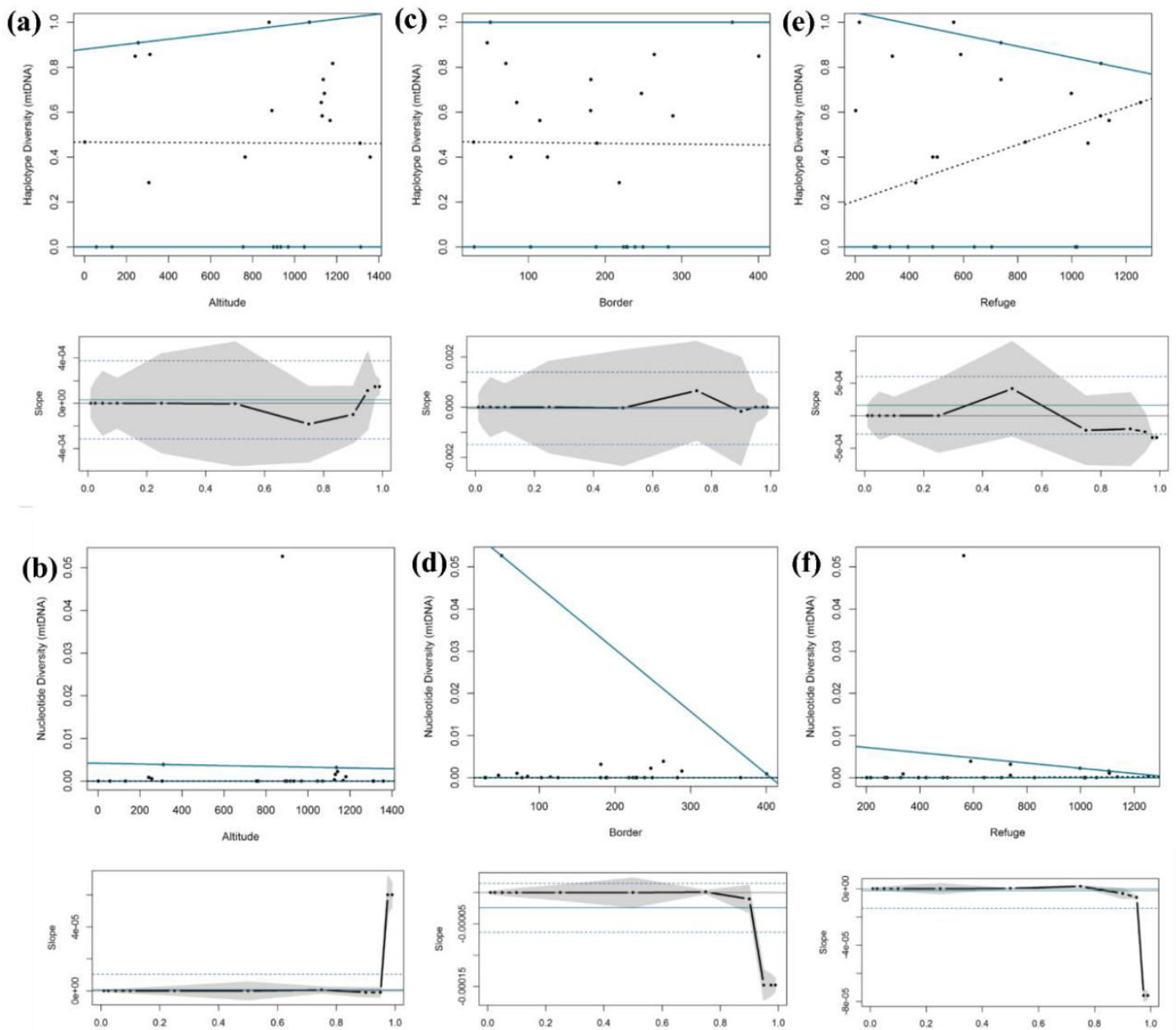


**Figure S3.12** Quantile regression for the relationships of haplotype and nucleotide diversities (mtDNA) among the 26 populations with altitude, edges and centroid distances of the historical refuge occupied by *S. squalirostris* through the last glacial period: (a) and (b) altitude (in meters), (c) and (d) distance from the edge of the historical refuge (in kilometers), and (e) and (f) distance from the centroid of the historical refuge (in kilometers). The upper figures show the triangle-shaped envelopes from 0.05 (lower line) and 0.95 (upper line) quantiles. The lower figures show the slope estimates for 0.01, 0.025, 0.05, 0.1, 0.25, 0.5, 0.75, 0.9, 0.95, 0.975 and 0.99 quantiles (area in grey indicates 95% confidence interval around estimates).

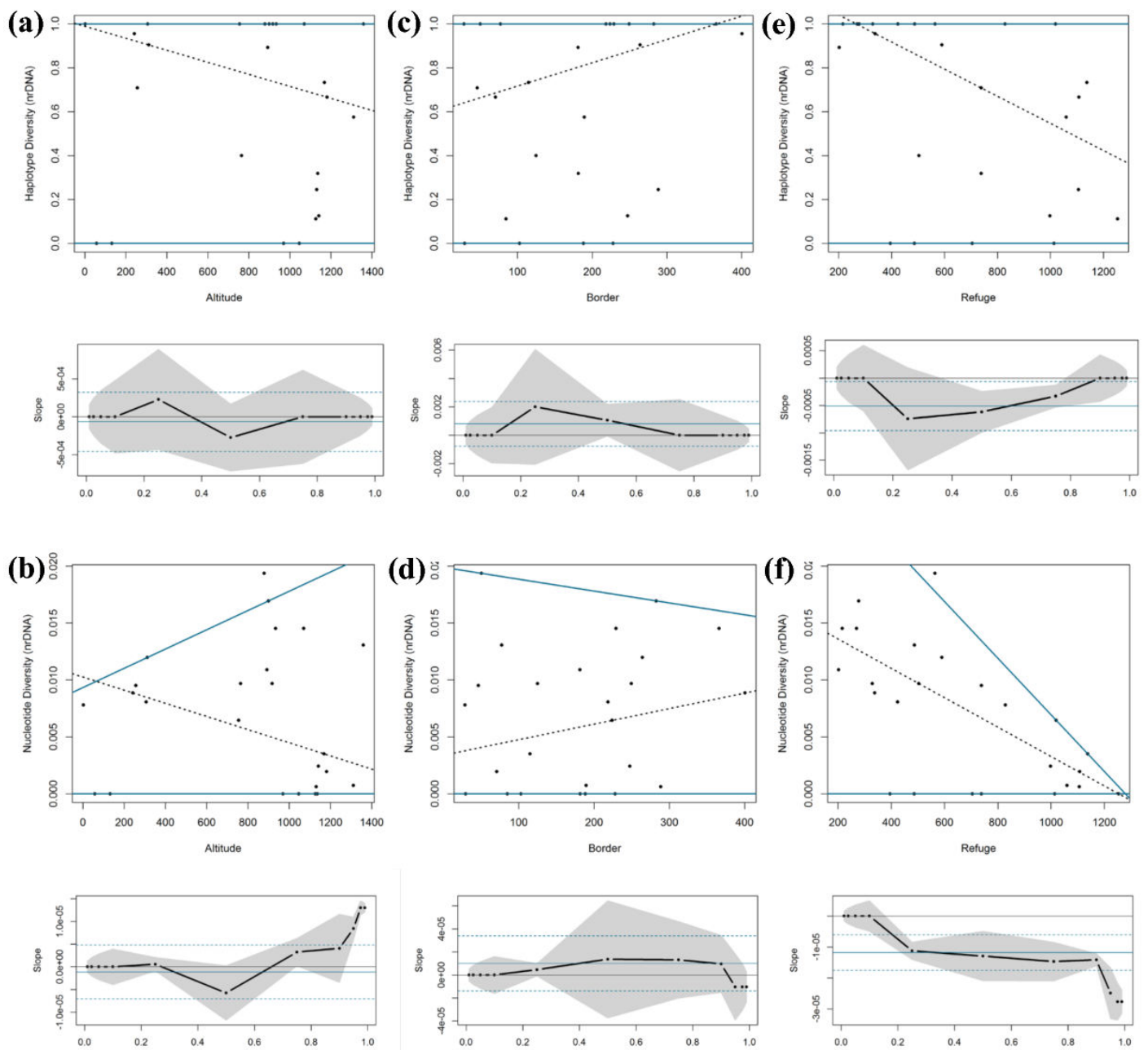


**Figure S3.13** Quantile regression for the relationships of haplotype and nucleotide diversities (nrDNA) among the 26 populations with altitude, edges and centroid distances of the historical refuge occupied by *S. squalirostris* through the last glacial period: (a) and (b) altitude (in meters), (c) and (d) distance from the edge of the historical refuge (in kilometers), and (e) and (f) distance from the centroid of the historical refuge (in kilometers). The upper figures show the triangle-shaped envelopes from 0.05 (lower line) and 0.95 (upper line) quantiles. The lower figures show the slope estimates for 0.01, 0.025, 0.05, 0.1, 0.25, 0.5, 0.75, 0.9, 0.95, 0.975 and 0.99 quantiles (area in grey indicates 95% confidence interval around estimates).



## Capítulo 2

---

**Revelando a diversidade do complexo de espécies de *Scinax squalirostris* (Lutz, 1925) (Anura, Hylidae), uma espécie com ampla distribuição disjunta**

Tatianne P. F. Abreu-Jardim<sup>1,2\*</sup>, Alejandro Valencia-Zuleta<sup>2</sup>, Natan M. Maciel<sup>2</sup> e Rosane G. Collevatti<sup>1</sup>

\*Autor de Correspondência: tatibio1@gmail.com

<sup>1</sup>Laboratório de Genética & Biodiversidade, Instituto de Ciências Biológicas, Universidade Federal de Goiás (UFG), Campus Samambaia, 74001-970, Goiânia, Goiás, Brazil.

<sup>2</sup>Laboratório de Herpetologia e Comportamento Animal, Departamento de Ecologia, Instituto de Ciências Biológicas, Universidade Federal de Goiás, Campus Samambaia, 74001-970, Goiânia, Goiás, Brazil.

**Título de cabeçalho:** Revelando o complexo *Scinax squalirostris*.

**Resumo**

A falta de conhecimento sobre as espécies pode afetar a compreensão de aspectos relacionados à biodiversidade em diversos níveis, como o entendimento dos padrões e processos que a regem. A ausência do conhecimento sobre espécies é denominada de lacuna Linneana. Um dos problemas associados a essa lacuna é o número elevado de

espécies não descritas. A presença de espécies crípticas (i.e. espécies diferentes com morfologias similares) podem elevar a complexidade do conhecimento real dos organismos. A taxonomia integrativa busca, através da utilização de várias fontes independentes, compreender a riqueza de espécies existentes. Assim, estratégias como a utilização de dados ditos não tradicionais como os moleculares, que levam em conta a história demográfica passada das espécies, e o uso de caracteres morfométricos e análises estatísticas, provém uma maior robustez na delimitação de uma espécie e na busca para revelar a cripticidade existente em nossa biodiversidade. Neste trabalho utilizamos medidas morfométricas e sequências de duas regiões mitocondriais e uma nuclear para verificar a possível existência de mais de uma espécie sob o mesmo nome de uma perereca Sul-Americana amplamente distribuída e com ocorrência disjunta, *Scinax squalirostris*. Os dados moleculares indicaram a existência de três linhagens evolutivamente distintas como possíveis candidatas a espécie. Entretanto, ao combinar as evidências destes dados como análises morfométricas revelaram a existência de duas linhagens, sendo uma candidata a espécie, em uma abordagem mais conservativa. A espécie candidata ocorre na região Centro-Oeste do Brasil, e não teria ainda nome constituindo uma nova espécie a ser descrita. Além disso, nossos resultados revelam a necessidade da realização de testes adicionais de hipóteses de relação entre as linhagens, com utilização de modelos de delimitação independentes e ainda a inclusão de dados morfológicos para melhor compreender esse complexo de espécie.

**Palavras-chave:** anfíbios, coalescente, delimitação, taxonomia integrativa, multiespécies.

## 1. INTRODUÇÃO

A ausência de informação e conhecimento sobre as espécies é um problema que pode afetar o acesso da biodiversidade, estudos ecológicos e evolutivos (Beheregaray & Caccione, 2007), pois ainda existe uma quantidade (desconhecida) de espécies a serem identificadas e descritas (Wilson, 2003). Essa falta de informação em relação ao conhecimento taxômico de espécies é denominada como lacuna Linneana (Lomolino, 2004; Hortal et al., 2015). Essa lacuna abrange duas categorias de ausência de informação sobre espécies, uma delas é que ainda existem espécies que não foram amostradas e a outra é que existem espécies que foram amostradas, mas não foram descritas (Hortal et al., 2015). Essa segunda categoria está em constante mudança, pois novas espécies são descritas, há um grande número de revisões taxonômicas e sinonimização de espécies. Um outro desafio ainda é a dificuldade em estabelecer um conceito unificado de espécie e como delimitá-las (De Queiroz, 2007; Freudenstein et al., 2017).

A utilização da taxonomia tradicional para delimitar espécies pode ser problemática, por basear-se apenas em caracteres fenotípicos, pois grupos de organismos podem apresentar pouca ou nenhuma variação morfológica (morfologia conservada), o que impede a sua descrição como espécie distinta, podendo gerar problemas de ações de conservação e o conhecimento real da riqueza global (Bickford et al., 2007). Esses grupos morfológicamente indistinguíveis são denominados de espécies crípticas, e geralmente são erroneamente associados a um único táxon (Beheregaray & Caccione, 2007). Métodos de taxonomia integrativa podem ajudar a revelar a diversidade críptica dos organismos, utilizando múltiplas fontes de dados (molecular, morfologia, comportamental, ecológico, etc) (Dayrat, 2005, Fujita et al., 2012). Com isso, houve o aumento do número de estudos utilizando dados morfológicos, morfométricos e genéticos na última década (Pante et al., 2015). Essa integração metodológica é funcional, pois cada método apresenta limites

intrínsecos para o delineamento das espécies, e mesmo quando dados morfológicos ou moleculares, por si só sejam capazes de delimitar uma unidade evolutiva como espécie, outras abordagens podem auxiliar e promover robustez na denominação de espécie (Bickford et al., 2007).

Recentemente, um dos métodos de delimitação mais utilizados tem sido inferir árvores de espécies através de múltiplas árvores gênicas (Knowles & Carstens, 2007). A abordagem de múltiplos genes pode fornecer hipóteses mais robustas, uma vez que combinam regiões do DNA com diferentes taxas evolutivas (Yang & Rannala, 2010). Métodos moleculares sob abordagens baseadas em modelos estatísticos vêm sendo utilizados para delimitar os limites de espécies, usando por exemplo, o modelo coalescente de multiespécies (Yang & Rannala, 2010).

A inferência sob o modelo coalescente de multiespécies fornece poder considerável na identificação de limites dos táxons recentemente divergidos e leva em conta a alta variância estocástica de processos genéticos (Sukumaran & Knowles, 2017). Assim, os dados genéticos podem ser utilizados para delimitar a espécie através de um critério de monofiletismo recíproco (Knowles & Carstens, 2007), em que se espera que haplótipos amostrados em uma espécie sejam mais intimamente relacionados entre si do qualquer haplótipo da outra espécie, devido ao longo tempo de divergência após a interrupção do fluxo gênico (Avice, 2000).

A ausência reciprocidade monofilética não indica a ausência de divergência de espécies, sendo que as espécies recentemente derivadas tenderão a não ser reveladas sob um critério monofilético (Knowles & Carstens, 2007). Eventos como esse, são caracterizados pela existência de um arranjo incompleto de linhagens, devido à ausência de tempo substancial para a separação completa das linhagens (Knowles & Carstens,

2007; Sukumaran & Knowles, 2017). Assim, o método de coalescência multiespécies, estima a árvore de espécie com múltiplas árvores gênicas, considerando a incongruência das árvores gênicas devido a retenção de polimorfismo ancestral, variação nas sequências moleculares e variação nos parâmetros demográficos (Yang & Rannala, 2010; Leaché & Fujita, 2010). Além disso, este método fornece um modelo apropriado para investigar e determinar linhagens separadas dentro de complexos de espécies (Yang & Rannala, 2010; Heled e Drummond, 2010), juntamente com a utilização de fontes de dados alternativos (Fujita et al., 2012; Olivier et al., 2014).

Anfíbios são um grupo de vertebrados com cerca de 7932 espécies reconhecidas (Frost, 2018), e com uma alta taxa de descoberta e descrição de espécies (Köhler et al., 2005). Porém, muitos de seus grupos refletem uma morfologia conservada, tornando-os um grupo desafiadores em sua taxonomia, o que poderia indicar que as espécies ainda se encontram no processo contínuo de especiação (De Queiroz, 2007). Assim, anfíbios que possuem ampla distribuição, que apresentam baixa capacidade de dispersão e alta filopatria (Duellman & Trueb, 1994; Blaustein *et al.*, 1994), podem apresentar uma alta estruturação geográfica, o que pode levar a representar um complexo de espécies. A utilização da taxonomia integrativa com dados moleculares pode trazer a luz essa diversidade críptica e categorizar as espécies candidatas, além de entender os processos que envolveram a diversificação dessas espécies (e.g. Gehara et al., 2014; Correia et al., 2017).

O gênero *Scinax* Wagler, 1830 possui ampla distribuição geográfica desde o México até a Argentina (Frost, 2018). Além disso apresenta uma taxonomia complexa devido ao grande número de espécies que compõem o grupo, inclusive morfologicamente semelhantes (Faivovich, 2002). Segundo Faivovich (2002), o gênero tem dois clados, *Scinax ruber* e *Scinax catharinae*, e alguns estudos mostram que o clado *S. ruber* pode

possuir uma alta diversidade críptica (Duellman et al., 2016, Ferrão et al., 2016). Entre essa diversidade críptica do clado *S. ruber*, encontra-se o caso de *Scinax squalirostris* (Lutz, 1925), uma pequena perereca (23 to 28mm) (Cei, 1980), que possui uma ampla distribuição geográfica, porém disjunta em formações de Campos nos Pampas, Chaco, Mata Atlântica e Cerrado. Essa espécie possui alta variação acústica (Faria et al., 2013) e morfológica, e vem sendo considerada como um complexo de espécies crípticas (Eterovick & Sazima, 2004). Assim neste trabalho, utilizamos a abordagem de taxonomia integrativa com *Scinax squalirostris* como modelo, combinando dados moleculares e morfométricos, com o objetivo de identificar e delimitar linhagens evolutivamente distintas que possam ser candidatas a espécie.

## **2. MATERIAL E MÉTODOS**

### **2.1 Amostragem e dados moleculares**

Foram amostrados 219 indivíduos de *Scinax squalirostris* em 26 localidades (Tabela 1), ao longo de sua distribuição geográfica no Brasil, Uruguai e Paraguai (Figura 1; Tabela 1). A extração do DNA foi realizada a partir de amostras de fígado ou tecido muscular preservados em etanol absoluto, utilizando o Kit Dneasy Blood & Tissue (Qiagen®, InR Chatsworth, CA). O DNA foi amplificado por reação em cadeia de polimerase (PCR) e sequenciado em um sequenciador automático de DNA ABI 3500 (Applied Biosystems® CA) usando o kit BigDye® Terminator Cycle Sequencing. Foi utilizado dois fragmentos mitocondriais (mtDNA), 12S e citocromo B (Cytb), e um nuclear (nDNA) gene de ativação de recombinação (RAG1) (para detalhes sobre primers, ampliações e condições de sequenciamento, consulte o Apêndice S1: Tabelas S1.1-S1.3 no material suplementar). As sequências consenso foram montadas para cada indivíduo usando o software Seqscape 2.7 (Applied Biosystems) e o alinhamento múltiplo foi feito pelo

software ClustalW (Thompson et al., 1997) implementado no software Bioedit 7.2.5 (Hall, 1999). Foi verificado a existência de saturação na segunda e terceira posição do códon, pelas transições e transversões com a distância TN93 (Tamura & Nei, 1993) usando o software Dambé (Xia, 2013). Como as posições do terceiro códon de CytB mostraram altos níveis de saturação (ver Apêndice S2: Figura S2.1 em material suplementar), elas foram excluídas do alinhamento final. As sequências de RAG1 mostraram indivíduos heterozigotos (138 indivíduos, 47 caracteres), portanto, utilizamos o haplótipo mais frequente, estimado pelo Phased implementado no DNAsp 5.0 (Librado & Rozas, 2009).

## **2.2 Dados morfométricos**

Medidas morfométricas de 365 indivíduos, sendo 269 machos, de oito museus/coleções (Apêndice S1: Tabela S1.4; Apêndice S3 para detalhes de números dos tombos e localidades), foram obtidas para integrar em uma análise discriminante baseado nos cladogramas gerados a partir da análise de delimitação (veja resultados). A identificação do sexo foi baseada na presença do saco vocal em machos. Os indivíduos representaram populações de toda a distribuição geográfica de *Scinax squalirostris* (Figura 1). As medidas foram baseadas em Heyer et al. (1990) e Watters et al. (2016), aferindo 15 caracteres morfométricos: comprimento rostro-cloacal (SVL), desde a ponta do focinho até a abertura cloacal; comprimento da cabeça (HL), distância perpendicular desde o tímpano até a ponta da boca; largura da cabeça (HW), entre na porção média dos tímpanos; diâmetro do olho (ED), entre a borda anterior e posterior do olho; diâmetro do tímpano (TD), entre a borda anterior e posterior do tímpano; distância interorbital (IOD), entre a base das pálpebras; distância internarinas (IND), entre as bordas das narinas; distância da narina à focinho (NSD), desde a borda da narina até a ponta do focinho;

distância olho-narina (E-N), desde a borda anterior à olho até a narina; comprimento do antebraço (FaL), desde a articulação braço-antebraço até a borda posterior do tubérculo palmar; comprimento da mão (HaL), desde a borda posterior do tubérculo palmar até a ponta do dedo III; comprimento da coxa (THL), desde a abertura cloacal até a articulação fêmur-tíbia; comprimento da tíbia (TiL), desde a articulação fêmur-tíbia até a articulação tíbia-tarso; comprimento do tarso (TaL), desde a articulação fêmur-tíbia até a articulação tarso-metatarso; comprimento do pé (FoL), desde a borda posterior do tubérculo metatarsal até a ponta do artelho IV. Todas as medidas foram realizadas utilizando um paquímetro digital (Mitutoyo) de precisão 0,01 mm.

### **2.3 Análises moleculares**

Para a análise de delimitação molecular, foi utilizado os dados genéticos combinados (mtDNA + nDNA), totalizando 1002pb. Foi utilizado duas espécies como grupo externo *Sphaenorhynchus lacteus* (12S: EF217472.1; RAG1: AY844527.1 e Cytb: AY549420.1) e *Pseudis paradoxa* (RAG1: AY844506.1), baseado em Duellman et al. (2016) e na disponibilidade dos dados no GenBank. O melhor modelo de substituição para cada partição (12S, Cytb e RAG) foi selecionado com base no Critério de Informação de Akaike corrigido (AICc) implementado no software jModelTest 2 (Darriba *et al.*, 2012) (Apêndice S1: Tabela S1.5). Para a datação molecular, foi usado taxas de mutação previamente estimadas para fragmentos mitocondriais e nuclear para a datação molecular de anfíbios anuros (Apêndice S1: Tabela S1.6) devido à falta de fósseis de Scinaxinae.

Para levar em conta o arranjo incompleto de linhagens, a análise de árvores de espécies foi realizada usando o modelo coalescente de multiespécies implementado no Beast 2.4.8 configurado no template \*Beast (*StarBeast*) (Bouckaert et al., 2014). Para

selecionar as possíveis linhagens, alocamos grupos de espécies de acordo com a localidade, sem a utilização de uma árvore guia previamente gerada, e utilizamos o template *StarBeastwithStacey*, que considera que cada haplótipo ou população pode ser uma linhagem independente. Foi selecionado o relógio molecular lognormal não correlacionado e o modelo de processo de especiação de Yule como *prior* para a árvore. Duas corridas independentes foram realizadas, cada uma com 150 milhões de gerações, amostrando a cada 1.500 gerações. A convergência e estacionariedade foram avaliadas (Tamanho efetivo amostral - ESS  $\geq$  200) usando o software Tracer 1.6 (Rambaut et al., 2014). As corridas e árvores foram combinadas após a remoção de 20% do *burn-in* com software LogCombiner 2.4.8 (Bouckaert et al., 2014) e a árvore de *Maximum Clade Credibility* (MCC) foi obtida com o software TreeAnnotator 2.4.8 (Bouckaert et al., 2014). A árvore foi visualizada e editada no software Figtree 1.4.3 (Rambaut, 2012). A análise foi realizada na plataforma Cipres 3.3 - *Cyberinfrastructure for Phylogenetic Research* (Miller et al., 2010).

## **2.4 Análises morfométricas**

Considerando que existe variação no tamanho corporal por dimorfismo sexual, nas análises só foram incluídos os machos (Hayek et al., 2001), pois apresentavam uma amostra mais representativa das populações em relação às fêmeas. Assim, variáveis morfométricas, foram integradas em uma análise discriminante (AD) com a função *lda* do pacote MASS (Venables & Ripley 2002). O AD é um método estatístico multivariado usado para discriminar e classificar grupos (variável categórica), o qual se baseia na combinação das variáveis que mais contribuem na separação desses grupos. O AD foi combinado com uma seleção de variáveis passo-a-passo segundo o critério de Lambda de Wilk's (função *greedy.wilks*, no pacote klaR: Weihs et al., 2005), com nível de 0.05 para

a decisão do teste de F. Esta seleção passo-a-passo baseia-se no desvio das variáveis dentro de cada grupo em relação ao desvio total sem distinção dos grupos. A decisão de entrada da variável é feita de acordo com o Lambda de Wilk's, assim, a primeira variável a entrar no modelo será aquela que proporciona a melhor diferenciação dos grupos. Além disso, foram feitas análises específicas para as três primeiras variáveis que mais contribuíram na discriminação dos grupos. Para essas variáveis foram feitas análises de variância (ANOVA) ou teste de Kruskal-Wallis, e posteriormente análises *post-hoc* para determinar de onde estava vindo essa variação entre os grupos. Todos os testes estatísticos foram feitos no programa R (R Core Team, 2016).

### **3. RESULTADOS**

#### **3.1 Análises moleculares**

As análises do \*Beast alcançaram convergência aparente, com ESS de pelo menos 300 para todos os parâmetros, mostrando convergência entre as corridas. Mas ainda assim, baixos valores de probabilidade a posteriori foram estimados para os clados formados (Figura 2). Contudo, não podemos desconsiderar a relação e a possível conformação dessas linhagens. Assim, para a realização das análises morfométricas, consideramos clados suportados acima de 60% de probabilidade a posteriori, adotando uma medida mais conservadora. A árvore de espécie estimada sugere a existência de três possíveis linhagens candidatas a espécie (Figura 2). Os iniciais eventos de divisão foram antigos, ~6 milhões de anos atrás (Ma) para o clado 1 em relação aos clados 2 e 3. Os outros eventos de cladogenese foram mais recentes, datando de ~ 4.0 Ma, entre os clados 2 e 3. O clado 1 inclui as populações do Paraguai e de Poços de Caldas em Minas Gerais (PMG). O clado 2 inclui as populações do Centro-Oeste brasileiro (BDF e CGO). Enquanto, o clado 3 agrupa o restante de populações presentes no Sudeste e Sul do Brasil (Figura 2).

### **3.2 Análises morfométricas**

Indivíduos das populações medidas foram distribuídas nos três agrupamentos gerados na análise de delimitação (ver subtópico 3.1). Como o número de populações medidas foi maior que nas amostras genéticas, populações não amostradas pelos dados genéticos foram alocadas nesses agrupamentos por similaridade morfológica e distância geográfica. Um resumo das medidas morfométricas para cada agrupamento está disponível na Tabela 2. As populações do clado 2 em média foram menores do que as outras populações (Tabela 2).

O AD incluiu em seus dois primeiros eixos o 99.97% da variação, sendo que o primeiro compilou o 96.8% (Tabela 3). Segundo o AD, só foi possível observar dois agrupamentos dos clados obtidos pelo método de delimitação de espécies (Figura 3). O clado 3, inclui dentro de sua variação o clado 1, incorporando indivíduos de populações do sul e sudeste do Brasil, junto com as populações de Paraguai, Uruguai e Argentina. Enquanto o clado 2 foi mais consistente, incluindo indivíduos somente do Centro-Oeste do Brasil (Figura 3). As variáveis mais importantes nessa separação foram a distância interorbital (IOD), comprimento da mão (HaL) e largura da cabeça (HW) (Tabela 4), as quais variaram entre os três clados (IOD:  $\chi^2=137.38$ ,  $p<0.001$ ; HaL:  $F=106.6$ ,  $p<0.001$ ; HW:  $F=104.2$ ,  $p<0.001$ ). Essa variação foi dada principalmente pelo clado 2, em relação aos outros dois clados (Tabela 5), sendo as populações desse clado em média, menores que os outros dois (Figura 4).

## **4. DISCUSSÃO**

Nossos resultados indicaram a formação três possíveis linhagens candidatas à espécie, porém com baixo suporte. De acordo os dados morfométricos, apenas dois clados podem

ser suportados a partir dessa evidência externa. Uma formação seria composta por populações da região Centro-Oeste e outra composta por populações das regiões Sul/Sudeste do Brasil, Paraguai e Uruguai.

#### **4.1 Delimitação Molecular**

A utilização do critério coalescente de múltiplas espécies pode gerar uma delimitação precisa de espécies (Maddison & Knowles, 2007), juntamente com dados independentes, como os morfométricos, morfológicos, acústicos, etc (Sólis-Lemus & Knowles, 2015). No caso de *Scinax squalirostris*, com a utilização dos dados moleculares e morfométricos foi possível categorizar duas linhagens como candidatas a espécie. Como o modelo coalescente de multiespécies considera um arranjo incompleto de linhagens, se espera incongruências genéticas na árvore de espécies (Sukumaran & Knowles, 2017), pois o evento de divisão de linhagens não corresponde um evento de especiação instantânea, mas sim uma especiação primária, que representa o isolamento inicial das populações (Sukumaran & Knowles, 2017). Isso ocorre, porque é necessária uma quantidade substancial de tempo após a divergência inicial para que haja um monofilismo recíproco observado na árvore de espécies (Knowles & Carstens, 2007; Mehta et al., 2016). Na árvore de espécies, o clado 2 foi monofilético, bem suportado e corroborado pelas diagnoses morfométrica. A cladogenese desse clado foi ~4.0Ma, que mostrou-se suficiente, indicando a ausência de fluxo gênico atual e de retenção de polimorfismo ancestral. Essas linhagens podem estar isoladas a mais tempo que os outros clados (clado 1 e clado 3), e de fato, a ocorrência dessas populações estão restritas a região do Centro-Oeste do Brasil, sendo geograficamente distantes das outras populações, o que facilitaria a divergência dessa linhagem em relação às outras. Em um estudo feito por Faria e colaboradores (2013) com avaliação canto de anúncio de *S. squalirostris* entraram

divergência de canto em populações da região Centro-Oeste do Brasil em relação as outras regiões, indicando a existência de uma linhagem críptica e reforçando nossos resultados de uma linhagem candidata a espécie. Essa linhagem se torna uma candidata a espécie, e ainda, sem um nome disponível para a sua associação, podendo ser descrito (ver abaixo em 4.3 Nomenclatura).

A árvore estimada neste trabalho foi baseada em uma abordagem não restritiva, ou seja, não foram estabelecidos e nem testados possíveis *constrains* de linhagens como espécies para testes de hipóteses de relações e nem utilizamos uma árvore guia *a priori*. Com essa abordagem obtivemos a formação dos clados 1 e 3, porém com baixo suporte e que não foram separados pela análise morfométrica. Como a delimitação de espécie consiste nessa etapa inicial de verificação de possíveis linhagens evolutivamente distintas sem a atribuição *à priori* e depois o teste de hipóteses baseado nas linhagens já atribuídas (Ence & Carstens, 2011), se faz necessário testar diferentes hipóteses de relação e conformação dos clados 1 e 3. Assim, ainda devemos testar modelos de espécies hipotéticas e analisar sob diferentes modelos de especiação (*Yule process* ou *Birth-Death model*) com os modelos coalescentes, levando em conta a estocasticidade genética. Com isso, a abordagem de limite e validação de espécies será mais robusta (Carstens et al., 2013).

## **4.2 Análise Morfométrica**

As análises morfométricas permitiram confirmar duas das linhagens obtidas pelas análises moleculares dentro do nome *S. squalirostris*. O clado 1 indicou variação morfométrica similar ao clado 3, sendo assim, difícil assimilar esses dois agrupamentos como linhagens evolutivas diferentes. Porém, isso não descarta a possibilidade dos clados

1 e 3 serem espécies candidatas diferentes. Dentro de anfíbios anuros, existem diferentes casos de espécies com diferenciação genética, mas sem clara evidência morfológica/morfométrica, e conformam unidades taxonômicas consistentes a partir de outras evidências (ver o caso de *Dendropsophus luddekei* e *D. molitor* [Guarnizo et al., 2012] ou das espécies de *Melanophryniscus* [Rojas-Zamora et al., 2018]). No entanto, no caso *S. squalirostris* para os clados 1 e 3, considerando o baixo suporte das análises de delimitação, seguimos uma abordagem conservadora na ausência de outras evidências disponíveis. O clado 2, que incluiu nas análises morfométricas populações do centro-oeste brasileiro de Goiás e de São Paulo, pode ser diagnosticado morfometricamente do clado 1+ clado 3 em tamanho, sendo a distância interorbital (IOD), a largura da cabeça (HW) e a longitude da mão (HaL) menores. Essa diferenciação pode vir acompanhada por mudança no padrão morfológico dos indivíduos (Bookstein, 1991; Kaliontzopoulou, 2011). Como por exemplo, o formato da cabeça (Figura 5), é subovóide (*subovoid*) para os clados 1 e 3, e pontuda (*pointed*) para o clado 2 segundo os formatos de Heyer et al. (1990) (Figura 5). No entanto, a morfometria necessita de análises morfológicas mais específicas, como variação do padrão de coloração e membranas interdigitais dos pés, acompanhados de outras linhas de evidências comportamentais e ecológicas, que permitam suportar mais robustamente as espécies candidatas.

### 4.3 Nomenclatura

Considerando a provável nomenclatura dos dois clados suportados pelas análises morfométricas, temos quatro nomes associados para *S. squalirostris*. (1) O sinônimo senior da espécie, *Hyla leucotaenia* descrita pelo Burmeister (1861) de lagos ao longo do rio Paraná, na Argentina, sendo um nome recuperado e designado como um nome esquecido (*nomem oblitum*) associado com *S. squalirostris* por Pinheiro et al. (2014). (2)

O nome *Hyla squalirostris* descrito pelo Lutz (1925) de Serra da Bocaina, São Paulo, Brazil. (3) O nome *Hyla lindneri* descrito pelo Müller & Hellmich (1936) em Formosa, Argentina. E (4) o nome *Hyla evelynae* descrito pelo Schmidt (1944) em San Carlos, Uruguai. Todos os nomes encontram-se limitados para o sudeste do Brasil, Uruguai e Argentina, o que incluiria as populações geograficamente limitadas nos clados 1 e 3, assumindo assim, o nome válido para a espécie, que seria *Scinax squalirostris*. Enquanto que, as populações do clado 2, não possuem nenhum nome descrito na sua área geográfica, portanto, ficariam sem nome disponível. Assim, o clado 2 poderia ser nomeado e descrito formalmente para as populações do Centro-Oeste brasileiro.

Em conclusão nossos resultados indicam a existência de duas possíveis linhagens candidata a espécie: (i) as populações de Centro-Oeste brasileiro e (ii) as populações presentes no Sudeste e Sul do Brasil, Uruguai, Paraguai e Argentina. Mesmo que com baixo suporte e levando em conta a estocasticidade genética, não podemos descartar a formação desses grupos acima mencionados, que foram corroborados pelos dados morfométricos. Além disso, nossos resultados mostram que ainda é necessário a utilização de métodos e teste de hipóteses de relação de espécies, bem como a utilização de mais dados como fonte externa para a corroboração da delimitação molecular, tais como a inclusão de dados morfológicos e acústicos.

## **AGRADECIMENTOS**

Este trabalho foi financiado pelo CNPq (projeto no. 475333/2011-0) e CAPES/PROCAD (projeto no. 88881.068425/2014-01). TPF AJ recebeu bolsa de doutorado da FAPEG (projeto no. 201410267000553), e AVZ recebeu bolsa da CAPES (projeto no. 1692475). NMM e RGC recebem bolsa de produtividade do CNPq, ao qual agradecemos.

Agradecemos a todas as pessoas e suas instituições que gentilmente coletaram, doaram espécimes, enviaram amostras de tecidos e amostras de empréstimos.

## REFERÊNCIAS

- Avise, J. C. 2000. *Phylogeography: the history and formation of species*. Cambridge: Harvard University Press.
- Beheregaray, L. B., and A. Caccone. 2007. Cryptic biodiversity in a changing world. *Journal of Biology*, 6-9.
- Bickford, D., D. J. Lohman, N. S. Sodhi, P. K. L. Ng, R. Meier, K. Winker, K. K. Ingram, and I. Das. 2007. Cryptic species as a window on diversity and conservation. *Trends in Ecology and Evolution*, 22, 148–155.
- Blaustein, A. R., Wake, D. B. & Sousa, W. P. 1994. Amphibian Declines: Judging Stability, Persistence, and Susceptibility of Populations to Local and Global Extinctions. *Conservation Biology*, 8, 60-71.
- Bookstein, F. L. 1991. *Morphometric Tools for Landmark Data: Geometry and Biology*. Cambridge University press, Cambridge, United kingdom.
- Bouckaert, R., Heled, J., Kühnert, D., Vaughan, T., Wu, C. H., Xie, D., Suchard, MA., Rambaut, A., and Drummond, A. J. 2014. BEAST 2: A Software Platform for Bayesian Evolutionary Analysis. *PLoS Computational Biology*, 10, e1003537.
- Burmeister, H. 1861. *Reise durch die La Plata-Staaten mit besonderer Rücksicht auf die Physische Beschaffenheit und den Culturzustand der Argentinische Republik. Ausgeführt in den Jahren 1857, 1858, 1859 un 1860. Volume 2.* Halle: H. W. Schmidt.
- Carstens, B. C., Pelletier, T. A., Reid, N.M. and Satler, J. D. 2013. How to fail at species delimitation. *Molecular Ecology*, 22, 4369–4383.
- Cei, J. M. 1980. Amphibians of Argentina. *Monitore Zoologico Italiano. Nuova Serie, Monographia*, 2, 1-609.

- Correa, C., Vásquez, D., Castro-Carrasco, C., Zúñiga-Reinoso, Á., Ortiz, J.C. and Palma, R.E. 2017. Species delimitation in frogs from South American temperate forests: The case of *Eupsophus*, a taxonomically complex genus with high phenotypic variation. *PLoS ONE*, 12, e0181026.
- Dayrat, B. 2005. Towards integrative taxonomy. *Biological Journal of the Linnean Society*, 85, 407–415.
- Duellman, W. E., Marion, A. B. and Hedges, S. B. 2016. Phylogenetics classification and biogeography of the treefrogs (Amphibia: Anura: Arboranae). *Zootaxa*, 4104, 001-109.
- Duellman, W. E., and Trueb, L. 1994. Biology of amphibians. The Johns Hopkins University Press. USA. pp. 1-670.
- Ence, D. D. and Carstens, B. C. 2011. SpedeSTEM: a rapid and accurate method for species delimitation. *Molecular Ecology Resources*, 11, 473–480.
- Eterovik, P. C. and Sazima, I. 2004. Anfíbios da Serra do Cipó-Minas Gerais-Brasil. Belo Horizonte. Ed. PUCMINAS.
- Faivovich, J. 2002. A cladistics analysis of *Scinax* (Anura: Hylidae). *Cladistics*, 18, 367–393.
- Faria, D.C. C, Signorelli, L., Morais, A. R., Bastos, R. P. and Maciel, N. M. 2013. Geographic structure and acoustic variation in populations of *Scinax squalirostris* (A. Lutz, 1925) (Anura: Hylidae). *North-Western Journal of Zoology*, 9, 329-336.
- Ferrão, M., Colatreli, O., de Fraga, R., Kaefer, I. L., Moravec, J. and Lima, A. P. 2016. High Species Richness of *Scinax* Treefrogs (Hylidae) in a Threatened Amazonian Landscape Revealed by an Integrative Approach. *PLoS ONE*, 11,e0165679.
- Frost, D. R. (2018). Amphibian Species of the World: An Online Reference. Version 5.7. Electronic Database accessible at <http://research.amnh.org/herpetology/amphibia/index.html>. American Museum of Natural History, New York, USA.
- Fujita, M. K., Leaché, A. D., Burbrink, F. T., McGuire, J. A. and Moritz, C. 2012. Coalescent-based species delimitation in an integrative taxonomy. *Trends in Ecology and Evolution*, 27, 480–488.

- Gehara, M., Crawford, A. J., Orrico, V. G. D., Rodríguez, A. et al. 2014. High Levels of Diversity Uncovered in a Widespread Nominal Taxon: Continental Phylogeography of the Neotropical Tree Frog *Dendropsophus minutus*. *PLoS ONE*, 9, e103958.
- Guarnizo, C. E., Escallón, D. C. Cannatella, and A. Amézquita. 2012. Congruence between acoustic traits and genealogical history reveals a new species of *Dendropsophus* (Anura: Hylidae) in the high Andes of Colombia. *Herpetologica*, 68, 523–540.
- Hall, T. A. 1999. BioEdit: a user-friendly biological sequence alignment editor and analysis program for Windows 95/98/NT. *Nucleic Acids Symposium Series*, 41, 95- 98.
- Hayer, L. A., Heyer, W. R. & Gascon, C. 2001. Frog morphometric: a cautionary tale. *Alytes*, 18, 153-177.
- Heled, J. and Drummond, A. J. 2010. Bayesian inference of species trees from multilocus data. *Molecular Biology and Evolution*, 27, 570-580.
- Heyer, W. R., Rand, A. S., da Cruz, C. A. G., Peixoto, O. L., and Nelson, C. E. 1990. Frogs of Boracéia. *Arquivos de Zoologia* (São Paulo), 31, 231-410.
- Hortal, J., de Bello, F., Diniz-Filho, J. A. F., Lewinsohn, T. M., Lobo, J. M. and Ladle, R. J. 2015. Seven Shortfalls that Beset Large-Scale Knowledge of Biodiversity. *Annual Review of Ecology, Evolution and Systematics*, 46, 523–549.
- Kaliontzopoulou, A. 2011. Geometric morphometrics in herpetology: modern tools for enhancing the study of morphological variation in amphibians and reptiles. *Basic and Applied Herpetology*, 25, 5-32.
- Köhler, J., Vieites, D. R., Bonett, R. M., García, F. H., Glaw, F., Steinke, D., and Vences, M. 2005. New amphibians and global conservation: a boost in species discoveries in a highly endangered vertebrate group. *AIBS Bulletin*, 55, 693-696.
- Librado, P. and Rozas, J. 2009. Dnasp: software for comprehensive analysis of DNA polymorphism data.

- Leaché, A. D. and Fujita, M.K. 2010. Bayesian species delimitation in West African forest geckos (*Hemidactylus fasciatus*). *Proceedings of the Royal Society of London B*, 277, 3071–3077.
- Lomolino, M. V. 2004. Conservation biogeography. In *Frontiers of Biogeography: New Directions in the Geography of Nature*, ed. MV Lomolino, LR Heaney, pp. 293–96. Sunderland, MA: Sinauer.
- Lutz, A. 1925. Batraciens du Brésil. *Comptes Rendus et Mémoires Hebdomadaires des Séances de la Société de Biologie et des ses Filiales*, vol. 2, Paris, pp. 211–214.
- Müller, L., and W. Hellmich. 1936. Amphibien und Reptilien. I. Teil: Amphibia, Chelonia, Loricata. *Wissenschaftliche Ergebnisse der Deutschen Gran Chaco-Expedition. Amphibien und Reptilien: 1–120*. Stuttgart, Strecker und Schröder.
- Oliver, P. M., Laver, R. J., Melville, J. and Doughty, P. 2014. A new species of Velvet Gecko (Order: Diplodactylidae) from the limestone ranges of the southern Kimberley, Western Australia. *Zootaxa*, 3873, 49–61.
- Pante, E., Schoelinck, C. and Puillandre, N. 2015. From Integrative Taxonomy to Species Description: One Step Beyond. *Systematic Biology*, 64, 152–160.
- R Core Team. 2018. R: A language and environment for statistical computing. R Foundation for Statistical Computing, Vienna, Austria. URL: <https://www.R-project.org/>.
- Venables, W. N. and Ripley, B. D. 2002. *Modern Applied Statistics with S*. Fourth Edition. Springer, New York.
- Rambaut, A. 2012. Figtree 1.4.0. <http://tree.bio.ed.ac.uk/software/figtree/>.
- Rojas-Zamora, R. R., Fouquet, A., Ron, S. R., Hernández-Ruz, E. J., Melo-Sampaio, P. R., Chaparro, J. C., Vogt, R. C., de Carvalho, V. T., Pinheiro, L. C., Ávila, R. W., Farias, I. P., Gordo, M. and Hrbek, T. 2018. A Pan-Amazonian species delimitation: high species diversity within the genus *Amazophrynella* (Anura: Bufonidae). *PeerJ*, 6, 1–56.
- Schmidt, K. P. 1944. New frogs from Misiones and Uruguay. *Field Museum of Natural History Publication. Zoological Series*, 29, 153–160.

- Tamura, K. and Nei, M. 1993. Estimation of the number of nucleotide substitutions in the control region of mitochondrial DNA in humans and chimpanzees. *Molecular Biology and Evolution*, 10, 512-526.
- Thompson, J. D., Gibson, T. J., Plewniak, F., Jeanmougin, F. & Higgins, D. G. 1997. The Clustal W windows interface: flexible strategies for multiple sequence alignment aided by quality analysis tools. *Nucleic Acids Research*, 24, 4876–4882.
- Xia, X. 2013. DAMBE5: A comprehensive software package for data analysis in molecular biology and evolution. *Molecular Biology and Evolution*, 30, 1720-1728.
- Yang, Z. and Rannala, B. 2010. Bayesian species delimitation using multilocus sequence data. *Proceedings of the National Academy of Sciences of the United States of America*, 107, 9264–9269.
- Watters, J. L., Cummings, S., Flanagan, R. L. & Silver, C. D. 2016. Review of morphometric measurements used in anuran species descriptions and recommendations for a standardized approach. *Zootaxa*, 4, 477- 495.
- Weihs, C., Ligges, U., Luebke, K. and Raabe, N. 2005. klaR Analyzing German Business Cycles. In Baier, D., Decker, R. and Schmidt-Thieme, L. (eds.). *Data Analysis and Decision Support*, 335-343, Springer-Verlag, Berlin.
- Wilson, E. O. 2003. *The encyclopedia of life*. *Trends Ecology and Evolution*, 18, 77–80.

## **MATERIAL SUPLEMENTAR**

**Apêndice S1** Tabelas Suplementares (Tabelas S1.1 - S1.6) contendo informações sobre primers, amplificação, sequenciamento, locais das amostras cedidas para as medidas morfométricas, modelos evolutivos e taxas de mutação.

**Apêndice S2** Figura suplementar (Figuras S3.1) gráfico de saturação com as taxas de transição e transversão.

**Apêndice S3** Detalhes de número tombo e localidades das espécimes utilizadas na análise morfométrica.

**Declaração de conflito de interesse:** Os autores declaram não ter conflito de interesses.

**Tabela 1.** Locais de amostragem das 26 populações de *Scinax squalirostris*. Nome das localidades, abreviação de estados brasileiros e departamento paraguaio. Coluna de coleção nós apresentamos a abreviação de instituições doadoras. (Coleção de Anfíbios Célio F. B. Haddad (CFBH), Coleção da Universidade Federal de Minas Gerais (UFMG), Coleção Zoológica da Universidade Federal de Goiás (ZUFG), Coleção Elaine Maria Lucas Gonsales (EMLG), Museu de Ciências e Tecnologia da PUCRS (MCT), Coleção da Universidade Federal do Rio Grande do Sul (UFRGS), Coleção de Herpetologia do Instituto de Investigação Biológica do Paraguai (IIBPH).

Localidade	Código da População	Número de indivíduos	Coleção	Latitude	Longitude
Itirapina - São Paulo	ISP	5	CFBH	-22.2744	-47.796
Bocaina - São Paulo	BSP	12	CFBH	-23.3458	-44.483
São Roque - Minas Gerais	SRMG	11	CFBH	-20.1461	-46.663
Ouro Preto - Minas Gerais	OMG	16	CFBH	-20.2875	-43.508
Catas Altas - Minas Gerais	CMG	3	UFMG	-20.0747	-43.408
Poços de Caldas - Minas Gerais	PMG	1	UFMG	-21.7878	-46.561
Serra do Cabral - Minas Gerais	SMG	16	LOD	-17.6992	-44.271
Sempre Vivas - Minas Gerais	SVMG	22	ZUFG	-17.7883	-43.798
Serra do Cipó - Minas Gerais	SCMG	13	ZUFG	-19.2469	-43.510
Chapada dos Veadeiros - Goiás	CGO	24	ZUFG	-14.0833	-47.467
Brasília- Goiás	BDF	19	ZUFG	-15.7797	-47.930
Bonito- Mato Grosso do Sul	BMS	7	ZUFG	-21.1211	-56.482
Itapiranga - Santa Catarina	ISC	26	CFBH	-27.1833	-53.733
São José do Norte - Rio Grande do Sul	SJRS	10	UFRGS	-32.0147	-52.042
São Francisco de Paula - Rio Grande do Sul	SFRS	2	MCP	-29.4481	-50.584
Bom Jesus - Rio Grande do Sul	BRS	1	CFBH	-28.6678	-50.417
Palmas- Paraná	PPR	2	ZUFG	-26.4842	-51.991
Ponta Grossa - Paraná	PGPR	8	ZUFG	-25.095	-50.162
Campo Belo - Santa Catarina	CBSC	1	MCP	-27.8992	-50.761
Campos Novos - Santa Catarina	CNSC	2	CFBH	-27.4017	-51.225
Bom Jardim - Santa Catarina	BSC	5	CFBH	-28.3369	-49.625
Caçador- Santa Catarina	CSC	3	EMLG	-26.7753	-51.015
Água Doce - Santa Catarina	ASC	1	EMLG	-26.9978	-51.556
Estancia San José -Ñeembucú - Paraguai	EPY	1	IIBPH	-27.2016	-58.449
Alto Vera - Paraguai	APY	7	IIBPH	-26.5833	-55.633
Uruguai	URU	1	-	-33.0000	-56.000

**Tabela 2.** Resumo das medidas morfométricas de machos de *Scinax squalirostris*. Para cada variável é mostrado a média com o desvio padrão, e entre parênteses o range com o valor máximo e mínimo. Siglas das medidas: comprimento focinho-cloaca (**SVL**), comprimento da cabeça (**HL**), largura da cabeça (**HW**), diâmetro do olho (**ED**), diâmetro do tímpano (**TD**), distância interorbital (**IOD**), distância internarinas (**IND**), distância da narina à focinho (**NSD**), distância olho-narina (**E-N**), comprimento do antebraço (**FaL**), comprimento da mão (**HaL**), comprimento da coxa (**THL**), comprimento da tíbia (**TiL**), comprimento do tarso (**TaL**), comprimento do pé (**FoL**).

Variável	Clado 1 (n=12)	Clado 2 (n=76)	Clado 3 (n=181)
SVL	22.9 ± 1.01 (21.62–24.86)	20.74 ± 1.13 (17.84–23.48)	23.24 ± 1.51 (18.99–26.54)
HL	8.47 ± 0.39 (7.92–9.3)	7.47 ± 0.77 (5.51–9.11)	8.3 ± 0.64 (6.36–10.18)
HW	5.65 ± 0.4 (5.1–6.18)	5.11 ± 0.39 (4.21–5.97)	5.99 ± 0.49 (4.9–7.42)
ED	2.19 ± 0.21 (1.87–2.52)	2.08 ± 0.28 (1.58–2.7)	2.34 ± 0.27 (1.54–3.1)
TD	1.24 ± 0.08 (1.12–1.34)	1.13 ± 0.25 (0.75–2.39)	1.25 ± 0.18 (0.72–1.67)
IOD	2.47 ± 0.26 (2.08–2.98)	1.95 ± 0.17 (1.55–2.42)	2.47 ± 0.28 (1.95–3.59)
IND	1.81 ± 0.18 (1.47–2.05)	1.54 ± 0.2 (1.11–2.08)	1.76 ± 0.22 (1–2.69)
E-N	2.81 ± 0.2 (2.43–3.07)	2.66 ± 0.35 (1.97–3.5)	2.95 ± 0.36 (2.04–3.83)
NSD	1.4 ± 0.21 (1.05–1.72)	1.44 ± 0.23 (0.93–1.89)	1.5 ± 0.2 (0.96–1.98)
THL	10.12 ± 0.66 (9.28–11.07)	9.44 ± 0.7 (6.92–10.81)	10.41 ± 0.82 (8.28–12.79)
TiL	12.19 ± 0.68 (11.06–13.21)	11.23 ± 0.67 (9.76–12.56)	12.33 ± 0.93 (9.99–15.06)
TaL	6.2 ± 0.47 (5.49–7.18)	6.12 ± 0.58 (4.75–7.33)	6.61 ± 0.7 (4.76–8.48)
FoL	9.73 ± 0.91 (8.08–11.07)	9.27 ± 0.8 (7.46–11.63)	10.21 ± 1.03 (7.39–13.33)
FaL	3.42 ± 0.3 (2.96–3.87)	3.29 ± 0.3 (2.64–4.12)	3.68 ± 0.39 (2.64–5.03)
HaL	5.45 ± 0.36 (5.02–6.23)	4.51 ± 0.42 (3.09–5.2)	5.45 ± 0.5 (3.66–6.62)

**Tabela 3.** Coeficientes de variação da análise discriminante (AD) para os indivíduos machos das populações de *Scinax squalirostris*. Siglas: distância interorbital (**IOD**), comprimento da mão (**HaL**), largura da cabeça (**HW**), distância da narina à focinho (**NSD**), distância internarinas (**IND**), diâmetro do olho (**ED**), comprimento do antebraço (**FaL**), comprimento do pé (**FoL**).

<b>Variáveis</b>	<b>LD1</b>	<b>LD2</b>
IOD	-1.9677	-0.298
HaL	-1.156	-1.4178
HW	-0.9416	0.92573
NSD	1.65699	0.74628
IND	-0.6072	-2.5382
ED	-0.6141	1.68076
FaL	-0.5215	1.23947
FoL	0.22177	0.34809
Proporção dos eixos	0.9683	0.0317

**Tabela 4.** Variáveis que mais contribuem na discriminação dos agrupamentos segundo o critério do Lambda de Wilk's com 0.05 para decisão para a estatística F. A estatística F da diferença compara o modelo incluindo a nova variável com o modelo que não a incluem. Siglas: distância interorbital (**IOD**), comprimento da mão (**HaL**), largura da cabeça (**HW**), distância da narina à focinho (**NSD**), distância internarinas (**IND**), diâmetro do olho (**ED**), comprimento do antebraço (**FaL**), comprimento do pé (**FoL**).

	<b>Variáveis</b>	<b>Lambda de Wilk's</b>	<b>Estatística F</b>	<b>p</b>	<b>F da diferença</b>	<b>p da diferença</b>
1	IOD	0.5441142	111.43398	<0.0001	111.433981	<0.0001
2	HaL	0.4138502	73.46541	<0.0001	41.705864	<0.0001
3	HW	0.3688121	56.90391	<0.0001	16.119403	<0.0001
4	NSD	0.349366	45.48858	<0.0001	7.319427	0.0008
5	IND	0.3397214	37.5021	<0.0001	3.71907	0.0255
6	ED	0.331049	32.10371	<0.0001	3.418644	0.0342
7	FAL	0.3228558	28.22602	<0.0001	3.29906	0.0385
8	FoL	0.3153119	25.28035	<0.0001	3.098312	0.0468

**Tabela 5.** Valores de significância das comparações múltiplas das médias das três variáveis que mais contribuíram na diferenciação dos clados ( $p > 0.05$ ). Siglas: distância interorbital (**IOD**), comprimento da mão (**HaL**), largura da cabeça (**HW**).

<b>Comparação</b>	<b>IOD</b>	<b>HaL</b>	<b>HW</b>
Clado 1 vs Clado 2	<0.0001	<0.0001	<0.0001
Clado 1 vs Clado 3	0.9928	0.9999	0.0501
Clado 2 vs Clado 3	<0.0001	<0.0001	<0.0001

## Lista de Figuras

**Figura 1.** Distribuição da amostragem de *Scinax squalirostris*. (A) Área de amostragem. (B). Os pontos pretos representam a amostragem dos dados genéticos, e os pontos rosas apresentam os pontos de amostragem para as medidas morfométricas.

**Figura 2.** Árvore de espécies estimada pelo modelo coalescente multiespécies no \*Beast. (A) Árvore consenso de espécies. As barras cinzas correspondem ao intervalo de credibilidade a 95% do tempo estimado para a idade do nó. Os números abaixo dos ramos correspondem ao suporte do nó (probabilidades a posteriori) e os números acima dos ramos representam a idade do nó. A escala está em milhões de anos (Ma) antes do presente. Para obter detalhes sobre códigos e localidades das populações consulte a Tabela 1. (B) Visualização de todas as árvores obtidas (10.000 árvores) com as duas análises estimadas no \*Beast. As cores dos clados representam as divisões utilizadas para fazer as análises discriminantes.

**Figura 3.** Análise discriminante baseado nos clados gerados pela análise de delimitação de espécies no \*Beast. As cores representam os clados como descrito na legenda.

**Figura 4.** Variáveis que mais influenciaram a separação dos clados na análise discriminante. As cores representam os clados estimados na árvore de espécie pelo \*Beast. Siglas: distância interorbital (IOD), comprimento da mão (HaL), largura da cabeça (HW).

**Figura 5.** Cabeça em vista dorsal de *Scinax squalirostris*. (A) ZUFG 5417 de Alto Paraíso de Goiás, Goiás, Brasil. (B) CBFH 30890 de Serra da Bocaina, São Paulo, Brasil.

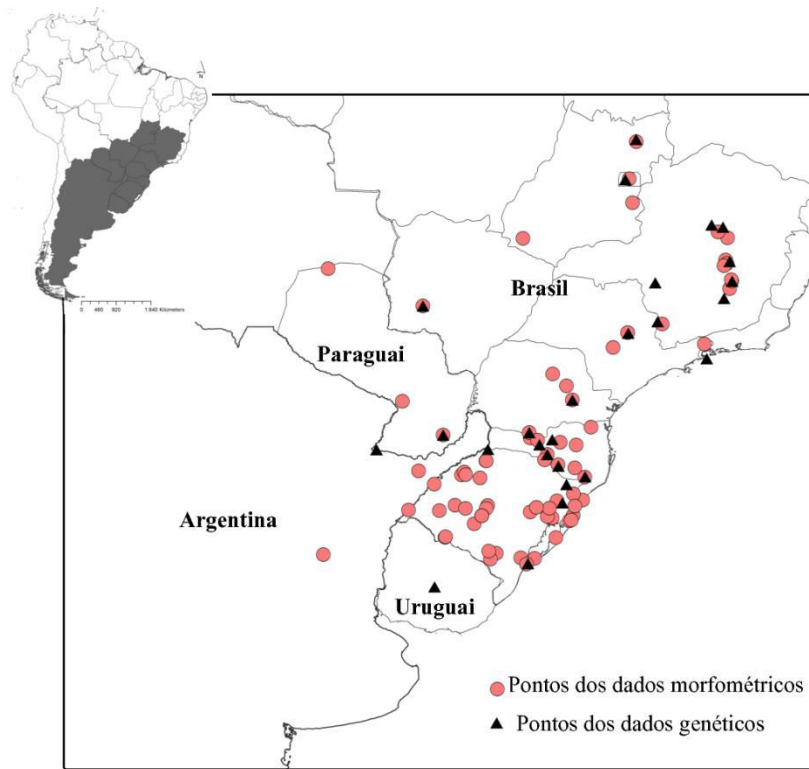


**Figura 1**

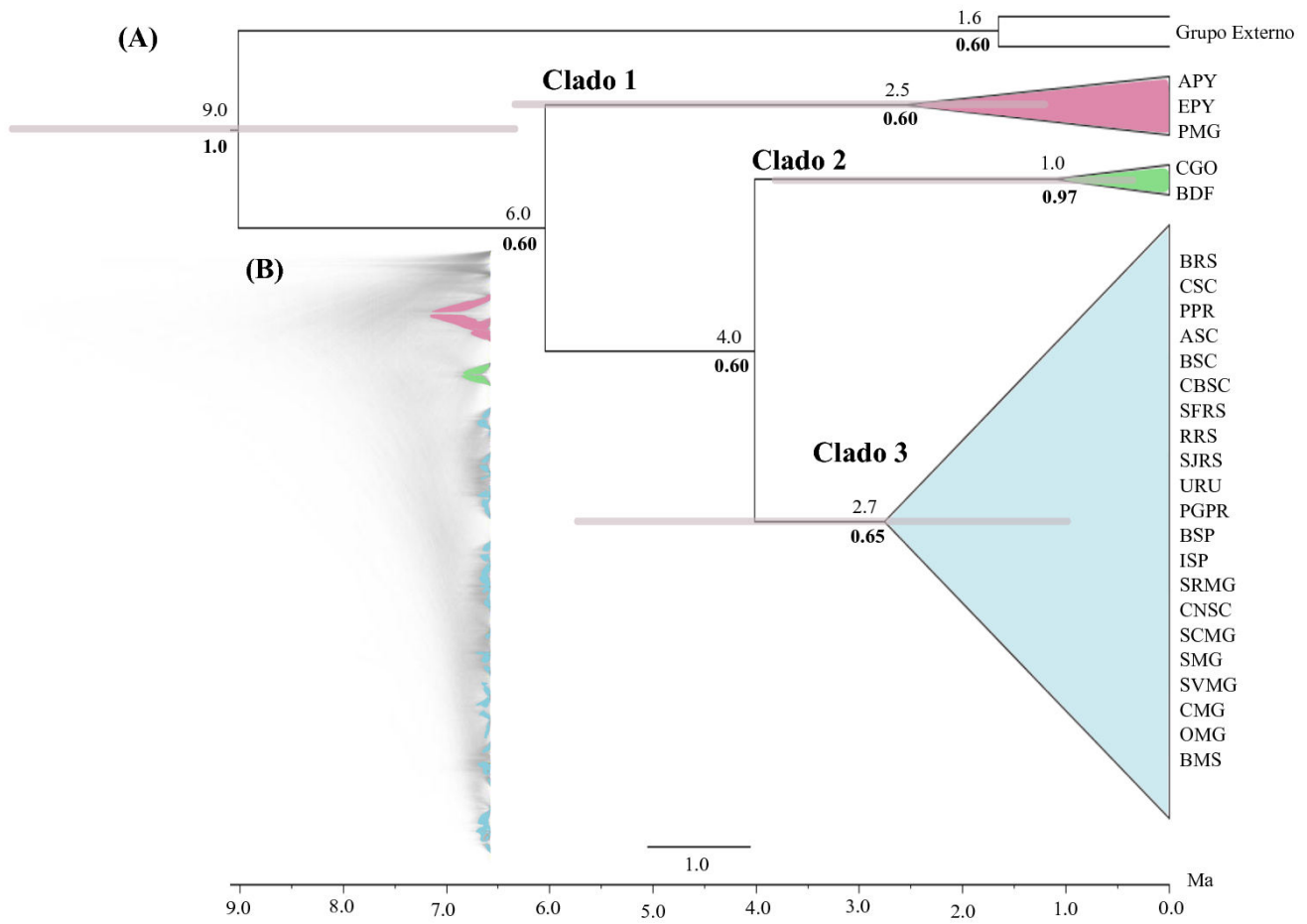


**Figura 2**

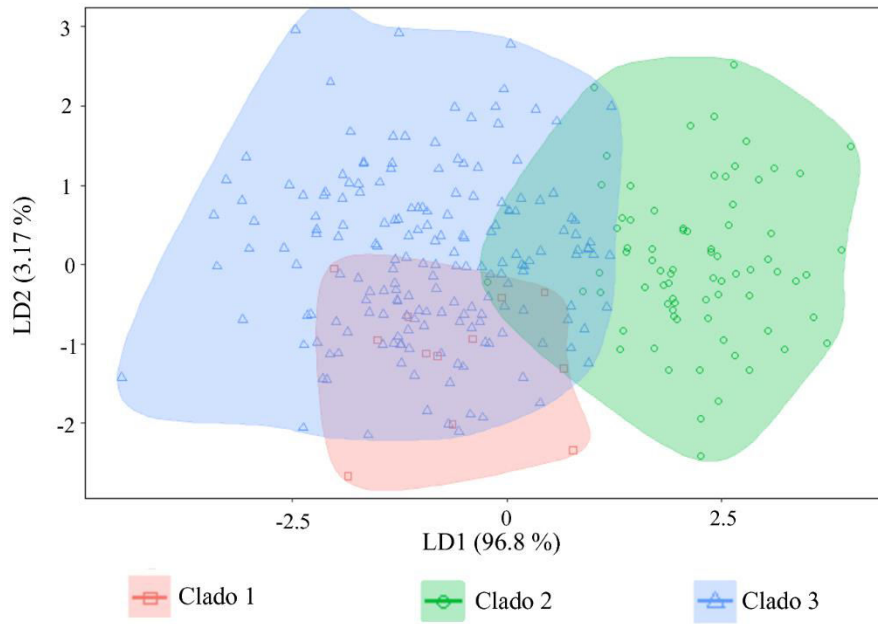


**Figura 3**

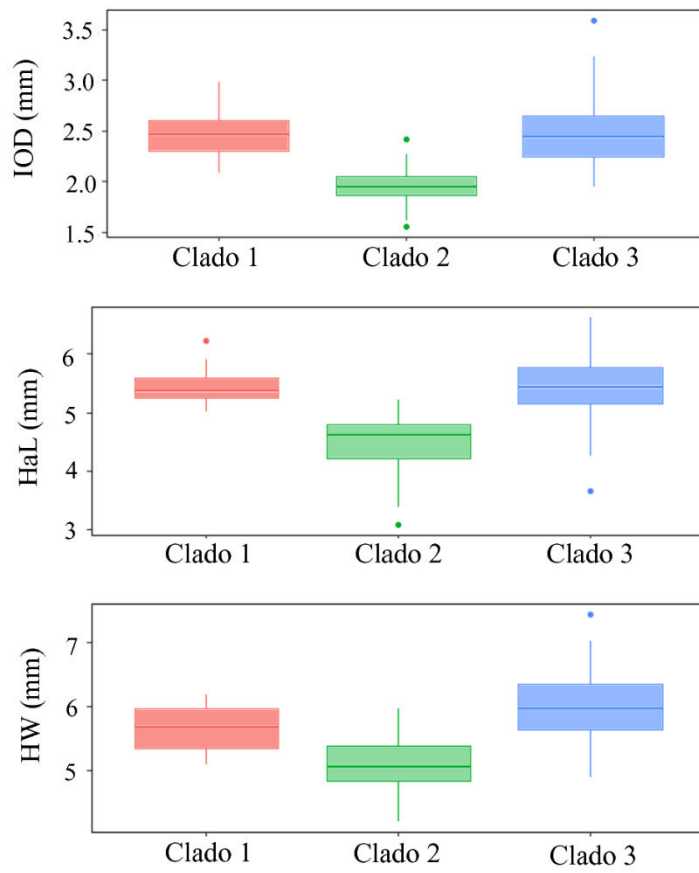


**Figura 4**

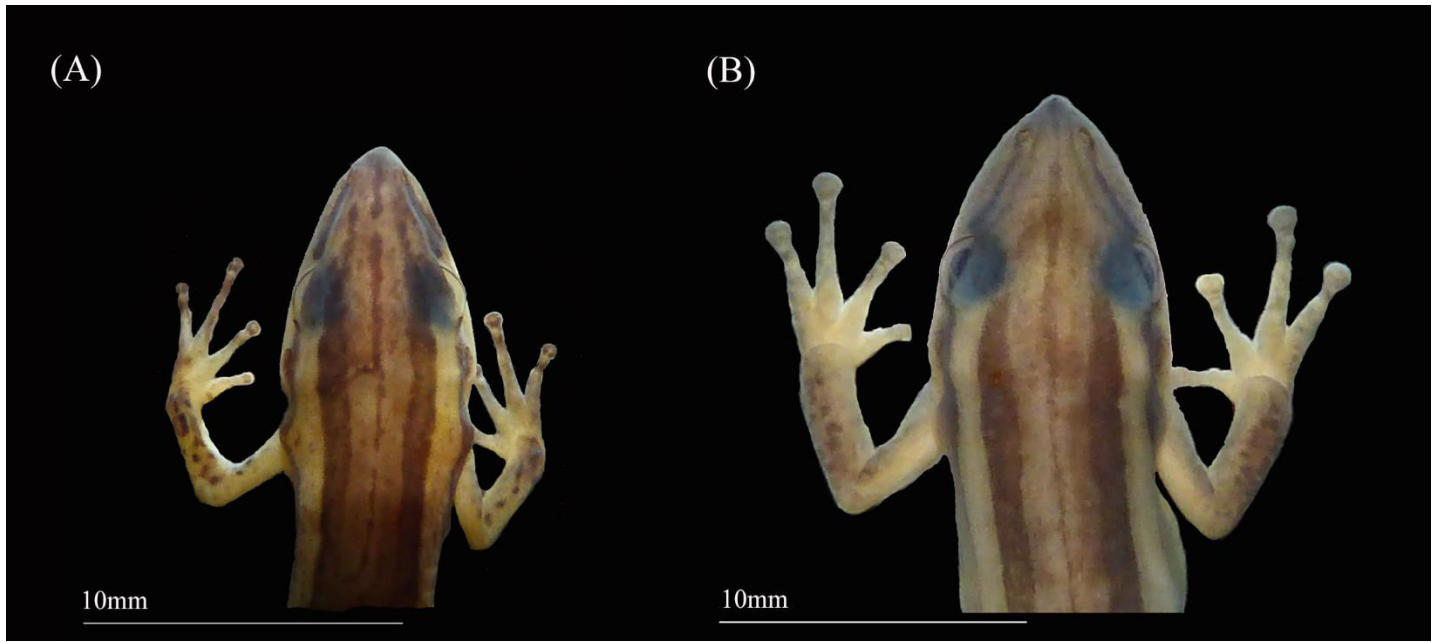


**Figura 5**

## Material Suplementar

### Revelando a diversidade do complexo de espécies de *Scinax squalirostris* (Lutz, 1925)

(Anura, Hylidae).

Tatianne P. F. Abreu-Jardim, Alejandro Valencia-Zuleta, Natan M. Maciel e

Rosane G. Collevatti.

**Apêndice S1** Suplementar de Tabelas S1: Tabelas S1.1-S1.6 contendo informações sobre *primers*, amplificação, sequenciamento, locais das amostras cedidas para as medidas morfométricas, modelos evolutivos e taxas de mutação.

**Tabela S1.1** Pares de primers usados PCR e sequenciamento: CytB, 12S e RAG-1

Região	Primer	Direção	Sequência Nucleotídica (5'-3')
CytB	MVZ15	<i>forward</i>	GAACTAATGGCCCACACWWTACGNAA
	H1415 (cyt-b2) (H15149)	<i>reverse</i>	AAACTGCAGCCCCTCAGAATGATATTTGTCCTCA
12S	12S	<i>forward</i>	AAACTGGGATTAGATACCCCACTAT
	12S	<i>reverse</i>	GAGGGTGACGGGCGGTGTGT
RAG	RAG1	<i>forward</i>	ATGCATCRAAAATTCARCAAT
	RAG1	<i>reverse</i>	CCYCCTTTRTTGATAKGGWCATA

**Tabela S1.2** Componentes de quantidades dos reagentes para o mix de PCR para cada um dos fragmentos utilizados nesse estudo.

<b>Reagentes</b>	<b>Cytb, 12S e RAG-1</b>
Deionized water	8.5 $\mu$ L
DNA	2.0 $\mu$ L
Forward primer (2 mM)	3.0 $\mu$ L
Reverse primer (2mM)	3.0 $\mu$ L
Buffer 1X*	2.0 $\mu$ L
DNTPs (2,5 mM)	1,2 $\mu$ L
Taq polymerase (5u/ $\mu$ L)	0.3 $\mu$ L
Total volume	20 $\mu$ L

\*Buffer 1X (10 mM Tris-HCl, pH 8.3, 50 mM KCl, 1.5 mM MgCl<sub>2</sub>)

**Tabela S1.3** Programa do termo de PCR para cada um dos fragmentos utilizados nesse estudo.

<b>Região</b>	<b>Aquecimento Inicial</b>	<b>Desnaturação</b>	<b>Anelamento</b>	<b>Extensão</b>	<b>Extensão final</b>
	<b>35 cycles</b>				
CytB	2 min at 94°C	60 sec at 94°C	60 sec at 56°C	90 sec at 72°C	6 min at 72°C
12S	2 min at 94°C	60 sec at 94°C	60 sec at 54°C	90 sec at 72°C	6 min at 72°C
RAG	2 min at 94°C	60 sec at 94°C	60 sec at 58°C	90 sec at 72°C	6 min at 72°C

**Tabela S1.4** Museus/Coleções onde foi revisado o material morfométricos de *Scinax squalirostris*.

<b>Museu/Coleção</b>	<b>Sigla</b>
Coleção Celio F. B. Haddad, Departamento de Zoologia, Universidade Estadual Paulista, Campus de Rio Claro, São Paulo, Brasil	CFBH
Coleção herpetológica, Universidade de Brasília, Brasília, D.F., Brasil.	CHUNB
Colección Biológica Arnoldo da Winkelried Bertoni, Instituto de Investigación Biológica del Paraguay, Asunción, Paraguai.	IIBP-H
Museu de Ciências e Tecnologia, Pontifícia Universidade Católica do Rio Grande do Sul, Porto Alegre, Rio Grande do Sul, Brasil	MCP
Museu Nacional do Rio de Janeiro, Universidade Federal de Rio de Janeiro, Rio de Janeiro, Brasil.	MNRJ
Coleção do setor de herpetologia, Universidade Federal do Rio Grande do Sul, Porto Alegre, Rio Grande do Sul, Brasil	UFRGS
Coleção de herpetologia, Universidade Federal de Goiás, Goiânia, Goiás, Brasil.	ZUFG
Coleção herpetológica, setor de Zoologia, Universidade Federal de Santa Maria, Santa Maria, Rio Grande do Sul, Brasil.	ZUFSM

**Tabela S1.5** Modelos evolutivos e parâmetros utilizado para *S. squalirostris*.

<b>Dados</b>	<b>Cytb</b>	<b>12S</b>	<b>RAG-1</b>
<b>Modelo</b>	K80+I	K80+G	JC
<b>p-inv</b>	0.8790	-	-
<b>Kappa</b>	17.7938	5.4465	
<b>gamma shape</b>	-	0.1200	-
<b>Nst</b>	2	2	1
<b>Ncat</b>	-	4	-

**Tabela S1.6** Taxa de mutação para cada região utilizado no estudo para gerar a árvore de espécie.

	Taxa de mutação (substituição/milhão de anos) Média - Desvio	Referência
12S	0.0026 - 0.0001	Evans <i>et al.</i> , 2004
CytB	0.0069 - 0.0010	Macey <i>et al.</i> , 1998
RAG	0.0015 - 0.0001	Heinicke <i>et al.</i> , 2007

Evans, B. J., Kelley, D. B., Tinsley, R. C., Melnick, D. J. & Cannatella, D. C. (2004) A mitochondrial DNA phylogeny of African clawed frogs: phylogeography and implications for polyploid evolution. *Molecular Phylogenetics and Evolution*, 33, 197-213.

Macey, J. R., Schulte, J. A., Larson, A., Fang, Z. L., Wang, Y. Z., Tuniyev, B.S. & Papenfuss, T. J. (1998) Phylogenetic relationships of toads in the *Bufo bufo* species group from the eastern escarpment of the Tibetan Plateau: a case of vicariance and dispersal. *Molecular Phylogenetics and Evolution*, 9, 80-87.

Heinicke, M. P., Duellman, W. E. & Hedges, S. B. (2007) Major Caribbean and Central American frog faunas originated by ancient oceanic dispersal. *Proceedings of the National Academy of Sciences*, 104, 10092–10097.

## Material Suplementar

### Revelando a diversidade do complexo de espécies de *Scinax squalirostris* (Lutz, 1925)

(Anura, Hylidae)

Tatianne P. F. Abreu-Jardim, Alejandro Valencia-Zuleta, Natan M. Maciel e

Rosane G. Collevatti

**Apêndice S2** Suplementar de Figura S2 gráfico de saturação com as taxas de transição e transversão.

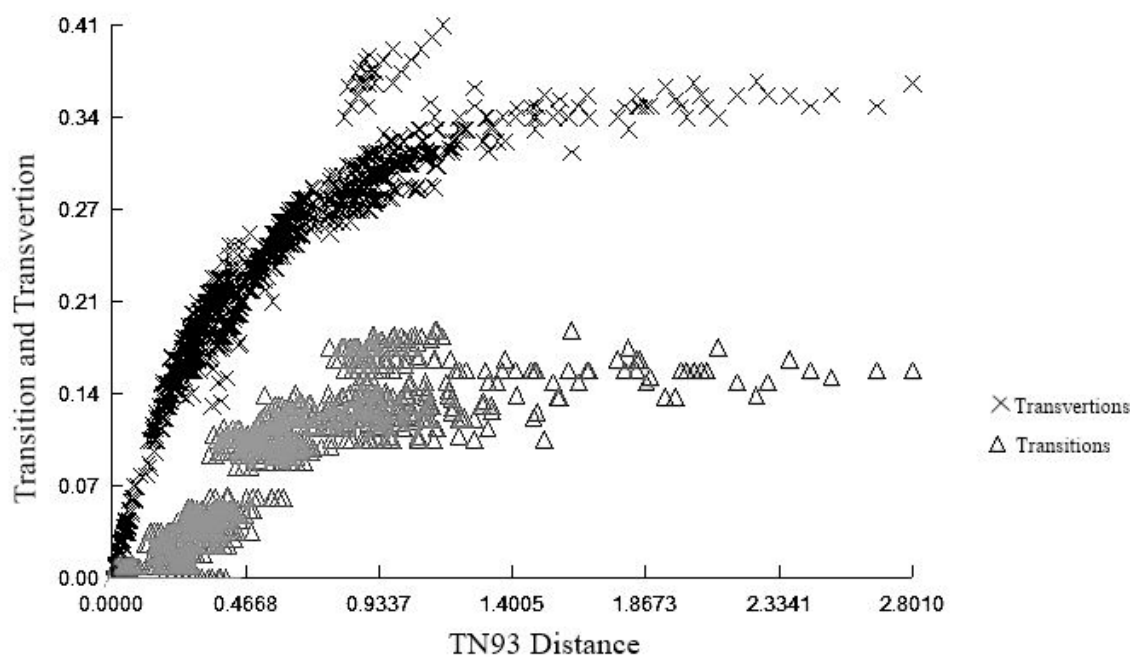


**Figure S3.1** Gráfico de saturação de transição e transversão para as posições dos terceiros códon das sequências do Citocromo b (Cytb).

## Revelando a diversidade do complexo de espécies de *Scinax squalirostris* (Lutz, 1925)

(Anura, Hylidae)

Tatianne P. F. Abreu-Jardim, Alejandro Valencia-Zuleta, Natan M. Maciel e

Rosane G. Collevatti

**Apêndice S3** Detalhes de número tombo e localidades das espécimes utilizadas na análise morfométrica.

Clado 1: **Brasil:** MINAS Gerais: Poços de Caldas: MNRJ 35579-81, 87812-16. **Paraguai:** Distrito Alto Verá: IIBP-H 1215-17, 2773-75; Emboscada: IIBP-H 1953-1955; Estancia San José: IIBP-H 267.

Clado 2: **Brasil:** DISTRITO FEDERAL: Brasília: CHUNB 16894-95, 16897, 16899-02, 16904-06, 25058, 42501-03, 50308-10; ZUFG 4754-59, 5476-88, 5651. GOIÁS: Alto Paraíso de Goiás: CHUNB 58392, 58395, 58397, 58768-73, 72679-80, ZUFG 5414-29, 6266, 6268; Cristalina: ZUFG 2717-24, 4949-53. SÃO PAULO: Botucatu: MNRJ 67337-52, 69864-65; Itirapina: CFBH 5709, 5666-69, 5708, 6551, 7067, 7069-70, 7072-74, 7076-77, 12847.

Clado 3: **Argentina:** CORRIENTES: Galarza: MNRJ 39989. SANTA FE: Villa Constitución: MCP 6505. **Brasil:** MINAS GERAIS: Alto Palácio: ZUFG 4740-41, 4767-69, 4771-79; Catas Altas: MNRJ 60634-42, 60655-59, 77745-65; Diamantina ZUFG 6309, 6350, 6353, 6357, 6364-81, 7625; Ibitipoca: MNRJ 59363-69; Jaboticatubas: MNRJ,45341,45344; Ouro Preto: CFBH 24377, 34626-29; Santa Barbara: MNRJ 72979-80; Santana do Riacho: CFBH 35053; Serra do Cipó: ZUFG 4785-87. MATO GROSSO DO SUL: Bonito: CHUNB 44058-59, 49342-44, 49347-50, 49352. PARANÁ: Guaíra: MNRJ 85613; Palmas: ZUFG 5660-61; Ponta Grossa: ZUFG 5652-59; Tibagi: ZUFG 7316, 7513. RIO GRANDE DO SUL: Alegrete: UFRGS 4244, ZUFMS 8509; Bagé: UFRGS 5715; Balneario Pinhal: MCP 3267, 3919, 4226-27; Braga: ZUFMS 4436;

Caibaté: UFRGS 4908; Cambara do Sul: CHUNB 69058-61, 69201, MCP 11408; Campos Novos: MCP 9463; Candiota: MCP 4059; Canela: UFRGS 2379; Canguçu: UFRGS 5393-94; Cerro Largo: ZUFISM 3333; Cidreira: MCP 11744; Coronel Barros: UFRGS 4915; General Câmara: MCP 3852-54; Itaáira: ZUFISM 4149; Manuel Viana: UFRGS 4453, ZUFISM 2430-31; Mato Queimado: UFRGS 4878-79; Mostardas: MCP 12639-40; Muitos Capois: MCP 11265; Nonoia: UFRGS 4074-75; Novo Hamburgo: MCP 9125; Pedras Altas: UFRGS 4834; Pinheiro Machado: UFRGS 5210, 5795, 6794; Porto Alegre: MCP 3290; Rio Grande: MCP 3214, 10803; Rolador: ZUFISM 3965, 4039; Santa Maria: ZUFISM 3119, 3737, 5157; Santana do Livramento: MCP 12138; São Borja: MCP 5771-73, ZUFISM 5009; São Francisco de Assis: UFRGS 5772, 5776, ZUFISM 3048; São Francisco de Paula: MCP 2473, 3430, 3482, 3655, 11037; São Gabriel : ZUFISM 9769; São João: ZUFISM 4097; São Joaquim: MCP 10364; São José do Norte: UFRGS 5271; São Lourenço do Sul: MCP 11290-92; São Luiza Conzaga: ZUFISM 4052; São Vicente: ZUFISM 2414; Santa Margarida do Sul: UFRGS 2534; Terra de Areia: MCP 5224-25; Torres: MCP 8688, ZUFISM 9992; Tramandaí: UFRGS 2129, 2131; Uruguaiana: UFRGS 1803-05; Viamão: UFRGS 1371. SÃO PAULO: São José do Barreiro: CFBH 21981, 28778-79, 28781, 30884, 30888-90, 35247. SANTA CATARINA: Água Doce: ZUFISM 8920; Bom Jardim da Serra: CFBH 9858, 11009, 11024, 11026; Campo Belo do Sul: MCP 10600-01, UFRGS 4044; Campos Novos: CFBH 14082; Celso Ramos: MCP 9006-07; Içara: UFRGS 6338, 6340; Lebon Régis: MCP 9663-64; Paniel: ZUFISM 2346; Passos Maia: CFBH 25775, UFRGS 5931; São Bento do Sul: CFBH 39252-53. **Uruguai:** Rivera: CHUNB 48026, ZUFG 13340-42.



# Capítulo 3

---

**Predicting impacts of global climatic change on distribution and genetic diversity  
of the treefrog *Scinax squalirostris* (Lutz, 1925) (Anura, Hylidae)**

Tatianne P. F. Abreu-Jardim<sup>1,2\*</sup>, Lucas Jardim<sup>3</sup>, Liliana Ballesteros-Meija<sup>4</sup>, Natan M. Maciel<sup>2</sup>, Rosane G. Collevatti<sup>1</sup>

\*Correspondence: tatibio1@gmail.com

<sup>1</sup>Laboratório de Genética & Biodiversidade, Departamento de Genética, Instituto de Ciências Biológicas, Universidade Federal de Goiás (UFG), Campus Samambaia, 74001-970, Goiânia, Goiás, Brazil.

<sup>2</sup>Laboratório de Herpetologia e Comportamento Animal, Departamento de Ecologia, Instituto de Ciências Biológicas, Universidade Federal de Goiás, Campus Samambaia, 74001-970, Goiânia, Goiás, Brazil.

<sup>3</sup>Instituto Nacional de Ciência e Tecnologia (INCT) em Evolução e Conservação da Biodiversidade, Instituto de Ciências Biológicas, Departamento de Ecologia, Universidade Federal de Goiás, Campus Samambaia, 74001-970, Goiânia, Goiás, Brazil.

<sup>4</sup>Muséum National d'Histoire Naturelle, Sorbonne Université, Institut de Systématique, Evolution, Biodiversité (ISYEB), UMR 7205 – CNRS, MNHN, UMPC, EPHE, Paris, France.

**Abstract**

Future climate changes caused by the increasing emission of greenhouse gases can affect negatively species distribution and their genetic diversity, hampering species adaption to the new climate or range shifting tracking the environment changes. Amphibians have

high sensitivity to environmental degradation and changes in temperature and humidity. Thus, the expected climatic changes to the end-of-century (EOC - 2100) may affect their ability to adapt to local conditions and may cause the local extinction of some species. In this work, we used Ecological Niche Modelling (ENM) and genetic simulations to predict the effects of climate change on the geographical distribution, genetic diversity and structure of *Scinax squalirostris*, a South American treefrog, using two scenarios of different CO<sub>2</sub> emission from the RCP database v 2.0.5 (Representative Concentration Pathways). We also performed a spatial analysis to verify how Protection Areas (PAs) are protecting the genetic diversity of the species. We found a reduction in the potential distribution of *S. squalirostris* under a future climate 8.5 RCP scenario. Genetic diversity and the number of haplotypes will decrease in both future scenarios, leading to a homogenization of genetic diversity across the geographical range of *S. squalirostris*. Populations may have difficulty adapting to new climatic conditions due to the displacement of genetic ancestry clusters from their ideal conditions. Although PAs conserve the current genetic diversity of *S. squalirostris*, only PAs in Southern Brazil and West Argentina will maintain high genetic diversity in the future, since most PAs will be in areas that will no longer be suitable for *S. squalirostris*.

**Keywords:** Bayesian clustering, conservation, ENMs, genetic clusters, global warming, South America.

**Short running head:** Climatic changing and genetic diversity in *Scinax squalirostris*.

## 1. INTRODUCTION

Genetic diversity represents the evolutionary potential of the species, in which natural selection acts to promote the evolution of organisms and their adaptation to environmental changes (Urban *et al.*, 2012, 2013). High levels of genetic diversity may favour a rapid evolutionary response, but populations with low genetic diversity have their evolutionary potential reduced and making them prone to local extinction (Spielman, *et al.*, 2004; Frankham, 2005). Anthropogenic impacts such as habitat fragmentation, invasive species, hunting pressures and climatic changes, have been associated with current extinctions (Purvis *et al.*, 2000; Fahrig, 2003; Loyola *et al.*, 2014; Bellard *et al.*, 2016). For instance, climatic dynamics (e.g. increase in temperature and variation in precipitation) may increase the effect of genetic stochasticity (e.g. loss of genetic diversity and inbreeding) in small populations and, therefore, fixation of poorly adapted haplotypes, causing extinction (Urban *et al.*, 2013; Pauls *et al.*, 2013). Furthermore, climatic changes force species to track suitable areas (Chen *et al.*, 2011), but some species cannot follow their optimal climatic niche because they have little dispersal capacity or cannot disperse through natural or anthropic barriers (Urban *et al.*, 2012). Species with low dispersal capacity have high extinction rates and population declines (Duan *et al.*, 2016).

Climatic changes can modify aspects of the biological system from the level of genes to ecosystems, thus, identifying populations that will be more vulnerable to these changes is a concern of biology and genetic conservation. Perhaps, one of the most worrisome groups are amphibians, with about 50% of all populations declining or threatened of extinction (Stuart *et al.*, 2004; Gibbons *et al.*, 2000; Houlahan *et al.*, 2000; Alroy, 2015; Duan *et al.*, 2016), amongst the most vulnerable vertebrates, declining even faster than birds and mammals (Stuart *et al.*, 2004). Because amphibians are highly reliable on environmental conditions (Duellman & Trueb, 1994), climatic change will

cause the extinction of approximately 40% of the species, with greater impact in the endemic groups (Gibbons *et al.*, 2000; Thomas *et al.*, 2004), making them the most threatened group of animals (Stuart *et al.*, 2004, Mendelson *et al.*, 2006).

Amphibians have low vagility, sensitivity to environmental degradation and changes in environmental temperature and humidity, mainly due to their permeable skin and life cycle, which includes stages in water and land (Duellman & Trueb, 1994, Stuart *et al.*, 2004; Storfer *et al.*, 2009). Changes in temperature and precipitation can lead to changes in geographic distribution and abundance (Chen *et al.*, 2011) of amphibian populations. Furthermore, climate changes could affect the hydro period available for amphibian populations, i.e. the time period that a temporary pond retains water for mating and metamorphosis (Rowe & Dunson, 1995; Carey & Alexander, 2003).

The global climate is changing drastically due to the emission of greenhouse gases, cause by anthropogenic action (Solomon, 2007; IPCC, 2014; 2018), since the last century there has been an increase of 0.6°C (Jones *et al.*, 2001) and climate models predict an increase of 2°C - 4°C in world temperature by the middle of the century (New *et al.*, 2011; Fischer *et al.*, 2018). Ecological niche modelling (ENM) is widely used to predict changes in the geographical distribution of species under climate change (e.g. Thomas *et al.*, 2004; Lima *et al.*, 2014; Collevatti *et al.*, 2015; Lima *et al.*, 2017). This framework uses current distribution data of species to model their fundamental environmental niches and, then, forecast potential distributions under various climatic scenarios (Peterson *et al.*, 2011), enabling the understanding of spatial dynamics and the impact of climatic changes on species in the future (Zhang *et al.*, 2012; Simon *et al.*, 2013; Mendoza-González *et al.*, 2013; Vasconcelos *et al.*, 2018). Future distributions are forecasted projecting the current suitable climatic conditions of species onto a map of future climatic scenarios (Midgley *et al.*, 2002; Lima *et al.*, 2017), assuming that species conserve their

current environmental niche and that they will be able to track future suitable climatic conditions (Elith & Leathwick, 2009). Coupling ENM to simulations of genetic parameters within and among populations can improve our understanding of climate change effects on genetic diversity and genetic clusters (Lima *et al.*, 2017). So, our knowledge about how climate change will affect genetic diversity will help predictions concerning how amphibian populations will cope with rapid future changes (Corn, 2005), especially guiding appropriate conservation policy scenarios (Duan *et al.*, 2016), protecting the future viability and genetic diversity of species and their ecosystems (Mendelson *et al.*, 2006; Schwartz *et al.*, 2007).

As the decline of amphibians is already a conservation concern, because of their great risk of extinction, it becomes urgent to understand how climate change will affect amphibian genetic diversities. In this work, we aimed to understand if and how the effects of future climate change on the distribution of the South American treefrog *Scinax squalirostris* Lutz, 1925 as a model group. This treefrog is widely distributed throughout the southeast and south of South America, occurring from the Central-West to the northern region of Argentina (Frost, 2018). We performed ecological niche modelling (ENM) to forecast the future geographical distribution based on two different scenarios of greenhouse gas emissions, 4.5 and 8.5 RCP. In order to understand the effects of climate change on genetic diversity, we performed genetic simulations conditioned to climatic and topographic variables, restricted to dispersal and establishment of anuran amphibians. In addition, since conservation of genetic diversity is a worldwide concern (Convention on Biological Diversity-Target 13 – CBD, Strategic Goal, <https://www.cbd.int/sp/targets/>), we performed a spatial analysis of the current genetic diversity and analyzed how much of this diversity is covered by Protection Areas (PAs) and predict PAs that will maintain genetic diversity even with future climate changes.

## 2. MATERIAL AND METHODS

### 2.1 Population sampling and genetic diversity

We sampled 26 localities across the distribution of *S. squalirostris* (Brazil, Uruguay and Paraguay) and collected 228 individuals with a sampling effort ranging between 1 and 10 individuals per locality (Table 1; Figure 1). Genetic data was obtained of tissue (muscle and liver) taken from specimens and preserved in ethanol 95%. DNA samples were obtained using Dneasy Blood & Tissue Kit (Quiagen<sup>®</sup>, InR. Chatsworth, CA). We sequenced two fragments of the mitochondrial DNA (mtDNA henceforward), 12S (353 bp, primers 12Sa-12Sb; Reeder, 1995), Cytochrome B (236 bp, primers MVZ15L, Moritz *et al.*, 1992, and H15149, Kocher *et al.*, 1989) and the nuclear (nDNA henceforward) RAG-1 gene (413 bp, Heinicke *et al.*, 2007). Fragments were amplified by polymerase chain reaction (details for the primers, PCR conditions and amplifications are summarized in Supporting Information, see Appendix S1: Tables S1.2-S1.4) and sequenced on an ABI GS3500 Genetic Analyser (Applied Biosystems<sup>®</sup>, CA) using the BigDye<sup>®</sup> Terminator Cycle Sequencing kit, according to the manufacturer's instructions. We sequenced all fragments in forward and reverse directions and consensus were obtained using the software SEQSCAPE 2.7 (Applied Biosystems, CA). Further, we used CLUSTALW (Thompson *et al.*, 1997) to obtain the multiple sequence alignments. Coding sequences were tested for saturation by plotting transitions and transversions with TN93 distance (Tamura & Nei, 1993) using DAMBE software (Xia, 2013). We excluded from the final alignment the third codon position of Cytb, which showed high levels of saturation (Appendix S2: Figure S2.1 in Supporting Information).

We estimated the overall and population nucleotide ( $\pi$ ) and haplotype ( $h$ ) diversities, using the concatenated fragments (mtDNA and nDNA = 1002 bp) in

ARLEQUIN 3.11 (Excoffier *et al.*, 2005). We also estimated the number of population and overall haplotypes (k) in DNAsp 5.0 (Librado & Rozas, 2009).

## **2.2 Ecological niche modelling: Future predictions**

To model the present and future potential geographical distributions of *S. squalirostris* in the Neotropics, we obtained occurrence records in literature and in open-access digital databases, such as VerNet (<http://portal.vertnet.org>), GBIF (the Global Biodiversity Information Facility-<http://www.gbif.org/>) and SpeciesLink project (<http://splink.cria.org.br/>). All records were examined for errors and duplicate occurrences were removed, thus, we obtained 257 unique occurrence records for *S. squalirostris* (Figure 1A; Table S1.5 in Appendix S1). We mapped the occurrence records in a grid cells of 0.5 x 0.5° (longitude x latitude) of spatial resolution, encompassing the Neotropics to generate the matrix of presences used to calibrate the ENMs. The environmental climatic conditions were characterized by climatic models for pre-industrial (representing current climate conditions) and two future scenarios of different CO<sub>2</sub> emission from the RCP database v 2.0.5 (Representative Concentration Pathways, <http://tntcat.iiasa.ac.at/RcpDb>). The scenario 4.5 RCP (rising radioactive forcing pathway leading to 4.5 W/m<sup>2</sup> in 2100), predicts a temperature increase of 1.8°C and stabilization before the EOC (end-of-century, 2100) due to the decrease in emissions of greenhouse gas. The scenario 8.5 RCP (rising radioactive forcing pathway leading to 8.5 W/m<sup>2</sup> in 2100), predicts a temperature increase of 3.7°C until the year 2100 and a continuing rising, due to a constant increase in representative concentration pathways (IPCC, 2013). These climatic conditions are derived from four Atmosphere-Ocean General Circulation Models (AOGCMs) (see Appendix S1: Table S1.6), with spatial resolution of 0.5° (ca. 55 km cell size). To overcome the multicollinearity problem among all bioclimatic variables

in the ENMs predictions, we performed a factorial analysis using *Varimax rotation* from 19 bioclimatic variables obtained in the EcoClimate database ([www.ecoclimate.org](http://www.ecoclimate.org)) which are available at 0.5° x 0.5° of resolution (Lima-Ribeiro *et al.*, 2015). We obtained five bioclimatic variables: annual mean temperature, mean diurnal range, isothermality-mean diurnal range/temperature annual range, precipitation of wettest three months and precipitation of driest three months. The current and future potential distributions of the treefrog were inferred using presence-only and presence–absence algorithms (Appendix S1: Table S1.7), represented by 12 algorithms. Some ENM algorithms based on presence-absence need absence data for model fitting and testing, however, there are not reliable real absence data available for this species. Therefore, we generated pseudo-absences randomly across the Neotropical area excluding cells with presence, maintaining prevalence equal to 0.5 to maximize model performance (Barbet-Massin *et al.*, 2012). To assess the model stability, we used a random data partitioning 75% training (calibration) and 25% testing (evaluation), replicated 50 repetitions for each model, due to the absence of independent testing data. This procedure and ENMs were run in the integrated computational platform BIOENSEMBLES (Diniz-Filho *et al.*, 2009). Model accuracy was assessed using the calculation of the area under the receiver operator characteristics (ROC) curve AUC (Allouche *et al.*, 2006) and with the metric true skill statistic (TSS), which take into account both omission and commission errors (Allouche *et al.*, 2006). We used an ensemble approach (Araújo & New, 2007) to calculate a consensus map that included only models with AUC > 0.75 and TSS>0.5 (Appendix S1: Table S1.8), and the models with poor performance were eliminated from the ensemble process. The frequency of occurrence in each cell provided a surrogate of the environmental suitability and was used for *Scinax squalirostris* across the Neotropical grid cells.

The combination of all ENMs and AOGCMs resulted in 48 independent predictive maps (12 ENMs x 4 AOGCMs) for each period of time (pre-industrial, 4.5 and 8.5 RCPs). We applied a hierarchical ANOVA using the predicted suitability from all models (12 ENMs x 4 AOGCMs x 3 times periods) as response variables to identify and map the uncertainties due to modelling components. For this, the ENMs and AOGCMs components were nested into the time component, but crossed by a two-way factorial design within each period of time (see Terrible *et al.*, 2012). The 48 predictive maps were combined to obtain the consensus map for each period of time. To quantify the range sizes and range shift between the three time periods, we first tested 0.5 and 0.75 binary thresholds and selected 0.5 because it better recovered the current distribution area of *S. squalirostris*. Then, we used this threshold to transform occurrence frequency maps into presence and absence maps, and then we calculated range size by summing the number of cells predicted as presence for each of the 48 predictive maps.

### **2.3 Simulations of genetic diversity under climatic changes**

To understand how climate change can affect genetic diversity, we simulated the extinction of some populations according to the occurrence thresholds estimated for two future scenarios (4.5 and 8.5 RCP). Ecological niche modelling predicts climatically suitable areas for species occurrence given predicted climate changes (see results below). Based on this, we assume that only populations occurring in climatically suitable areas in 2100 will persist and contribute to the gene pool for the next generations (see Collevatti *et al.*, 2011). Then, we simulated the extinction of populations below suitability thresholds ranging from 0.1 to 0.9 (Table 1) and re-calculated genetic diversity ( $\pi$ ,  $h$  and  $k$ ) for the remaining populations under two future scenarios (4.5 and 8.5 RCP), using the software ARLEQUIN 3.11 (Excoffier *et al.*, 2005).

## 2.4 Forecasting and dynamic genetic clusters in future scenarios

We performed spatially explicit simulations to predict the dynamics of climatic clusters conditioned to climatic changes using the software POPs (Jay *et al.*, 2015). In this analysis, Bayesian grouping is based on genetic, geographic and environmental variables, assigning individuals to genetic clusters, based on genetic coancestry. POPs models the effects of climatic and landscape variables in such cluster assignments and predicts changes in the genetic structure in response to climatic changes (Jay *et al.*, 2012). For the simulations, we selected two environmental variables for current and future scenarios: minimum temperature of the coldest month and precipitation of the coldest quarter, which were the two climatic predictors with the highest variance among populations. In addition, we selected topographic variables that may affect the dispersal and occurrence of anurans, such as slope and altitude (Table 1). We performed simulations for mitochondrial and nuclear haplotypes separated and excluded rare haplotypes (Appendix S1: Table S1.9). In order to define the rare haplotypes, we made an abundance rank curve and set a sample selection of 85% of the relative frequency, that is, haplotypes present in less than 15% of the individuals were excluded.

We simulated genetic clusters under current climatic conditions combining genetic, climatic and topographic variables. The analysis was performed using Markov Chain Monte Carlo (MCMC) implemented in POPS (Jay *et al.*, 2015). The MCMC runtime was set for 50,000 sweeps and the burn-in period for 5,000 sweeps using models with admixture. To define the number of clusters (K), we run the simulations four times for each K varying between 2 and 23 for both mitochondrial and nuclear data. The subset of runs minimizing the deviation information criterion (DIC, Spiegelhalter *et al.*, 2002) and the lowest DIC values were selected. Finally, we predicted the genetic clusters for both future scenarios (4.5 and 8.5 RCP) conditioned on future climatic and topographic

conditions. We measured the changes in ancestry among contemporary and predicted ancestry coefficients (intraspecific turnover, Jay *et al.* 2012) for both 4.5 and 8.5 RCP future scenarios to understand the impact of climate change on spatial genetic structure. Topographic variables were extracted from the occurrence points of the *S. squalirostris* populations in ArcGIS® 10.2 (ESRI, 2014) using a Digital Elevation Model (DEM) raster from the ALOS – Advanced Land Observing Satellite database (<https://www.eorc.jaxa.jp/ALOS/en/index.htm>). Since we expect no changes to altitude and slope in a few years (up to 2100), we use the same values of the present to make the future simulations.

## **2.5 Accessing the genetic richness and conservation of genetic diversity**

To obtain the genetic richness of *S. squalirostris*, we defined the genetic richness as the number of haplotypes in a population divided by the number of individuals sampled within population. Then, we performed a spatial interpolation of genetic richness over a raster of the current distribution area predicted by ENM with a resolution of 0.5°. We fitted a spherical variogram model and performed interpolation using R package *gstat* (Gräler *et al.*, 2016).

We also verified the effectiveness of the current PAs across the geographical range of *S. squalirostris* to conserve genetic richness. We obtained CU data from Protect Planet website ([www.protectedplanet.net](http://www.protectedplanet.net)) and maintained only PAs with area higher than 1% of the cell of the interpolated genetic richness raster. Then, we calculated the mean genetic richness covered by each PAs and performed PAs clustering using k-means method (Hartigan & Wong 1979), implemented in *kmeans* function of R package *stats* (R Core Team, 2016). The clusters were optimized by minimizing the sum of squares within

groups. The number of groups were optimized by a grid search ranging from 2 to 15 clusters.

### 3. RESULTS

#### 3.1 Ecological niche modelling: Future predictions

*Scinax squalirostris* shows a preference to cooler and drier habitats (Figure 2). The ENMs predicted range shift and loss of suitability in the future for both climatic scenarios (Figure 1; Appendix S2: Figure S2.3A). The average number of cells for current geographical range is 1,286 and decreases to 1,050 cells under 4.5 RCP scenario and to 901 cells under 8.5 RCP (Appendix S2: Figure S2.3A). The ENMs also predicted a higher range shift between the current conditions and the 8.5 RCP scenario than for the 4.5 RCP (Appendix S2: Figure S2.3B) with a potential loss of climatic suitability mainly at the Eastern Brazil (Figure 1C, D). At 8.5 RCP scenario (Figure 1D) the potential geographical range is restricted to the Southern Brazil to Central Argentina and eastern Andean slopes (Figure 1D).

The analysis of uncertainty using hierarchical ANOVA showed high proportional variance from both ENMs algorithms and AOGCM (Appendix S1: Table S1.10). However, variation was higher on cells outside *S. squalirostris*' occurrence range (Figure S2.2 in Appendix S2). Variation through time was higher within *S. squalirostris* range, therefore, the ENMs were able to detect the effects of climatic changes on the distribution dynamics of *S. squalirostris* through time, despite the AOGCM variation.

### **3.2 Simulations of genetic diversity under climatic changes**

Although number of haplotypes will be rapidly lost at both scenarios (Figure 3), haplotype diversity will decrease only under 8.5 RCP scenario (Figure 3). The number of haplotypes will decrease, with a steeper decrease for the 8.5 RCP scenario and there is not a drastic decrease for the 4.5 RCP scenario, since the suitability thresholds cover the areas with the most haplotypes (Figure 3 and 4). Nucleotide diversity is shown to be constant over the course of climate change, being little affected by range retraction, for both 4.5 and 8.5 RCP scenarios (Figure 3).

### **3.3 Forecasting and dynamics in genetic clusters in future scenarios v**

The most likely number of mitochondrial genetic clusters conditioned to environmental and topographic variables (precipitation, temperature, altitude and slope) was  $K = 8$  (DIC = 980.274) (Appendix S1: Tables S1.11-S1.13) and for nuclear genetic clusters conditioned to environmental variables was  $K = 9$  (DIC = 700.11) (Appendix S1: Tables S1.14-S1.16). The correlation between estimated and predicted admixture coefficients of geographic and environmental covariates was 0.99 for both mitochondrial and nuclear data, these values indicate that predictions of environmental variables were accurate.

Overall, spatial explicit simulations showed loss of variation over time due to environmental climate changes (Figure 5). Some climatic clusters were lost for mitochondrial (clusters 1, 2, 4, 5, 6 and 8) predictions for both climate change scenarios (4.5 and 8.5 RCP) (Figure 5A, B and C) leading to a genetic homogenization in the South Brazil, Paraguay and Uruguay and in the Central, West Brazil and Northwest South America (Figures 5B and 5C). Nuclear data showed a displacement in clusters (5D, E and F) and loss of clusters for all scenarios (clusters 7, 8 and 9) (Figure 5D, E and F). In

addition, the simulations evidenced a homogenization in the spatial conformation of the genetic variability in Central, Northeast and East Brazil (cluster 1) (Figure 5F).

Turnover analysis showed the impact of climatic changes in spatial genetic structure, but the clusters, in general, showed congruent responses (Figure 5G, H). The mitochondrial genetic clusters 3 and 7, remained constant from the current to 4.5 RCP and 8.5 RCP scenarios (Appendix S2: Figure S2.4A). The other clusters showed a change from the current to the 4.5 RCP scenario, but did not show great changes and remained practically constant, except clusters 1 and 5 (Appendix S2: Figure S2.4A). For nuclear sequences, clusters 3 and 5 had little or no shifts in ancestry. Most clusters shifted the ancestry from current scenario to 4.5 RCP and 8.5 RCP, with increase (clusters 1 and 6) or decrease (clusters 2, 4, 7, 8 and 9) (Appendix S2: Figure S2.4B).

### **3.4 Conservation of genetic diversity**

Populations at the South and Southeast Brazil showed higher genetic richness (Figure 6A, B). Spatial interpolation (Figure 6C) showed that the genetic richness is lower in the northeaster geographical distribution of *S. squalirostris*. Higher genetic richness can be found mainly in the Southern region of the *S. squalirostris* distribution area.

The cluster analysis found 5 groups (Appendix S2: Figure S2.4) classified according to the amount of genetic richness and size of the PAs area (Figure 7A; Table S1.17 in Appendix S1). Four groups were composed by PAs smaller than 4000 km<sup>2</sup>, but with different genetic richness (clusters 1, 2, 3 and 4, Figure 7A). Cluster 5 comprises PAs larger than 4000 km<sup>2</sup> with high genetic richness. However, PAs clusters had no spatial pattern (Figure 7B), with Protection Areas with high or low genetic richness spread throughout *S. squalirostris* geographical distribution.

#### 4. DISCUSSION

Our findings showed that climatic changes can affect *S. squalirostris* populations, leading to a reduction in its geographical distribution and loss of genetic diversity. However, loss of genetic diversity will be greater and faster at 8.5 RCP scenario, although haplotypes will be rapidly lost at both scenarios 4.5 and 8.5 RCP.

ENMs showed a decrease in suitability in the Central-West and Southeastern region of *S. squalirostris*, leading to a shift in suitable areas towards the South Brazil and Central and West Argentina. The scenarios 4.5 RCP will cause 18% reduction of suitable areas for *S. squalirostris* and the scenario 8.5 RCP will reach 30% of loss in suitable areas. South American amphibians and reptiles also showed retraction and shift in geographical distribution due to future climatic changes, affecting both widely-distributed (Mesquita *et al.*, 2010; Vasconcelos *et al.*, 2014; 2016; 2018) and locally restricted species (Vilela *et al.*, 2018). The co-generic widely-distributed species *Scinax fuscomarginatus* and *S. fuscovarius* showed reduction of 31 to 43% of suitable areas by 2050 (Vasconcelos *et al.*, 2014). Thus, the scenario of reduction in suitable areas in the future due to climatic changes seem common among amphibians and reptiles, two taxa highly affected by environment conditions (e.g. Mesquita *et al.*, 2010; Vasconcelos *et al.*, 2014; López-Alcaide & Macip-Ríos, 2014).

The decrease in suitable areas will lead to a negative effect on the genetic diversity of *S. squalirostris*. Although nucleotide diversity will not reduce, haplotype diversity and the number of different haplotypes will decrease sharply for 8.5 RCP. Populations of *S. squalirostris* from the South Brazil have higher genetic diversity, thus, haplotype diversity at 4.5 RCP scenario will not decrease, because this area will be the most stable with the least reduction of climatic suitability. Thus, with the displacement of suitable areas towards the South and Southeast Brazil for the 4.5 RCP scenario, populations with

high genetic diversity will remain. On the other hand, many haplotypes will be potentially lost, and even if the remaining populations can maintain high diversity, this loss may hinder response to climate change and lead to local extinction risk (Wright *et al.*, 2008; Foden *et al.*, 2013). The low genetic diversity and richness in population from the Central-West and Southeast region of the distribution of *S. squalirostris* may be due to demographic history and habitat fragmentation. The loss of habitat in the past may have led to the loss of haplotypes in the Central-West populations, reducing the genetic diversity (Abreu-Jardim *et al.*, 2018).

Due to the low genetic diversity of *S. squalirostris* populations in less suitable areas, the adaptation to new environmental conditions may be difficult (Hoffmann & Willi, 2008). In addition, there is no guarantee that those vulnerable *S. squalirostris* populations will track its adequate climatic conditions, due to the speed of climate changes (Chen *et al.*, 2011; Arenas *et al.*, 2012), the low dispersion capacity (Blaustein *et al.*, 1994; Hillman *et al.*, 2014) or by failing to disperse through natural or anthropogenic barriers (Urban *et al.*, 2012). The ENMs predicted a change and spatial restriction on habitat suitability for *S. squalirostris* from Southern Brazil to the West of Argentina. In these areas the anthropogenic disturbances as urbanization (Lopéz *et al.*, 2015), agriculture (Moreira & Maltchik, 2015; Lopéz *et al.*, 2015; Laufer & Gobel, 2017) and cattle grazing cropping (Medan *et al.*, 2011; Lopéz *et al.*, 2015) are strong and the tendency is to increase in the future. These factors can affect population persistence through time under the scenarios of climatic changes, despite their high genetic diversity.

Our simulations showed a loss of genetic variation among populations. *Scinax squalirostris* prefers cold and dry climates, so temperature increasing and changes in precipitation regimes predicted for the EOC will affect the geographical distribution and the spatial patterns of genetic diversity distribution. Temperature regimes are expected to

change dramatically according to 8.5 RCP scenario (Figure 2), particularly colder month temperatures will increase in some regions resulting in the loss of some genetic clusters and homogenization of climatic genetic clusters through the distribution range of *S. squalirostris*. Species require a diverse gene pool to rapid adaptation to environmental changes (Barrett & Schluter, 2008). The predicted loss of variation among populations and within populations will potentially threat *S. squalirostris* long-term conservation under climatic change.

During the evolution of the species the climatic niches may evolve (Peterson *et al.*, 1999; Wiens & Graham, 2005; Wiens *et al.*, 2010), but as climatic changes will happen rapidly and abruptly due to high intensity of anthropic disturbs, niche conservatism can disable vulnerable populations to respond to climatic changes, leading to local extinction (Wiens, 2004). Thus, climatic change will challenge the adaptation of vulnerable populations to new environmental conditions due to the displacement of genetic ancestry clusters from their ideal conditions.

Our results indicate that even small PAs can preserve high levels of genetic richness of *S. squalirostris*. However, climatic change will decrease suitability in areas with higher density of PAs through *S. squalirostris* geographical range, such as the Central-West and Southeast Brazil (Figure 7). In addition, the areas with higher density of PAs have lower levels of genetic richness. Thus, PAs at the Southern, the more climatic stable area through time and with higher genetic richness are more important to maintain the genetic diversity of *S. squalirostris* in the future. However, it is important note that the Southern has low density of PAs, which may potentially threat the species long-term conservation. The reduction of suitable areas and the decline of amphibian species within PAs due to climatic changes are of major concern in conservation planning (e.g. Loyola *et al.*, 2008; Loyola *et al.*, 2014; Vasconcelos *et al.*, 2018). Amphibians from the Atlantic

Forest will be misrepresented by current PAs, because those PAs will be in climatically inadequate places to sustain species richness and diversity (Loyola *et al.*, 2014). Further, global warming and the reduction of suitable areas for species coupled with the loss of genetic diversity may lead to the extinction of undescribed and cryptic species (Bálint *et al.*, 2011). *Scinax squalirostris* has high genetic differentiation among populations and populations in Central-West Brazil are specially highly differentiated (Abreu-Jardim *et al.*, 2018). This region is characterized by low levels of genetic diversity, with low suitability through the Quaternary. Our findings show that this region will also have low suitability in the EOC. Therefore, we have a pessimistic scenario, in which lineages in Central-West will probably extinct or be highly threaten. The problem of losing cryptic lineages is that it can affect ongoing diversification processes and thus affect future biodiversity (Bálint *et al.*, 2011). Thus, under a more unpredictable climate and with very rapid changes, leading to a decrease and shift in the geographical range the genetic diversity becomes increasingly important for the survival of populations and species.

In conclusion, our results show that populations of *S. squalirostris* can be negatively affected by climatic changes, mainly by reducing and shifting suitable areas in EOC. The contraction of suitable areas can lead to local extinction and range retraction and, in turn, decrease the genetic diversity, becoming *S. squalirostris* less able to respond to the fast climatic changes. Thus, *S. squalirostris* will become more threatened in future, as distribution size is the main criteria to assign extinction risk category of species. Moreover, populations of the Central-West and Southeast Brazil have low genetic diversity, and may lose their suitable area due to climatic changes leading to a potential extinction of lineages in the EOC. These regions will lose climatic suitability in the areas with high density of PAs, making it difficult to preserve this species and its genetic diversity. Furthermore, climatic changes will result in loss and changes in genetic

clusters, leading to a homogenization of diversity, which will decrease evolutionary potential of *S. squalirostris* to deal with future climate changes.

## **ACKNOWLEDGEMENTS**

This work was supported by a grant from CNPq (project no. 475333/2011-0, 475333/2011-0) and CAPES/PROCAD (project no. 88881.068425/2014-01). TPFAJ received a fellowship from FAPEG (Fundação de Amparo à Pesquisa do Estado de Goiás, project no. 201410267000553). The authors would like to thank TF Rangel for providing access to the computational platform Bioensembles, and E. Barreto and A. Anjos for help in generated the genetic data. We thank P. Cabral and A. Valencia-Zuleta for help in English editing and J. Silva and O. François for the help with POPs analysis. We are grateful to many people and their institutions that kindly collected, donated specimens, sent sample tissues and loan specimens. CNPq have continuously support NMM, GRC, CFBH and RGC with grants and fellowships, which we gratefully acknowledge.

## REFERENCES

- Allouche, O., Tsoar, A. & Kadmon, R. 2006. Assessing the accuracy of species distribution models: prevalence, kappa and the true skill statistic (TSS). *Journal of Applied Ecology*, 43,1223-1232.
- Alroy, J. 2015. Current extinction rates of reptiles and amphibians. *Proceedings of the National Academy of Sciences*, 112, 13003-13008.
- Araújo, B. M. & New, M. 2007. Ensemble forecasting of species distributions. *Trends in Ecology and Evolution*, 22, 42-47.
- Arenas, M., Ray, N., Currat, M. & Excoffier, L. 2012. Consequences of range contractions and range shifts on molecular diversity. *Molecular Biology and Evolution*, 29, 207-218.
- Bálint, M., Domisch, S., Engelhardt, C. H. M., Haase, P., Lehrian, S., Sauer, J., Theissinger, K., Pauls, S. U. & Nowak, C. 2011. Cryptic biodiversity loss linked to global climate change. *Nature Climate Change*, 1, 313-318.
- Barbet-Massin, M., Jiguet, F., Albert, C. H., & Wilfried, T. 2012. Modelling species distributions to map the road towards carnivore conservation in the tropics. *Methods in Ecology and Evolution*, 3, 327–338.
- Barrett, R. D. H. & Schluter, D. 2008. Adaptation from standing genetic variation. *Trends in Ecology & Evolution*, 23, 38-44.
- Bellard, C., Phillip. C. & Blackburn, T. M. 2016. Alien species as a driver of recent extinctions. *Biology Letters*, 12.
- Blaustein, A. R., Wake, D. B. & Sousa, W. P. 1994. Amphibian Declines: Judging Stability, Persistence, and Susceptibility of Populations to Local and Global Extinctions. *Conservation Biology*, 8, 60-71.
- Carey, C. & Alexander, M. A. 2003. Climate change and amphibian declines: is there a link? *Diversity and Distributions*, 9, 111–121.

- Chen, I. C., Hill, J. K., Ohlemuller, R., Roy, D. B. & Thomas, C. D. 2011. Rapid range shifts of species associated with high levels of climate warming. *Science*, 333, 1024–1026.
- Collevatti, R. G., Nabout, J. C., & Diniz-Filho, J. A. F. 2011. Range shift and loss of genetic diversity under climate change in *Caryocar brasiliense*, a Neotropical tree species. *Tree Genetics and Genomes*, 7, 1237–1247.
- Collevatti, R. G., Terribile, L. C., Rabelo, S. G. & Lima-Ribeiro, M. S. 2015. Relaxed random walk model coupled with ecological niche modeling unravel the dispersal dynamics of a Neotropical savanna tree species in the deeper Quaternary. *Frontiers in Plant Science*, 6.
- Corn, P. S. 2005. Climate change and amphibians. *Animal Biodiversity and Conservation*, 28, 59-67.
- Diniz-Filho, J. A. F., Bini, L. M., Rangel, T. F.; Loyola, R. D., Hof, C., Nogués-Bravo, D. & Araújo, M. B. 2009. Partitioning and mapping uncertainties in ensembles of forecasts of species turnover under climate change. *Ecography*, 32, 897-906.
- Duan, R. Y., Kong, X. Q., Huang, M. Y., Varela, S. & Ji, X. 2016. The potential effects of climates change on amphibian distribution range fragmentation and turnover in China. *PeerJ*, 4, 1-17.
- Duellman, W. E., & Trueb, L. 1994. Biology of amphibians. The Johns Hopkins University Press. USA. pp. 1-670.
- Elith, J. & Leathwick, J. R. 2009. Species distribution models: ecological explanation and prediction across space and time. *Annual Review of Ecology, Evolution, and Systematics*, 40, 677–697.
- Environmental Systems Research Institute (ESRI). 2014. ArcGIS Desktop Help 10.2. Geostatistical Analyst.
- Excoffier, L., Laval, G. & Schneider, S. 2005. Arlequin ver. 3.0: an integrated software package for population genetics data analysis. *Evolutionary Bioinformatics Online*, 1, 47-50.

- Fahrig L. 2003. Effects of habitat fragmentation on biodiversity. *Annual Review of Ecology, Evolution and Systematics*, 34, 487-515.
- Fischer, H., Meissner, K. J., Mix, A. C, Abram, N. J., Austermann, J. *et al.* 2018. Paleoclimate constraints on the impact of 2°C anthropogenic warming and beyond. *Nature Geoscience*, 11, 474-485.
- Foden, W. B. *et al.* 2013. Identifying the world's most climate change vulnerable species: A systematic trait-based assessment of all birds, amphibians and corals. *PLoS ONE*, 8, e65427.
- Frankham, R. 2005. Genetics and extinction. *Biology Conservation*, 126,131–140.
- Frost, D. R. (2018). Amphibian Species of the World: An Online Reference. Version 5.7. Electronic Database accessible at <http://research.amnh.org/herpetology/>.
- Gibbons, J. W., Scott, D. E., Ryan, T. J., Buhlmann, K. A., Tuberville, T. D., Metts, B. S., Greene, J. L. *et al.* 2000. The global decline of reptiles, dejavu amphibians. *BioScience*, 50, 653–666.
- Gräler, B., Pebesma E. & Heuvelink, G. 2016. Spatio-Temporal Interpolation using gstat. *The R Journal*, 8, 204-218.
- Hall, T. A. 1999. BioEdit: a user-friendly biological sequence alignment editor and analysis program for Windows 95/98/NT. *Nucleic Acids Symposium Series*, 41, 95-98.
- Hartigan, J. A. & Wong, M. A. 1979. A K-means clustering algorithm. *Applied Statistics*, 28, 100–108.
- Heinicke, M. P., Duellman, W. E. & Hedges, S. B. 2007. Major Caribbean and Central American frog faunas originated by ancient oceanic dispersal. *Proceedings of the National Academy of Sciences*, 104, 10092-10097.
- Hillman, S. S., Drewes, R. C., Hedrick, M. S. & Hancock, T. V. 2014. Physiological Vagility: Correlations with Dispersal and Population Genetic Structure of Amphibians. *Physiological and Biochemical Zoology*, 87, 105-112.

- Hoffmann, A. A., & Willi, Y. 2008. Detecting genetic responses to environmental change. *Nature Reviews Genetics*, 9, 421–432.
- Houlahan, J. E., Findlay, C. S., Schmidt, B. R., Meyer, A. H. & Kuzmin, S. L. 2000. Quantitative evidence for global amphibian population declines. *Nature*, 404,752–755.
- IPCC Climate Change 2013: The Physical Science Basis (eds Stocker, T. F. et al.) (Cambridge Univ. Press, Cambridge, 2013).
- IPCC Climate Change 2014: Synthesis Report. Contribution of Working Groups I, II and III to the Fifth Assessment Report of the Intergovernmental Panel on Climate Change [Core Writing Team, R.K. Pachauri and L.A. Meyer (eds.)]. IPCC, Geneva, Switzerland, 151 pp.
- IPCC Climate Change 2018: Global Warming of 1.5°C: an IPCC special report on the impacts of global warming of 1.5°C above pre-industrial levels and related global greenhouse gas emission pathways, in the context of strengthening the global response to the threat of climate change, sustainable development, and efforts to eradicate poverty.
- Jay, F., Francois, O., Durand, E. Y., & Blum, M. G. B. 2015. POPS: A software for prediction of population genetic structure using latent regression models. *Journal of Statistical Software*, 68, 1–19.
- Jay, F., Manel, S., Alvarez, N., Durand, E. Y., Thuiller, W., Holderegger, R., Taberlet, P., Francois, O. 2012. Forecasting changes in population genetic structure of alpine plants in response to global warming. *Molecular Ecology*, 21, 2354–2368.
- Jones, P. D., Osborn, T. J. & Briffa, K. R. 2001. The evolution of climate over the last millennium. *Science*, 292, 662–667.
- Kocher, T. D., Thomas, W. K., Meyer, A., Edwards, S. V., Pääbo, S., Villablanca, F. X. & Wilson, C. 1989. Dynamics of mitochondrial DNA evolution in animals: amplification and sequencing with conserved primers. *Proceedings of the National Academy of Sciences*, 86, 6196–6200.

- Laufer, G., & Gobel, N. 2017. Habitat degradation and biological invasions as a cause of amphibian richness loss: a case report in Aceguá, Cerro Largo, Uruguay. *Phyllomedusa: Journal of Herpetology*, 16, 289-293.
- Librado, P. & Rozas, J. 2009. Dnasp: software for comprehensive analysis of DNA polymorphism data.
- Lima, J. S., Ballesteros-Meija, L., Lima-Ribeiro, M. S. & Collevatti, R. G. 2017. Climatic changes can drive the loss of genetic diversity in a Neotropical savanna tree species. *Global Change Biology*, 1-12.
- Lima, N. E., Lima-Ribeiro, M. S., Tinoco, C. F., Terribile, L. C., & Collevatti, R. G. 2014. Phylogeography and ecological niche modelling, coupled with the fossil pollen record, unravel the demographic history of a Neotropical swamp palm through the Quaternary. *Journal of Biogeography*, 41, 673–686.
- Lima-Ribeiro, M. S., Varela, S., González-Hernández, J., Oliveira, G., Diniz-Filho, J. A. F. & Terribile, L. C. 2015. ecoClimate: a database of climate data from multiple models for past, present and future for Macroecologists and Biogeographers. *Biodiversity Informatics*, 10, 1-21.
- Lopez, J. A., Scarabotti, P. A., & Ghirardi, R. 2015. Amphibian trophic ecology in increasingly human-altered wetlands. *Herpetological Conservation and Biology*, 10, 819-832.
- Loyola, R. D. et al. 2008. Hung out to dry: choice of priority ecoregions for conserving threatened neotropical anurans depends on life-history traits. *PloS One*, 3, e2120.
- Loyola, R. D., Lemes, P., Brum, F. T., Provete, D. B., & Duarte, L. D. 2014. Clade-specific consequences of climate change to amphibians in Atlantic Forest protected areas. *Ecography*, 37, 65-72.
- Medan, D., Torretta, J. P., Hodara, K., Elba, B., & Montaldo, N. H. 2011. Effects of agriculture expansion and intensification on the vertebrate and invertebrate diversity in the Pampas of Argentina. *Biodiversity and Conservation*, 20, 3077-3100.
- Mendelson JR III, et al. 2006. Confronting amphibian declines and extinctions. *Science*, 313, 48.

- Mendoza-González, G., Martínez, M. L., Rojas-Soto, O. R., Vázquez, G., Gallego-Fernández, J. B. 2013. Ecological niche modeling of coastal dune plants and future potential distribution in response to climate change and sea level rise. *Global Change Biology*, 19, 2524–2535.
- Mesquita, P. C. M. D., Pinheiro-Mesquita, S. F., & Pietczak, C. 2013. Are common species endangered by climate change: Habitat suitability projections for the royal ground snake, *Liophis reginae* (Serpentes, Dipsadidae). *North-Western Journal of Zoology*, 9, 51-56.
- Midgley, G. F., Hannah, L., Rutherford, M. C. & Powrie, L. W. 2002. Assessing the vulnerability of species richness to anthropogenic climate change in a biodiversity hotspot. *Global Ecology and Biogeography*, 11, 445 - 451.
- Moreira, L. F. B., & Maltchik, L. 2015. Our time will come: is anuran community structure related to crop age? *Austral Ecology*, 40, 827-835.
- Moritz, C., Schneider, C. & Wake, D. 1992. Evolutionary relationships within the *Ensatina eschscholtzii* complex confirm the ring species interpretation. *Systematic Biology*, 41, 273-291.
- New, M. D., Liverman, H., Schroeder, H., & Anderson, K. 2011. Four degrees and beyond: The potential for a global temperature increase of four degrees and its implications. *Philosophical Transactions of the Royal Society A: Mathematical, Physical and Engineering Sciences*, 369, 4–5.
- Pauls, S. U., Nowak, C., Bálint, M. & Pfenninger, M. 2013. The impact of global climate change on genetic diversity within populations and species. *Molecular Ecology*, 22, 925-946.
- Peterson, A. T., Soberón, J., Pearson, R. G., et al. 2011. Ecological niches and geographic distributions. Princeton, Princeton University Press.
- Peterson, A.T., Soberón, J.J., Sánchez-Cordero, V. 1999. Conservatism of ecological niches in evolutionary time. *Science*, 285,1265-1267.
- Purvis, A., Gittleman, J. L., Cowlishaw, G. & Mace, G. M. 2000. Predicting extinction risk in declining species. *Proceedings of the royal society B*, 267, 1947-1952.

- Reeder, T. W. 1995. Phylogenetic relationships among Phrynosomatid lizards as inferred from mitochondrial ribosomal DNA sequences: substitutional bias and information content of transitions relative to transversions. *Molecular Phylogenetics and Evolution*, 4, 203-222.
- Rowe, C. L. & Dunson, W. A. 1995. Impacts of hydroperiod on growth and survival of larval amphibians in temporary ponds of Central Pennsylvania, USA. *Oecologia*, 102, 397-403.
- Schwartz, M. K., Luikart, G. & Waples, R. S. 2007. Genetic monitoring as a promising tool for conservation and management. *Trends in Ecology and Evolution*, 22, 25-33.
- Simon, L. M., Oliveira, G., Barreto, B. S., Nabout, J. C., Rangel, T. F. L. V. B., Diniz-Filho, J. A. F. 2013. Effects of global climate changes on geographical distribution patterns of economically important plant species in cerrado. *Revista Árvore*, 37, 267-274.
- Solomon, S. 2007. Climate Change. The Physical Science Basis: Working Group I Contribution to the Fourth Assessment Report of the IPCC. Cambridge: Cambridge University Press.
- Spielman, D., Brook, B. W. & Frankham, R. 2004. Most species are not driven to extinction before genetic factors impact them. *Proceedings of the National Academy of Sciences of USA*, 101, 15261-15264.
- Storfer, A., Jonathan, M. E. & Stephen, F. S. 2009. Modern molecular methods for amphibian conservation. *BioScience*, 59, 559-571.
- Stuart, S. N., Chanson, J. S., Cox, N. A., Young, B. E., Rodrigues, A. S. L., Fischman, D. L., & Waller, R. W. 2004. Status and trends of amphibian declines and extinctions worldwide. *Science*, 306, 1783-1786.
- Tamura, K. & M. Nei. 1993. Estimation of the number of nucleotide substitutions in the control region of mitochondrial DNA in humans and chimpanzees. *Molecular Biology and Evolution*, 10, 512-526.

- Terribile, L. C., Lima-Ribeiro, M. S., Araújo, M. B., Bizão, N., Collevatti, R. G. *et al.* 2012. Areas of Climate Stability of Species ranges in the Brazilian Cerrado: Disentangling Uncertainties through Time. *Natureza & Conservação*, 10, 152-159.
- Thomas, C. D., A. Cameron, R. E. Green, M. Bakkenes, L. J. Beaumont, Y. C. Collingham, B. F. N. Erasmus *et al.* 2004. Extinction risk from climate change. *Nature*, 427, 145–148.
- Thompson, J. D., Gibson, T. J., Plewniak, F., Jeanmougin, F. & Higgins, D. G. 1997. The Clustal X windows interface: flexible strategies for multiple sequence alignment aided by quality analysis tools. *Nucleic Acids Research*, 24, 4876–4882.
- Urban, M. C., De Meester, L., Vellend, M., Stoks, R. & Vanoverbeke, J. 2012. A crucial step toward realism: responses to climate change from an evolving metacommunity perspective. *Evolutionary Applications*, 5, 154–167.
- Urban, M. C., Richardson, J. L. & Freidenfelds, N. A. 2013. Plasticity and genetic adaptation mediate amphibian and reptile responses to climate changes. *Evolutionary Applications*, 7, 88-103.
- Vasconcelos, T. S. 2014. Tracking climatically suitable areas for an endemic Cerrado snake under climate change. *Natureza Conservação*, 12, 47–52.
- Vasconcelos, T. S., & Do Nascimento, B. T. 2016. Potential climate-driven impacts on the distribution of generalist treefrogs in South America. *Herpetologica*, 72, 23-31.
- Vasconcelos, T. S., do Nascimento, B. T., & Prado, V. H. 2018. Expected impacts of climate change threaten the anuran diversity in the Brazilian hotspots. *Ecology and Evolution*.
- Vilela, B., Nascimento, F. A., & Vital, M. V. C. 2018. Impacts of climate change on small-ranged amphibians of the northern Atlantic Forest. *Oecologia Australis*, 22.
- Wiens, J. J., Ackerly, D. D., Allen, A. P., Anacker, B. L., Buckley, L. B., Cornell, H.V., Damschen, E. I., Davies, T. J., Grytnes, J. A., Harrison, S. P., Hawkins, B. A., Holt, R. D., McCain, C. M. & Stephens, P. R. 2010. Niche conservatism as an emerging principle in ecology and conservation biology. *Ecology Letters*, 13, 1310–1324.

- Wiens, J. J. & Graham, C. H. 2005. Niche conservatism: integrating evolution, ecology, and conservation biology. *Annual Review of Ecology, Evolution and Systematics* 36, 519–539.
- Wiens, J. J. 2004. Speciation and ecology revisited: phylogenetic niche conservatism and the origin of species. *Evolution*, 58, 193-97.
- Wright, L. I., Tregenza, T., & Hosken, D. J. 2008. Inbreeding, inbreeding depression and extinction. *Conservation Genetics*, 9, 833–843.
- Xia, X. 2013. DAMBE5: A comprehensive software package for data analysis in molecular biology and evolution. *Molecular Biology and Evolution*, 30, 1720-1728.
- Zhang, M. G., Zhou, Z. K., Chen, W. Y., Slik, J. W. F., Cannon, C. H. & Raes, N. 2012. Using species distribution modeling to improve conservation and land use planning of Yunnan, China. *Biological Conservation*, 153, 257–264

## **BIOSKETCH**

The authors work with bridging macroecology and population genetics, with particular emphasis on phylogeography and geographical patterns of genetic diversity in Neotropical species.

**Author contributions:** RGC, NMM, and TPFAJ conceived the study; TPFAJ generated the genetic data, and performed the genetic analysis and niche modelling analyses. LBM and T PFAJ performed the forecasting and dynamics in genetic clusters in future scenarios. LBM, LJ and TPFAJ performed kriging and spatial genetic analysis. All authors contributed and approved the final version of the manuscript.

## **SUPPORTING INFORMATION**

Additional Supporting information may be found in the online version of this article:

**Appendix S1** Supplementary tables (Tables S1.1- S1.17) with details of sampling, PCR amplification, sampling and models used in ecological niche modelling, number of haplotypes and results of genetic ancestry clusters.

**Appendix S2** Supplementary figures (Figures S2.1-S2.4) with saturation result, maps of uncertainty, graph of range size and range shift and Sum of squares within clusters by number of clusters.

**Conflict of Interest Statement:** The authors declare no conflict of interest.

**Table 1** Genetic diversity and environmental variables of *Scinax squaleirostris* populations. Population – Population code, Coordinates (longitude e latitude), N – sample size, *h* – haplotype diversity,  $\pi$  - nucleotide diversity and k - number of haplotypes, Altitude, Slope, aspect, and suitability values for each time (Current, 4.5 RCP and 8.5 RCP future scenarios).

Population	Coordinates		N	Genetic Diversities			Altitude	Slope	Suitability		
	Longitude	Latitude		<i>h</i>	$\pi$	k			Current	Future 4.5 RCP	Future 8.5 RCP
ISP	-47.7958	-22.2744	5	0.70000	0.006163 ± 0.004322	3	764	1.159	0.861	0.333	0.091
BSP	-44.4825	-23.3458	13	0.98718	0.006163 ± 0.004322	12	256	0.000	0.772	0.334	0.061
SRMG	-46.6628	-20.1461	12	0.83333	0.001527 ± 0.001107	5	1136	2.565	0.914	0.398	0.083
OMG	-43.5081	-20.2875	16	0.68333	0.002304 ± 0.001490	5	1141	3.646	0.939	0.659	0.190
CMG	-43.4075	-20.0747	3	1.00000	0.001527 ± 0.001107	2	755	2.100	0.935	0.638	0.165
PMG	-46.5614	-21.7878	1	0.00000	0.000000 ± 0.000000	1	1314	4.174	0.950	0.632	0.180
SMG	-44.2714	-17.6992	16	0.93333	0.002016 ± 0.001486	11	1181	0.292	0.728	0.140	0.070
SVMG	-43.7977	-17.7883	22	0.86147	0.001408 ± 0.000999	11	1169	3.146	0.828	0.189	0.071
SCMG	-43.5100	-19.2469	13	0.79487	0.000256 ± 0.000341	5	1311	1.428	0.901	0.386	0.115
CGO	-47.4667	-14.0833	24	0.64855	0.001146 ± 0.000856	8	1131	5.362	0.223	0.064	0.050
BDF	-47.9297	-15.7797	19	0.70175	0.000187 ± 0.000279	5	1127	0.529	0.535	0.118	0.059
BMS	-56.4819	-21.1211	7	1.00000	0.007311 ± 0.004469	6	312	0.896	0.195	0.081	0.062
RRS	-53.7333	-27.1833	27	0.99715	0.003332 ± 0.001965	25	242	0.157	0.997	0.858	0.360
SJRS	-52.0417	-32.0147	10	1.00000	0.003216 ± 0.002048	10	2	0.048	0.890	0.753	0.609
SFRS	-50.5836	-29.4481	2	1.00000	0.038922 ± 0.039418	2	879	2.609	0.965	0.860	0.732
BRS	-50.4167	-28.6678	1	0.00000	0.000000 ± 0.000000	1	1046	1.197	0.922	0.826	0.745
PPR	-51.9906	-26.4842	2	1.00000	0.005988 ± 0.006468	2	1070	0.454	0.996	0.965	0.692

PGPR	-50.1619	-25.095	8	0.94290	$0.004491 \pm 0.002815$	7	892	0.723	0.977	0.875	0.619
CBSC	-50.7608	-27.8992	1	0.00000	$0.000000 \pm 0.000000$	1	970	0.424	0.949	0.895	0.759
CNSC	-51.2250	-27.4017	2	1.00000	$0.006163 \pm 0.006891$	2	917	0.435	0.998	0.946	0.757
BSC	-49.6247	-28.3369	5	1.00000	$0.008320 \pm 0.005639$	5	1359	0.464	0.901	0.810	0.644
CSC	-51.0150	-26.7753	3	1.00000	$0.003082 \pm 0.002905$	3	934	0.896	0.997	0.949	0.748
ASC	-51.5561	-26.9978	2	1.00000	$0.010786 \pm 0.011531$	2	899	1.763	0.999	0.953	0.720
EPY	-58.4486	-27.2016	1	0.00000	$0.000000 \pm 0.000000$	1	57	0.045	0.964	0.336	0.236
APY	-55.6333	-26.5833	7	0.95238	$0.002054 \pm 0.001651$	5	306	0.864	0.992	0.334	0.186
URU	-56.0000	-33.0000	1	0.00000	$0.000000 \pm 0.000000$	1	132	0.249	0.986	0.991	0.946

## Figures Labels

**Figure 1.** Current geographical distribution of *Scinax squalirostris* and environmental suitability modelled using ecological niche modelling. A) The 257 occurrence records (black dots) used in ecological niche modelling. B) Distribution of suitability for the current climate conditions. C) Distribution of suitability for the future climatic scenario of CO<sub>2</sub> emission for 4.5 RCP and D) Distribution of suitability for the future climate scenarios of CO<sub>2</sub> emission for 8.5 RCP. Black dots in B, C and D represent the 26 sampled populations from where genetic data were collected.

**Figure 2.** Ecological space of climatic conditions across the Neotropics during current time (light blue), 4.5 RCP future scenario (blue) and 8.5 RCP future scenario (purple). The climatic preferences from current occurrence records of *Scinax squalirostris* are represented by black dots. The bioclimatic variable values used here were obtained from AOGCM CCSM4.

**Figure 3.** Simulations of shifts in genetic diversity for sequence data under different levels of suitability threshold for A) 4.5 RCP and B) 8.5 scenarios, based on 26 populations of *Scinax squalirostris*.  $h$  – haplotype diversity,  $\pi$  - nucleotide diversity and  $k$  - number of haplotypes.

**Figure 4.** Geographical distribution of nucleotide and haplotype genetic diversity and number of haplotypes for *Scinax squalirostris* populations: A) nucleotide diversity, B) haplotype diversity, C) number of haplotypes. For details on population codes and localities see Table S1.1 in Appendix S1.

**Figure 5.** Spatial distribution of genetic clusters conditioned to environmental variables simulated for *Scinax squalirostris*, for mitochondrial (A, B and C) and nuclear data (D, E and F), for present-day (A and D), 4.5 RCP scenario (B and E), 8.5 RCP scenario (C and F). Each colour set represents a cluster in the figure legend. Shifts in ancestry between contemporary and predicted ancestry coefficients for both future scenarios based on the simulation of genetic clusters of all individuals of *Scinax squalirostris*. G) Shifts in ancestry for the eight genetic clusters based on mitochondrial data. H) Shifts in ancestry for the three genetic clusters based on nuclear data.

**Figure 6.** Spatial distributions of genetic information from nuclear and mitochondrial sequences. A) Raw data of spatial distribution of haplotypes; B) Observed genetic richness measured by the number haplotypes divided by number of individuals per cell. C) Estimated genetic richness in 0.5° cell size measured as the estimated genetic richness using kriging.

**Figure 7.** Spatial distributions of clusters of Protection Areas, based on *k-mean* clusters analysis. A) Relationship of estimated genetic richness and Protection Areas size; B) Spatial distribution of genetic richness and the Protection Areas clusters. The colour of polygons representing Protection Areas corresponds to the clusters in the *k-mean* cluster analysis following the figure legends.

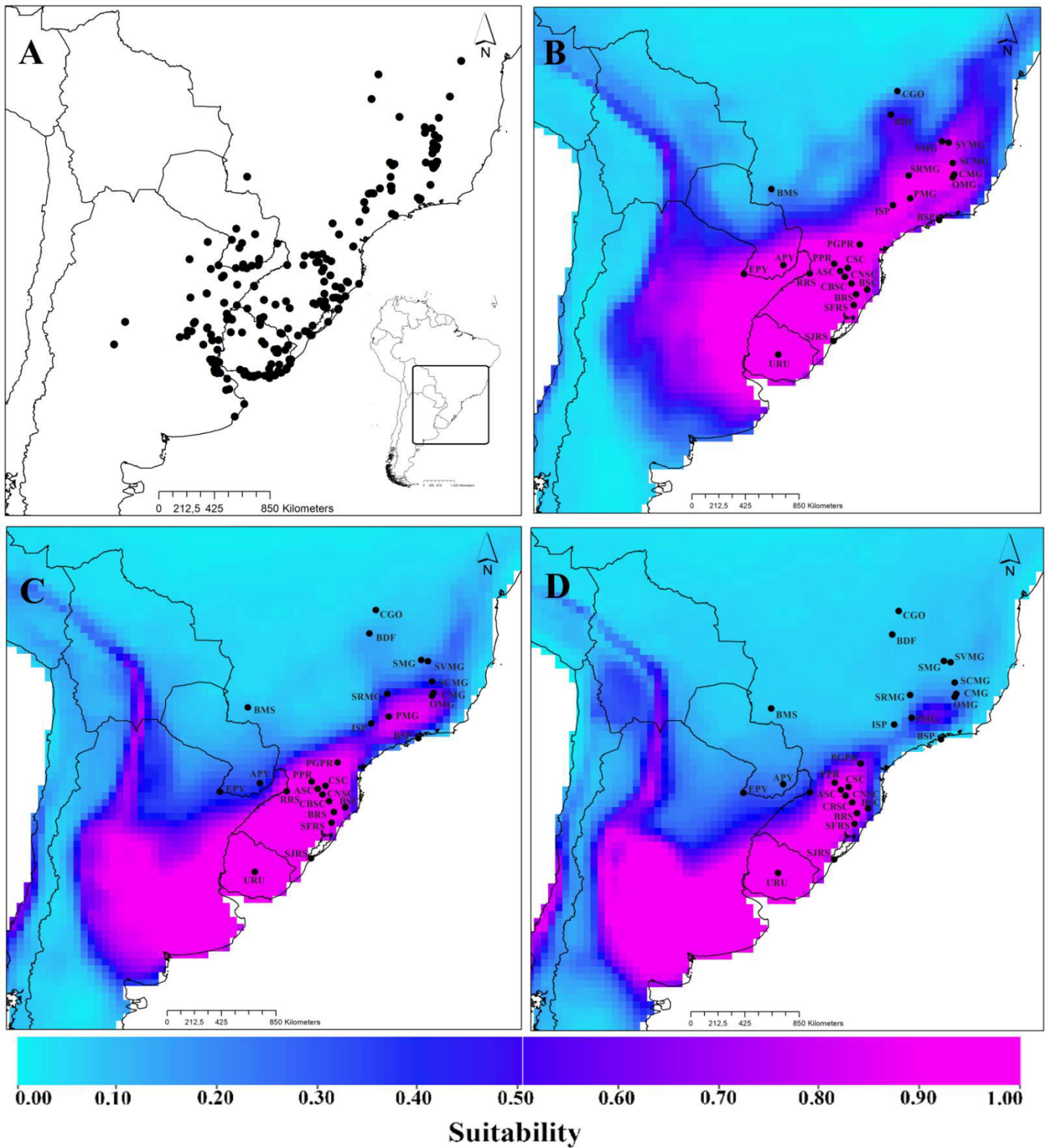
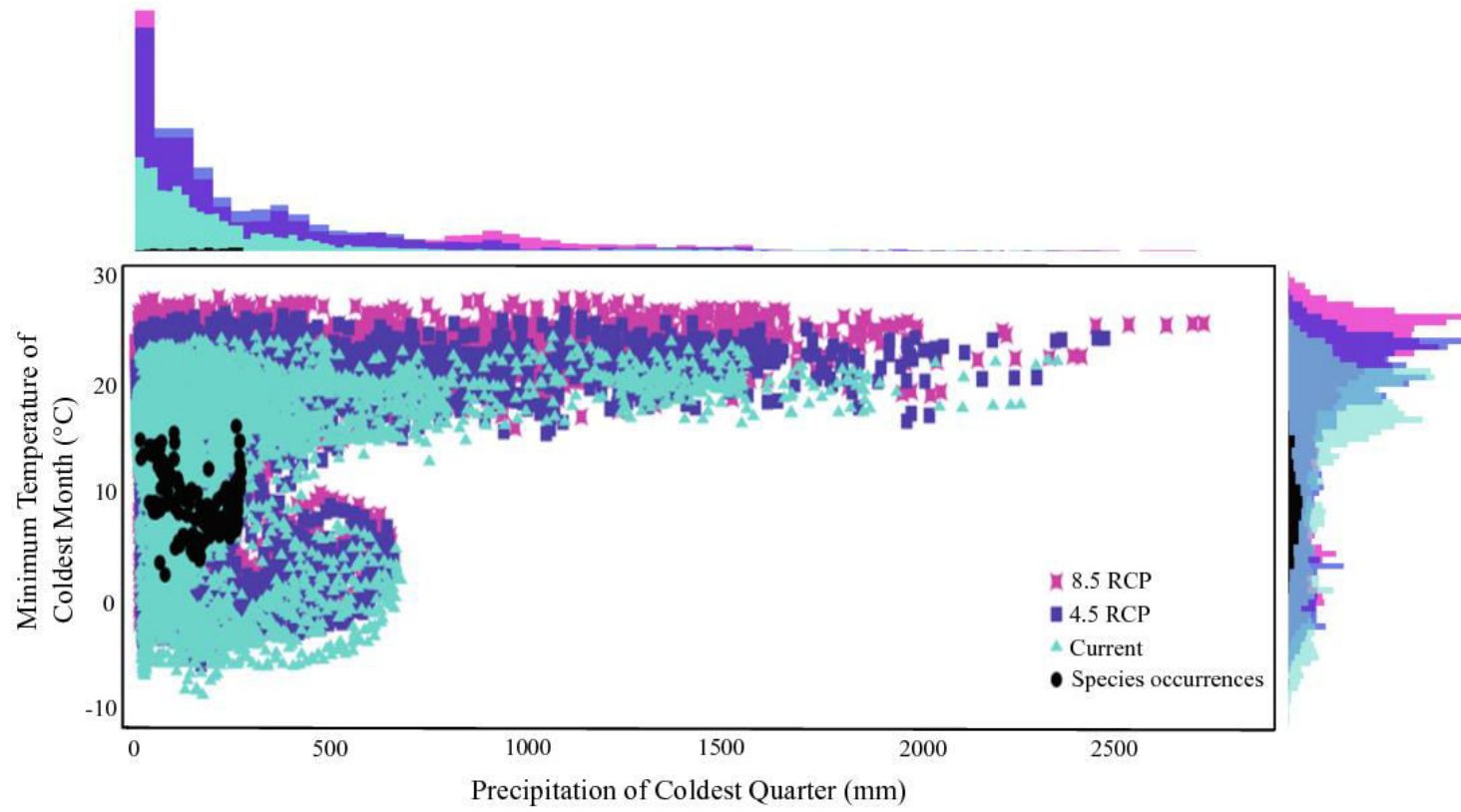
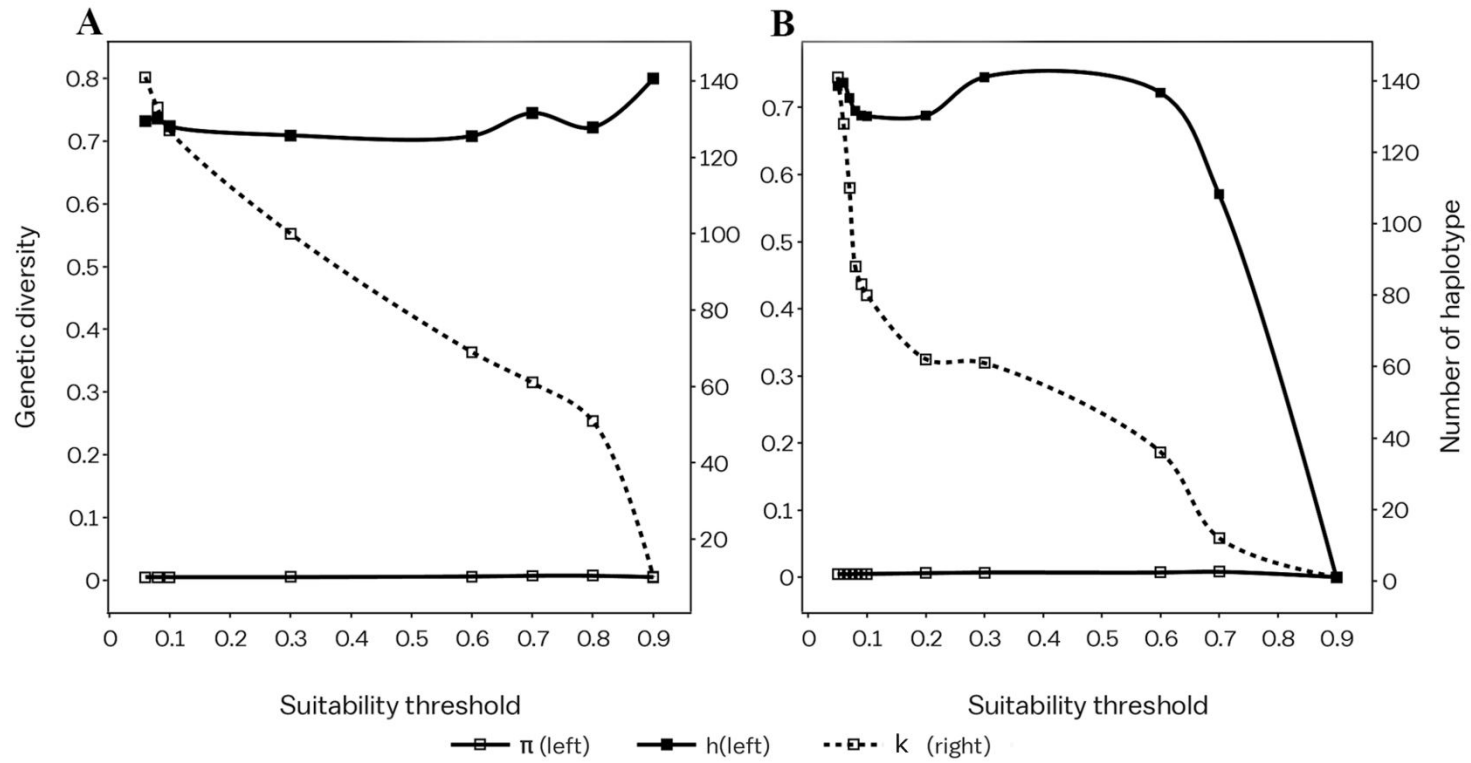


Figura 1



**Figura 2**



**Figure 3**

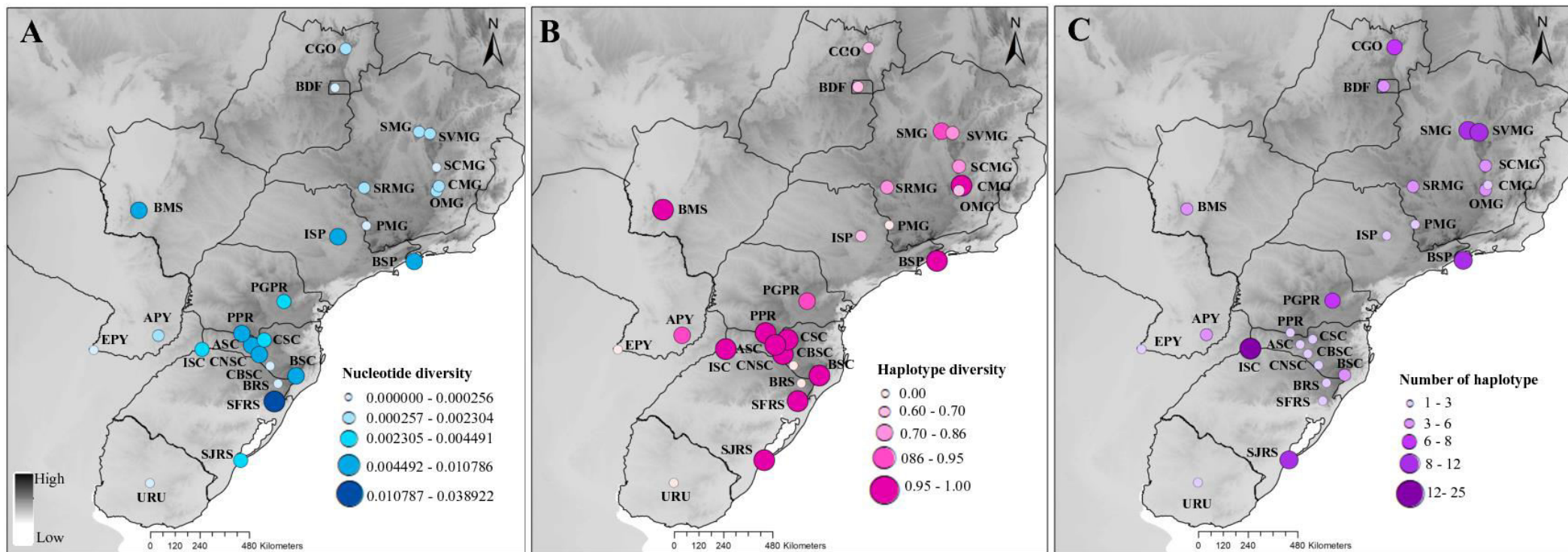


Figura 4

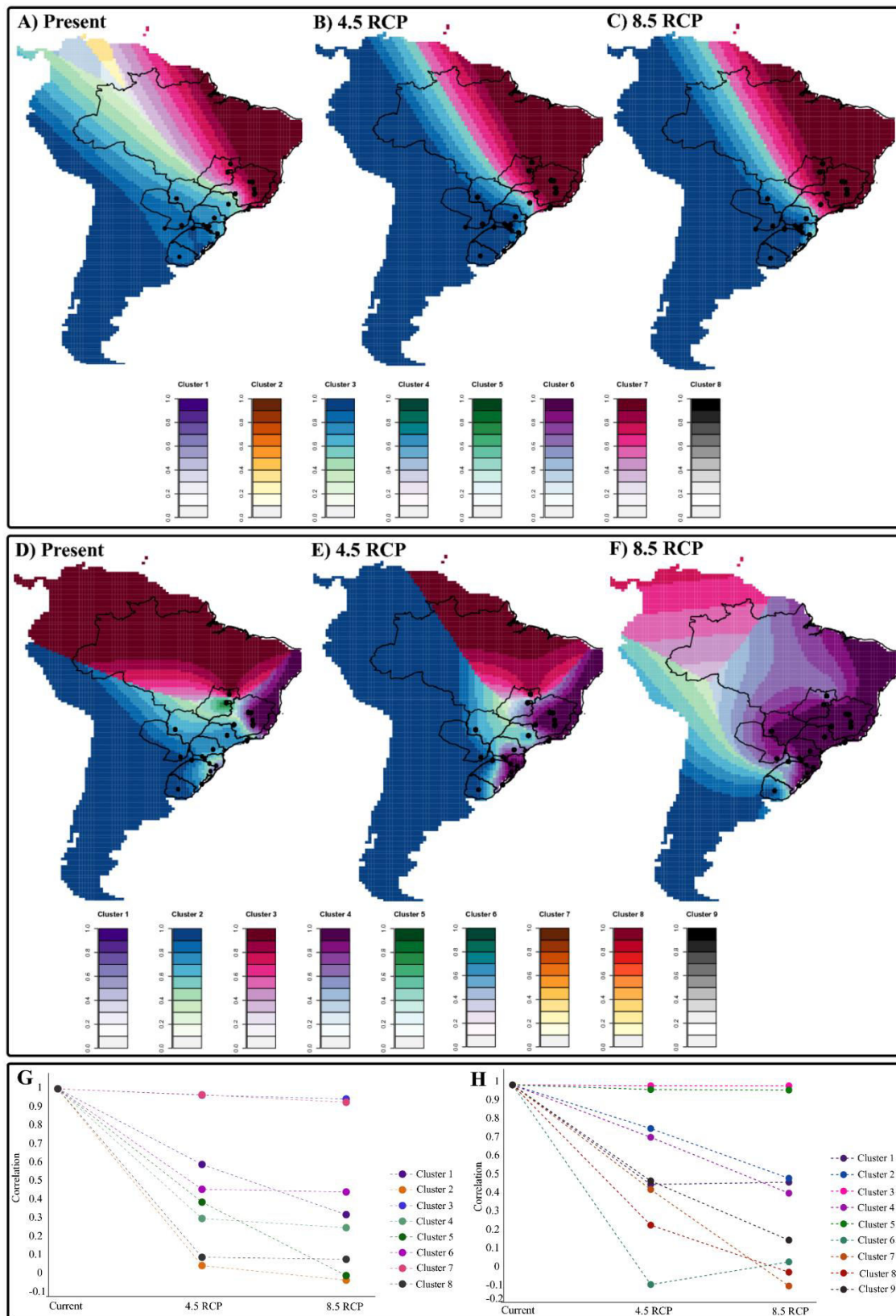
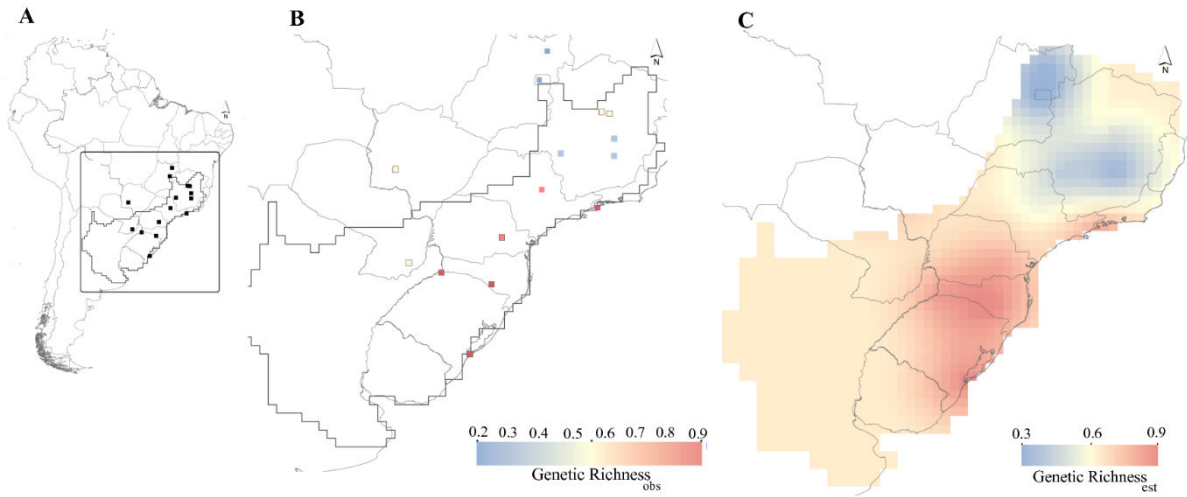
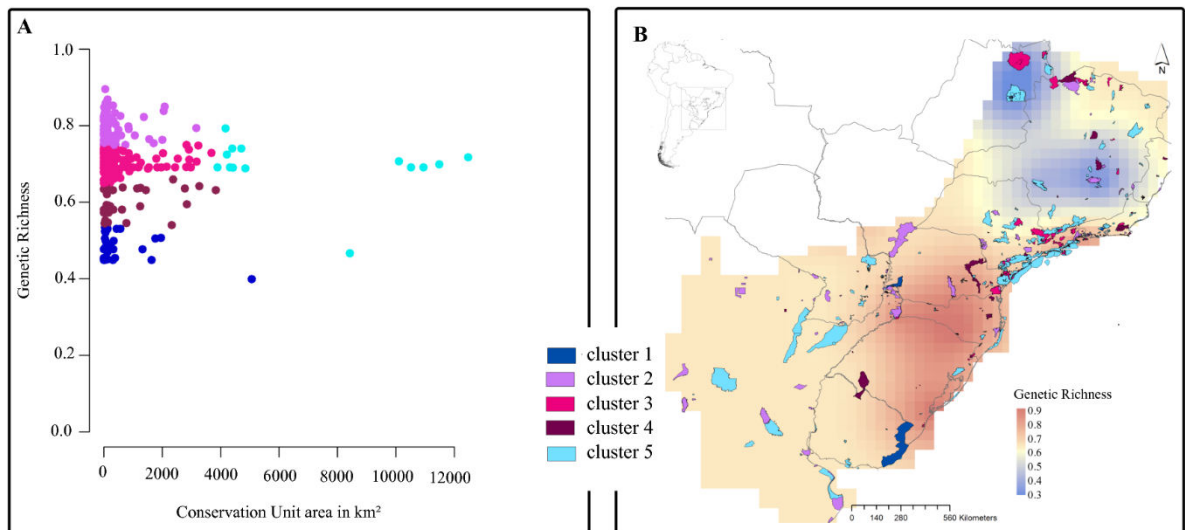


Figure 5



**Figure 6**



**Figure 7**

## SUPPORTING INFORMATION

### **Predicting impacts of global climatic change on distribution and genetic diversity of the treefrog *Scinax squalirostris* (Lutz, 1925) (Anura, Hylidae)**

Tatianne P. F. Abreu-Jardim, Lucas Jardim, Liliana Ballesteros-Meija, Natan M.

Maciel, Rosane G. Collevatti

**Appendix S1** Supplementary tables (Tables S1- S11) with details of sampling, PCR amplification, sampling and models used in ecological niche modelling, number of haplotypes and results of genetic ancestry clusters.

**Table S1.1** Sampling locations of the 26 populations of *Scinax squalirostris*. Name of localities in the Population column we presented the abbreviation of Brazilian states and a Paraguayan

department. Collection column we presented the abbreviation of donor institutions. (Amphibian Collection Célio F. B. Haddad (CFBH), Collection of the Universidade Federal de Minas Gerais (UFMG), Zoological Collection of the Universidade Federal de Goiás (ZUFG), Collection Elaine Maria Lucas Gonsales (EMLG), Museum of Ciências e Tecnologia da PUCRS (MCT), Collection of the Universidade Federal do Rio Grande do Sul (UFRGS), Herpetology Collection of the Instituto de Investigación Biológica del Paraguay (IIBPH).

<b>Population</b>	<b>Population Code</b>	<b>Collection</b>	<b>Latitude</b>	<b>Longitude</b>
Itirapina-SP	ISP	CFBH	-22.2744	-47.7958
PARNA Bocaina-SP	BSP	CFBH	-23.3458	-44.4825
São Roque de Minas-MG	SRMG	CFBH	-20.1461	-46.6628
Ouro Preto-MG	OMG	CFBH	-20.2875	-43.5081
Catas Altas-MG	CMG	UFMG	-20.0747	-43.4075
Poços de Caldas-MG	PMG	UFMG	-21.7878	-46.5614
Serra do Cabral-MG	SMG	LOD	-17.6992	-44.2714
PARNA Sempre Vivas-MG	SVMG	ZUFG	-17.7883	-43.7977
PARNA Serra do Cipó-MG	SCMG	ZUFG	-19.2469	-43.5100
PARNA Chapada dos Veadeiros-GO	CGO	ZUFG	-14.0833	-47.4667
Brasília-DF	BDF	ZUFG	-15.7797	-47.9297
Bonito-MS	BMS	ZUFG	-21.1211	-56.4819
Itaparanga-SC	ISC	CFBH	-27.1833	-53.7333
São José do Norte-RS	SJRS	UFRGS	-32.0147	-52.0417
São Francisco de Paula-RS	SFRS	MCP	-29.4481	-50.5836
Bom Jesus-RS	BRS	CFBH	-28.6678	-50.4167
Palmas-PR	PPR	ZUFG	-26.4842	-51.9906
Ponta Grossa-PR	PGPR	ZUFG	-25.095	-50.1619
Campo Belo do Sul-SC	CBSC	MCP	-27.8992	-50.7608
Campos Novos-SC	CNSC	CFBH	-27.4017	-51.2250
Bom Jardim da Serra-SC	BSC	CFBH	-28.3369	-49.6247
Caçador-SC	CSC	EMLG	-26.7753	-51.0150
Água Doce-SC	ASC	EMLG	-26.9978	-51.5561
Estancia San José-Ñeembucú-Py	EPY	IIBPH	-27.2016	-58.4486
Alto Vera, Yataí-Itapuá-Py	APY	IIBPH	-26.5833	-55.6333
Uruguai	URU	-	-33.0000	-56.0000

**Table S1.2** PCR Primers used to sequence CytB, 12S rRNA, and RAG-1 genes used in this study.

Gene region	Primer	Direction	Nucleotide Sequence (5'-3')
CytB	MVZ15	forward	GAACTAATGGCCCACACWWTACGNAA
	H1415 (cyt-b2) (H15149)	reverse	AAACTGCAGCCCCTCAGAATGATATTTGTCCTCA
12S	12S	forward	AAACTGGGATTAGATACCCCACTAT
	12S	reverse	GAGGGTGACGGGCGGTGTGT
RAG	RAG1	forward	ATGCATCRAAAATTCARCAAT
	RAG1	reverse	CCYCCTTTRTTGATAKGGWCATA

**Table S1.3** PCR mix components and quantities for each of the amplified fragments used in this study.

Reagent	Cytb, 12S and RAG-1
Deionized water	8.5 $\mu$ L
DNA	2.0 $\mu$ L
Forward primer (2 mM)	3.0 $\mu$ L
Reverse primer (2mM)	3.0 $\mu$ L
Buffer 1X*	2.0 $\mu$ L
DNTPs (2,5 mM)	1,2 $\mu$ L
Taq polymerase (5u/ $\mu$ L)	0.3 $\mu$ L
Total volume	20 $\mu$ L

\*Buffer 1X (10 mM Tris-HCl, pH 8.3, 50 mM KCl, 1.5 mM MgCl<sub>2</sub>)

**Table S1.4** PCR thermal program for each of the amplified fragments used in this study.

Gene region	Initial heating	Desnaturation	Annealing	Extension	Final extension
	<b>35 cycles</b>				
CytB	2 min at 94°C	60 sec at 94°C	60 sec at 56°C	90 sec at 72°C	6 min at 72°C
12S	2 min at 94°C	60 sec at 94°C	60 sec at 54°C	90 sec at 72°C	6 min at 72°C
RAG	2 min at 94°C	60 sec at 94°C	60 sec at 58°C	90 sec at 72°C	6 min at 72°C

**Table S1.5** Geographic coordinates of 257 occurrence records of *Scinax squalirostris* used in ecological niche modelling.

longitude	latitude	longitude	latitude	longitude	latitude
-54.80	-34.70	-55.67	-26.83	-50.42	-28.67
-56.46	-34.75	-56.17	-27.23	-51.23	-27.40
-54.92	-34.80	-49.63	-28.33	-53.57	-30.16
-54.10	-31.92	-56.77	-27.14	-43.31	-17.06
-54.28	-34.03	-57.02	-26.01	-44.27	-18.11
-56.69	-34.71	-58.40	-33.87	-46.01	-17.01
-53.77	-34.35	-58.58	-34.33	-50.58	-29.45
-57.54	-30.90	-58.23	-28.05	-51.18	-29.17
-55.67	-26.76	-64.87	-31.10	-52.53	-26.56
-56.74	-27.36	-54.42	-25.72	-43.68	-18.81
-56.50	-27.42	-65.63	-32.65	-43.69	-20.52
-56.17	-27.23	-56.68	-36.75	-42.54	-15.61
-55.94	-25.07	-58.54	-34.63	-44.18	-17.87
-56.76	-27.14	-58.05	-29.79	-41.77	-13.15
-57.23	-24.69	-59.26	-29.14	-43.80	-20.25
-55.73	-27.18	-61.11	-32.16	-55.06	-34.83
-56.83	-25.68	-58.60	-33.78	-58.52	-33.01
-57.27	-27.40	-58.88	-32.37	-60.08	-31.10
-57.54	-25.46	-58.54	-34.58	-46.37	-20.25
-55.67	-26.83	-58.52	-33.02	-46.62	-21.13
-46.52	-23.67	-60.44	-26.79	-48.35	-23.40
-47.35	-21.92	-60.64	-32.06	-56.33	-34.86
-44.75	-22.57	-60.57	-31.71	-44.57	-22.64
-49.55	-28.40	-59.02	-33.69	-58.99	-27.47
-46.32	-23.78	-60.30	-31.73	-46.56	-21.79
-35.73	-84.83	-58.44	-32.35	-51.32	-264.28
-48.43	-22.87	-59.22	-31.48	-49.20	-25.93
-59.50	-32.67	-60.52	-31.73	-51.32	-26.43
-58.73	-34.38	-57.85	-35.02	-51.63	-26.52
-58.84	-33.69	-57.33	-37.62	-46.62	-21.78

-58.87	-32.37	-54.91	-34.80	-44.58	-22.65
-58.96	-31.99	-54.28	-34.04	-51.74	-27.01
-59.24	-31.54	-54.13	-34.58	-46.37	-20.25
-58.88	-33.91	-57.53	-30.95	-51.02	-30.08
-57.17	-28.54	-56.45	-34.74	-50.23	-30.25
-58.70	-34.58	-54.17	-31.87	-50.21	-30.18
-58.10	-27.92	-55.06	-34.83	-52.10	-32.04
-58.64	-34.36	-56.30	-34.87	-51.23	-30.03
-60.38	-29.42	-55.60	-30.87	-50.07	-28.75
-58.06	-29.79	-53.80	-34.39	-51.93	-29.83
-58.87	-33.89	-57.88	-30.53	-51.76	-29.91
-57.93	-35.78	-57.87	-30.58	-53.67	-31.56
-58.35	-34.61	-57.73	-30.78	-56.00	-28.66
-60.15	-31.19	-55.90	-34.82	-50.07	-29.59
-59.26	-29.15	-56.03	-34.82	-48.78	-28.48
-57.17	-28.54	-56.03	-34.88	-52.34	-31.77
-57.72	-35.73	-55.72	-34.73	-49.73	-29.34
-58.44	-34.54	-54.20	-31.87	-51.34	-27.63
-59.19	-25.61	-53.67	-32.72	-51.13	-29.68
-43.75	-19.51	-55.28	-32.63	-50.70	-26.93
-43.71	-19.17	-56.65	-34.50	-50.76	-27.90
-43.71	-19.17	-54.98	-34.33	-50.22	-29.45
-43.74	-19.51	-54.57	-34.78	-52.10	-32.04
-46.57	-22.07	-55.27	-34.80	-50.38	-29.42
-43.88	-21.68	-54.95	-34.97	-51.18	-28.33
-43.41	-20.07	-56.35	-34.80	-51.98	-31.36
-44.18	-17.87	-56.83	-31.83	-50.01	-28.84
-44.20	-20.14	-57.62	-31.82	-50.22	-30.20
-43.43	-19.04	-55.55	-31.03	-55.36	-30.77
-43.60	-18.25	-55.60	-31.32	-52.99	-32.05
-43.31	-18.47	-53.45	-33.68	-57.18	-29.95
-43.61	-20.45	-53.58	-33.68	-55.34	-29.60
-43.47	-20.08	-53.53	-33.98	-54.54	-29.92

-46.53	-23.67	-53.77	-34.28	-56.47	-30.18
-46.53	-23.67	-53.78	-34.33	-56.01	-28.62
-47.82	-22.25	-53.78	-34.35	-52.52	-31.74
-48.44	-22.88	-54.33	-34.48	-50.92	-31.11
-47.35	-21.92	-54.15	-34.60	-48.43	-22.87
-44.75	-22.57	-57.87	-30.93	-57.54	-30.90
-46.32	-23.78	-57.53	-30.95	-53.77	-34.35
-48.13	-22.28	-56.67	-34.73	-49.55	28.40
-48.77	-24.22	-56.97	-34.38	-47.80	-22.27
-53.81	-29.68	-56.37	-34.82	-46.48	-20.35
-51.02	-30.08	-55.47	-32.43	-46.66	-20.15
-51.46	-29.69	-54.40	-32.97	-46.56	-21.79
-51.18	-29.92	-54.62	-33.00	-44.27	-17.70
-52.34	-31.77	-54.48	-33.22	-43.80	-17.79
-52.15	-32.02	-54.38	-33.23	-43.51	-19.25
-50.16	-25.10	-54.83	-34.00	-51.56	-27.00
-51.99	-26.48	-53.87	-33.03	-51.02	-26.78
-50.62	-24.32	-48.00	-22.25	-52.04	-32.01
-49.18	-25.92	-44.61	-22.72	-53.73	-27.18
-52.62	-27.19	-43.51	-20.29	-47.47	-14.08
-47.82	-22.25	-49.62	-28.34	-47.93	-15.78
-44.57	-22.64	-56.48	-21.12	-58.45	-27.20
-50.16	-25.10	-51.99	-26.48		

---

**Table S1.6** Details on atmosphere-ocean global circulation models (AOGCMs) used for ecological niche modelling of *Scinax squalirostris*

<b>Model ID</b>	<b>Modelling Centre</b>	<b>Resolution*</b>	<b>Source</b>	<b>Year</b>
CCSM4	University of Miami – RSMAS, USA	0.9° × 1.25°	CMIP5/PMIP3	2012
CNRM-CM5	Centre National de Recherches Meteorologiques / Centre Europeen de Recherche et Formation Avancees en Calcul Scientifique, France	1.4° x 1.4°	CMIP5/PMIP3	2012
MIROC-ESM	Atmosphere and Ocean Research Institute (University of Tokyo), National Institute for Environmental Studies, and Japan Agency for Marine-Earth Science and Technology, Japan	2.8° × 2.8°	CMIP5/PMIP3	2012
MPI-ESM-P	Max Planck Institute for Meteorology, Germany	1.9° × 1.9°	CMIP5/PMIP3	2011
MRI-CGCM3	Meteorological Research Institute, Japan	1.1° x 1.1°	CMIP5/PMIP3	2012

\* longitude × latitude

CMIP5 –Coupled Model Intercomparison Project, Phase 5 (<http://cmip-pcmdi.llnl.gov/>)

PMIP3 –Paleoclimate Modelling Intercomparison Project, Phase 3 (<http://pmip3.lsce.ipsl.fr/>)

**Table S1.7** Ecological niche modeling methods used to estimate *Scinax squalirostris* potential distribution.

<b>Method</b>	<b>Species data type</b>
Bioclimatic Envelope (BioClim)	Presence only
Ecological Niche Factor Analysis (ENFA)	Presence only
Euclidian Distance (EuclidDist)	Presence only
Flexible discriminant analysis (FDA)	Presence and absence
Generalized additive models (GAM)	Presence and absence
Generalized Linear Models (GLM)	Presence and absence
Gower Distance (GowerDist)	Presence only
Mahalanobis Distance (MahalDist)	Presence only
Multivariate adaptive regression splines (MARS)	Presence and absence
Maximum Entropy (MaxEnt)	Presence/background
Neural Networks (NNet)	Presence and absence
Random Forest (RNDFOR)	Presence and absence

**Table S1.8** Values of true skill statistics (TSS) and values of area under the curve (AUC), with mean and standard deviation, for all ecological niche models (ENM) and atmosphere-ocean global circulation model (AOGCM) combinations (ENM x AOGCM) in *Scinax squaleirostris* paleodistribution modelling.

ENM/AOGCM	CCSM		CNRM		MIROC		MPI		MRI		Mean		SD	
	TSS	AUC	TSS	AUC	TSS	AUC	TSS	AUC	TSS	AUC	TSS	AUC	TSS	AUC
BioClim	0.698	0.937	0.690	0.936	0.678	0.920	0.722	0.949	0.647	0.927	0.690	0.936	0.028	0.011
ENFA	0.515	0.849	0.480	0.798	0.503	0.840	0.521	0.841	0.541	0.841	0.515	0.841	0.022	0.020
EuclidDist	0.645	0.895	0.465	0.825	0.625	0.888	0.673	0.903	0.551	0.883	0.625	0.888	0.084	0.031
FDA	0.759	0.961	0.730	0.945	0.724	0.940	0.793	0.963	0.751	0.950	0.751	0.950	0.027	0.010
GAM	0.768	0.960	0.780	0.967	0.767	0.942	0.821	0.966	0.758	0.956	0.768	0.960	0.025	0.010
GowerDist	0.662	0.921	0.647	0.889	0.683	0.900	0.746	0.927	0.616	0.915	0.662	0.915	0.049	0.016
MahalonobisDist	0.725	0.935	0.561	0.845	0.545	0.867	0.724	0.927	0.707	0.923	0.707	0.923	0.091	0.041
GLM	0.714	0.942	0.761	0.952	0.704	0.915	0.820	0.967	0.754	0.954	0.754	0.952	0.046	0.020
MARS	0.747	0.951	0.761	0.952	0.780	0.955	0.837	0.969	0.761	0.954	0.761	0.954	0.035	0.007
MaxEnt	0.762	0.958	0.727	0.957	0.768	0.960	0.836	0.978	0.777	0.972	0.768	0.960	0.039	0.009
NNet	0.564	0.882	0.686	0.962	0.688	0.951	0.694	0.920	0.670	0.966	0.686	0.951	0.054	0.035
RndFor	0.792	1.000	0.767	1.000	0.789	1.000	0.827	1.000	0.798	1.000	0.792	1.000	0.022	0.000
<b>Mean</b>	0.720	0.939	0.709	0.948	0.696	0.930	0.769	0.956	0.729	0.952	-	-	-	-
<b>SD</b>	0.085	0.041	0.111	0.064	0.091	0.044	0.093	0.043	0.089	0.043	-	-	-	-

**Table S1.9** Characteristics of the 26 populations sampled for the analysis Phylogeography of *Scinax squalirostris*. Individuals (N), haplotypes by population (K) and relation of the haplotypes by population. Haplotypes in bold show the haplotype shared among some populations.

Population	mtDNA		nrDNA	
	N	k	Haplotypes	Haplotypes
ISP	5	2	h01, h02	h01, h02
BSP	12	8	h01, h02, h03, h04, h05, h06, h07, h08	h02, h03, h04, h05
SRMG	11	4	h09, h10, h11, h12	h04
OMG	16	5	h13, h14, h15, h16, h17	h06, h07
CMG	3	1	h14	h06, h08, h09
PMG	1	1	h18	-
SMG	16	7	h19, h20, h21, h22, h23, h24, h25	h06, h10, h11, h12, h13
SVMG	22	5	h26, h27, h28, h29, h30	h06, h10, h14, h15, h16, h17, h18, h19
SCMG	13	2	h26, h31	h06, h20, h21
CGO	24	5	h32, h33, h34, h35, h36	h22, h23, h24
BDF	19	4	h37, h38, h39, h40	h25
BMS	7	3	h41, h42, h43	h06, h07, h26, h27, h28
ISC	26	12	h44, h45, h46, h47, h48, h49, h50, h51, h52, h53, h54, h55	h01, h29, h30, h31, h32, h33, h34, h35, h36, h37, h38, h39, h40, h41, h42, h43, h44, h45

SJRS	10	2	h44, h46	10	10	h26, h30, h32, h36, h37, h46, h47, h48, h49, h50
SFRS	2	2	h56, h57	2	2	h51, h52
BRS	1	1	h58	1	1	h53
PPR	2	2	h59, h60	2	2	h06, h54
PGPR	8	3	h01, h05, h61	8	6	h55, h56, h57, h58, h59, h60
CBSC	1	1	h62	1	1	h51
CNSC	2	1	h01	2	2	h61, h62
BSC	5	2	h01, h62	5	5	h31, h63, h64, h65, h66
CSC	3	2	h59	2	2	h67, h68
ASC	1	2	h59	2	2	h29, h69
EPY	1	1	h41	1	1	h70
APY	7	2	h41, h63	4	3	h71, h72, h73
URU	1	1	h45	1	1	h30

---

**Table S1.10** Relative contributions of each modeling component (time, methods, AOGCMs and their interaction) to the variability of the predictions of the ENMs for *Scinax squalirostris*. The suitability column shows the median proportion and amplitude of the sum of squares from the hierarchical ANOVA calculated for each cell of the grid covering the Neotropical region.

Sources of uncertainty	Median (SS)%	Min-Max
ENMs*Time	0.26	0.00 - 0.78
AOGCMs*Time	0.14	0.00 - 0.76
Time	0.04	0.02 - 0.92
Residual	0.46	0.06 - 0.78

**Table S1.11** Proportion on ancestry for individuals of *Scinax squalirostris*, conditioned to environmental variables, inferred by Bayesian analysis of mitochondrial for present climatic conditions.

Individual	Inferred Cluster							
	Cluster 1	Cluster 2	Cluster 3	Cluster 4	Cluster 5	Cluster 6	Cluster 7	Cluster 8
1	0.004344828	0.007167816	0.593778544	0.004300383	0.005538697	0.201199234	0.178868199	0.004802299
2	0.004407663	0.007630651	0.596	0.004133333	0.005888889	0.200182375	0.177249808	0.00450728
3	0.004271264	0.00762682	0.59643908	0.004165517	0.00560613	0.200652107	0.17651954	0.00471954
4	0.004250575	0.007413027	0.594255172	0.004298851	0.005630651	0.200624521	0.178816092	0.004711111
5	0.004195402	0.007236782	0.594556322	0.004347126	0.006088123	0.199836782	0.178898851	0.004840613
6	0.005784674	0.004825287	0.290354023	0.006108812	0.020458238	0.006009962	0.660121073	0.006337931

7	0.005827586	0.004735632	0.288455939	0.00597931	0.02034023	0.006071264	0.662344061	0.006245977
8	0.00574023	0.004747893	0.288927203	0.006095785	0.020748659	0.005927969	0.661275096	0.006537165
9	0.005836782	0.004922605	0.287701916	0.005921839	0.020900383	0.005985441	0.662208429	0.006522605
10	0.005527203	0.004824521	0.287843678	0.005839847	0.020557854	0.006023755	0.663285057	0.006098084
11	0.005359387	0.005091188	0.288165517	0.005822989	0.020461303	0.005966284	0.663057471	0.006075862
12	0.005625287	0.005043678	0.289311111	0.006016858	0.020701916	0.006016092	0.661153257	0.006131801
13	0.005550192	0.005045977	0.288970881	0.00617931	0.020388506	0.005790805	0.661572414	0.006501916
14	0.005414559	0.004969349	0.289145594	0.006422989	0.020476628	0.006224521	0.660870498	0.006475862
15	0.0050659	0.007944828	0.357798467	0.003902682	0.004614559	0.211132567	0.404449808	0.005091188
16	0.005363218	0.007902682	0.356860536	0.004134866	0.004497318	0.211509579	0.404496552	0.005235249
17	0.005011494	0.008087356	0.357956322	0.003933333	0.004485824	0.211491954	0.403898851	0.005134866
18	0.005143295	0.007944061	0.356460536	0.004083525	0.004229885	0.211537931	0.405425287	0.005175479
19	0.005002299	0.007750958	0.356767816	0.004046743	0.004543295	0.21100613	0.40577318	0.005109579
20	0.00489272	0.008150192	0.356413793	0.004282759	0.004704981	0.211198467	0.405017625	0.005339464
21	0.004870498	0.008216858	0.357268966	0.003679693	0.004673563	0.210915709	0.405391571	0.004983142
22	0.005216858	0.007790038	0.356971648	0.003962452	0.004753257	0.211382375	0.404828352	0.005095019
23	0.00512567	0.007924904	0.359766284	0.0042	0.00472567	0.211154023	0.40194023	0.005163218
24	0.004987739	0.008050575	0.357062069	0.003976245	0.00431954	0.211240613	0.405375479	0.004987739
25	0.002547893	0.00647433	0.036866667	0.002298084	0.002284291	0.015028352	0.931223755	0.003276628
26	0.002477395	0.006499617	0.036362452	0.002249808	0.002232184	0.015263602	0.931894253	0.00302069
27	0.002652874	0.006723372	0.036400766	0.002227586	0.002198467	0.014619157	0.932207663	0.002970115
28	0.002580843	0.00663295	0.036370881	0.002294253	0.002269732	0.015127969	0.931712644	0.003010728
29	0.002577778	0.006222222	0.037219157	0.002299617	0.002213793	0.01511954	0.931424521	0.002923372
30	0.002535632	0.006551724	0.036463602	0.002285824	0.002316475	0.015599234	0.931177011	0.003070498
31	0.002602299	0.006591571	0.035731034	0.002285057	0.002285824	0.014816858	0.932737931	0.002949425
32	0.002431418	0.006695019	0.036096552	0.00242069	0.002243678	0.01550728	0.931532567	0.003072797

33	0.002600766	0.006354023	0.037070498	0.002390038	0.002224521	0.015182375	0.931150192	0.003027586
34	0.002454406	0.006518774	0.03614636	0.002229885	0.002354789	0.015590805	0.931691188	0.003013793
35	0.002547126	0.006331034	0.036642146	0.002303448	0.002324904	0.015425287	0.93145977	0.002966284
36	0.0024659	0.006385441	0.036079693	0.002236015	0.002161686	0.015222989	0.932549425	0.002898851
37	0.002341762	0.006539464	0.036412261	0.002301149	0.002243678	0.015310345	0.931704215	0.003147126
38	0.003997701	0.01102069	0.049704215	0.003458238	0.014724904	0.003428352	0.909532567	0.004133333
39	0.004273563	0.011411494	0.050548659	0.003652107	0.015298084	0.003342529	0.9071341	0.004339464
40	0.00414023	0.01108659	0.050728736	0.003716475	0.015645211	0.003137165	0.907510345	0.004035249
41	0.001463602	0.00097931	0.011255172	0.001454406	0.068785441	0.004529502	0.910097318	0.001435249
42	0.001427586	0.00105977	0.01145364	0.001258238	0.068837548	0.004655939	0.910029119	0.001278161
43	0.001345594	0.001087356	0.011242912	0.001315709	0.068523372	0.004717241	0.910343295	0.001424521
44	0.001436015	0.001096552	0.011043678	0.001426054	0.068283525	0.00471341	0.910759387	0.001241379
45	0.001354789	0.001008429	0.011540996	0.001343295	0.068930268	0.004783142	0.909636015	0.001403065
46	0.001386207	0.001061303	0.011214559	0.001403831	0.069731034	0.004568582	0.909260536	0.001373946
47	0.001362452	0.00111954	0.010893487	0.001324138	0.068560153	0.004619923	0.910663602	0.001456705
48	0.001318008	0.00107433	0.011006897	0.001337931	0.06947433	0.004535632	0.909854406	0.001398467
49	0.00132567	0.001104215	0.011213793	0.001349425	0.068176245	0.004882759	0.910610728	0.001337165
50	0.001377778	0.001029119	0.011485824	0.001305747	0.068694253	0.00459387	0.910132567	0.001380843
51	0.001422989	0.001030651	0.011216858	0.001251341	0.069818391	0.004628352	0.909310345	0.001321073
52	0.001472031	0.001049808	0.01112567	0.00136705	0.068603065	0.004564751	0.910321073	0.001496552
53	0.000948659	0.005016858	0.001969349	0.000834483	0.001970881	0.002636782	0.985649042	0.000973946
54	0.000931801	0.005033716	0.001954789	0.00083295	0.002042146	0.002467433	0.985757854	0.00097931
55	0.000975479	0.005038314	0.002000766	0.000852874	0.001927203	0.002433716	0.985839847	0.000931801
56	0.000854406	0.00477931	0.001883525	0.000912644	0.001870498	0.002580843	0.986251341	0.000867433
57	0.000901916	0.004961686	0.00185977	0.0008659	0.001940996	0.002781609	0.985748659	0.000939464
58	0.00092567	0.004849042	0.001950192	0.000805364	0.002004598	0.002580843	0.985942529	0.000941762

59	0.000893487	0.005081992	0.00203908	0.000836015	0.002064368	0.002601533	0.985427586	0.001055939
60	0.000887356	0.004898084	0.002028352	0.000785441	0.001770115	0.002414559	0.986212261	0.001003831
61	0.00096092	0.004849042	0.002016092	0.000855172	0.001943295	0.002488889	0.985964751	0.000921839
62	0.000953257	0.005072031	0.002061303	0.000743295	0.001896552	0.002530268	0.985783142	0.000960153
63	0.000954023	0.004989272	0.00192567	0.000838314	0.001832184	0.002641379	0.985896552	0.000922605
64	0.000910345	0.005037548	0.001898084	0.000967816	0.001911877	0.002629119	0.985649042	0.000996169
65	0.00096092	0.005042912	0.001990805	0.000839847	0.001954789	0.002695019	0.985434483	0.001081226
66	0.000844444	0.005008429	0.002024521	0.000802299	0.001966284	0.002809962	0.985509579	0.001034483
67	0.000868199	0.005228352	0.001917241	0.00087433	0.001931034	0.002470498	0.985731801	0.000978544
68	0.000878161	0.005003831	0.001977778	0.000908812	0.002006897	0.00231341	0.985941762	0.000969349
69	0.000918008	0.005186973	0.001901916	0.000785441	0.001924904	0.002458238	0.985835249	0.000989272
70	0.000995402	0.005091188	0.002003831	0.000798467	0.001878927	0.002460536	0.985861303	0.000910345
71	0.000910345	0.005069732	0.00187433	0.000795402	0.00194636	0.002624521	0.98587433	0.000904981
72	0.001684291	0.001450575	0.015961686	0.001478161	0.009900383	0.015608429	0.95217318	0.001743295
73	0.001665134	0.001511877	0.01642069	0.001459004	0.010038314	0.015574713	0.951672797	0.001657471
74	0.001744061	0.001225287	0.016487356	0.001425287	0.009871264	0.015586207	0.951970881	0.001689655
75	0.001634483	0.001436015	0.016295019	0.001314176	0.01054023	0.015630651	0.951530268	0.001619157
76	0.001696552	0.001422222	0.016354023	0.001427586	0.009891188	0.0161341	0.951359387	0.001714943
77	0.001651341	0.001340996	0.016301149	0.001366284	0.010186207	0.015999234	0.951357088	0.001797701
78	0.001652874	0.001398467	0.016659004	0.001388506	0.009882759	0.016394636	0.950964751	0.001659004
79	0.001744828	0.001318774	0.016344061	0.001402299	0.010206897	0.016005364	0.951233716	0.001744061
80	0.001823755	0.00142069	0.016408429	0.00134023	0.010121073	0.015977011	0.951175479	0.001733333
81	0.001607663	0.001363985	0.016524904	0.001347893	0.010177011	0.015813027	0.951380843	0.001784674
82	0.001785441	0.001378544	0.016254406	0.001481992	0.01010728	0.015683525	0.951545594	0.001763218
83	0.001632184	0.001377778	0.016641379	0.00151341	0.009943295	0.016004598	0.95119387	0.001693487
84	0.00162069	0.001396935	0.016266667	0.001466667	0.010151724	0.015550958	0.951836015	0.001710345

85	0.001329502	0.192845977	0.006281992	0.001485824	0.004344828	0.00257931	0.789097318	0.002035249
86	0.00136705	0.192629119	0.006145594	0.001517241	0.004318774	0.002491954	0.789443678	0.00208659
87	0.001455939	0.19367433	0.00605977	0.001448276	0.004181609	0.002609195	0.788526437	0.002044444
88	0.001562452	0.192793103	0.006009195	0.001542529	0.004311111	0.002527203	0.789162452	0.002091954
89	0.001596935	0.192937165	0.006277395	0.001523372	0.004248276	0.002570881	0.788681992	0.002163985
90	0.001375479	0.193332567	0.005956322	0.001520307	0.004278927	0.002505747	0.789	0.002030651
91	0.001517241	0.193277395	0.005977778	0.001669732	0.004043678	0.002245211	0.789273563	0.001995402
92	0.001564751	0.192625287	0.006345594	0.001491188	0.004291188	0.002504215	0.789087356	0.002090421
93	0.001386207	0.192962452	0.006003065	0.001539464	0.003996169	0.002735632	0.789309579	0.002067433
94	0.001499617	0.19334636	0.006062835	0.001471264	0.003935632	0.002586207	0.78895249	0.002145594
95	0.001429885	0.193544061	0.005936398	0.001504215	0.004126437	0.002568582	0.788784674	0.002105747
96	0.001508046	0.193445977	0.006065134	0.00148046	0.004236015	0.002463602	0.788741762	0.002059004
97	0.001482759	0.192856705	0.006057471	0.001409962	0.004308812	0.002308046	0.789468199	0.002108046
98	0.001603065	0.193012261	0.00615249	0.001514176	0.00415249	0.002708812	0.788780843	0.002075862
99	0.001433716	0.193061303	0.005936398	0.001583908	0.004180077	0.00239387	0.789306513	0.002104215
100	0.001596935	0.193002299	0.006327969	0.001462069	0.00396705	0.002468199	0.789117241	0.002058238
101	0.00151341	0.193373946	0.006067433	0.001462069	0.004170115	0.002285824	0.78917318	0.001954023
102	0.001399234	0.192163218	0.006171648	0.001488889	0.004376245	0.002493487	0.789733333	0.002173946
103	0.001496552	0.193340996	0.006171648	0.001553257	0.004103448	0.002503448	0.788678161	0.00215249
104	0.001468199	0.193099617	0.006109579	0.001426054	0.004291188	0.002577011	0.788895019	0.002133333
105	0.001462835	0.193381609	0.006162452	0.001423755	0.004321839	0.00251341	0.78862682	0.00210728
106	0.00144751	0.192764751	0.006145594	0.001527969	0.004235249	0.002541762	0.789248276	0.002088889
107	0.00303908	0.006829885	0.022931034	0.002891954	0.17891341	0.011808429	0.770701149	0.002885057
108	0.002953257	0.0066659	0.022414559	0.002826054	0.178403065	0.012190038	0.77185977	0.002687356
109	0.002856705	0.006977011	0.022409195	0.002652107	0.178345594	0.011905747	0.77188046	0.00297318
110	0.003001533	0.006914176	0.022729502	0.00290728	0.17771954	0.012121073	0.771479693	0.003127203

111	0.002898084	0.00656092	0.022544061	0.002967816	0.179234483	0.012354789	0.770676628	0.002763218
112	0.002773946	0.006740996	0.022483525	0.002970115	0.178488123	0.012132567	0.77134023	0.003070498
113	0.003017625	0.006889655	0.022749425	0.00296705	0.178285057	0.012084291	0.771130268	0.002876628
114	0.002934866	0.006687356	0.02270728	0.002953257	0.179482759	0.01154636	0.770730268	0.002957854
115	0.00305364	0.00691341	0.022843678	0.002881992	0.178506513	0.012407663	0.77054636	0.002846743
116	0.002727969	0.006682759	0.022549425	0.00282069	0.178150192	0.012421456	0.771675096	0.002972414
117	0.00282682	0.00635249	0.022836015	0.002850575	0.179436782	0.012308812	0.770386973	0.003001533
118	0.002682759	0.007358621	0.022640613	0.002734866	0.178613793	0.012184674	0.770910345	0.00287433
119	0.002839847	0.006796935	0.022628352	0.002915709	0.179396169	0.011704215	0.770809195	0.002909579
120	0.00294636	0.006790038	0.02228659	0.002747893	0.178798467	0.011831418	0.771660536	0.002938697
121	0.002889655	0.006753257	0.022786207	0.002831418	0.17822682	0.012373946	0.771364751	0.002773946
122	0.002957854	0.006318008	0.02283295	0.002815326	0.178967816	0.012052874	0.771139464	0.002915709
123	0.002908046	0.006586973	0.022467433	0.002757088	0.179314943	0.011418391	0.771593103	0.002954023
124	0.005399234	0.010770115	0.762583908	0.004333333	0.009008429	0.168145594	0.03496092	0.004798467
125	0.005479693	0.010310345	0.76316092	0.004308046	0.009574713	0.167731801	0.034580843	0.00485364
126	0.005521839	0.010655172	0.762199234	0.004481226	0.009311877	0.167708046	0.035068199	0.005054406
127	0.005573946	0.010370115	0.762417625	0.004336398	0.009308046	0.167927969	0.035097318	0.004968582
128	0.005388506	0.010403065	0.761311877	0.004493487	0.009485057	0.168362452	0.035597701	0.004957854
129	0.005072031	0.01040613	0.76191954	0.004332567	0.009666667	0.167914176	0.035592337	0.005096552
130	0.001208429	0.004745594	0.954174713	0.001477395	0.006563985	0.027392337	0.003211494	0.001226054
131	0.001245977	0.004417625	0.954858238	0.001568582	0.006392337	0.026983142	0.003367816	0.001166284
132	0.001154023	0.00452567	0.95480613	0.001649042	0.006566284	0.026922605	0.003137165	0.00123908
133	0.001259004	0.004659004	0.954695019	0.001624521	0.006506513	0.0268659	0.003157088	0.00123295
134	0.001222222	0.004445977	0.954485824	0.001497318	0.006803831	0.026932567	0.003357088	0.001255172
135	0.001240613	0.00437931	0.954560153	0.001454406	0.00644751	0.02768046	0.003190038	0.00104751
136	0.001206897	0.004518774	0.954899617	0.001541762	0.006575479	0.02692567	0.003178544	0.001153257

137	0.001209195	0.004624521	0.954697318	0.001475862	0.006498084	0.027101149	0.003188506	0.001205364
138	0.00117318	0.00454023	0.954694253	0.001634483	0.006359387	0.027240613	0.0032659	0.001091954
139	0.001217625	0.00468659	0.954771648	0.001516475	0.006550958	0.026788506	0.003391571	0.001076628
140	0.001182375	0.004726437	0.954363218	0.001604598	0.006567816	0.026914943	0.003384674	0.001255939
141	0.001203065	0.004436015	0.954583908	0.001612261	0.006396935	0.027216092	0.003372414	0.00117931
142	0.001216092	0.004347126	0.95462069	0.001636015	0.006595402	0.026976245	0.003430651	0.001177778
143	0.001168582	0.004498851	0.955441379	0.001583908	0.006176245	0.026749425	0.003229119	0.00115249
144	0.001236015	0.004398467	0.954862835	0.001599234	0.006695785	0.026758621	0.0032	0.001249042
145	0.001147893	0.004565517	0.95496092	0.001558621	0.006521839	0.026862835	0.003162452	0.001219923
146	0.001273563	0.004597701	0.954283525	0.001529502	0.006339464	0.027385441	0.003386207	0.001204598
147	0.00168046	0.003603065	0.942478927	0.001922605	0.001267433	0.008656705	0.038934866	0.001455939
148	0.001533333	0.00363295	0.943449042	0.001756322	0.001160153	0.008563218	0.038572414	0.001332567
149	0.001730268	0.003586973	0.942553257	0.001731801	0.001290421	0.008436015	0.039317241	0.001354023
150	0.001706513	0.003575479	0.943085057	0.00183295	0.001190805	0.008381609	0.038875096	0.00135249
151	0.001715709	0.003657471	0.942498084	0.001852874	0.001302682	0.008574713	0.038956322	0.001442146
152	0.001729502	0.003862835	0.94229272	0.001956322	0.001396169	0.008268199	0.039093487	0.001400766
153	0.00163295	0.0036	0.942087356	0.001938697	0.001344828	0.008743295	0.039222989	0.001429885
154	0.001777011	0.003671264	0.942298851	0.001921073	0.001378544	0.008041379	0.039495019	0.001416858
155	0.0016659	0.003642146	0.942695019	0.001860536	0.00129272	0.008354789	0.039055172	0.001433716
156	0.001676628	0.003768582	0.941648276	0.001904981	0.00125977	0.008594636	0.039721073	0.001426054
157	0.000687356	0.000990038	0.739391571	0.001042146	0.001	0.247595402	0.008527203	0.000766284
158	0.002123372	0.003956322	0.732327969	0.00282682	0.007002299	0.216891954	0.03239387	0.002477395
159	0.002171648	0.003949425	0.731008429	0.002947893	0.00665364	0.218170881	0.032659004	0.00243908
160	0.002265134	0.003988506	0.731337931	0.003088123	0.006688889	0.217601533	0.032514943	0.002514943
161	0.002136398	0.004036782	0.731944061	0.002911111	0.006684291	0.217682759	0.031968582	0.002636015
162	0.002324138	0.004042146	0.732332567	0.002947126	0.006771648	0.217304215	0.031965517	0.002312644

163	0.002345594	0.00411954	0.731478927	0.002929502	0.006938697	0.217215326	0.032390038	0.002582375
164	0.002327203	0.004073563	0.731493487	0.003045211	0.00708659	0.217408429	0.031992337	0.00257318
165	0.002329502	0.004045977	0.732350958	0.002865134	0.00702069	0.217439847	0.031594636	0.002353257
166	0.002295019	0.00595249	0.779038314	0.003608429	0.010196169	0.178060536	0.018256705	0.002592337
167	0.001547126	0.003881226	0.775214559	0.002367816	0.006998467	0.196785441	0.011582375	0.001622989
168	0.001504981	0.003636782	0.774332567	0.002468199	0.00671341	0.198109579	0.0114659	0.001768582
169	0.004516475	0.005412261	0.658881992	0.006629885	0.008150192	0.212267433	0.098751724	0.005390038
170	0.004629885	0.005455172	0.658843678	0.006585441	0.008271264	0.212025287	0.098705747	0.005483525
171	0.004481992	0.00569272	0.659852107	0.006673563	0.008151724	0.211287356	0.09823908	0.005621456
172	0.004557088	0.005629885	0.659145594	0.006731801	0.008744828	0.211362452	0.098046743	0.005781609
173	0.004675862	0.005843678	0.659592337	0.006360153	0.008305747	0.210988506	0.098605364	0.005628352
174	0.001648276	0.003845977	0.756729502	0.002221456	0.003966284	0.215950958	0.013867433	0.001770115
175	0.001488123	0.003915709	0.754914176	0.002284291	0.004073563	0.216951724	0.014591571	0.001780843
176	0.001557088	0.003918008	0.756717241	0.002088889	0.004016092	0.215154023	0.014672797	0.001875862
177	0.001272031	0.00334023	0.750560153	0.001799234	0.001139464	0.229381609	0.011193103	0.001314176
178	0.000211494	0.000436015	0.815682759	0.000268199	0.000305747	0.182842146	5.05747E-05	0.000203065
179	0.000587739	0.001673563	0.82076705	0.000672797	0.000531801	0.174353257	0.000774713	0.00063908
180	0.000586207	0.001754789	0.820947126	0.00063908	0.000548659	0.174270498	0.000668199	0.000585441
181	0.000581609	0.001643678	0.820898084	0.000670498	0.000570115	0.174239847	0.000829119	0.00056705
182	0.00055249	0.001721839	0.820737931	0.000682759	0.00055249	0.174422222	0.000758621	0.000571648
183	0.000524138	0.001649808	0.821162452	0.00070728	0.000574713	0.17399387	0.000842912	0.000544828
184	0.000572414	0.001666667	0.82122682	0.000632184	0.000568582	0.173992337	0.000772414	0.000568582
185	0.000121073	0.000267433	0.796537165	0.000123372	3.06513E-05	0.202780843	4.90421E-05	9.04215E-05

**Table S1.12** Proportion on ancestry for individuals of *Scinax squalirostris*, conditioned to environmental variables, inferred by Bayesian analysis of mitochondrial for 4.5RCP climatic conditions.

Individual	Inferred Cluster							
	Cluster 1	Cluster 2	Cluster 3	Cluster 4	Cluster 5	Cluster 6	Cluster 7	Cluster 8
1	1.91E-06	0.00E+00	0.64226	2.10E-14	0.00E+00	0.03833	0.319371	3.96E-05
2	0.00E+00	0.00E+00	0.69923	2.00E-15	0.00E+00	0.00000	0.273014	2.78E-02
3	1.68E-07	7.60E-14	0.51629	4.38E-13	3.61E-07	0.00114	0.482572	0.00E+00
4	2.00E-15	1.01E-06	0.46421	6.03E-03	3.33E-12	0.01787	0.511246	6.39E-04
5	3.42E-08	0.00E+00	0.48759	2.63E-02	2.74E-09	0.02938	0.456125	5.74E-04
6	2.50E-02	4.01E-09	0.02723	2.70E-10	0.00E+00	0.00000	0.947788	1.52E-11
7	2.72E-04	3.68E-05	0.02333	9.00E-07	6.70E-03	0.00000	0.968184	1.47E-03
8	1.61E-10	5.57E-08	0.03495	7.43E-11	2.03E-02	0.00000	0.944371	3.52E-04
9	1.31E-12	0.00E+00	0.03458	4.73E-13	3.06E-03	0.00279	0.959567	9.50E-08
10	3.20E-04	0.00E+00	0.05797	0.00E+00	0.00E+00	0.00000	0.941701	7.87E-06
11	3.16E-12	0.00E+00	0.06618	2.44E-04	0.00E+00	0.00005	0.933531	1.17E-07
12	1.34E-07	0.00E+00	0.04238	1.57E-07	1.00E-15	0.00000	0.953744	3.87E-03
13	3.58E-06	0.00E+00	0.02941	0.00E+00	5.54E-11	0.00000	0.970587	1.31E-08
14	8.90E-10	0.00E+00	0.01236	2.97E-07	1.47E-05	0.00000	0.987625	1.00E-15
15	7.57E-09	5.66E-08	0.12568	2.23E-10	0.00E+00	0.11636	0.757961	4.62E-10
16	2.01E-09	2.67E-11	0.08749	5.80E-14	3.00E-15	0.00069	0.911817	0.00E+00
17	1.17E-07	0.00E+00	0.06781	3.18E-10	0.00E+00	0.00011	0.928914	3.17E-03
18	1.30E-03	0.00E+00	0.01116	1.14E-08	0.00E+00	0.00000	0.987538	6.20E-08
19	1.05E-03	0.00E+00	0.11430	0.00E+00	2.16E-03	0.00000	0.882490	2.69E-06
20	5.10E-14	0.00E+00	0.09867	1.72E-09	0.00E+00	0.00005	0.901284	8.00E-12

21	0.00E+00	3.58E-07	0.00361	1.00E-10	0.00E+00	0.00013	0.996258	0.00E+00
22	2.97E-04	1.60E-03	0.10186	0.00E+00	0.00E+00	0.01600	0.880233	0.00E+00
23	1.39E-12	0.00E+00	0.01663	4.20E-14	0.00E+00	0.00000	0.983366	9.90E-14
24	2.04E-05	5.97E-04	0.15773	4.90E-04	2.05E-06	0.00385	0.837305	0.00E+00
25	6.61E-09	1.43E-08	0.00119	2.45E-03	2.61E-08	0.00000	0.996348	1.07E-05
26	0.00E+00	1.54E-08	0.01390	4.66E-12	1.10E-03	0.00000	0.984999	1.09E-10
27	1.06E-08	1.45E-08	0.00570	1.22E-11	2.65E-10	0.00000	0.994303	4.06E-11
28	0.00E+00	1.43E-10	0.00237	1.09E-07	0.00E+00	0.00000	0.997602	2.39E-05
29	1.33E-04	1.23E-06	0.00000	8.72E-13	0.00E+00	0.00000	0.997751	2.11E-03
30	2.36E-05	6.26E-10	0.00009	2.72E-06	5.77E-11	0.00018	0.999701	1.25E-13
31	0.00E+00	1.85E-03	0.00433	6.40E-05	0.00E+00	0.00000	0.993758	1.30E-13
32	4.21E-11	3.65E-10	0.00005	5.78E-10	0.00E+00	0.00000	0.999949	0.00E+00
33	4.13E-11	0.00E+00	0.00000	0.00E+00	4.05E-11	0.00000	0.999999	6.83E-10
34	1.11E-09	2.11E-05	0.00000	2.73E-05	2.53E-11	0.00050	0.999448	1.00E-15
35	0.00E+00	0.00E+00	0.00000	1.62E-03	6.09E-10	0.00002	0.997196	1.16E-03
36	3.60E-14	1.04E-07	0.00319	5.35E-06	0.00E+00	0.00010	0.996699	0.00E+00
37	0.00E+00	5.82E-10	0.00105	4.47E-03	2.61E-04	0.00000	0.993775	4.42E-04
38	0.00E+00	0.00E+00	0.00000	1.50E-14	2.66E-04	0.00000	0.999730	3.92E-12
39	2.33E-05	0.00E+00	0.02095	0.00E+00	5.40E-03	0.00000	0.973627	0.00E+00
40	0.00E+00	7.90E-12	0.00000	0.00E+00	4.22E-06	0.00000	0.999996	0.00E+00
41	1.10E-09	1.90E-12	0.00007	2.60E-10	8.12E-09	0.00000	0.999927	1.83E-06
42	1.35E-09	1.68E-05	0.00000	0.00E+00	2.28E-04	0.00000	0.999755	7.12E-11
43	5.59E-06	0.00E+00	0.00000	0.00E+00	1.32E-05	0.00001	0.999973	7.00E-15
44	2.49E-09	0.00E+00	0.00000	3.70E-08	1.45E-06	0.00225	0.997746	2.49E-11
45	3.07E-09	0.00E+00	0.00000	1.96E-11	4.03E-05	0.00001	0.999930	1.63E-05
46	3.08E-10	5.14E-07	0.00053	0.00E+00	1.23E-12	0.00000	0.999266	2.01E-04

47	0.00E+00	5.47E-08	0.00001	5.98E-05	5.54E-08	0.00000	0.999925	7.86E-07
48	1.60E-06	0.00E+00	0.00000	0.00E+00	3.89E-04	0.00000	0.999605	4.98E-07
49	4.35E-05	0.00E+00	0.00000	3.15E-13	7.32E-04	0.00001	0.999219	1.65E-12
50	2.49E-06	1.84E-09	0.00000	1.72E-06	1.05E-08	0.00000	0.999996	1.88E-10
51	2.78E-09	6.96E-08	0.00000	2.57E-07	8.87E-04	0.00000	0.999110	1.38E-09
52	8.00E-15	0.00E+00	0.00000	3.32E-06	2.74E-07	0.00000	0.999996	2.95E-11
53	6.94E-13	0.00E+00	0.00011	0.00E+00	5.77E-05	0.00011	0.999709	8.52E-06
54	2.68E-05	2.31E-06	0.00018	1.04E-10	1.35E-08	0.00022	0.999446	1.25E-04
55	8.88E-06	3.15E-05	0.00000	3.28E-05	0.00E+00	0.00000	0.999927	1.06E-07
56	6.55E-05	3.09E-09	0.00001	1.99E-06	5.69E-10	0.00000	0.999918	2.16E-10
57	1.49E-07	5.90E-04	0.00005	1.47E-08	5.86E-11	0.00000	0.999357	1.65E-12
58	0.00E+00	0.00E+00	0.00010	0.00E+00	1.52E-04	0.00000	0.999749	0.00E+00
59	0.00E+00	5.16E-13	0.00014	0.00E+00	3.63E-05	0.00000	0.999828	2.00E-14
60	5.37E-13	0.00E+00	0.00000	2.42E-07	9.37E-08	0.00000	1.000000	5.56E-09
61	3.66E-13	0.00E+00	0.00000	8.23E-06	0.00E+00	0.00000	0.999992	0.00E+00
62	4.85E-09	6.60E-04	0.00000	1.93E-07	0.00E+00	0.00000	0.999336	4.11E-07
63	1.28E-08	8.18E-04	0.00000	3.52E-05	7.60E-07	0.00018	0.998856	1.06E-04
64	1.10E-13	1.17E-03	0.00000	0.00E+00	0.00E+00	0.00000	0.998827	0.00E+00
65	1.05E-08	2.04E-07	0.00000	0.00E+00	5.96E-09	0.00014	0.999809	5.00E-05
66	5.99E-05	4.01E-06	0.00000	0.00E+00	5.10E-14	0.00012	0.999821	2.44E-12
67	4.65E-08	1.73E-08	0.00122	3.60E-10	3.19E-10	0.00000	0.998780	6.50E-11
68	0.00E+00	0.00E+00	0.00003	3.89E-05	5.43E-04	0.00000	0.999360	2.84E-05
69	0.00E+00	2.25E-04	0.00001	0.00E+00	2.68E-08	0.00000	0.999769	0.00E+00
70	1.31E-04	1.55E-04	0.00041	7.25E-12	1.69E-03	0.00000	0.997614	4.29E-07
71	3.00E-10	0.00E+00	0.00000	1.74E-05	0.00E+00	0.00000	0.999978	0.00E+00
72	8.56E-11	0.00E+00	0.00000	1.57E-10	2.76E-05	0.00070	0.996372	2.90E-03

73	5.13E-09	2.21E-13	0.00000	0.00E+00	3.28E-05	0.00001	0.999951	1.06E-06
74	2.01E-12	0.00E+00	0.00002	2.17E-03	0.00E+00	0.00002	0.997790	3.64E-11
75	1.86E-08	0.00E+00	0.00000	2.46E-05	1.61E-03	0.00000	0.996762	1.60E-03
76	0.00E+00	1.06E-10	0.00000	0.00E+00	1.53E-12	0.00000	0.999997	1.11E-07
77	2.34E-05	0.00E+00	0.00004	9.15E-05	4.32E-08	0.00227	0.997582	1.61E-10
78	1.06E-03	2.04E-08	0.00040	1.50E-14	8.13E-06	0.00000	0.998531	1.50E-11
79	5.28E-06	0.00E+00	0.00405	0.00E+00	2.05E-09	0.00000	0.995948	0.00E+00
80	0.00E+00	0.00E+00	0.00000	0.00E+00	1.10E-09	0.00054	0.999464	0.00E+00
81	0.00E+00	0.00E+00	0.00036	1.46E-07	1.13E-04	0.00000	0.999526	6.88E-11
82	0.00E+00	0.00E+00	0.00057	4.05E-03	2.61E-10	0.00000	0.995373	1.69E-07
83	1.86E-09	3.12E-05	0.00000	0.00E+00	2.35E-03	0.00001	0.997607	0.00E+00
84	4.11E-13	2.75E-06	0.00000	3.38E-05	4.01E-09	0.00242	0.997542	0.00E+00
85	3.82E-04	2.42E-07	0.00000	3.00E-15	2.14E-05	0.00281	0.996789	0.00E+00
86	5.15E-05	2.18E-03	0.00002	3.59E-09	4.30E-14	0.00000	0.997748	7.27E-08
87	5.20E-11	1.21E-05	0.00061	1.21E-07	0.00E+00	0.00000	0.999375	4.07E-07
88	0.00E+00	3.36E-04	0.00000	3.12E-07	0.00E+00	0.00000	0.999663	5.35E-08
89	0.00E+00	2.29E-05	0.00000	9.92E-11	3.14E-12	0.00000	0.999977	1.28E-12
90	0.00E+00	8.68E-04	0.00001	0.00E+00	3.64E-03	0.00000	0.995120	3.66E-04
91	9.44E-04	1.68E-04	0.00000	2.00E-15	2.47E-03	0.00000	0.996421	1.40E-09
92	1.20E-03	4.65E-04	0.00000	5.31E-05	2.05E-07	0.00000	0.998275	2.71E-06
93	1.21E-06	1.17E-04	0.00000	7.10E-14	8.43E-10	0.00000	0.999881	8.50E-14
94	0.00E+00	1.07E-04	0.00124	0.00E+00	0.00E+00	0.00000	0.998655	1.20E-11
95	0.00E+00	1.39E-05	0.00000	1.33E-09	5.58E-04	0.00000	0.999409	1.82E-05
96	0.00E+00	2.87E-07	0.00000	9.00E-15	0.00E+00	0.00000	0.999998	4.43E-07
97	3.26E-08	8.75E-04	0.00000	1.81E-03	4.54E-05	0.00000	0.997267	5.38E-10
98	1.30E-05	3.42E-06	0.00000	4.15E-07	3.05E-05	0.00000	0.999950	3.34E-09

99	1.08E-04	3.54E-03	0.00000	2.02E-07	1.76E-12	0.00033	0.995976	3.99E-05
100	2.04E-11	0.00E+00	0.00000	2.76E-05	1.82E-06	0.00000	0.999970	0.00E+00
101	0.00E+00	5.46E-04	0.00000	0.00E+00	2.42E-06	0.00000	0.999452	4.16E-13
102	0.00E+00	1.17E-05	0.00000	0.00E+00	1.13E-04	0.00000	0.999876	3.56E-10
103	5.24E-03	8.92E-04	0.00001	1.00E-15	0.00E+00	0.00000	0.993866	1.68E-08
104	0.00E+00	2.37E-06	0.00000	3.53E-06	2.38E-05	0.00000	0.997673	2.30E-03
105	2.14E-09	1.02E-03	0.00000	3.00E-14	0.00E+00	0.00000	0.998974	4.08E-08
106	0.00E+00	6.70E-06	0.00000	2.52E-07	5.21E-08	0.00000	0.999499	4.93E-04
107	7.00E-15	4.80E-03	0.00163	2.34E-02	3.14E-05	0.00000	0.970175	0.00E+00
108	1.46E-07	3.60E-04	0.01305	0.00E+00	1.02E-02	0.00002	0.976198	1.58E-04
109	0.00E+00	4.60E-11	0.00000	0.00E+00	2.77E-06	0.00627	0.993731	0.00E+00
110	1.61E-11	0.00E+00	0.00000	0.00E+00	4.81E-03	0.00000	0.995184	2.34E-06
111	3.48E-09	9.78E-09	0.00000	1.97E-12	4.33E-03	0.00000	0.995664	0.00E+00
112	0.00E+00	1.04E-04	0.00000	1.49E-04	2.63E-02	0.00000	0.973394	2.33E-06
113	8.70E-08	3.88E-07	0.00292	3.80E-14	9.35E-05	0.00000	0.996987	0.00E+00
114	3.79E-04	3.08E-07	0.00010	1.69E-03	2.81E-03	0.00553	0.986583	2.91E-03
115	2.03E-13	3.61E-12	0.00061	1.26E-09	1.86E-10	0.00000	0.999394	0.00E+00
116	0.00E+00	4.93E-05	0.00579	3.78E-05	3.51E-08	0.00000	0.992790	1.33E-03
117	9.83E-05	1.58E-09	0.00029	1.02E-06	1.01E-04	0.00009	0.997880	1.54E-03
118	1.45E-13	1.81E-07	0.00022	6.45E-05	1.80E-03	0.00145	0.996459	1.15E-06
119	1.43E-02	0.00E+00	0.04467	0.00E+00	2.06E-08	0.00000	0.941030	2.53E-05
120	0.00E+00	6.96E-04	0.00293	1.20E-03	1.59E-04	0.00000	0.995011	0.00E+00
121	1.77E-05	8.15E-07	0.00467	0.00E+00	8.16E-03	0.00001	0.987145	4.61E-12
122	4.67E-05	0.00E+00	0.00001	2.11E-09	2.01E-03	0.00000	0.997934	0.00E+00
123	0.00E+00	1.53E-03	0.00000	0.00E+00	6.76E-11	0.00000	0.998466	2.37E-10
124	4.46E-05	1.83E-03	0.97345	1.12E-03	1.48E-06	0.01308	0.010431	4.71E-05

125	1.05E-09	1.76E-04	0.96958	1.81E-06	7.67E-03	0.00973	0.012836	1.13E-05
126	2.17E-04	1.17E-05	0.98084	2.04E-05	8.57E-04	0.00007	0.017374	6.06E-04
127	2.69E-02	4.97E-05	0.93871	1.17E-05	1.29E-05	0.00279	0.031504	1.73E-05
128	0.00E+00	1.88E-06	0.93831	3.39E-04	5.00E-15	0.01277	0.048564	1.47E-05
129	1.97E-07	4.47E-03	0.94214	2.21E-05	1.00E-14	0.00188	0.051485	1.00E-15
130	2.61E-08	2.50E-08	0.99510	1.31E-04	4.22E-09	0.00002	0.004584	1.67E-04
131	0.00E+00	1.78E-08	0.99936	1.21E-08	1.01E-04	0.00038	0.000165	0.00E+00
132	1.67E-06	2.06E-06	0.99447	1.00E-05	4.79E-07	0.00000	0.005511	8.14E-09
133	0.00E+00	4.83E-04	0.99644	2.92E-06	4.10E-07	0.00073	0.002299	4.06E-05
134	1.08E-06	1.64E-06	0.99974	0.00E+00	2.87E-07	0.00026	0.000001	4.97E-07
135	0.00E+00	1.06E-04	0.99848	1.95E-12	3.23E-11	0.00002	0.000573	8.27E-04
136	3.12E-05	4.45E-03	0.99494	0.00E+00	0.00E+00	0.00001	0.000569	2.90E-07
137	5.17E-07	1.05E-06	0.99407	1.00E-15	8.00E-04	0.00026	0.004864	1.39E-09
138	1.06E-11	4.08E-09	0.99945	1.14E-10	3.33E-04	0.00008	0.000137	1.10E-14
139	2.34E-08	4.89E-03	0.99444	5.92E-04	4.76E-07	0.00000	0.000075	6.41E-10
140	0.00E+00	1.42E-06	0.99548	3.41E-05	5.05E-12	0.00096	0.003524	7.77E-11
141	9.85E-05	7.14E-08	0.99808	4.45E-09	1.82E-03	0.00000	0.000000	0.00E+00
142	3.47E-10	3.34E-04	0.99965	1.13E-05	3.14E-10	0.00000	0.000000	7.37E-12
143	1.07E-13	1.48E-05	0.99982	1.18E-09	1.48E-12	0.00015	0.000011	9.41E-06
144	5.55E-05	1.64E-04	0.99665	4.22E-06	4.40E-12	0.00098	0.002145	1.38E-10
145	0.00E+00	2.15E-03	0.99705	4.58E-04	1.36E-07	0.00000	0.000337	0.00E+00
146	0.00E+00	8.96E-05	0.99870	0.00E+00	9.12E-09	0.00000	0.001208	3.49E-07
147	5.59E-05	1.61E-05	0.99418	1.09E-04	2.36E-03	0.00029	0.002971	2.34E-05
148	1.46E-09	1.84E-06	0.99585	1.39E-04	0.00E+00	0.00000	0.004008	7.56E-12
149	2.00E-15	1.08E-13	0.99941	1.56E-04	1.64E-04	0.00023	0.000045	2.24E-09
150	4.03E-04	5.09E-04	0.98825	3.29E-06	0.00E+00	0.00996	0.000663	2.09E-04

151	2.30E-10	1.69E-05	0.99536	2.07E-05	6.60E-14	0.00004	0.004556	0.00E+00
152	2.52E-08	3.41E-10	0.99822	4.19E-07	2.40E-14	0.00000	0.001769	7.96E-06
153	2.23E-12	6.76E-04	0.99360	5.92E-04	8.73E-11	0.00000	0.004410	7.21E-04
154	7.43E-08	4.90E-05	0.99296	3.21E-07	6.21E-04	0.00000	0.006373	0.00E+00
155	8.85E-05	6.91E-12	0.99966	2.13E-06	4.21E-11	0.00005	0.000199	8.93E-07
156	4.34E-08	5.54E-08	0.99598	7.86E-08	9.96E-06	0.00000	0.004014	2.86E-07
157	0.00E+00	2.00E-15	0.98793	3.94E-13	6.75E-08	0.00625	0.005822	3.47E-06
158	7.56E-08	2.10E-11	0.99289	0.00E+00	4.86E-04	0.00193	0.004696	2.14E-13
159	4.24E-05	1.00E-15	0.99710	1.98E-03	2.95E-09	0.00000	0.000864	0.00E+00
160	0.00E+00	0.00E+00	0.95787	6.10E-10	1.79E-12	0.00000	0.042127	0.00E+00
161	9.29E-03	5.65E-04	0.87225	0.00E+00	8.64E-06	0.00417	0.113718	1.55E-06
162	4.07E-11	7.75E-08	0.93806	1.97E-02	2.39E-06	0.00050	0.041711	9.26E-08
163	2.32E-05	1.07E-08	0.98707	5.08E-07	1.67E-04	0.00034	0.012394	0.00E+00
164	4.67E-04	2.85E-04	0.97074	3.42E-12	3.42E-12	0.02429	0.004215	0.00E+00
165	0.00E+00	1.60E-05	0.84311	4.44E-03	4.12E-05	0.00000	0.152392	1.86E-09
166	0.00E+00	1.02E-08	0.90739	1.46E-04	7.80E-04	0.05084	0.040847	1.17E-11
167	7.50E-10	4.40E-11	0.96926	2.00E-15	2.01E-05	0.00009	0.012411	1.82E-02
168	1.00E-15	1.45E-06	0.98819	0.00E+00	1.00E-15	0.00014	0.000597	1.11E-02
169	1.13E-05	0.00E+00	0.87566	3.88E-04	5.96E-04	0.00378	0.119570	1.09E-06
170	1.97E-09	6.08E-09	0.60549	0.00E+00	5.16E-10	0.00129	0.361592	3.16E-02
171	1.86E-02	1.01E-06	0.88443	3.73E-04	8.82E-11	0.00002	0.096559	1.63E-05
172	1.73E-06	2.93E-03	0.72747	1.87E-02	1.63E-05	0.00000	0.222391	2.85E-02
173	7.73E-03	9.59E-05	0.62929	2.04E-02	6.73E-13	0.00000	0.342456	2.71E-08
174	2.15E-12	1.47E-05	0.98481	3.27E-03	1.79E-12	0.00002	0.011884	8.22E-11
175	3.04E-06	0.00E+00	0.94448	9.18E-12	1.49E-03	0.00000	0.052625	1.40E-03
176	3.85E-10	0.00E+00	0.96866	9.86E-03	7.91E-07	0.00023	0.006825	1.44E-02

177	1.30E-05	2.11E-02	0.95519	1.00E-15	2.25E-07	0.00091	0.022782	3.43E-12
178	2.53E-06	5.73E-08	0.99983	4.68E-06	4.27E-13	0.00015	0.000001	1.83E-05
179	4.70E-05	1.25E-09	0.99739	3.12E-12	2.30E-11	0.00237	0.000191	1.25E-06
180	1.07E-05	3.20E-04	0.99819	1.35E-08	2.76E-04	0.00086	0.000087	2.59E-04
181	5.33E-07	6.22E-08	0.99845	9.16E-04	5.00E-15	0.00005	0.000584	2.00E-14
182	0.00E+00	1.71E-06	0.99870	0.00E+00	9.04E-04	0.00039	0.000000	6.58E-10
183	4.00E-15	2.49E-03	0.99299	3.18E-03	2.57E-08	0.00001	0.001220	1.00E-04
184	1.95E-06	1.51E-06	0.99955	9.09E-11	0.00E+00	0.00000	0.000443	1.80E-14
185	0.00E+00	6.72E-05	0.99987	4.93E-09	0.00E+00	0.00007	0.000000	4.85E-10

**Table S1.13** Proportion on ancestry for individuals of *Scinax squalirostris*, conditioned to environmental variables, inferred by Bayesian analysis of mitochondrial for 8.5RCP climatic conditions.

Individual	Inferred Cluster							
	Cluster 1	Cluster 2	Cluster 3	Cluster 4	Cluster 5	Cluster 6	Cluster 7	Cluster 8
1	5.88E-07	2.44E-07	1.72E-01	3.67E-03	2.30E-12	1.25E-05	8.24E-01	1.30E-08
2	4.06E-13	1.00E-15	2.71E-01	7.83E-07	0.00E+00	6.26E-07	7.29E-01	0.00E+00
3	7.13E-05	8.92E-13	1.67E-01	0.00E+00	2.29E-06	6.39E-05	8.32E-01	3.45E-13
4	2.60E-11	6.28E-05	3.94E-01	1.28E-03	2.26E-12	2.85E-03	6.02E-01	0.00E+00
5	4.78E-12	2.03E-05	3.32E-01	2.05E-02	0.00E+00	1.46E-08	6.47E-01	1.41E-07
6	3.84E-09	0.00E+00	2.88E-02	4.73E-09	3.71E-08	2.18E-06	9.71E-01	2.20E-14
7	0.00E+00	6.34E-12	6.74E-03	3.85E-08	0.00E+00	6.11E-07	9.93E-01	4.19E-10

8	1.90E-14	1.05E-13	1.45E-02	0.00E+00	4.34E-12	0.00E+00	9.85E-01	2.66E-13
9	0.00E+00	3.35E-04	1.31E-02	1.46E-04	5.97E-05	8.44E-11	9.86E-01	3.74E-10
10	9.62E-04	8.39E-09	1.69E-02	7.75E-05	3.43E-04	2.83E-09	9.80E-01	1.49E-03
11	9.40E-03	1.59E-03	6.12E-03	4.02E-03	2.06E-03	9.37E-09	9.77E-01	4.28E-06
12	9.70E-07	1.93E-07	1.03E-02	2.00E-15	8.25E-05	0.00E+00	9.89E-01	2.19E-04
13	4.73E-08	3.72E-11	7.69E-03	2.01E-10	2.99E-11	0.00E+00	9.92E-01	0.00E+00
14	5.30E-05	1.80E-03	2.19E-03	3.04E-04	3.56E-04	2.40E-14	9.92E-01	2.96E-03
15	6.50E-14	0.00E+00	4.77E-03	9.66E-07	8.65E-06	1.64E-03	9.94E-01	5.18E-10
16	1.02E-03	0.00E+00	5.25E-03	0.00E+00	0.00E+00	1.73E-03	9.92E-01	1.99E-07
17	5.66E-03	4.36E-13	3.70E-03	5.37E-10	9.10E-14	2.08E-03	9.89E-01	2.47E-05
18	0.00E+00	0.00E+00	1.61E-02	0.00E+00	2.00E-15	2.19E-03	9.82E-01	0.00E+00
19	3.98E-08	2.88E-04	1.61E-03	9.07E-13	0.00E+00	1.02E-04	9.98E-01	4.00E-15
20	6.49E-04	1.07E-12	1.94E-02	7.42E-05	2.02E-09	6.61E-04	9.79E-01	0.00E+00
21	8.70E-14	1.92E-07	8.47E-03	0.00E+00	0.00E+00	2.38E-04	9.91E-01	7.02E-13
22	0.00E+00	7.51E-11	4.18E-03	0.00E+00	2.34E-02	2.39E-04	9.72E-01	9.43E-07
23	2.55E-06	4.11E-06	5.33E-03	0.00E+00	0.00E+00	2.08E-05	9.90E-01	4.66E-03
24	0.00E+00	1.20E-14	3.83E-02	0.00E+00	0.00E+00	7.25E-05	9.62E-01	1.84E-12
25	0.00E+00	1.61E-06	2.05E-06	2.32E-05	0.00E+00	3.12E-11	1.00E+00	1.48E-11
26	2.68E-06	2.22E-04	2.35E-04	1.68E-12	1.35E-11	1.12E-07	9.99E-01	6.07E-05
27	0.00E+00	0.00E+00	4.88E-04	2.83E-07	0.00E+00	3.20E-08	9.99E-01	4.97E-04
28	1.16E-11	2.02E-08	1.37E-05	5.42E-06	0.00E+00	0.00E+00	1.00E+00	5.47E-05
29	7.29E-05	2.90E-14	1.14E-04	1.00E-15	0.00E+00	0.00E+00	1.00E+00	3.48E-08
30	8.65E-06	6.16E-09	1.70E-03	0.00E+00	0.00E+00	1.60E-09	9.98E-01	5.93E-09
31	5.21E-07	0.00E+00	3.16E-09	0.00E+00	2.15E-10	1.71E-10	9.99E-01	8.70E-04
32	6.90E-07	2.56E-06	3.25E-08	2.39E-06	7.68E-04	1.64E-03	9.98E-01	1.65E-11
33	3.97E-11	8.08E-11	7.26E-04	4.00E-14	1.16E-04	1.02E-05	9.99E-01	6.17E-10

34	2.02E-05	5.98E-13	1.61E-03	1.99E-07	0.00E+00	6.37E-11	9.98E-01	5.49E-05
35	6.52E-08	1.34E-04	1.57E-07	1.44E-06	3.06E-11	1.71E-09	1.00E+00	5.37E-06
36	4.55E-09	3.03E-13	1.25E-04	0.00E+00	0.00E+00	5.49E-11	1.00E+00	1.68E-04
37	0.00E+00	1.12E-05	1.50E-03	0.00E+00	0.00E+00	3.74E-09	9.98E-01	8.00E-15
38	0.00E+00	9.74E-11	3.95E-04	1.20E-09	2.67E-08	3.94E-03	9.96E-01	0.00E+00
39	0.00E+00	0.00E+00	1.25E-05	1.51E-03	3.88E-10	3.59E-06	9.98E-01	7.00E-15
40	0.00E+00	0.00E+00	7.37E-07	2.17E-03	2.34E-09	4.97E-04	9.97E-01	9.70E-06
41	1.15E-12	7.07E-05	2.80E-08	0.00E+00	1.34E-04	0.00E+00	1.00E+00	0.00E+00
42	1.34E-04	2.90E-07	3.64E-07	2.83E-08	1.31E-08	3.70E-08	1.00E+00	1.16E-09
43	1.98E-07	0.00E+00	0.00E+00	1.06E-06	1.08E-04	2.07E-06	1.00E+00	1.30E-14
44	4.13E-05	0.00E+00	1.59E-06	3.19E-11	7.01E-04	2.59E-06	9.99E-01	2.30E-12
45	0.00E+00	0.00E+00	7.00E-15	3.28E-13	3.72E-05	3.27E-12	1.00E+00	3.95E-11
46	3.93E-12	3.33E-07	1.60E-14	2.53E-09	2.78E-07	5.77E-07	1.00E+00	3.23E-08
47	3.91E-10	0.00E+00	7.59E-06	1.29E-04	6.71E-07	3.34E-12	1.00E+00	0.00E+00
48	0.00E+00	5.00E-15	3.94E-04	4.06E-10	2.08E-07	7.93E-06	1.00E+00	7.94E-09
49	1.04E-04	0.00E+00	1.84E-03	3.74E-13	2.51E-04	0.00E+00	9.98E-01	3.16E-08
50	1.14E-06	4.83E-07	1.21E-05	4.85E-05	1.28E-04	1.07E-10	1.00E+00	1.12E-05
51	9.75E-10	1.13E-10	6.88E-07	1.05E-09	1.69E-05	4.68E-07	1.00E+00	3.74E-04
52	2.24E-07	3.99E-09	3.70E-11	0.00E+00	3.63E-11	1.90E-11	1.00E+00	2.33E-06
53	0.00E+00	0.00E+00	9.83E-07	7.70E-09	5.80E-08	2.37E-10	1.00E+00	6.95E-05
54	0.00E+00	1.37E-11	1.27E-08	5.17E-04	4.85E-11	3.52E-06	9.99E-01	0.00E+00
55	1.00E-15	5.31E-05	2.64E-12	5.72E-05	5.27E-13	9.46E-06	1.00E+00	4.01E-06
56	3.86E-13	2.74E-10	0.00E+00	2.81E-05	2.33E-05	0.00E+00	1.00E+00	6.63E-05
57	1.21E-08	0.00E+00	2.67E-08	1.37E-05	3.61E-12	5.21E-06	1.00E+00	3.94E-07
58	2.83E-07	2.61E-06	3.90E-14	1.58E-12	0.00E+00	1.63E-09	1.00E+00	1.53E-08
59	0.00E+00	1.18E-04	0.00E+00	3.45E-06	1.74E-06	4.89E-08	1.00E+00	3.93E-06

60	3.54E-06	0.00E+00	0.00E+00	4.11E-12	1.62E-04	1.17E-04	1.00E+00	6.88E-07
61	9.13E-07	9.54E-07	0.00E+00	0.00E+00	4.66E-09	0.00E+00	1.00E+00	0.00E+00
62	7.10E-10	1.06E-11	4.31E-11	1.79E-04	1.86E-10	2.48E-12	1.00E+00	1.35E-07
63	2.79E-05	3.02E-07	0.00E+00	2.58E-11	3.62E-12	2.59E-07	1.00E+00	3.16E-05
64	2.00E-15	5.57E-09	0.00E+00	1.32E-05	8.40E-08	1.50E-06	1.00E+00	4.67E-04
65	2.48E-09	4.64E-04	2.67E-08	8.34E-05	1.07E-04	5.70E-09	9.99E-01	1.13E-09
66	0.00E+00	1.15E-03	7.52E-07	0.00E+00	0.00E+00	2.90E-14	9.99E-01	3.06E-05
67	0.00E+00	0.00E+00	2.88E-05	9.88E-07	0.00E+00	3.71E-06	1.00E+00	5.71E-10
68	2.69E-04	0.00E+00	1.00E-15	0.00E+00	1.10E-14	5.32E-08	1.00E+00	1.70E-06
69	2.54E-07	0.00E+00	0.00E+00	2.59E-07	4.60E-13	0.00E+00	1.00E+00	5.35E-06
70	0.00E+00	3.12E-05	5.38E-07	8.30E-06	0.00E+00	3.10E-14	1.00E+00	1.83E-08
71	5.86E-08	1.51E-04	8.38E-12	3.74E-10	4.00E-11	0.00E+00	1.00E+00	5.00E-15
72	0.00E+00	0.00E+00	8.29E-05	0.00E+00	1.67E-08	3.98E-07	1.00E+00	5.04E-08
73	9.00E-15	7.89E-05	2.54E-07	0.00E+00	1.15E-08	3.55E-05	1.00E+00	0.00E+00
74	2.36E-05	1.57E-06	2.87E-07	3.80E-14	2.22E-09	1.25E-07	1.00E+00	1.00E-15
75	9.87E-07	6.44E-10	1.10E-05	0.00E+00	0.00E+00	1.72E-07	1.00E+00	1.22E-07
76	1.60E-11	0.00E+00	2.62E-05	1.09E-05	0.00E+00	1.19E-09	1.00E+00	1.98E-11
77	4.77E-05	1.70E-11	0.00E+00	4.64E-05	0.00E+00	1.91E-12	1.00E+00	4.77E-05
78	2.95E-05	9.01E-10	5.44E-13	4.29E-08	1.92E-08	8.18E-10	9.99E-01	5.12E-04
79	2.45E-12	0.00E+00	1.27E-06	1.03E-09	3.57E-08	2.16E-05	1.00E+00	0.00E+00
80	1.34E-11	3.50E-14	1.85E-06	1.48E-05	0.00E+00	4.40E-14	1.00E+00	0.00E+00
81	3.18E-10	0.00E+00	7.18E-04	9.90E-14	1.52E-08	1.80E-14	9.99E-01	3.41E-13
82	6.63E-07	1.06E-03	1.14E-04	0.00E+00	7.21E-04	2.63E-07	9.98E-01	1.43E-09
83	0.00E+00	0.00E+00	1.60E-06	0.00E+00	1.70E-06	5.95E-04	9.99E-01	5.71E-04
84	9.16E-09	0.00E+00	4.80E-06	9.10E-09	2.35E-13	5.46E-08	1.00E+00	4.02E-12
85	0.00E+00	3.30E-05	5.60E-14	6.86E-08	2.34E-04	0.00E+00	1.00E+00	6.86E-13

86	0.00E+00	2.60E-05	1.90E-06	3.86E-06	0.00E+00	4.84E-06	1.00E+00	1.62E-04
87	6.28E-08	6.55E-04	0.00E+00	8.30E-05	7.13E-06	6.22E-09	9.99E-01	1.84E-04
88	2.35E-13	4.87E-10	8.29E-06	1.37E-09	3.78E-13	4.33E-12	1.00E+00	3.85E-12
89	2.87E-09	1.74E-06	4.22E-09	1.85E-06	3.42E-09	3.05E-08	1.00E+00	1.51E-10
90	7.55E-04	1.91E-05	0.00E+00	1.38E-09	2.25E-07	0.00E+00	9.99E-01	8.82E-05
91	2.01E-06	7.15E-04	2.36E-04	4.50E-04	0.00E+00	7.74E-08	9.99E-01	3.26E-10
92	4.33E-12	2.75E-04	0.00E+00	2.00E-06	1.38E-04	0.00E+00	9.99E-01	7.52E-04
93	4.20E-14	3.86E-06	0.00E+00	0.00E+00	2.64E-12	1.94E-05	1.00E+00	2.31E-10
94	6.43E-09	9.23E-06	2.28E-06	5.49E-05	9.70E-14	4.53E-06	1.00E+00	2.00E-10
95	1.35E-07	7.68E-05	0.00E+00	2.13E-11	5.38E-09	5.00E-15	1.00E+00	1.35E-09
96	3.60E-07	8.97E-05	1.26E-08	1.29E-04	7.70E-05	2.54E-08	1.00E+00	8.04E-08
97	0.00E+00	9.84E-07	0.00E+00	3.30E-07	1.00E-14	6.92E-06	1.00E+00	6.46E-06
98	0.00E+00	3.50E-05	1.08E-06	5.08E-08	1.20E-06	0.00E+00	1.00E+00	5.72E-05
99	2.13E-06	1.25E-04	0.00E+00	1.21E-09	2.27E-08	0.00E+00	1.00E+00	5.80E-14
100	7.89E-13	2.11E-07	0.00E+00	3.70E-10	8.00E-04	4.00E-15	9.99E-01	6.04E-04
101	5.90E-14	8.05E-06	3.65E-08	7.00E-15	2.38E-06	5.01E-09	1.00E+00	5.46E-11
102	1.00E-14	3.70E-05	2.25E-10	0.00E+00	1.55E-10	1.00E-15	1.00E+00	4.71E-05
103	3.81E-07	1.14E-06	7.08E-09	4.16E-07	0.00E+00	0.00E+00	1.00E+00	1.49E-04
104	6.64E-11	1.47E-09	3.05E-13	4.67E-08	0.00E+00	1.64E-04	1.00E+00	9.33E-06
105	1.04E-10	2.07E-04	0.00E+00	0.00E+00	5.16E-11	1.57E-05	1.00E+00	5.15E-13
106	1.27E-11	1.25E-05	2.17E-08	1.28E-07	4.31E-10	1.00E-15	1.00E+00	2.87E-13
107	3.46E-05	0.00E+00	7.04E-05	0.00E+00	2.51E-06	8.86E-05	9.99E-01	9.12E-04
108	0.00E+00	0.00E+00	3.90E-07	1.00E-15	4.14E-04	2.17E-04	9.99E-01	1.55E-06
109	2.29E-12	2.82E-12	2.09E-08	5.87E-08	1.01E-04	2.31E-08	1.00E+00	1.88E-06
110	1.27E-04	0.00E+00	3.09E-04	1.61E-09	5.36E-06	0.00E+00	1.00E+00	0.00E+00
111	3.76E-04	2.91E-04	7.62E-04	3.32E-06	1.15E-05	7.81E-06	9.99E-01	0.00E+00

112	2.10E-05	1.92E-10	3.79E-07	1.15E-06	5.29E-05	1.70E-12	1.00E+00	1.00E-15
113	0.00E+00	4.32E-08	2.45E-05	2.86E-09	1.68E-10	8.00E-15	1.00E+00	1.68E-08
114	1.60E-05	5.73E-07	2.81E-05	3.84E-04	4.93E-04	6.92E-03	9.92E-01	1.97E-12
115	2.27E-08	6.00E-15	6.41E-04	5.70E-12	5.27E-04	0.00E+00	9.99E-01	2.84E-13
116	4.98E-08	0.00E+00	6.84E-09	6.87E-07	2.13E-06	0.00E+00	1.00E+00	4.46E-07
117	6.50E-07	1.12E-06	3.89E-04	1.41E-07	4.71E-06	1.13E-04	9.99E-01	3.86E-05
118	1.20E-06	1.43E-04	1.01E-03	4.83E-04	4.47E-07	4.26E-04	9.89E-01	8.52E-03
119	0.00E+00	1.11E-03	3.25E-08	1.64E-05	3.00E-04	6.86E-07	9.99E-01	2.35E-08
120	3.86E-08	1.59E-03	8.56E-07	0.00E+00	3.16E-03	2.52E-04	9.95E-01	0.00E+00
121	9.02E-12	2.59E-11	1.60E-14	0.00E+00	4.75E-05	5.37E-06	1.00E+00	8.18E-10
122	1.89E-03	2.79E-04	5.91E-06	0.00E+00	1.45E-04	3.59E-10	9.98E-01	3.14E-09
123	1.16E-08	1.80E-04	3.68E-05	3.56E-05	2.58E-06	4.83E-04	9.99E-01	4.89E-06
124	3.10E-05	1.87E-07	9.11E-01	3.07E-03	8.04E-08	9.63E-03	7.66E-02	5.69E-07
125	4.30E-03	1.31E-04	9.10E-01	5.24E-05	4.61E-06	1.56E-04	8.49E-02	7.96E-07
126	2.57E-03	1.31E-03	8.86E-01	5.78E-04	1.53E-03	1.12E-08	1.08E-01	3.49E-06
127	1.52E-03	1.32E-05	8.26E-01	5.74E-05	2.09E-04	8.10E-04	1.70E-01	1.38E-03
128	8.48E-04	2.93E-05	9.00E-01	7.35E-08	0.00E+00	9.44E-04	9.81E-02	1.03E-05
129	1.15E-04	5.35E-03	8.22E-01	1.65E-02	0.00E+00	7.01E-03	1.49E-01	1.34E-06
130	1.69E-03	1.04E-06	9.97E-01	6.59E-09	1.17E-08	2.87E-04	1.46E-04	1.36E-03
131	9.20E-05	1.85E-04	9.95E-01	1.40E-04	1.26E-07	2.47E-05	5.00E-03	1.40E-14
132	1.06E-04	4.14E-06	9.84E-01	3.71E-10	3.33E-05	6.12E-06	1.37E-02	2.04E-03
133	1.56E-03	3.19E-07	9.98E-01	0.00E+00	0.00E+00	2.46E-05	6.39E-06	6.07E-13
134	1.74E-03	4.97E-09	9.82E-01	9.93E-08	3.78E-03	5.46E-03	6.26E-03	8.29E-04
135	1.80E-09	0.00E+00	9.91E-01	4.06E-05	1.56E-07	2.30E-03	7.12E-03	8.25E-07
136	4.83E-09	1.57E-10	9.94E-01	4.89E-05	3.67E-04	1.29E-06	5.87E-03	4.06E-05
137	0.00E+00	7.37E-12	9.98E-01	1.60E-07	1.81E-10	7.59E-05	2.17E-03	1.04E-11

138	1.21E-08	1.06E-08	9.96E-01	5.23E-06	3.38E-03	5.26E-08	2.86E-04	5.88E-09
139	1.00E-15	2.77E-05	9.92E-01	7.29E-09	4.90E-05	4.67E-03	2.65E-03	3.80E-04
140	3.12E-05	3.02E-08	9.99E-01	1.51E-07	1.41E-10	2.12E-11	5.64E-04	1.02E-13
141	2.00E-15	1.80E-14	9.96E-01	1.16E-08	5.20E-11	2.67E-04	3.63E-03	6.37E-10
142	8.99E-10	0.00E+00	9.96E-01	2.27E-09	2.26E-03	7.97E-07	2.00E-03	2.84E-09
143	8.15E-08	0.00E+00	9.96E-01	1.00E-15	7.46E-04	9.27E-06	2.98E-03	0.00E+00
144	3.43E-03	2.42E-04	9.93E-01	2.11E-07	2.69E-08	3.30E-04	2.51E-03	0.00E+00
145	3.75E-06	1.79E-03	9.92E-01	4.29E-03	6.72E-07	4.85E-05	1.11E-03	7.40E-04
146	8.07E-05	1.92E-10	9.99E-01	7.03E-08	5.27E-12	3.28E-05	4.11E-04	2.41E-07
147	5.45E-04	4.12E-04	9.86E-01	2.15E-03	2.02E-05	1.55E-03	9.02E-03	4.25E-04
148	1.53E-04	1.66E-05	9.92E-01	1.13E-07	2.08E-12	2.73E-06	7.35E-03	1.95E-04
149	4.04E-12	1.00E-15	9.88E-01	3.21E-03	7.25E-06	0.00E+00	8.09E-03	1.12E-03
150	8.50E-09	1.43E-05	9.81E-01	4.59E-04	0.00E+00	2.54E-12	1.83E-02	3.95E-06
151	5.89E-05	2.76E-06	9.85E-01	3.19E-03	1.60E-08	2.83E-04	1.11E-02	1.70E-08
152	0.00E+00	2.77E-05	9.89E-01	8.56E-07	9.93E-05	1.44E-09	1.09E-02	2.77E-04
153	8.25E-06	6.91E-13	9.76E-01	4.21E-06	5.74E-03	1.24E-11	1.35E-02	4.72E-03
154	8.77E-04	2.42E-05	9.86E-01	1.27E-07	3.00E-09	7.66E-12	1.36E-02	4.57E-09
155	7.52E-05	4.38E-04	9.90E-01	1.39E-05	0.00E+00	5.57E-08	9.56E-03	1.21E-04
156	5.54E-08	7.29E-04	9.94E-01	8.89E-06	9.28E-05	1.27E-05	5.19E-03	2.00E-15
157	8.85E-04	1.19E-08	9.45E-01	4.12E-02	7.00E-05	3.43E-05	1.26E-02	2.20E-09
158	0.00E+00	4.73E-06	8.46E-01	3.56E-03	1.99E-06	1.10E-03	1.49E-01	2.95E-06
159	2.35E-07	0.00E+00	7.42E-01	2.04E-08	1.10E-03	2.42E-03	2.13E-01	4.11E-02
160	2.74E-07	5.07E-07	8.06E-01	5.00E-15	2.44E-05	3.02E-04	1.94E-01	8.33E-05
161	6.91E-03	6.19E-06	8.29E-01	6.10E-03	0.00E+00	1.21E-06	1.58E-01	3.72E-12
162	0.00E+00	7.30E-02	7.83E-01	2.98E-05	2.74E-05	2.36E-04	1.42E-01	1.81E-03
163	1.16E-07	6.94E-04	8.57E-01	1.52E-12	1.84E-07	5.44E-08	1.42E-01	3.72E-09

164	1.90E-09	1.13E-10	6.87E-01	5.69E-03	9.97E-05	6.28E-02	1.55E-01	8.92E-02
165	1.38E-09	8.75E-06	8.81E-01	8.15E-03	1.55E-10	1.38E-02	9.66E-02	0.00E+00
166	2.02E-04	0.00E+00	9.79E-01	1.00E-15	0.00E+00	1.01E-08	2.10E-02	0.00E+00
167	5.75E-04	1.83E-08	9.64E-01	9.71E-08	1.10E-14	5.77E-03	2.92E-02	6.77E-08
168	0.00E+00	1.67E-03	9.55E-01	7.66E-05	1.00E-14	4.15E-08	4.37E-02	0.00E+00
169	3.57E-05	3.15E-04	4.09E-01	1.29E-03	3.42E-04	3.46E-06	5.89E-01	6.51E-11
170	5.69E-04	5.87E-04	3.99E-01	2.43E-13	1.40E-05	1.49E-04	6.00E-01	2.90E-05
171	9.34E-06	0.00E+00	6.62E-01	1.68E-08	1.96E-10	1.49E-06	3.14E-01	2.41E-02
172	5.86E-11	8.04E-06	7.28E-01	8.91E-09	5.47E-08	1.35E-05	2.72E-01	0.00E+00
173	3.82E-02	4.81E-04	5.30E-01	6.18E-10	7.01E-04	6.18E-03	4.24E-01	1.05E-04
174	7.21E-07	6.62E-11	9.72E-01	0.00E+00	7.13E-11	4.74E-04	2.80E-02	0.00E+00
175	6.10E-04	5.48E-13	9.79E-01	1.03E-09	8.08E-10	9.44E-04	1.77E-02	1.56E-03
176	0.00E+00	2.62E-03	9.18E-01	0.00E+00	5.72E-04	2.99E-05	7.89E-02	4.93E-13
177	1.09E-02	2.82E-06	9.81E-01	4.20E-04	4.30E-10	5.08E-03	2.81E-03	0.00E+00
178	2.10E-14	3.00E-15	9.99E-01	4.73E-08	1.70E-05	5.17E-04	3.34E-06	1.91E-06
179	2.45E-03	1.38E-06	9.94E-01	1.07E-06	8.05E-10	5.97E-04	2.49E-03	0.00E+00
180	5.05E-06	3.78E-08	9.97E-01	3.70E-04	1.51E-03	4.99E-05	6.89E-04	1.35E-06
181	1.24E-04	0.00E+00	9.97E-01	3.32E-07	0.00E+00	1.05E-03	2.29E-03	9.37E-06
182	4.40E-04	4.43E-05	9.94E-01	7.42E-04	0.00E+00	1.63E-03	2.64E-03	2.79E-04
183	9.95E-05	6.76E-05	9.99E-01	7.34E-13	0.00E+00	1.50E-04	1.79E-04	2.73E-04
184	6.00E-04	4.68E-06	9.96E-01	2.60E-04	1.16E-03	1.12E-03	4.55E-04	5.34E-06
185	3.41E-04	2.06E-04	9.99E-01	2.96E-05	2.99E-04	3.68E-05	4.05E-12	4.15E-06

---

**Table S1.14** Proportion on ancestry for individuals of *Scinax squalirostris*, conditioned to environmental variables, inferred by Bayesian analysis of nuclear for present climatic conditions.

Individual	Inferred Cluster								
	Cluster 1	Cluster 2	Cluster 3	Cluster 4	Cluster 5	Cluster 6	Cluster 7	Cluster 8	Cluster 9
1	0.000560	0.772864	0.000259	0.004862	0.006075	0.000599	0.000536	0.000366	0.213879
2	0.000587	0.772552	0.000205	0.004832	0.006089	0.000619	0.000542	0.000407	0.214168
3	0.000566	0.772619	0.000232	0.004766	0.006171	0.000685	0.000481	0.000398	0.214081
4	0.000597	0.772906	0.000250	0.004941	0.005920	0.000629	0.000539	0.000336	0.213882
5	0.000577	0.772784	0.000254	0.004811	0.005954	0.000570	0.000537	0.000413	0.214100
6	0.003443	0.720549	0.004989	0.087267	0.008823	0.003751	0.004271	0.003619	0.163288
7	0.003394	0.721781	0.004405	0.086321	0.008574	0.003723	0.004460	0.003700	0.163643
8	0.003231	0.720129	0.004709	0.087689	0.009246	0.003708	0.004443	0.003656	0.163189
9	0.003383	0.720784	0.005014	0.086426	0.009449	0.003482	0.004479	0.003496	0.163486
10	0.003260	0.720860	0.004641	0.086392	0.008802	0.003694	0.004347	0.003577	0.164427
11	0.003384	0.719718	0.004789	0.088244	0.008509	0.003651	0.004544	0.003419	0.163743
12	0.003219	0.720187	0.004699	0.086702	0.008886	0.003834	0.004333	0.003683	0.164456
13	0.003315	0.719731	0.004681	0.087356	0.008881	0.003846	0.004514	0.003478	0.164198
14	0.003447	0.722399	0.004640	0.085743	0.008797	0.003507	0.004481	0.003546	0.163439
15	0.003196	0.719990	0.004755	0.088016	0.008747	0.003773	0.004512	0.003623	0.163388
16	0.003343	0.676647	0.004680	0.096811	0.021194	0.003594	0.003205	0.002601	0.187927
17	0.003623	0.674833	0.004786	0.097601	0.021544	0.003779	0.003089	0.002679	0.188067
18	0.003542	0.676503	0.004697	0.097837	0.020599	0.003782	0.002839	0.002610	0.187591
19	0.003490	0.676302	0.004535	0.097709	0.021093	0.003575	0.003035	0.002662	0.187599
20	0.003631	0.675996	0.004741	0.097032	0.021705	0.003459	0.003023	0.002638	0.187774

21	0.003512	0.675993	0.004883	0.097565	0.021141	0.003444	0.003101	0.002716	0.187646
22	0.003418	0.676255	0.004829	0.097467	0.021119	0.003535	0.002995	0.002497	0.187885
23	0.003501	0.676235	0.004773	0.096758	0.021040	0.003655	0.002924	0.002708	0.188406
24	0.003401	0.676063	0.004853	0.097179	0.020970	0.003550	0.002935	0.002675	0.188374
25	0.003364	0.676643	0.004800	0.097075	0.020631	0.003563	0.003005	0.002576	0.188344
26	0.003480	0.676868	0.004877	0.096272	0.021194	0.003626	0.002890	0.002576	0.188218
27	0.003331	0.675819	0.004989	0.097087	0.021207	0.003647	0.003018	0.002700	0.188202
28	0.002339	0.057844	0.019120	0.896778	0.001021	0.002262	0.002142	0.002168	0.016326
29	0.002240	0.057904	0.019545	0.896629	0.001026	0.002183	0.002162	0.002236	0.016075
30	0.002083	0.057806	0.019131	0.897392	0.000981	0.002003	0.002189	0.002260	0.016155
31	0.002200	0.057931	0.019473	0.896322	0.000941	0.002141	0.002070	0.002313	0.016609
32	0.002210	0.057956	0.018554	0.897747	0.001008	0.002098	0.002146	0.002252	0.016029
33	0.002116	0.057544	0.019254	0.897711	0.000969	0.002108	0.002117	0.002259	0.015922
34	0.002124	0.057576	0.018432	0.897869	0.001033	0.002093	0.002369	0.002362	0.016142
35	0.002108	0.057969	0.019141	0.896397	0.001122	0.002209	0.002192	0.002331	0.016531
36	0.002009	0.058809	0.019302	0.895307	0.001047	0.002100	0.002311	0.002298	0.016816
37	0.002137	0.058258	0.019108	0.896431	0.001093	0.002128	0.002233	0.002395	0.016217
38	0.002269	0.058445	0.019719	0.895174	0.000978	0.002231	0.002119	0.002476	0.016589
39	0.002158	0.057824	0.019565	0.896410	0.001079	0.002167	0.002197	0.002309	0.016291
40	0.002160	0.057012	0.018602	0.898952	0.000896	0.002108	0.002092	0.002306	0.015872
41	0.002202	0.057731	0.018981	0.897081	0.001020	0.002066	0.002082	0.002476	0.016360
42	0.002282	0.057314	0.019259	0.897781	0.000975	0.002108	0.002169	0.002249	0.015861
43	0.002043	0.057221	0.019230	0.897972	0.000956	0.002118	0.002081	0.002187	0.016192
44	0.011200	0.378496	0.135743	0.282617	0.084289	0.016584	0.014591	0.011541	0.064940
45	0.002091	0.009486	0.001753	0.890574	0.084220	0.002180	0.001920	0.002140	0.005636
46	0.002355	0.009518	0.001891	0.889564	0.084455	0.002107	0.001861	0.002202	0.006048

47	0.002046	0.009601	0.001857	0.889505	0.085205	0.002194	0.001774	0.002156	0.005663
48	0.002293	0.009556	0.001999	0.889547	0.084256	0.002195	0.001856	0.002296	0.006002
49	0.002219	0.009399	0.001785	0.888744	0.085495	0.002107	0.001844	0.002081	0.006324
50	0.002227	0.009344	0.001992	0.889812	0.084467	0.002225	0.001832	0.002281	0.005820
51	0.002286	0.009182	0.001877	0.889515	0.085068	0.002122	0.002010	0.002247	0.005693
52	0.002126	0.009341	0.001954	0.889368	0.084854	0.002256	0.001852	0.002173	0.006078
53	0.002156	0.009586	0.001897	0.890059	0.084382	0.002248	0.001837	0.002142	0.005693
54	0.002153	0.009351	0.001811	0.890676	0.083965	0.002087	0.001781	0.002170	0.006006
55	0.002312	0.009685	0.001877	0.889663	0.084746	0.002118	0.001638	0.002180	0.005781
56	0.002227	0.009679	0.002017	0.890413	0.083505	0.002220	0.001919	0.002197	0.005824
57	0.002183	0.009681	0.001978	0.889489	0.084627	0.002067	0.001781	0.002231	0.005964
58	0.002244	0.009304	0.001784	0.889831	0.084745	0.002181	0.001712	0.002134	0.006063
59	0.001447	0.004210	0.022730	0.962131	0.002322	0.001229	0.001403	0.001475	0.003053
60	0.001525	0.004325	0.022891	0.961918	0.002130	0.001105	0.001451	0.001542	0.003115
61	0.001516	0.004101	0.023158	0.961716	0.002186	0.001250	0.001418	0.001550	0.003106
62	0.001488	0.004157	0.023070	0.961635	0.002231	0.001203	0.001531	0.001531	0.003153
63	0.001379	0.004192	0.023103	0.961766	0.002281	0.001169	0.001441	0.001552	0.003119
64	0.001452	0.004129	0.023278	0.961546	0.002321	0.001223	0.001350	0.001554	0.003147
65	0.001446	0.004294	0.023057	0.961752	0.002268	0.001195	0.001311	0.001566	0.003111
66	0.001543	0.004063	0.023155	0.961721	0.002132	0.001271	0.001416	0.001553	0.003146
67	0.001533	0.004090	0.023238	0.961517	0.002271	0.001260	0.001406	0.001576	0.003108
68	0.001452	0.004114	0.022886	0.961968	0.002131	0.001252	0.001473	0.001567	0.003157
69	0.001499	0.004100	0.023304	0.961467	0.002240	0.001302	0.001481	0.001456	0.003153
70	0.001513	0.004072	0.023352	0.961740	0.002300	0.001185	0.001411	0.001573	0.002854
71	0.001408	0.004042	0.023339	0.961557	0.002369	0.001078	0.001437	0.001584	0.003186
72	0.001520	0.004060	0.023084	0.962217	0.002229	0.001222	0.001305	0.001422	0.002941

73	0.001551	0.004226	0.023274	0.961466	0.002245	0.001168	0.001346	0.001513	0.003211
74	0.001398	0.003966	0.023122	0.962304	0.002227	0.001199	0.001326	0.001512	0.002946
75	0.000721	0.004485	0.000523	0.985403	0.004442	0.000591	0.000628	0.000610	0.002597
76	0.000681	0.004585	0.000583	0.985406	0.004302	0.000599	0.000589	0.000648	0.002606
77	0.000687	0.004745	0.000544	0.985039	0.004469	0.000535	0.000586	0.000722	0.002671
78	0.000693	0.004957	0.000611	0.984706	0.004570	0.000556	0.000583	0.000684	0.002639
79	0.000656	0.004534	0.000508	0.985170	0.004444	0.000677	0.000584	0.000725	0.002702
80	0.000634	0.004568	0.000541	0.985321	0.004370	0.000644	0.000609	0.000654	0.002658
81	0.000687	0.004723	0.000555	0.984784	0.004535	0.000685	0.000581	0.000734	0.002715
82	0.000607	0.004741	0.000588	0.985201	0.004534	0.000616	0.000569	0.000647	0.002496
83	0.000688	0.004548	0.000578	0.985240	0.004531	0.000575	0.000533	0.000639	0.002668
84	0.000619	0.004571	0.000589	0.984975	0.004461	0.000579	0.000549	0.000797	0.002859
85	0.001480	0.003372	0.944903	0.027527	0.016391	0.001569	0.001777	0.001493	0.001489
86	0.001512	0.003354	0.945492	0.027385	0.016359	0.001639	0.001543	0.001348	0.001369
87	0.001436	0.003393	0.945007	0.028079	0.015923	0.001639	0.001681	0.001508	0.001334
88	0.001382	0.003355	0.944976	0.027932	0.016124	0.001618	0.001610	0.001563	0.001440
89	0.001441	0.003583	0.944460	0.027775	0.016310	0.001623	0.001723	0.001579	0.001506
90	0.001440	0.003450	0.944798	0.028142	0.015804	0.001686	0.001705	0.001459	0.001517
91	0.001475	0.003482	0.945275	0.027383	0.016340	0.001551	0.001658	0.001445	0.001390
92	0.001379	0.003413	0.945244	0.027435	0.016588	0.001558	0.001560	0.001474	0.001348
93	0.001394	0.003465	0.944377	0.028418	0.016077	0.001591	0.001710	0.001555	0.001415
94	0.001444	0.003417	0.944694	0.028003	0.016192	0.001559	0.001673	0.001508	0.001510
95	0.001377	0.003582	0.944889	0.027808	0.016083	0.001687	0.001794	0.001391	0.001389
96	0.001572	0.003471	0.944001	0.028719	0.016010	0.001584	0.001772	0.001487	0.001383
97	0.001438	0.003377	0.944952	0.027943	0.016153	0.001422	0.001739	0.001491	0.001486
98	0.001422	0.003204	0.945966	0.027083	0.016119	0.001554	0.001791	0.001460	0.001402

99	0.001403	0.003473	0.945928	0.027213	0.015776	0.001594	0.001778	0.001439	0.001397
100	0.001329	0.003280	0.944979	0.027809	0.016353	0.001558	0.001722	0.001669	0.001301
101	0.001469	0.003535	0.944130	0.028294	0.016295	0.001582	0.001665	0.001569	0.001462
102	0.001528	0.003396	0.945084	0.027681	0.015982	0.001676	0.001726	0.001420	0.001506
103	0.001483	0.003544	0.944679	0.027596	0.016487	0.001509	0.001722	0.001516	0.001464
104	0.001481	0.003200	0.945791	0.027248	0.016115	0.001481	0.001764	0.001495	0.001424
105	0.001501	0.003541	0.944095	0.028679	0.016134	0.001568	0.001708	0.001356	0.001419
106	0.001473	0.003451	0.944361	0.028253	0.016155	0.001639	0.001730	0.001394	0.001545
107	0.002834	0.016005	0.015480	0.034507	0.916956	0.003098	0.002792	0.002368	0.005961
108	0.002919	0.015692	0.015695	0.034574	0.916769	0.003131	0.002676	0.002302	0.006243
109	0.002896	0.015294	0.015379	0.033921	0.918635	0.002950	0.002576	0.002462	0.005887
110	0.002781	0.015565	0.015549	0.034006	0.918380	0.002704	0.002647	0.002484	0.005883
111	0.002782	0.015810	0.015648	0.033996	0.917740	0.002974	0.002717	0.002544	0.005788
112	0.002704	0.015673	0.015609	0.033727	0.917804	0.002914	0.002713	0.002505	0.006352
113	0.002872	0.015230	0.015787	0.033481	0.918287	0.003036	0.002860	0.002494	0.005954
114	0.002746	0.015508	0.015922	0.034034	0.917856	0.003070	0.002733	0.002338	0.005791
115	0.002846	0.015381	0.015577	0.033368	0.919095	0.002810	0.002494	0.002397	0.006032
116	0.002728	0.015834	0.015872	0.034090	0.917246	0.002986	0.002828	0.002332	0.006083
117	0.002736	0.015264	0.015606	0.034713	0.917279	0.003188	0.002730	0.002477	0.006008
118	0.002881	0.015772	0.015269	0.033593	0.918413	0.003081	0.002645	0.002426	0.005919
119	0.002709	0.016085	0.015529	0.034675	0.917064	0.002983	0.002535	0.002369	0.006051
120	0.002665	0.015716	0.015306	0.034095	0.918043	0.002994	0.002745	0.002362	0.006075
121	0.002748	0.015683	0.015643	0.035052	0.916584	0.002984	0.002739	0.002341	0.006226
122	0.002675	0.015344	0.015700	0.033518	0.918308	0.002943	0.002684	0.002405	0.006424
123	0.002968	0.015674	0.015737	0.033259	0.918676	0.002784	0.002739	0.002413	0.005750
124	0.002826	0.015615	0.015877	0.033811	0.917989	0.002981	0.002613	0.002356	0.005932

125	0.009640	0.673896	0.054271	0.046647	0.069997	0.007722	0.009324	0.006563	0.121939
126	0.009482	0.673457	0.054484	0.045963	0.070356	0.007613	0.009481	0.006673	0.122490
127	0.009547	0.672744	0.054595	0.047057	0.070513	0.007292	0.009378	0.006495	0.122379
128	0.009687	0.673715	0.054275	0.046407	0.070318	0.007419	0.009382	0.006678	0.122119
129	0.009378	0.673768	0.054285	0.046646	0.070927	0.007671	0.009319	0.006314	0.121692
130	0.009496	0.673165	0.054470	0.046527	0.069670	0.007545	0.009327	0.006432	0.123367
131	0.009417	0.673208	0.054854	0.047132	0.070085	0.007494	0.009430	0.006481	0.121900
132	0.001331	0.937373	0.010036	0.000454	0.035746	0.002473	0.002760	0.001656	0.008170
133	0.001359	0.936846	0.009664	0.000405	0.036742	0.002309	0.002779	0.001775	0.008121
134	0.001400	0.936422	0.009965	0.000459	0.036550	0.002407	0.002833	0.001731	0.008232
135	0.001321	0.937577	0.009622	0.000479	0.036134	0.002527	0.002638	0.001718	0.007984
136	0.001268	0.937614	0.009569	0.000423	0.036198	0.002503	0.002731	0.001682	0.008011
137	0.001353	0.937192	0.009910	0.000377	0.035870	0.002442	0.002695	0.001768	0.008394
138	0.001355	0.936763	0.009817	0.000358	0.036305	0.002521	0.002490	0.001787	0.008605
139	0.001331	0.937883	0.009746	0.000469	0.035527	0.002371	0.002687	0.001767	0.008218
140	0.001348	0.937833	0.009660	0.000469	0.035904	0.002376	0.002706	0.001757	0.007946
141	0.001306	0.936978	0.009989	0.000462	0.036106	0.002405	0.002769	0.001781	0.008206
142	0.001309	0.937321	0.009852	0.000412	0.036154	0.002505	0.002682	0.001762	0.008003
143	0.001251	0.937862	0.009582	0.000418	0.035967	0.002480	0.002657	0.001748	0.008035
144	0.001349	0.937350	0.009768	0.000374	0.035931	0.002444	0.002705	0.001788	0.008292
145	0.007128	0.695919	0.019820	0.243230	0.000844	0.004313	0.010794	0.008225	0.009728
146	0.006864	0.697135	0.020156	0.242387	0.000786	0.004674	0.010635	0.008056	0.009307
147	0.007103	0.698399	0.019879	0.240835	0.000736	0.004599	0.010619	0.008213	0.009618
148	0.007225	0.696835	0.020099	0.242054	0.000713	0.004327	0.010991	0.008196	0.009560
149	0.007070	0.698719	0.019731	0.240339	0.000807	0.004597	0.010588	0.008358	0.009790
150	0.007256	0.205991	0.038508	0.720604	0.002920	0.004518	0.006618	0.009032	0.004554

151	0.007377	0.546651	0.007587	0.273287	0.123168	0.007130	0.008367	0.008642	0.017793
152	0.004766	0.757357	0.009966	0.055624	0.128426	0.005679	0.005739	0.005271	0.027172
153	0.004736	0.755645	0.010244	0.055806	0.128936	0.005668	0.005851	0.005306	0.027809
154	0.004438	0.756970	0.009834	0.055601	0.129245	0.005562	0.005841	0.005352	0.027156
155	0.007385	0.391352	0.047973	0.279569	0.216203	0.014391	0.015171	0.013714	0.014242
156	0.003015	0.076719	0.002454	0.887592	0.021836	0.001354	0.002824	0.003094	0.001114
157	0.005921	0.762548	0.036770	0.122094	0.033539	0.007380	0.008490	0.007271	0.015987
158	0.002681	0.891463	0.011282	0.005825	0.010298	0.001837	0.002666	0.002013	0.071934
159	0.002627	0.892194	0.011317	0.005803	0.010447	0.001923	0.002609	0.001893	0.071187
160	0.000327	0.945769	0.000094	0.000095	0.000195	0.000181	0.000257	0.000349	0.052733

**Table S1.15** Proportion on ancestry for individuals of *Scinax squalirostris*, conditioned to environmental variables, inferred by Bayesian analysis of nuclear for 4.5RCP climatic conditions.

Individual	Inferred Cluster								
	Cluster 1	Cluster 2	Cluster 3	Cluster 4	Cluster 5	Cluster 6	Cluster 7	Cluster 8	Cluster 9
1	0.000000	0.748363	0.000000	0.250356	0.000000	0.000000	0.000000	0.000001	0.001281
2	0.000002	0.811036	0.000000	0.187840	0.000191	0.000001	0.000000	0.000003	0.000927
3	0.000000	0.789702	0.000000	0.171008	0.000000	0.000000	0.000000	0.000001	0.039289
4	0.011692	0.802633	0.000000	0.185577	0.000000	0.000000	0.000000	0.000000	0.000098
5	0.000000	0.719585	0.000000	0.273016	0.000005	0.000000	0.000000	0.000000	0.007394
6	0.000004	0.336543	0.000000	0.651662	0.000000	0.000000	0.000002	0.000000	0.011789
7	0.000000	0.197504	0.000000	0.802463	0.000001	0.000000	0.000000	0.000000	0.000033
8	0.000000	0.266425	0.000000	0.732886	0.000000	0.000000	0.000000	0.000001	0.000688

9	0.000000	0.278994	0.000000	0.719808	0.000000	0.000000	0.000000	0.000000	0.001198
10	0.000000	0.217988	0.000000	0.668509	0.017277	0.000000	0.000001	0.000000	0.096225
11	0.000014	0.303278	0.000000	0.696707	0.000000	0.000000	0.000000	0.000000	0.000000
12	0.000000	0.200940	0.000000	0.798783	0.000000	0.000075	0.000005	0.000006	0.000191
13	0.000000	0.239793	0.000000	0.747632	0.000000	0.000000	0.004736	0.007797	0.000042
14	0.000000	0.138237	0.000000	0.861702	0.000000	0.000000	0.000000	0.000000	0.000061
15	0.001531	0.297267	0.000000	0.700792	0.000000	0.000000	0.000000	0.000000	0.000410
16	0.000001	0.012969	0.000000	0.962732	0.000000	0.019457	0.000010	0.000026	0.004806
17	0.000735	0.040187	0.000000	0.954510	0.004562	0.000000	0.000005	0.000000	0.000002
18	0.000000	0.032467	0.000000	0.967533	0.000000	0.000000	0.000000	0.000000	0.000000
19	0.000852	0.011815	0.000043	0.982875	0.000000	0.000000	0.000011	0.003942	0.000463
20	0.000000	0.047596	0.000000	0.949329	0.000000	0.000000	0.000002	0.000202	0.002871
21	0.000004	0.067479	0.000033	0.932351	0.000000	0.000000	0.000000	0.000000	0.000133
22	0.000000	0.021336	0.000000	0.966873	0.000000	0.000000	0.002913	0.008143	0.000736
23	0.000000	0.024855	0.000000	0.961951	0.000000	0.000008	0.002171	0.000000	0.011015
24	0.000000	0.011261	0.000007	0.985954	0.002740	0.000000	0.000000	0.000000	0.000037
25	0.000000	0.036019	0.000000	0.963621	0.000000	0.000000	0.000000	0.000000	0.000360
26	0.001142	0.021929	0.000000	0.976897	0.000000	0.000000	0.000000	0.000000	0.000032
27	0.000477	0.006711	0.000000	0.992812	0.000000	0.000000	0.000000	0.000000	0.000000
28	0.000001	0.000125	0.000013	0.999767	0.000000	0.000000	0.000000	0.000000	0.000094
29	0.000000	0.000000	0.000715	0.999196	0.000000	0.000088	0.000000	0.000000	0.000001
30	0.000016	0.002639	0.000000	0.997341	0.000000	0.000000	0.000000	0.000000	0.000004
31	0.000000	0.000001	0.000000	0.999997	0.000000	0.000000	0.000000	0.000000	0.000003
32	0.000000	0.000156	0.000002	0.999652	0.000000	0.000000	0.000000	0.000000	0.000190
33	0.000000	0.000014	0.000132	0.999749	0.000000	0.000003	0.000000	0.000001	0.000102
34	0.000146	0.000330	0.000000	0.999521	0.000000	0.000000	0.000000	0.000001	0.000002

35	0.000000	0.000001	0.000000	0.999517	0.000000	0.000002	0.000000	0.000480	0.000000
36	0.000000	0.000000	0.000105	0.999895	0.000000	0.000000	0.000000	0.000000	0.000000
37	0.000000	0.000033	0.000001	0.999966	0.000000	0.000000	0.000000	0.000000	0.000000
38	0.000000	0.001500	0.000000	0.998312	0.000000	0.000148	0.000000	0.000039	0.000000
39	0.000026	0.000020	0.000012	0.999730	0.000000	0.000000	0.000179	0.000000	0.000034
40	0.000000	0.001162	0.000000	0.995582	0.000000	0.003110	0.000000	0.000146	0.000000
41	0.000000	0.000004	0.001230	0.998752	0.000000	0.000000	0.000014	0.000000	0.000000
42	0.000000	0.000140	0.000000	0.999579	0.000000	0.000000	0.000006	0.000273	0.000002
43	0.000000	0.000000	0.000785	0.998585	0.000000	0.000092	0.000290	0.000247	0.000001
44	0.000000	0.033420	0.000025	0.956459	0.004966	0.000985	0.000000	0.004144	0.000000
45	0.000302	0.000000	0.000000	0.999419	0.000262	0.000000	0.000000	0.000011	0.000006
46	0.000000	0.000000	0.000019	0.999740	0.000241	0.000000	0.000000	0.000000	0.000000
47	0.000000	0.000033	0.000000	0.999124	0.000842	0.000001	0.000000	0.000000	0.000000
48	0.000020	0.000000	0.000000	0.998206	0.001774	0.000000	0.000000	0.000000	0.000000
49	0.000009	0.000331	0.000000	0.998231	0.000938	0.000000	0.000000	0.000490	0.000000
50	0.000000	0.000000	0.000094	0.999137	0.000548	0.000000	0.000221	0.000000	0.000000
51	0.000000	0.000000	0.000008	0.999947	0.000029	0.000017	0.000000	0.000000	0.000000
52	0.000000	0.000000	0.000000	1.000000	0.000000	0.000000	0.000000	0.000000	0.000000
53	0.000000	0.000000	0.000000	0.999078	0.000641	0.000000	0.000000	0.000078	0.000203
54	0.000000	0.000000	0.000000	0.999901	0.000000	0.000000	0.000001	0.000098	0.000000
55	0.000000	0.000000	0.000000	0.999616	0.000166	0.000000	0.000000	0.000000	0.000218
56	0.000000	0.000004	0.000000	0.999873	0.000123	0.000000	0.000000	0.000000	0.000000
57	0.000004	0.000002	0.000000	0.999945	0.000038	0.000000	0.000000	0.000011	0.000000
58	0.000001	0.000000	0.000000	0.998440	0.001559	0.000000	0.000000	0.000000	0.000000
59	0.000001	0.000000	0.000005	0.999994	0.000000	0.000000	0.000000	0.000000	0.000000
60	0.000442	0.000000	0.000228	0.999329	0.000000	0.000000	0.000000	0.000000	0.000000

61	0.000000	0.000000	0.000991	0.998899	0.000000	0.000108	0.000001	0.000000	0.000000
62	0.000000	0.000000	0.000051	0.999946	0.000000	0.000000	0.000000	0.000002	0.000001
63	0.000000	0.000000	0.000253	0.999636	0.000000	0.000000	0.000000	0.000000	0.000111
64	0.000000	0.000000	0.002659	0.997341	0.000000	0.000000	0.000000	0.000000	0.000000
65	0.000000	0.000000	0.000073	0.999854	0.000003	0.000000	0.000000	0.000071	0.000000
66	0.000005	0.000000	0.000024	0.999960	0.000000	0.000000	0.000000	0.000009	0.000001
67	0.000000	0.000000	0.000115	0.999447	0.000438	0.000000	0.000000	0.000000	0.000000
68	0.000000	0.000000	0.000082	0.999496	0.000000	0.000325	0.000027	0.000000	0.000069
69	0.000001	0.000000	0.000565	0.999427	0.000000	0.000000	0.000000	0.000000	0.000007
70	0.000000	0.000000	0.000000	1.000000	0.000000	0.000000	0.000000	0.000000	0.000000
71	0.000000	0.000000	0.000352	0.998879	0.000000	0.000001	0.000000	0.000769	0.000000
72	0.000000	0.000009	0.000089	0.999863	0.000000	0.000004	0.000035	0.000000	0.000000
73	0.000000	0.000000	0.000668	0.999192	0.000000	0.000124	0.000000	0.000001	0.000015
74	0.000000	0.000080	0.000481	0.999425	0.000000	0.000000	0.000000	0.000015	0.000000
75	0.000022	0.000000	0.000000	0.999717	0.000000	0.000000	0.000000	0.000000	0.000261
76	0.000000	0.000000	0.000000	0.999976	0.000000	0.000000	0.000000	0.000000	0.000024
77	0.000042	0.000000	0.000000	0.999958	0.000000	0.000000	0.000000	0.000000	0.000000
78	0.000020	0.000000	0.000009	0.999898	0.000001	0.000066	0.000000	0.000006	0.000000
79	0.000000	0.000000	0.000000	1.000000	0.000000	0.000000	0.000000	0.000000	0.000000
80	0.000000	0.000000	0.000000	0.999989	0.000000	0.000000	0.000000	0.000000	0.000010
81	0.000000	0.000003	0.000000	0.999996	0.000001	0.000000	0.000000	0.000000	0.000000
82	0.000042	0.000001	0.000000	0.999797	0.000000	0.000000	0.000000	0.000000	0.000161
83	0.000001	0.000000	0.000000	0.999999	0.000000	0.000000	0.000000	0.000000	0.000000
84	0.000000	0.000000	0.000000	0.999971	0.000000	0.000001	0.000000	0.000027	0.000000
85	0.000000	0.000000	0.833094	0.166785	0.000008	0.000010	0.000000	0.000067	0.000036
86	0.000000	0.000000	0.874003	0.110925	0.000000	0.015072	0.000000	0.000000	0.000000

87	0.006611	0.000000	0.857535	0.133859	0.001643	0.000000	0.000000	0.000348	0.000005
88	0.000000	0.000000	0.872510	0.127114	0.000005	0.000000	0.000337	0.000034	0.000000
89	0.000000	0.000000	0.883276	0.108676	0.000003	0.000000	0.003520	0.004525	0.000000
90	0.000000	0.000000	0.869316	0.130309	0.000374	0.000000	0.000001	0.000000	0.000000
91	0.000000	0.000000	0.869789	0.128859	0.000002	0.000000	0.000000	0.001346	0.000004
92	0.000000	0.000000	0.839961	0.156577	0.003198	0.000001	0.000036	0.000001	0.000228
93	0.000004	0.000000	0.835231	0.155287	0.000000	0.000000	0.009472	0.000004	0.000002
94	0.000000	0.000000	0.886197	0.113802	0.000000	0.000000	0.000000	0.000000	0.000000
95	0.007080	0.000000	0.815686	0.177234	0.000000	0.000000	0.000000	0.000000	0.000000
96	0.000000	0.000000	0.882174	0.113190	0.000000	0.000000	0.000001	0.004635	0.000000
97	0.000000	0.000000	0.803059	0.196204	0.000000	0.000000	0.000095	0.000641	0.000000
98	0.000000	0.000000	0.851876	0.148123	0.000000	0.000000	0.000000	0.000000	0.000000
99	0.000000	0.000000	0.877299	0.122695	0.000001	0.000000	0.000005	0.000000	0.000000
100	0.000000	0.000000	0.911999	0.088000	0.000000	0.000000	0.000000	0.000000	0.000001
101	0.000000	0.000000	0.834255	0.160319	0.000000	0.004381	0.000000	0.000000	0.001044
102	0.000000	0.000000	0.851569	0.147991	0.000000	0.000043	0.000395	0.000000	0.000002
103	0.000000	0.000000	0.856286	0.143714	0.000000	0.000000	0.000000	0.000000	0.000000
104	0.000000	0.000000	0.801907	0.198093	0.000000	0.000000	0.000000	0.000000	0.000000
105	0.000000	0.000000	0.867090	0.132908	0.000001	0.000000	0.000000	0.000001	0.000000
106	0.000000	0.000000	0.894934	0.101781	0.003285	0.000000	0.000000	0.000000	0.000000
107	0.000000	0.000000	0.020709	0.502846	0.476445	0.000000	0.000000	0.000000	0.000000
108	0.000000	0.000000	0.001321	0.554068	0.444611	0.000000	0.000000	0.000000	0.000000
109	0.000000	0.000000	0.000216	0.626440	0.366358	0.000002	0.000000	0.006984	0.000000
110	0.000000	0.000000	0.001472	0.677522	0.313166	0.000000	0.000000	0.000000	0.007839
111	0.000000	0.000000	0.000062	0.744356	0.252779	0.000000	0.000000	0.000000	0.002803
112	0.000000	0.000003	0.000195	0.536893	0.456878	0.005040	0.000991	0.000000	0.000000

113	0.000000	0.000000	0.000416	0.613552	0.356298	0.000000	0.000000	0.029662	0.000072
114	0.000000	0.000049	0.000006	0.655536	0.344407	0.000000	0.000001	0.000000	0.000002
115	0.000000	0.000000	0.015807	0.519676	0.464515	0.000000	0.000000	0.000000	0.000001
116	0.000000	0.000000	0.014246	0.555688	0.426818	0.000000	0.000000	0.003248	0.000000
117	0.000000	0.000005	0.000238	0.545016	0.454740	0.000000	0.000000	0.000000	0.000000
118	0.000000	0.004557	0.000127	0.712675	0.280718	0.000000	0.000000	0.000000	0.001924
119	0.000000	0.000000	0.049675	0.408232	0.542093	0.000000	0.000000	0.000000	0.000000
120	0.002377	0.000000	0.000000	0.911637	0.084650	0.000000	0.000000	0.001327	0.000009
121	0.000000	0.000000	0.000017	0.668279	0.290590	0.023281	0.000000	0.000000	0.017833
122	0.000000	0.000000	0.001624	0.457210	0.522825	0.000000	0.000004	0.000000	0.018338
123	0.000000	0.024186	0.000000	0.541315	0.433794	0.000000	0.000677	0.000028	0.000000
124	0.000049	0.000000	0.000000	0.612493	0.387458	0.000000	0.000000	0.000000	0.000000
125	0.000693	0.527822	0.000263	0.300891	0.069692	0.000095	0.000086	0.057821	0.042636
126	0.022203	0.543592	0.004061	0.275140	0.000000	0.000000	0.000011	0.000219	0.154773
127	0.000870	0.612981	0.058702	0.258636	0.000122	0.009686	0.000023	0.047735	0.011244
128	0.000652	0.609855	0.003880	0.260087	0.060103	0.002022	0.000000	0.000115	0.063286
129	0.018761	0.777086	0.013269	0.083179	0.001290	0.001095	0.007164	0.000015	0.098142
130	0.017377	0.777739	0.000711	0.196619	0.000000	0.000035	0.000029	0.000892	0.006596
131	0.067363	0.782926	0.027344	0.060995	0.000001	0.000000	0.003353	0.000000	0.058018
132	0.000014	0.968260	0.014212	0.017372	0.000045	0.000000	0.000038	0.000059	0.000001
133	0.007702	0.974032	0.015314	0.000638	0.001643	0.000018	0.000000	0.000083	0.000569
134	0.000000	0.985745	0.005230	0.002856	0.005384	0.000348	0.000000	0.000000	0.000437
135	0.004068	0.925051	0.001286	0.006593	0.045644	0.000177	0.013913	0.000182	0.003086
136	0.000000	0.989384	0.001646	0.003419	0.003857	0.000033	0.001352	0.000001	0.000308
137	0.000000	0.967161	0.012830	0.000008	0.003215	0.003278	0.000169	0.013337	0.000001
138	0.001333	0.945377	0.047529	0.000880	0.001835	0.002674	0.000044	0.000328	0.000000

139	0.004380	0.992605	0.000017	0.002589	0.000088	0.000205	0.000046	0.000006	0.000064
140	0.000002	0.978439	0.001040	0.015327	0.000539	0.000000	0.001657	0.000000	0.002997
141	0.000001	0.945579	0.000344	0.005364	0.006459	0.001192	0.000002	0.040376	0.000682
142	0.024489	0.963016	0.003000	0.000000	0.003673	0.003710	0.000002	0.002109	0.000000
143	0.000571	0.985669	0.007969	0.001417	0.000596	0.003554	0.000000	0.000001	0.000222
144	0.000000	0.918633	0.008459	0.000939	0.028671	0.043263	0.000002	0.000000	0.000032
145	0.000036	0.044879	0.008330	0.940754	0.000000	0.000324	0.001650	0.004027	0.000000
146	0.000000	0.095820	0.003768	0.894770	0.000000	0.000009	0.000579	0.000170	0.004884
147	0.000010	0.060986	0.005313	0.925713	0.000000	0.007705	0.000015	0.000259	0.000000
148	0.000000	0.083372	0.001058	0.911821	0.000468	0.000015	0.000149	0.000340	0.002777
149	0.000000	0.033269	0.002210	0.954727	0.000000	0.000114	0.008362	0.000402	0.000915
150	0.000001	0.000008	0.002162	0.997803	0.000000	0.000000	0.000002	0.000024	0.000000
151	0.000000	0.043703	0.000000	0.953585	0.000068	0.002586	0.000000	0.000002	0.000055
152	0.000073	0.323245	0.000000	0.655610	0.019530	0.000192	0.000000	0.000018	0.001333
153	0.001474	0.316506	0.000000	0.678941	0.000013	0.003055	0.000001	0.000008	0.000004
154	0.000000	0.446718	0.000000	0.534017	0.000000	0.000000	0.015680	0.000000	0.003584
155	0.000021	0.010397	0.000392	0.985656	0.003511	0.000010	0.000012	0.000000	0.000000
156	0.000000	0.000000	0.000000	0.999999	0.000000	0.000000	0.000000	0.000000	0.000000
157	0.000000	0.181842	0.024944	0.768523	0.000000	0.000000	0.024692	0.000000	0.000000
158	0.001047	0.961999	0.000000	0.029909	0.000000	0.000000	0.001688	0.002914	0.002442
159	0.000000	0.944947	0.020278	0.034603	0.000000	0.000000	0.000001	0.000002	0.000168
160	0.000002	0.999501	0.000000	0.000243	0.000000	0.000000	0.000074	0.000000	0.000180

---

**Table S1.16** Proportion on ancestry for individuals of *Scinax squalirostris*, conditioned to environmental variables, inferred by Bayesian analysis of nuclear for 8.5RCP climatic conditions.

Individual	Inferred Cluster								
	Cluster 1	Cluster 2	Cluster 3	Cluster 4	Cluster 5	Cluster 6	Cluster 7	Cluster 8	Cluster 9
1	1.9923E-05	2.2609E-02	0.0000E+00	9.7714E-01	0.0000E+00	7.2946E-09	0.0000E+00	1.8500E-13	2.2710E-04
2	1.8812E-06	6.4153E-03	3.8083E-09	9.9161E-01	1.5154E-03	0.0000E+00	1.2439E-10	1.7297E-04	2.8680E-04
3	9.2239E-04	1.3147E-02	1.0361E-06	9.8588E-01	0.0000E+00	6.0376E-09	0.0000E+00	0.0000E+00	4.8797E-05
4	9.1963E-10	2.4587E-02	0.0000E+00	9.7516E-01	0.0000E+00	1.4006E-08	0.0000E+00	5.3286E-05	1.9577E-04
5	2.3637E-07	6.3682E-03	0.0000E+00	9.9230E-01	0.0000E+00	8.4637E-10	6.6903E-06	6.1175E-08	1.3291E-03
6	0.0000E+00	1.3529E-02	0.0000E+00	9.8230E-01	0.0000E+00	0.0000E+00	0.0000E+00	2.5551E-07	4.1719E-03
7	5.4259E-11	5.5265E-03	0.0000E+00	9.9430E-01	0.0000E+00	2.8993E-05	3.3371E-08	8.9600E-13	1.4622E-04
8	4.8050E-05	1.0271E-02	0.0000E+00	9.8947E-01	0.0000E+00	1.3682E-05	3.4499E-05	3.6000E-14	1.6681E-04
9	1.7302E-10	6.8327E-03	1.3229E-10	9.9108E-01	0.0000E+00	0.0000E+00	1.5760E-05	1.8827E-11	2.0672E-03
10	4.0000E-15	8.7383E-03	0.0000E+00	9.9123E-01	0.0000E+00	5.3148E-10	1.0000E-15	2.8094E-05	7.3459E-08
11	6.7242E-05	1.2618E-02	0.0000E+00	9.8728E-01	0.0000E+00	1.0299E-06	4.5100E-13	1.4318E-11	2.9652E-05
12	1.2327E-09	1.5565E-02	0.0000E+00	9.8443E-01	0.0000E+00	3.0046E-07	1.4687E-07	0.0000E+00	2.7712E-07
13	5.4830E-03	4.8950E-03	0.0000E+00	9.8856E-01	0.0000E+00	9.4402E-10	5.7485E-07	4.0971E-10	1.0653E-03
14	7.5159E-09	3.1585E-03	0.0000E+00	9.9683E-01	0.0000E+00	4.2005E-08	1.8583E-07	1.0776E-05	2.5160E-06
15	8.6470E-07	3.9654E-03	3.9304E-07	9.9603E-01	0.0000E+00	2.9320E-12	0.0000E+00	1.4933E-07	4.0835E-11
16	2.7499E-09	6.7471E-04	0.0000E+00	9.9925E-01	0.0000E+00	0.0000E+00	1.8350E-12	6.2000E-14	7.8148E-05
17	2.0628E-08	6.0880E-06	0.0000E+00	9.9770E-01	0.0000E+00	3.1000E-14	4.8047E-04	2.2358E-04	1.5856E-03
18	3.6894E-09	9.8002E-04	0.0000E+00	9.9901E-01	7.2429E-09	0.0000E+00	0.0000E+00	8.4225E-06	7.8635E-10
19	1.4417E-11	6.1401E-04	0.0000E+00	9.9906E-01	0.0000E+00	2.0000E-15	1.6997E-08	2.4819E-08	3.2613E-04

20	2.6092E-06	9.9411E-04	0.0000E+00	9.9801E-01	1.7394E-09	4.0934E-07	5.8000E-14	2.6388E-04	7.2570E-04
21	7.3327E-08	2.4886E-03	2.9467E-06	9.9648E-01	0.0000E+00	2.2400E-08	0.0000E+00	1.0503E-05	1.0214E-03
22	5.1054E-09	2.2711E-03	1.5304E-03	9.9590E-01	0.0000E+00	3.0005E-08	5.5546E-10	1.5010E-12	2.9906E-04
23	0.0000E+00	2.4826E-04	1.0101E-08	9.9964E-01	0.0000E+00	4.0700E-13	0.0000E+00	1.6096E-10	1.0847E-04
24	0.0000E+00	8.4705E-05	0.0000E+00	9.9879E-01	0.0000E+00	0.0000E+00	7.9727E-06	0.0000E+00	1.1138E-03
25	3.4937E-04	1.9834E-04	0.0000E+00	9.9945E-01	0.0000E+00	0.0000E+00	2.1203E-10	0.0000E+00	9.4555E-07
26	5.6000E-13	3.8451E-04	0.0000E+00	9.9949E-01	0.0000E+00	0.0000E+00	4.8486E-07	2.2150E-12	1.2738E-04
27	1.1388E-06	1.4576E-03	2.2695E-06	9.9853E-01	0.0000E+00	3.1927E-08	1.3552E-06	3.1893E-08	3.9564E-06
28	4.2990E-12	7.8467E-06	1.9712E-06	9.9998E-01	0.0000E+00	0.0000E+00	3.2150E-12	0.0000E+00	1.4334E-05
29	0.0000E+00	2.4690E-12	2.1614E-06	1.0000E+00	0.0000E+00	0.0000E+00	3.9626E-09	2.7697E-09	9.5875E-10
30	3.0831E-08	2.1496E-05	5.7507E-06	9.9997E-01	0.0000E+00	7.6383E-08	3.1001E-06	1.1438E-09	2.1776E-11
31	2.5223E-08	0.0000E+00	3.4360E-07	1.0000E+00	0.0000E+00	0.0000E+00	1.2726E-08	0.0000E+00	0.0000E+00
32	1.3939E-11	9.6200E-13	4.4899E-07	9.9988E-01	0.0000E+00	0.0000E+00	0.0000E+00	0.0000E+00	1.2065E-04
33	1.5763E-07	2.2819E-07	2.1823E-08	9.9985E-01	0.0000E+00	1.7000E-14	0.0000E+00	5.7381E-11	1.5177E-04
34	5.4324E-10	1.0389E-05	2.1784E-05	9.9994E-01	0.0000E+00	0.0000E+00	1.3880E-12	9.4546E-07	2.6776E-05
35	3.8512E-10	3.5043E-07	1.3279E-11	1.0000E+00	0.0000E+00	5.1016E-08	1.0000E-15	5.5225E-09	1.0000E-15
36	1.8644E-05	9.1958E-10	3.8664E-08	9.9997E-01	0.0000E+00	2.2459E-08	1.6966E-08	2.5328E-10	1.2401E-05
37	4.9206E-10	1.1373E-08	7.8515E-08	1.0000E+00	0.0000E+00	2.1208E-07	2.8300E-13	1.1348E-09	1.4381E-08
38	1.3443E-06	6.6942E-08	1.8371E-06	1.0000E+00	0.0000E+00	0.0000E+00	0.0000E+00	1.7742E-08	0.0000E+00
39	3.8508E-05	6.6201E-07	1.8144E-07	9.9989E-01	0.0000E+00	1.7000E-14	7.3045E-07	2.1469E-08	7.2042E-05
40	7.9700E-13	5.7994E-10	7.5078E-07	9.9998E-01	0.0000E+00	1.5772E-05	1.7876E-07	3.2193E-07	6.8210E-10
41	3.4413E-08	0.0000E+00	1.1191E-04	9.9989E-01	0.0000E+00	1.2677E-09	4.7670E-12	5.7482E-09	5.7602E-07
42	7.8050E-10	4.0435E-11	1.1142E-05	9.9967E-01	0.0000E+00	3.2067E-04	6.6638E-08	9.0100E-09	6.4181E-08
43	5.7361E-10	3.7950E-12	2.3222E-07	9.9998E-01	0.0000E+00	8.1000E-14	1.8271E-05	7.3000E-14	1.3350E-08
44	3.4712E-04	2.5000E-13	7.6317E-04	9.9883E-01	0.0000E+00	0.0000E+00	0.0000E+00	5.6831E-05	0.0000E+00
45	0.0000E+00	1.0000E-15	0.0000E+00	9.9982E-01	1.2880E-12	0.0000E+00	2.0737E-05	1.5728E-04	6.3852E-09

46	8.2664E-10	0.0000E+00	0.0000E+00	9.9998E-01	1.8409E-08	0.0000E+00	6.1103E-10	2.0000E-15	1.5929E-05
47	2.4935E-06	2.0000E-14	0.0000E+00	9.9998E-01	1.1758E-05	0.0000E+00	3.5570E-07	4.9073E-07	1.0000E-15
48	3.8482E-11	1.4293E-09	0.0000E+00	9.9986E-01	1.3547E-04	2.0000E-15	0.0000E+00	2.0000E-15	2.6336E-11
49	0.0000E+00	0.0000E+00	1.7002E-07	9.9996E-01	9.7128E-08	4.4275E-05	2.8365E-07	9.9951E-11	0.0000E+00
50	3.8603E-11	0.0000E+00	0.0000E+00	9.9982E-01	2.5659E-05	1.5132E-04	0.0000E+00	1.8238E-08	0.0000E+00
51	7.7369E-10	0.0000E+00	2.8334E-11	9.9995E-01	7.6706E-08	1.0000E-15	9.0300E-12	5.0296E-05	1.4696E-09
52	1.9993E-06	1.7603E-08	4.5600E-13	1.0000E+00	4.5817E-07	0.0000E+00	0.0000E+00	0.0000E+00	0.0000E+00
53	2.6035E-05	0.0000E+00	0.0000E+00	9.9988E-01	8.3525E-05	9.2146E-10	1.1333E-05	6.4046E-07	0.0000E+00
54	0.0000E+00	0.0000E+00	0.0000E+00	9.9988E-01	7.7173E-05	5.3514E-11	5.4328E-10	4.7159E-05	2.5550E-12
55	9.5500E-13	0.0000E+00	0.0000E+00	1.0000E+00	1.8148E-08	0.0000E+00	1.3000E-14	1.4162E-06	1.8000E-14
56	0.0000E+00	0.0000E+00	0.0000E+00	1.0000E+00	4.2059E-06	9.1000E-14	5.9642E-08	6.8209E-10	3.4821E-07
57	4.9543E-09	0.0000E+00	0.0000E+00	1.0000E+00	3.0028E-07	0.0000E+00	0.0000E+00	1.1436E-10	7.0941E-10
58	1.0000E-15	0.0000E+00	4.9848E-09	9.9990E-01	3.3849E-06	0.0000E+00	5.0200E-13	1.0000E-15	1.0108E-04
59	3.1475E-06	4.0300E-13	3.3438E-06	9.9999E-01	7.5000E-14	0.0000E+00	1.0000E-15	9.4593E-09	1.8007E-10
60	0.0000E+00	0.0000E+00	1.3604E-04	9.9984E-01	0.0000E+00	0.0000E+00	1.9000E-14	2.4817E-05	3.7632E-06
61	0.0000E+00	2.7000E-14	1.3067E-04	9.9987E-01	0.0000E+00	1.5500E-13	6.1762E-10	2.5217E-07	0.0000E+00
62	6.7649E-07	2.0709E-06	8.3477E-05	9.9988E-01	0.0000E+00	1.5529E-09	1.1833E-05	2.4574E-05	1.3064E-07
63	5.9309E-08	0.0000E+00	1.3302E-06	1.0000E+00	0.0000E+00	1.0472E-10	1.2335E-08	7.8501E-10	7.1997E-09
64	4.0347E-10	1.7163E-09	1.1595E-05	9.9999E-01	0.0000E+00	1.9900E-13	1.7327E-08	3.3647E-08	1.2845E-09
65	4.5806E-08	0.0000E+00	3.8641E-05	9.9996E-01	3.5000E-14	1.9825E-09	2.6410E-12	0.0000E+00	3.3254E-06
66	1.0079E-04	0.0000E+00	8.9910E-06	9.9988E-01	0.0000E+00	1.7410E-12	1.1509E-09	8.1387E-06	1.2244E-07
67	5.9670E-12	3.4635E-09	4.1324E-05	9.9996E-01	0.0000E+00	0.0000E+00	1.0800E-13	3.8196E-09	3.6600E-13
68	1.3130E-05	0.0000E+00	4.1978E-05	9.9994E-01	0.0000E+00	0.0000E+00	1.6660E-12	4.3200E-13	0.0000E+00
69	5.9000E-14	7.8436E-05	1.8382E-04	9.9971E-01	0.0000E+00	2.5014E-05	0.0000E+00	0.0000E+00	2.6668E-07
70	3.9027E-07	0.0000E+00	3.2748E-05	9.9997E-01	0.0000E+00	0.0000E+00	0.0000E+00	8.9000E-13	2.0000E-15
71	3.4000E-14	4.8818E-09	1.8587E-06	1.0000E+00	0.0000E+00	0.0000E+00	3.1500E-13	1.3462E-08	0.0000E+00

72	4.7727E-07	0.0000E+00	3.7972E-05	9.9996E-01	0.0000E+00	0.0000E+00	3.6620E-12	0.0000E+00	1.3724E-06
73	2.0000E-14	0.0000E+00	1.8608E-04	9.9981E-01	0.0000E+00	1.2934E-10	2.9776E-09	0.0000E+00	4.7020E-11
74	1.2809E-10	0.0000E+00	1.0482E-06	1.0000E+00	0.0000E+00	1.6779E-07	5.1021E-07	4.4072E-09	9.6452E-11
75	3.6457E-09	0.0000E+00	1.3000E-14	1.0000E+00	5.0000E-15	1.0670E-12	0.0000E+00	0.0000E+00	4.1793E-10
76	6.6168E-06	0.0000E+00	0.0000E+00	9.9999E-01	0.0000E+00	0.0000E+00	2.2930E-07	1.9591E-07	0.0000E+00
77	1.5586E-09	0.0000E+00	1.1681E-06	1.0000E+00	0.0000E+00	0.0000E+00	1.0000E-15	2.5949E-10	2.3622E-10
78	8.0323E-11	0.0000E+00	1.6600E-13	9.9998E-01	1.0637E-06	0.0000E+00	0.0000E+00	1.2883E-11	1.9630E-05
79	0.0000E+00	0.0000E+00	4.3000E-13	1.0000E+00	0.0000E+00	3.6335E-07	1.9115E-07	4.8398E-07	1.9000E-14
80	9.3267E-07	0.0000E+00	0.0000E+00	1.0000E+00	0.0000E+00	0.0000E+00	1.8723E-07	1.1500E-13	0.0000E+00
81	1.4163E-10	0.0000E+00	0.0000E+00	1.0000E+00	7.3100E-13	6.4310E-12	6.9000E-14	0.0000E+00	2.5048E-07
82	9.4052E-09	9.2340E-12	5.0020E-12	9.9999E-01	1.2239E-09	5.3561E-07	0.0000E+00	5.0730E-06	0.0000E+00
83	4.5156E-06	1.3138E-11	0.0000E+00	9.9998E-01	1.1070E-12	7.8138E-11	1.0599E-10	1.3766E-07	1.3072E-05
84	1.9097E-10	0.0000E+00	1.6062E-05	9.9998E-01	0.0000E+00	4.9736E-08	2.3152E-06	2.0090E-09	1.0393E-11
85	2.9727E-04	0.0000E+00	4.5527E-01	5.4442E-01	1.7888E-06	3.7980E-11	3.3451E-09	5.3652E-06	8.3271E-07
86	0.0000E+00	0.0000E+00	4.1262E-01	5.8737E-01	5.1349E-07	1.1018E-10	0.0000E+00	0.0000E+00	5.5489E-07
87	2.1830E-08	0.0000E+00	3.7501E-01	6.2349E-01	0.0000E+00	1.3827E-03	0.0000E+00	1.1798E-04	0.0000E+00
88	1.0000E-15	0.0000E+00	4.7862E-01	5.2138E-01	0.0000E+00	3.7000E-14	1.3824E-08	0.0000E+00	4.7100E-13
89	5.6564E-10	0.0000E+00	4.0613E-01	5.9370E-01	0.0000E+00	1.7054E-04	4.7580E-12	0.0000E+00	0.0000E+00
90	2.6406E-06	0.0000E+00	4.1727E-01	5.8256E-01	0.0000E+00	1.5884E-04	0.0000E+00	0.0000E+00	0.0000E+00
91	0.0000E+00	0.0000E+00	4.6480E-01	5.3504E-01	0.0000E+00	0.0000E+00	1.2315E-08	1.6115E-04	0.0000E+00
92	1.1153E-05	0.0000E+00	3.9739E-01	6.0165E-01	2.0001E-06	0.0000E+00	9.4024E-04	1.6750E-06	1.3423E-10
93	0.0000E+00	0.0000E+00	3.9888E-01	6.0112E-01	6.0300E-11	0.0000E+00	0.0000E+00	4.3095E-08	7.5008E-11
94	0.0000E+00	0.0000E+00	4.5316E-01	5.4683E-01	0.0000E+00	0.0000E+00	3.0906E-06	9.3247E-07	1.8533E-08
95	2.1221E-07	0.0000E+00	4.5039E-01	5.4388E-01	0.0000E+00	3.4647E-04	9.0000E-15	5.3780E-03	1.0389E-08
96	1.7782E-05	0.0000E+00	4.0579E-01	5.9419E-01	0.0000E+00	6.7243E-08	1.9721E-06	4.6300E-07	1.3229E-11
97	8.7675E-06	0.0000E+00	3.6608E-01	6.3382E-01	0.0000E+00	2.1279E-06	3.9500E-13	8.4623E-05	6.0000E-14

98	1.2797E-10	0.0000E+00	4.1477E-01	5.8522E-01	0.0000E+00	5.3542E-06	0.0000E+00	6.4067E-09	1.8416E-07
99	7.2694E-05	0.0000E+00	4.2617E-01	5.7318E-01	2.2579E-04	0.0000E+00	3.4666E-04	2.7000E-14	6.0000E-15
100	3.2543E-04	0.0000E+00	4.5785E-01	5.4183E-01	2.2986E-07	0.0000E+00	1.0982E-09	7.5225E-08	5.0309E-10
101	1.8213E-06	0.0000E+00	4.0184E-01	5.9814E-01	0.0000E+00	1.4222E-09	5.0846E-06	2.9440E-08	8.3003E-06
102	2.3174E-05	0.0000E+00	4.1540E-01	5.8458E-01	0.0000E+00	0.0000E+00	7.5870E-08	1.0562E-07	0.0000E+00
103	3.3564E-10	0.0000E+00	4.0689E-01	5.9256E-01	0.0000E+00	0.0000E+00	1.9271E-10	5.5278E-04	6.6314E-10
104	7.0482E-07	0.0000E+00	4.2671E-01	5.7328E-01	0.0000E+00	0.0000E+00	0.0000E+00	2.0699E-06	0.0000E+00
105	0.0000E+00	0.0000E+00	4.2218E-01	5.7782E-01	0.0000E+00	0.0000E+00	0.0000E+00	0.0000E+00	1.0000E-15
106	4.7621E-05	0.0000E+00	4.3235E-01	5.6760E-01	0.0000E+00	3.3760E-09	1.7482E-07	0.0000E+00	0.0000E+00
107	2.2887E-10	0.0000E+00	1.4682E-04	9.9842E-01	1.3494E-03	7.9126E-05	1.0000E-15	0.0000E+00	1.0000E-15
108	4.4000E-13	0.0000E+00	3.6237E-03	9.7130E-01	2.3580E-02	1.4888E-03	6.3852E-06	2.9865E-11	7.6800E-13
109	0.0000E+00	2.7000E-14	3.4395E-06	9.7030E-01	1.5469E-02	4.9100E-13	1.4088E-02	9.9685E-10	1.4322E-04
110	9.5042E-05	0.0000E+00	2.6003E-10	9.7083E-01	2.9075E-02	1.1537E-08	8.7444E-07	4.1093E-11	6.9284E-10
111	2.5640E-04	1.8645E-10	8.7087E-03	9.8122E-01	9.8173E-03	5.1087E-10	1.5100E-13	0.0000E+00	0.0000E+00
112	3.5004E-06	4.6856E-06	4.9680E-08	9.8981E-01	3.8990E-03	8.5000E-14	2.4742E-03	3.7943E-03	1.1045E-05
113	1.6543E-05	0.0000E+00	2.8382E-05	9.6415E-01	2.7938E-02	7.5542E-06	7.4869E-08	7.8631E-03	2.4234E-11
114	5.5500E-13	0.0000E+00	6.9946E-03	9.7560E-01	1.7319E-02	1.2400E-13	8.7685E-05	7.1006E-07	6.8774E-07
115	6.3066E-09	0.0000E+00	7.2993E-04	9.3868E-01	6.0589E-02	7.6715E-11	5.7285E-07	2.6700E-13	0.0000E+00
116	3.6006E-05	0.0000E+00	4.3511E-04	9.9166E-01	7.3349E-03	1.1233E-05	1.3751E-08	5.1799E-04	0.0000E+00
117	2.2805E-07	0.0000E+00	5.5415E-04	9.9249E-01	6.9566E-03	5.3954E-07	0.0000E+00	3.7790E-11	1.0800E-13
118	0.0000E+00	0.0000E+00	7.6246E-04	9.9136E-01	7.7941E-03	0.0000E+00	8.4793E-05	8.4055E-07	0.0000E+00
119	2.0848E-11	0.0000E+00	8.7645E-05	9.6698E-01	2.7158E-02	6.2902E-04	1.8106E-07	5.1495E-03	4.4382E-11
120	3.0326E-08	0.0000E+00	5.2506E-03	9.8734E-01	7.4007E-03	3.6900E-06	0.0000E+00	3.3629E-06	0.0000E+00
121	3.4000E-14	0.0000E+00	2.2931E-03	9.7855E-01	1.9093E-02	1.0000E-15	4.9125E-05	6.9948E-09	1.4889E-05
122	1.4460E-04	0.0000E+00	2.2836E-04	9.6115E-01	3.7578E-02	2.5665E-06	9.5876E-10	8.9586E-04	0.0000E+00
123	1.7001E-09	3.5965E-06	5.9555E-10	9.8259E-01	1.7404E-02	4.4014E-07	6.7013E-07	6.0954E-09	0.0000E+00

124	1.0000E-15	3.4004E-11	2.2784E-05	9.8621E-01	1.3767E-02	2.5781E-06	2.7900E-12	0.0000E+00	0.0000E+00
125	9.9641E-03	8.0334E-03	9.1630E-04	9.5067E-01	0.0000E+00	1.6076E-02	6.0036E-03	1.4906E-09	8.3332E-03
126	3.3922E-03	3.5791E-02	5.7002E-05	9.2571E-01	1.1729E-07	2.5435E-02	2.6608E-03	1.5918E-03	5.3625E-03
127	3.2240E-03	9.4926E-03	2.0516E-04	9.3267E-01	4.2015E-06	1.2658E-05	2.2420E-03	2.5511E-03	4.9597E-02
128	1.8437E-02	2.9242E-02	3.3585E-06	9.4385E-01	0.0000E+00	3.7883E-03	8.5650E-04	8.4303E-04	2.9763E-03
129	6.0617E-03	3.7337E-02	8.1497E-07	9.4852E-01	0.0000E+00	1.3908E-08	1.0172E-03	1.4849E-04	6.9121E-03
130	4.0809E-03	2.8053E-02	1.5701E-03	9.5419E-01	0.0000E+00	3.8562E-05	8.5130E-03	2.5518E-03	1.0018E-03
131	1.1838E-06	6.3672E-03	2.9898E-02	9.4954E-01	1.2700E-13	1.0000E-15	1.0768E-05	7.2215E-03	6.9615E-03
132	2.3649E-03	5.8062E-01	1.1492E-03	4.0192E-01	0.0000E+00	1.6179E-06	2.5425E-03	4.5493E-03	6.8465E-03
133	2.5617E-04	5.5801E-01	5.5682E-05	4.1216E-01	0.0000E+00	4.0816E-07	1.8251E-02	6.9401E-06	1.1261E-02
134	3.5493E-07	7.3641E-01	1.8623E-02	2.4452E-01	3.6981E-05	6.4644E-06	3.9610E-06	3.4119E-04	5.4983E-05
135	7.3640E-07	5.3677E-01	5.0311E-06	4.4705E-01	1.5737E-02	8.7796E-05	4.5896E-07	3.5318E-05	3.0872E-04
136	1.9620E-10	6.7954E-01	3.3801E-08	3.0948E-01	8.0997E-03	1.6870E-03	2.9538E-07	5.8736E-05	1.1305E-03
137	4.5678E-02	5.3948E-01	7.3321E-02	3.3075E-01	0.0000E+00	1.0142E-02	2.0896E-04	6.8916E-06	4.0563E-04
138	7.9463E-03	5.5917E-01	5.6107E-04	4.2821E-01	2.0014E-03	4.1894E-11	5.1279E-05	7.2982E-04	1.3221E-03
139	2.4098E-06	5.8404E-01	1.6395E-03	4.0799E-01	3.0000E-15	6.7290E-08	5.3734E-07	5.7601E-03	5.6822E-04
140	1.1974E-03	6.4028E-01	2.0807E-02	3.1817E-01	7.2142E-03	1.2335E-02	1.9871E-07	1.1922E-11	4.7910E-08
141	4.7485E-05	5.3440E-01	8.7023E-05	4.4804E-01	2.5600E-13	5.6993E-11	2.1509E-08	1.6791E-02	6.3509E-04
142	1.0172E-07	5.7092E-01	5.6035E-03	3.8186E-01	1.8294E-11	1.0224E-04	6.4199E-05	5.3025E-03	3.6145E-02
143	6.2320E-03	6.6849E-01	2.6500E-04	3.1581E-01	7.4395E-05	2.5860E-07	7.0745E-05	9.0339E-03	2.3165E-05
144	9.6248E-06	6.1519E-01	5.9378E-04	3.7771E-01	0.0000E+00	1.6376E-09	1.8998E-05	3.8688E-03	2.6091E-03
145	4.2736E-05	1.0104E-03	2.7844E-03	9.9392E-01	0.0000E+00	4.2703E-09	4.8686E-04	4.5511E-04	1.2956E-03
146	2.6365E-04	1.1162E-03	2.2547E-03	9.9617E-01	0.0000E+00	5.6941E-05	1.4823E-05	1.2623E-04	0.0000E+00
147	1.4159E-04	4.8394E-04	3.1798E-03	9.9614E-01	0.0000E+00	3.9574E-09	2.1293E-05	2.8933E-05	2.6029E-07
148	1.2748E-04	5.7296E-04	1.6209E-03	9.9553E-01	0.0000E+00	5.1592E-07	1.3821E-03	7.6774E-04	6.0000E-14
149	4.1535E-05	5.7592E-05	2.5596E-03	9.9713E-01	0.0000E+00	7.6023E-06	1.0671E-04	4.7163E-05	4.6427E-05

150	3.0553E-10	1.1300E-13	3.0306E-05	9.9995E-01	0.0000E+00	1.2769E-07	1.9381E-06	1.9036E-06	1.5857E-05
151	1.3355E-04	2.7916E-04	0.0000E+00	9.9943E-01	0.0000E+00	8.6568E-07	2.9483E-07	1.6002E-04	1.1046E-11
152	1.9491E-11	7.1169E-04	0.0000E+00	9.9924E-01	3.7600E-13	3.8032E-07	1.9257E-05	4.7305E-06	2.5649E-05
153	1.5561E-03	4.3867E-03	8.2758E-08	9.9314E-01	8.0400E-13	0.0000E+00	4.2462E-08	9.1625E-04	1.7469E-08
154	1.2279E-03	3.9359E-03	1.5202E-05	9.8712E-01	7.4520E-03	6.9922E-05	1.4303E-04	1.1320E-12	3.1169E-05
155	8.2612E-05	4.3558E-04	4.9482E-05	9.9918E-01	2.8312E-08	0.0000E+00	3.9277E-09	2.5294E-04	0.0000E+00
156	7.7575E-09	0.0000E+00	5.0803E-09	1.0000E+00	0.0000E+00	0.0000E+00	6.2279E-09	7.3217E-07	9.6408E-09
157	9.6920E-09	2.7757E-03	3.1877E-06	9.9695E-01	0.0000E+00	7.2978E-07	2.6387E-04	2.4201E-07	3.0427E-06
158	4.2612E-06	1.1427E-01	2.3244E-09	8.8086E-01	0.0000E+00	1.2909E-08	3.6347E-04	2.3241E-07	4.5002E-03
159	6.0177E-04	1.2522E-01	1.1296E-03	8.6825E-01	0.0000E+00	3.8940E-11	2.0673E-04	4.6462E-04	4.1322E-03
160	1.1336E-06	9.9265E-01	1.9166E-04	6.5176E-03	0.0000E+00	5.8084E-08	2.6586E-04	3.6779E-04	1.4263E-06

---

**Table S1.17** Protection Areas clusters based on *k-mean* cluster analysis.

Cluster number	Cluster size	Protection Areas (km <sup>2</sup> )	Genetic richness	Sum of Square within clusters
1	41	-0.12295820	-2.60794521	18.10607
2	133	-0.21967676	1.069904709	30.1519
3	311	-0.16779237	0.03600683	68.01019
4	39	0.06994206	-1.16858556	23.13335
5	20	4.18569915	-0.04499571	95.65173

## REFERENCES

- Allouche, O., Tsoar, A. & Kadmon, R. (2006) Assessing the accuracy of species distribution models: prevalence, kappa and the true skill statistic (TSS). *Journal of Applied Ecology*, 43,1223-1232.
- Araújo, B. M. & New, M. (2007) Ensemble forecasting of species distributions. *Trends in Ecology and Evolution*, 22, 42-47.
- Barbet-Massin, M., Jiguet, F., Albert, C. H., & Wilfried, T. (2012). Modelling species distributions to map the road towards carnivore conservation in the tropics. *Methods in Ecology and Evolution*, 3, 327–338.
- Diniz-Filho, J. A. F., Bini, L. M., Rangel, T. F.; Loyola, R. D., Hof, C., Nogués-Bravo, D. & Araújo, M. B. (2009) Partitioning and mapping uncertainties in ensembles of forecasts of species turnover under climate change. *Ecography*, 32, 897-906.
- Hall, T. A. (1999) BioEdit: a user-friendly biological sequence alignment editor and analysis program for Windows 95/98/NT. *Nucleic Acids Symposium Series*, 41, 95-98.
- Lima-Ribeiro, M. S., Varela, S., González-Hernández, J., Oliveira, G., Diniz-Filho, J. A. F. & Terribile, L. C. (2015) ecoClimate: a database of climate data from

- multiple models for past, present and future for Macroecologists and Biogeographers. *Biodiversity Informatics*, 10, 1-21.
- Tamura, K. & M. Nei. (1993) Estimation of the number of nucleotide substitutions in the control region of mitochondrial DNA in humans and chimpanzees. *Molecular Biology and Evolution*, 10, 512-526.
- Terribile, L. C., Lima-Ribeiro, M. S., Araújo, M. B., Bizão, N., Collevatti, R. G. *et al.* (2012) Areas of Climate Stability of Species ranges in the Brazilian Cerrado: Disentangling Uncertainties through Time. *Natureza & Conservação*, 10, 152-159.
- Thompson, J. D., Gibson, T. J., Plewniak, F., Jeanmougin, F. & Higgins, D. G. (1997) The Clustal X windows interface: flexible strategies for multiple sequence alignment aided by quality analysis tools. *Nucleic Acids Research*, 24, 4876–4882.
- Xia, X. (2013) DAMBE5: A comprehensive software package for data analysis in molecular biology and evolution. *Molecular Biology and Evolution*, 30, 1720-1728.

## SUPPORTING INFORMATION

### Predicting impacts of global climatic change on distribution and genetic diversity of the treefrog *Scinax squalirostris* (Lutz, 1925) (Anura, Hylidae)

Tatianne P. F. Abreu-Jardim, Lucas Jardim, Liliana Ballesteros-Meija, Natan M.

Maciel, Rosane G. Collevatti

**Appendix S2** Supplementary figures (Figs S2.1-S2.5) with saturation result, maps of uncertainty, graph of range size and range shift, shifts in ancestry between contemporary and predicted ancestry coefficients and Sum of squares within clusters by number of clusters.

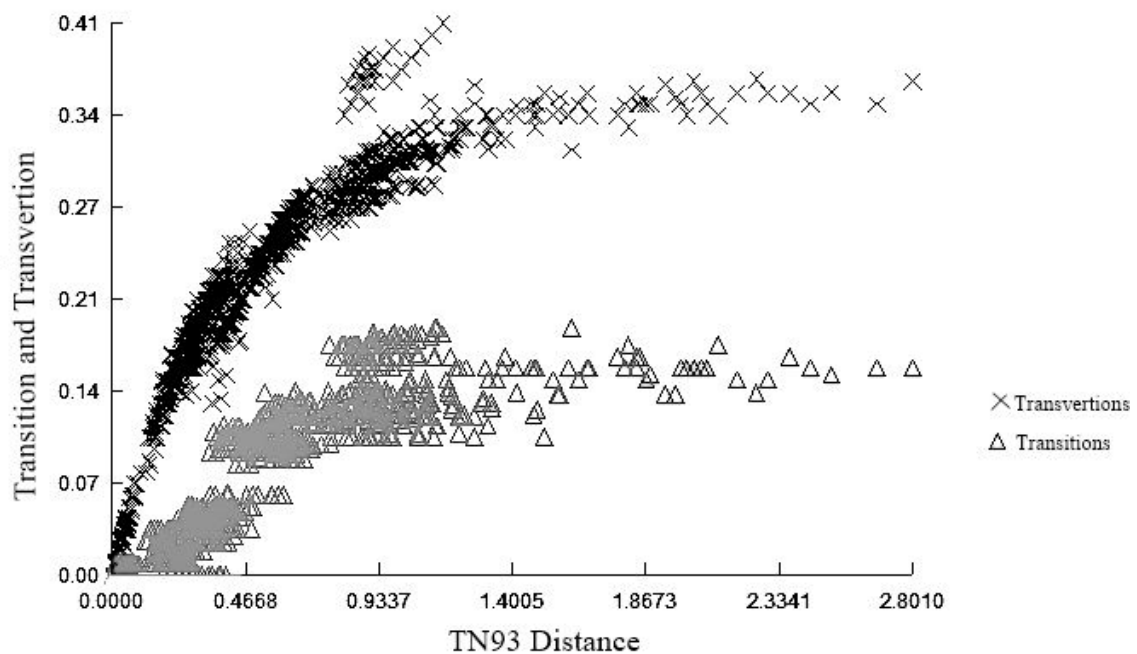


**Figure S2.1** Transition and transversion saturation plot for third codon positions of Cytochrome b sequences.

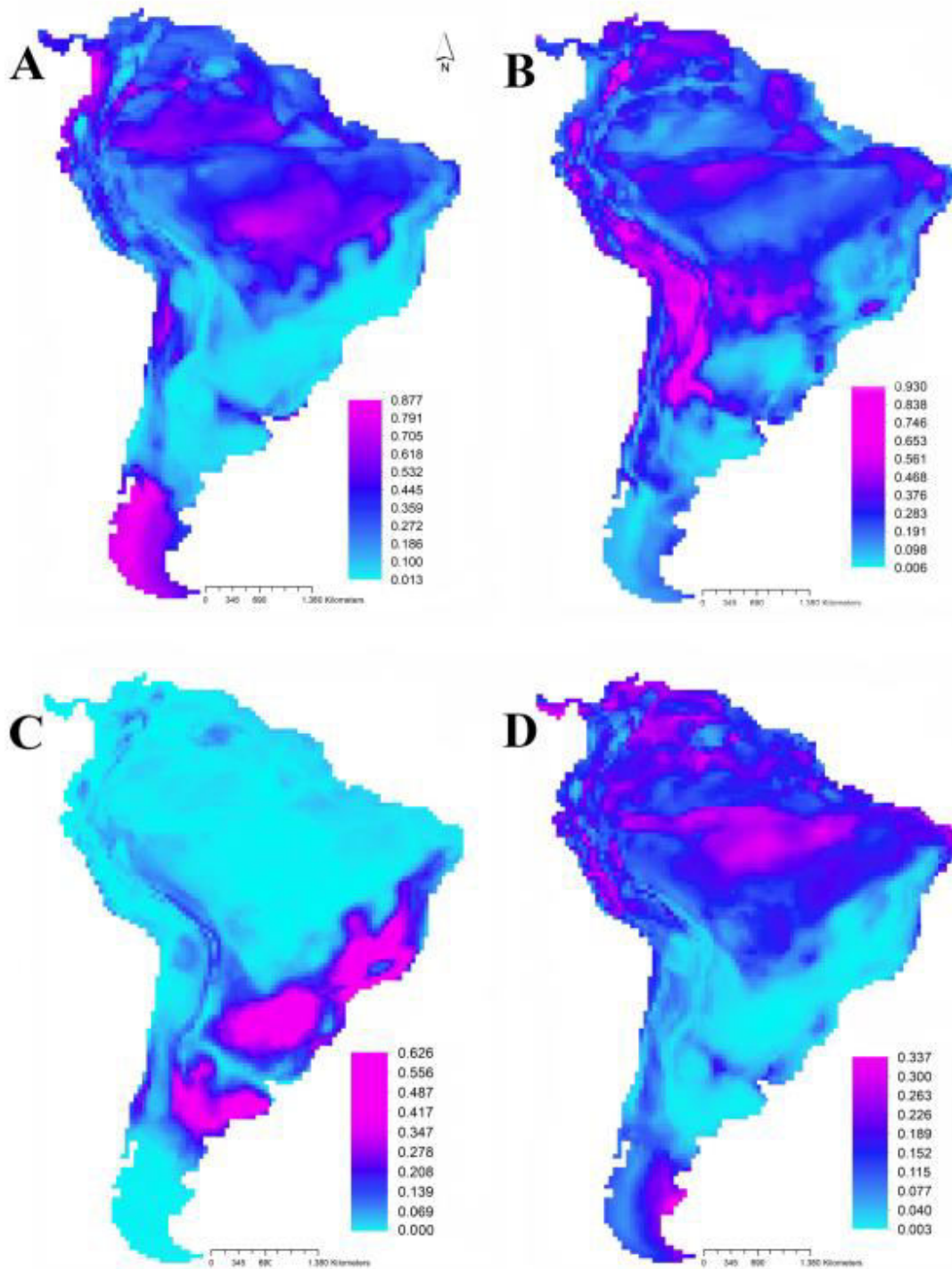


**Figure S2.2** Maps of uncertainty (relative sum of squares) for the modelling components for *Scinax squalirostris*: A) ecological niche models (ENMs), B) atmosphere–ocean global circulation models (AOGCMs), C) time, and D) residual (ENM \* AOGCM interaction).

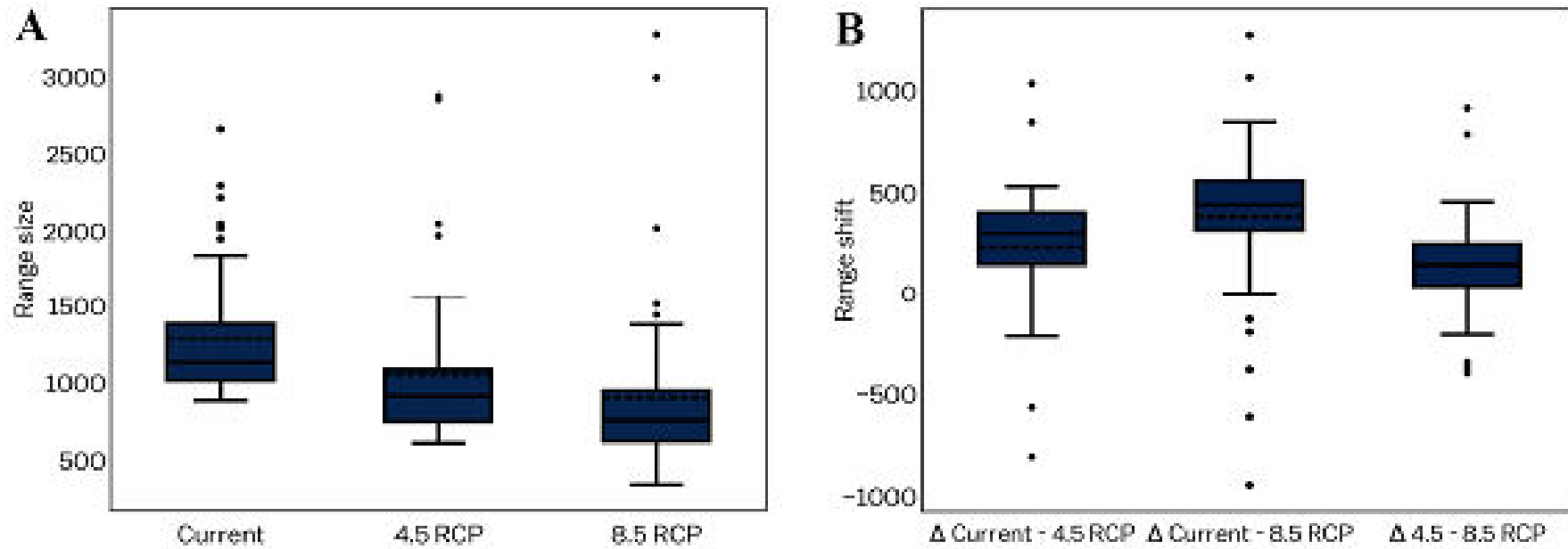


**Figure S2.3** Median and 0.05 – 0.95 quantile among the 48 maps of A) range size and B) shift (difference of range size among time periods in number of cells) predicted for *Scinax squalirostris* at present-day (0 Kya), 4.5 RCP scenario and 8.5 RCP scenario.

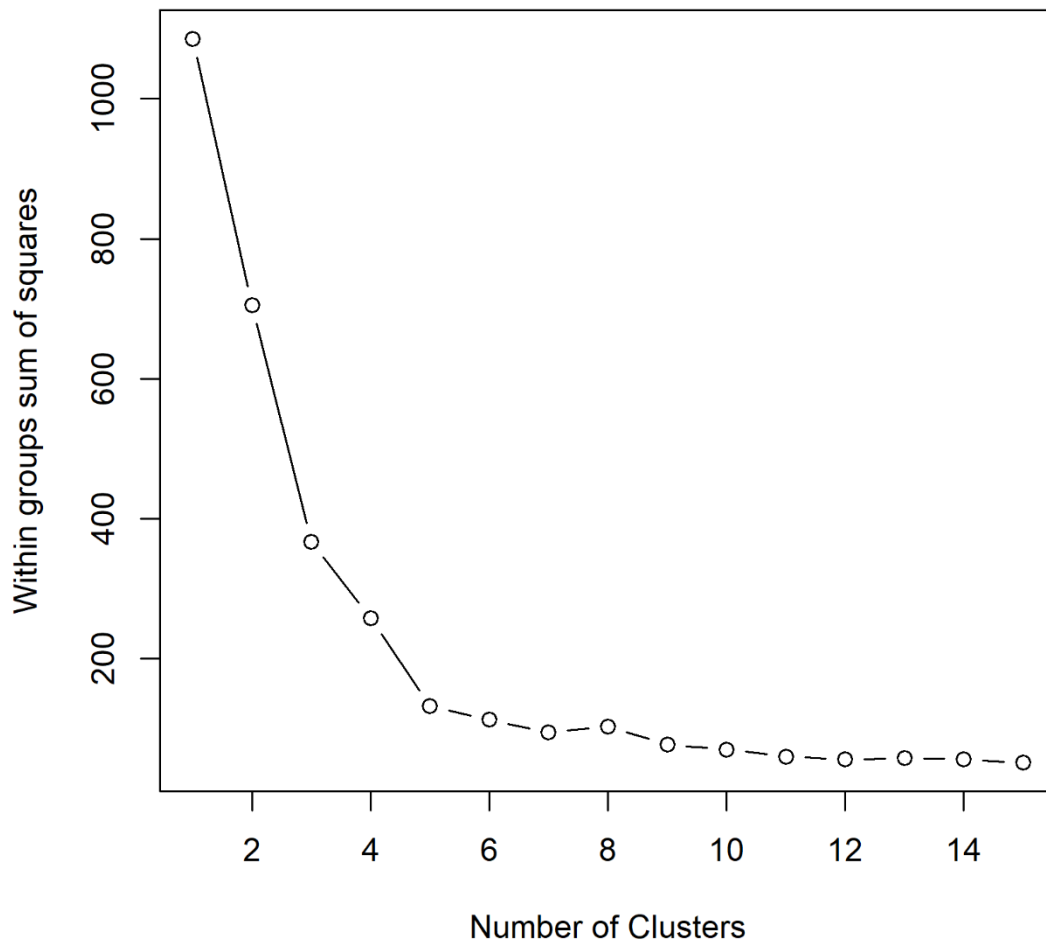


**Figure S2.4** Sum of squares within clusters by number of clusters.

## CONCLUSÃO GERAL

Nesta tese foi avaliado como os eventos históricos podem ter moldado e influenciado a atual distribuição disjunta e diversidade genética de *Scinax squalirostris*. Além disso, avaliamos se essa espécie pode apresentar mais de uma espécie sob o mesmo nome, devido ao isolamento geográfico e restrição ao fluxo gênico. E por fim, avaliamos como as mudanças climáticas esperadas para o fim do século (2100), irão afetar a distribuição geográfica das populações de *S. squalirostris* e se com a perda de áreas adequadas, poderia levar a perda da diversidade genética e assim, uma diminuição do seu potencial de se adaptar as mudanças climáticas, podendo levar a extinção local. Avaliamos essas questões utilizando abordagens de filogeografia estatística, múltiplos genes de herança e taxas de evolução diferentes, simulações coalescentes e modelagem de nicho ecológico.

No primeiro capítulo verificamos que as populações de *S. squalirostris* apresentam alta diferenciação genética e história demográfica constante ao longo do tempo, com eventos de coalescência e origem de dispersão que datam no Plioceno-Pleistoceno, com compartilhamento de haplótipos entre populações geograficamente distantes, o que indicaria um arranjo incompleto de linhagens. Esses resultados nos levaram a concluir que a atual distribuição disjunta e diversidade genética de *S. squalirostris* é devido a contração de uma área amplamente distribuída no passado, gerada pela dinâmica de retração de *grasslands* nos períodos mais quentes devido à perda de áreas adequadas para sua ocorrência.

No segundo capítulo, através de uma abordagem de taxonomia integrativa, com a utilização de dados moleculares e dados morfométricos resgatou-se a formação de dois grupos evolutivamente distintos. A linhagem restrita a região Centro-Oeste do Brasil é uma candidata a espécie e sem nome para a sua associação, podendo ser descrita. O outro grupo abrange populações do Sul e Sudeste do Brasil, Paraguai, Uruguai e Argentina, e devido a essa relação com populações geograficamente distantes, ainda se faz necessário mais testes de hipóteses de delimitação, afim de verificar a existência de mais linhagens candidatas à espécie.

No terceiro capítulo, utilizamos simulações de dados genéticos e modelagem de nicho ecológico e assim fizemos previsões para os efeitos das mudanças climáticas esperadas para o fim do século, que indicaram que *S. squalirostris* terá sua área de distribuição retraída e haverá perda da diversidade genética, que poderá levar a

diminuição do seu potencial em se adaptar as condições locais, principalmente devido as mudanças climáticas serem previstas a acontecer de forma rápida e brusca. Neste capítulo também verificamos que as populações da região Centro-Oeste do Brasil poderão ser extintas devido à ausência de área adequada para a sua ocorrência, essas são as populações que representam ser linhagens evolutivamente distintas candidatas a espécie. Refletindo a problemática em que uma nova espécie pode ser descrita, porém já como ameaçada de extinção. Como a área adequada para a ocorrência irá diminuir, as Unidades de Conservação presentes nessa região, não irão conseguir preservar a sua diversidade genética. Apenas as Unidades de Conservação na região Sul do Brasil, Paraguai, Uruguai e Argentina conseguiram manter a atual riqueza genética encontrada para essas espécies. Porém, nossas simulações genéticas indicaram que haverá perda dos clusters genéticos estimados e poderá haver uma homogeneização da diversidade, em toda a área de ocorrência de *S. squalirostris* e isso poderia levar a uma baixa capacidade de lidar com as mudanças climáticas.

Assim, nosso trabalho indica que *Scinax squalirostris* possui uma história evolutiva complexa, em que os eventos climáticos do passado levaram a uma diminuição de sua distribuição ampla no passado, moldando a sua distribuição atual e sua diversidade genética, e devido à restrição ao fluxo gênico essas populações apresentaram alta estruturação genética. E assim, com a essa estruturação e isolamento, essas populações começaram a se diversificar e hoje podem apresentar pelo menos uma espécie a mais sob o mesmo nome. Com isso, nos deparamos com um cenário em que uma nova espécie pode ser descrita e possivelmente em breve, se enquadrar em uma categoria de ameaça de extinção, devido à perda de áreas adequadas para a sua ocorrência e permanência, mediada pelas mudanças climáticas futuras.

## REFERÊNCIAS

- Awise, J. C.; Arnold, J.; Ball, R. M.; Bermingham, E.; Lamb, T.; Neigel, J. E.; Reeb, C. A. & Saunders, N. C. 1987. Intraspecific phylogeography – the mitochondrial DNA Bridge between population genetics and systematics. *Annual Review of Ecology and Systematics*, 18, 489-522.
- Behling, H. 2002. South and Southeast Brazilian grasslands during Late Quaternary times: a synthesis. *Palaeogeography, Palaeoclimatology and Palaeoecology*, 177, 19-27.
- Brandão, R. A.; Duar, B. A. & Sebben, A. 1997. Geographic Distribution. *Scinax squalirostris*. *Herpetological Reviews*, 28, 93.
- Burnham, R. J. & Graham, A. 1999. The history of Neotropical vegetation: new developments and status. *Annual Missouri Botanic Garden*, 86, 546–589.
- Cei, J. M. 1980. Amphibians of Argentina. *Monitore Zoologico Italiano. Nuova Serie, Monographia*, 2, 1-609.
- Collevatti, R. G., Terribile, L. C., Rabelo, S. G. & Lima-Ribeiro, M. S. 2015. Relaxed random walk model coupled with ecological niche modeling unravel the dispersal dynamics of a Neotropical savanna tree species in the deeper Quaternary. *Frontiers in Plant Science*, 6.
- Cruz, C. A.G; Feio, R. N. & Caramaschi, U. 2009. Anfíbio do Ibitipoca. Ed. Bicho do Mato. Belo Horizonte.
- Duellman, W. E., Marion, A. B. & Hedges, S. B. 2016. Phylogenetics classification and biogeography of the treefrogs (Amphibia: Anura: Arboranae). *Zootaxa*, 4104, 001-109.
- Eterovik, P. C. & Sazima, I. 2004. Anfíbios da Serra do Cipó-Minas Gerais-Brasil. Belo Horizonte. Ed. PUCMINAS.
- Faivovich, J.; Haddad, C. F. B.; Garcia, P. C. A.; Frost, D. R.; Campbell, J. A. & Wheeler, W. C. 2005. Systematic review of the frog family Hylidae, with special reference to Hylinae: phylogenetic analysis and taxonomic revision. *Bulletin of the American Museum of Natural History*, 294, 1-240.

- Faria, D.C. C, Signorelli, L., Morais, A. R., Bastos, R. P. & Maciel, N. M. 2013. Geographic structure and acoustic variation in populations of *Scinax squalirostris* (A. Lutz, 1925) (Anura: Hylidae). *North-Western Journal of Zoology*, 9, 329-336.
- Fischer, H., Meissner, K. J., Mix, A. C, Abram, N. J., Austermann, J. *et al.* 2018. Paleoclimate constraints on the impact of 2°C anthropogenic warming and beyond. *Nature Geoscience*, 11, 474-485.
- Fouquet, A.; Vences, M.; Salducci, M.; Meyer, A.; Marty, C.; Blanc, M. & Gilles, A. 2007. Revealing cryptic diversity using molecular phylogenetics and phylogeography in frogs of the *Scinax ruber* and *Rhinella margaritifera* species groups. *Molecular Phylogenetics and Evolution*, 43, 567-582.
- Frankham, R. 2005. Genetics and extinction. *Biology Conservation*, 126,131–140.
- Freeland, J. 2005. In: *Molecular Ecology*, John Wiley and Sons Ltd, the Atrium, Southern Gate, Chichester, England.
- IPCC, 2014: Climate Change 2014: Synthesis Report. Contribution of Working Groups I, II and III to the Fifth Assessment Report of the Intergovernmental Panel on Climate Change [Core Writing Team, R.K. Pachauri and L.A. Meyer (eds.)]. IPCC, Geneva, Switzerland, 151 pp.
- IUCN 2018. IUCN Red List of Threatened Species. Version 2010.1. <[www.iucnredlist.org](http://www.iucnredlist.org)>.
- Knowles, L. L. & Maddison, W. P. 2002. Statistical phylogeography. *Molecular Ecology*, 11, 2623-2635.
- Kwet, A. & Di-Bernardo, M. 1999. Pró-Mata -Anfíbios. Amphibian. Amphibians. EDIPUCRS. Porto Alegre, Brazil.
- Lima, J. S., Ballesteros-Meija, L., Lima-Ribeiro, M. S. & Collevatti, R. G. 2017. Climatic changes can drive the loss of genetic diversity in a Neotropical savanna tree species. *Global Change Biology*, 1-12.
- Lima, N. E., Lima-Ribeiro, M. S., Tinoco, C. F., Terribile, L. C., & Collevatti, R. G. 2014. Phylogeography and ecological niche modelling, coupled with the fossil pollen record, unravel the demographic history of a Neotropical swamp palm through the Quaternary. *Journal of Biogeography*, 41, 673–686.

- Loyola, R. D., Lemes, P., Brum, F. T., Provete, D. B., & Duarte, L. D. 2014. Clade-specific consequences of climate change to amphibians in Atlantic Forest protected areas. *Ecography*, 37, 65-72.
- Lutz, A. 1925. Batraciens du Brésil. Comptes Rendus et Mémoires Hebdomadaires des Séances de la Société de Biologie et des ses Filiales, vol. 2, Paris, pp. 211–214.
- New, M. D., Liverman, H., Schroeder, H., & Anderson, K. 2011. Four degrees and beyond: The potential for a global temperature increase of four degrees and its implications. *Philosophical Transactions of the Royal Society A: Mathematical, Physical and Engineering Sciences*, 369, 4–5.
- Ortiz-Jaureguizar, E. & Cladera, G. A. 2006. Paleoenvironmental evolution of Southern South America during the Cenozoic. *Journal of Arid Environments*, 66, 498-532.
- Overbeck, G. E.; Müller, S. C.; Fidelis, A.; Pfadenhauer, J.; Pillar, V. D.; Blanco, C. C.; Boldrini, I. I.; Both, R. & Forneck, E. D. 2007. Brazil's neglected biome: The South Brazilian Campos. *Perspectives in Plant Ecology, Evolution and Systematics*, 9, 101-116.
- Riddle, B. R.; Dawson, M. N.; Hadly, E. A.; Hafner, D. J.; Hickerson, M. J.; Mantooth, S. J. & Yoder, A. D. 2008. The role of molecular genetics in sculpting the future of biogeography. *Progress in Physical Geography*, 32, 173-202.
- Rull, V. 2011. Neotropical biodiversity: timing and potential drivers. *Trends in Ecology and Evolution*, 26, 508-513.
- Spielman, D., Brook, B. W. & Frankham, R. 2004. Most species are not driven to extinction before genetic factors impact them. *Proceedings of the National Academy of Sciences of USA*, 101, 15261–15264.
- Tuomisto, H. 2007. Interpreting the biogeography of South America. *Journal of Biogeography*, 34, 1294-1295.
- Turchetto-Zolet, A. C., Pinheiro, F., Salgueiro, F. & Palma-Silva, C. 2013. Phylogeographical patterns shed light on evolutionary process in South America. *Molecular Ecology*, 22, 1193-1213.

- Uetanabaro, M.; Souza, L. F.; Landgraf-Filho, P.; Beda, A. F. & Brandão, R. A. 2007. Anfíbios e Répteis do Parque Nacional da Serra da Bodoquena, Mato Grosso do Sul do Brasil. *Biota Neotropica*, 7, 279-289.
- Urban, M. C., De Meester, L., Vellend, M., Stoks, R. & Vanoverbeke, J. 2012. A crucial step toward realism: responses to climate change from an evolving metacommunity perspective. *Evolutionary Applications*, 5, 154–167.
- Urban, M. C., Richardson, J. L. & Freidenfelds, N. A. 2013. Plasticity and genetic adaptation mediate amphibian and reptile responses to climate changes. *Evolutionary Applications*, 7, 88-103.
- Vasconcelos, T. S., do Nascimento, B. T., & Prado, V. H. 2018. Expected impacts of climate change threaten the anuran diversity in the Brazilian hotspots. *Ecology and Evolution*.
- Vilela, B., Nascimento, F. A., & Vital, M. V. C. 2018. Impacts of climate change on small-ranged amphibians of the northern Atlantic Forest. *Oecologia Australis*, 22.
- Vitorino, L. C., Lima-Ribeiro, M. S., Terribile, L. C. & Collevatti, R. G. 2017. Demographical history and palaeodistribution modelling show range shift towards Amazon Basin for a Neotropical tree species in the LGM. *BMC Evolutionary Biology*, 16-213.